



European Radiology

The official journal of the European Society of
Gastrointestinal and Abdominal Radiology

Supplements online version

ESGAR 2008 Book of Abstracts / Volume 18 / Supplement 2 / June 2008



ESGAR 2008 / June 10 –13 / Istanbul, Turkey
19th Annual Meeting and Postgraduate Course

ESGAR

ISSN-Nummer: 1613-3757

EDUCATIONAL ACTIVITIES

European Society of Gastrointestinal and Abdominal Radiology



ANNUAL MEETINGS

ESGAR 2009

20th Annual Meeting and Postgraduate Course
Valencia, Spain
June 23 – 26, 2009

Meeting President:
Dr. Luis Marti-Bonmati, Valencia/ES

ESGAR 2010

21st Annual Meeting and Postgraduate Course
Dresden, Germany
June 1 – 4, 2010

Meeting President:
Prof. Michael Laniado, Dresden/DE

CT-COLONOGRAPHY HANDS-ON WORKSHOPS

9th ESGAR CT-Colonography Hands-on Workshop

September 11 – 13, 2008, Berlin, Germany

10th ESGAR CT-Colonography Hands-on Workshop

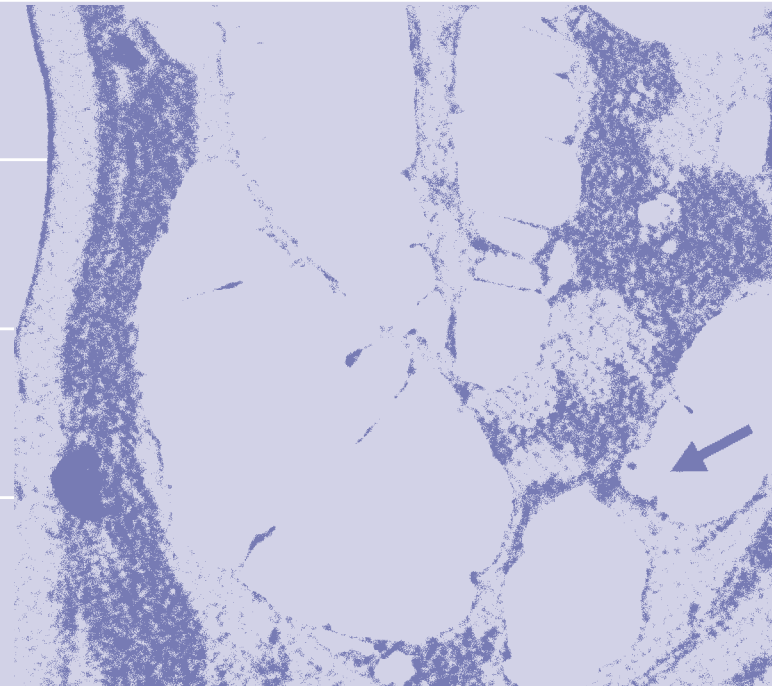
February 2 – 4, 2009, Harrogate, United Kingdom

11th ESGAR CT-Colonography Hands-on Workshop

September 17 – 19, 2009, Stresa, Italy

GE Doctor to Doctor Training on CT-Colonography

October 2 – 3, 2008, Buc, France



LIVER IMAGING WORKSHOP

3rd Liver Imaging Workshop

October 9 – 11, 2008, Munich, Germany



ESGAR thanks its Corporate Members for supporting the realisation of the aims of the Society



GE Healthcare



www.esgar.org



ISTANBUL / TR

EUROPEAN SOCIETY OF GASTROINTESTINAL AND ABDOMINAL RADIOLOGY

ESGAR 2008

BOOK OF ABSTRACTS

INCLUDES ABSTRACTS OF THE POSTGRADUATE COURSE,
SCIENTIFIC PRESENTATIONS AND LUNCH SYMPOSIA

JUNE 10 – 13

19TH ANNUAL MEETING AND POSTGRADUATE COURSE

IMPORTANT ADDRESSES

ORGANISING SECRETARIAT

Central ESGAR Office
Neutorgasse 9/2a
AT-1010 Vienna, Austria
Phone: +43 1 535 89 27
Fax: +43 1 535 70 37
E-mail: office@esgar.org

EXECUTIVE DIRECTOR

Ms. Brigitte Lindlbauer
blindlbauer@esgar.org

WEBSITE

www.esgar.org

EXHIBITION MANAGEMENT

MAW – Medizinische Ausstellungsgesellschaft
Freyung 6
AT-1010 Vienna, Austria
Phone: + 43 1 536 63 35
Fax: + 43 1 535 60 16
E-mail: maw@media.co.at

HOTEL ACCOMMODATION / TRAVEL AGENT

Figür Congress & Organisation Services
Mrs. Yesim Andic
Ayazmaderesi Cad. Karadut Sok. No: 7
TR – 34394 Dikilitas / Istanbul, Turkey
Phone: +90 212 258 6020 – ext. 124
Fax: +90 212 258 6078
E-Mail: esgar2008@figur.net

CONFERENCE VENUE

Istanbul Convention & Exhibition Centre (ICEC)
TR – 80230 Harbiye / Istanbul, Turkey
www.icec.org

PATRONAGE

TRD
Turkish Society of Radiology

TGRD
Turkish Society of Cardiovascular and Interventional
Radiology

Date of publishing: May 2008

CME

The European Society of Gastrointestinal and Abdominal Radiology, ESGAR, is accredited by the European Accreditation Council for Continuing Medical Education (EACCME). The EACCME is an institution of the European Union of Medical Specialists (UEMS), www.uems.be

ESGAR 2008 has been accredited with 24 CME Credits by the EACCME and with 23.5 CME/CPD Credits by the Turkish Medical Association.

SPONSORS

ESGAR wishes to gratefully acknowledge the support of its Corporate Members:



ESGAR also thanks the following companies and institutions for supporting ESGAR 2008:

ANGIOTECH/BERKA
BAYINDIR HOSPITALS
BRACCO
GE MEDICAL SYSTEMS-TURKEY
MINISTRY OF CULTURE AND TOURISM
OPAKIM
SIEMENS -TURKEY/SIMEKS
TUBITAK

The final programme of ESGAR 2008 is available on the ESGAR website www.esgar.org

European Society

ESCAR

Gastrointestinal and Abdominal Radiology

TABLE OF CONTENTS

| | |
|---|-----------|
| Postgraduate Course, Tuesday, June 10 | 05 - 09 |
| Lunch Symposia, Tuesday, June 10 / (SY 1, SY 2) | 11 |
| Lunch Symposia, Wednesday, June 11 / (SY 3, SY 4) | 12 - 13 |
| Lunch Symposia, Thursday, June 12 / (SY 5, SY 6) | 13 - 14 |
| Lunch Symposia, Friday, June 13 / (SY 7, SY 8) | 14 - 15 |
| Scientific Sessions, Wednesday, June 11 / (SS 1 - SS 5) | 17 - 27 |
| Scientific Sessions, Thursday, June 12 / (SS 6 - SS 10) | 28 - 38 |
| Scientific Sessions, Friday, June 13 / (SS 11 - SS 15) | 39 - 49 |
| EPOS™ Presentations (P-001 - P-305) | 51 - 109 |
| Authors' index | 111 - 119 |

COMMITTEES

ESGAR MEETING PRESIDENT

Prof. Dr. Okan Akhan
Department of Radiology
Hacettepe University
School of Medicine
Sihhiye
TR – 6100 Ankara, Turkey
Phone: +90 312 305 1188
Fax: +90 312 311 2145
E-Mail: akhano@tr.net

CO-MEETING PRESIDENT

Prof. Dr. Nevra Elmas
Department of Radiology
EGE University Medical School
Bornova
TR – 35100 Izmir, Turkey
Phone: +90 232 390 2209
Fax: +90 232 342 0001
E-Mail: nevraelmas@gmail.com

ESGAR EXECUTIVE COMMITTEE

PRESIDENT

B. Marincek (Zurich/CH)

PRESIDENT-ELECT

Y. Menu (Le Kremlin-Bicêtre/FR)

VICE PRESIDENT

F. Caseiro-Alves (Coimbra/PT)

SECRETARY

D.E. Malone (Dublin/IE)

TREASURER

S. Halligan (London/UK)

PAST PRESIDENT

C. Bartolozzi (Pisa/IT)

BY-LAWS COMMITTEE

A. Palkó (Szeged/HU)

EDUCATION COMMITTEE

A. Laghi (Latina/IT)

MEMBERSHIP COMMITTEE

J.S. Laméris (Amsterdam/NL)

MEETING PRESIDENT

O. Akhan (Ankara/TR)

PRE-MEETING PRESIDENT

L. Marti-Bonmati (Valencia/ES)

PRE-PRE-MEETING PRESIDENT

M. Laniado (Dresden/DE)

FELLOWS REPRESENTATIVES

L.H. Ros Mendoza (Zaragoza/ES)

W. Schima (Vienna/AT)

ESGAR PROGRAMME COMMITTEE

CHAIRMAN

C. Bartolozzi (Pisa/IT)

MEMBERS

O. Akhan (Ankara/TR)

F. Caseiro-Alves (Coimbra/PT)

N. Elmas (Izmir/TR)

N. Gourtsoyiannis (Heraklion/GR)

M. Laniado (Dresden/DE)

A. Laghi (Latina/IT)

D.E. Malone (Dublin/IE)

B. Marincek (Zurich/CH)

L. Marti-Bonmati (Valencia/ES)

Y. Menu (Le Kremlin-Bicêtre/FR)

LOCAL ORGANISING COMMITTEE

D. Akata (Ankara/TR)

M. Başak (Istanbul/TR)

O. Dicle (Izmir/TR)

M. Harman (Izmir/TR)

A. Kabaalioğlu (Antalya/TR)

U. Korman (Istanbul/TR)

F. Obuz (Izmir/TR)

M. Özmen (Ankara/TR)

G. Savci (Bursa/TR)

D. Tüney (Istanbul/TR)

COMMITTEES

REVIEWING PANEL

D. Akata, Ankara/TR
O. Akhan, Ankara/TR
M.-M. Amitai, Tel Aviv/IL
C.D. Becker, Geneva/CH
R.G.H. Beets-Tan, Maastricht/NL
R. Bouzas, Vigo/ES
G. Brancatelli, Palermo/IT
D.J. Breen, Southampton/UK
C. Bru, Barcelona/ES
J.-M. Bruel, Montpellier/FR
F. Caseiro-Alves, Coimbra/PT
C. Catalano, Rome/IT
D. Cioni, Pisa/IT
L. Crocetti, Pisa/IT
M.C. Della Pina, Pisa/IT
A. Denys, Lausanne/CH
N. Elmas, Izmir/TR
B. Fox, Plymouth/UK
A.H. Freeman, Cambridge/UK
A. Gillams, London/UK
P. Goffette, Brussels/BE
J.A. Guthrie, Leeds/UK
S. Halligan, London/UK
T. Helmberger, Munich/DE
F. Iafrate, Rome/IT
C. Kay, Bradford/UK
H.-U. Laasch, Manchester/UK
A. Laghi, Latina/IT
E. Leen, Glasgow/UK
P. Lefere, Roeselare/BE
R. Lencioni, Pisa/IT
D.J. Lomas, Cambridge/UK
M. Maher, Wilton, Cork/IE
T. Mang, Vienna/AT
B. Marincek, Zurich/CH
L. Marti-Bonmati, Valencia/ES
C. Matos, Brussels/BE
R.M. Mendelson, Perth/AU
Y. Menu, Le Kremlin-Bicêtre/FR
G. Morana, Treviso/IT
E. Neri, Pisa/IT
B. Op De Beeck, Edegem/BE
A. Palkó, Szeged/HU
O. Papakonstantinou, Athens/GR
N. Papanikolaou, Heraklion/GR
P.L. Pereira, Tübingen/DE
P. Pokieser, Vienna/AT
P. Prassopoulos, Alexandroupolis/GR
M. Puckett, Torquay/UK
J. Puig Domingo, Sabadell/ES
A.S. Roberts, Cardiff/UK
G.A. Rollandi, Genova/IT
P.R. Ros, Barcelona/ES
L.H. Ros Mendoza, Zaragoza/ES
W. Schima, Vienna/AT
S. Skehan, Dublin/IE
M. Staunton, Toronto, ON/CA
G.W. Stevenson, Victoria, BC/CA
J. Stoker, Amsterdam/NL
Z. Tarján, Budapest/HU
I. Távora, Lisbon/PT
S.A. Taylor, London/UK
V. Valek, Brno-Bohunice/CZ
D. Vanbeckevoort, Leuven/BE
D. Weishaupt, Zurich/CH
A. Wuttge-Hannig, Munich/DE
C.J. Zech, Munich/DE
C.L. Zollikofer, Winterthur/CH

EPOST™ JURY

R.G.H. Beets-Tan, Maastricht/NL
D.J. Breen, Southampton/UK
F. Caseiro-Alves, Coimbra/PT
L. Crocetti, Pisa/IT
A. Gillams, London/UK
J.A. Guthrie, Leeds/UK
S. Halligan, London/UK
A. Laghi, Latina/IT
M. Laniado, Dresden/DE
E. Leen, Glasgow/UK
A.J. Madureira, Porto/PT
M. Maher, Wilton, Cork/IE
B. Marincek, Zurich/CH
L. Marti-Bonmati, Valencia/ES
D.F. Martin, Manchester/UK
G. Morana, Treviso/IT
O. Papakonstantinou, Athens/GR
N. Papanikolaou, Heraklion/GR
P. Pokieser, Vienna/AT
P. Prassopoulos, Alexandroupolis/GR
L.H. Ros-Mendoza, Zaragoza/ES
W. Schima, Vienna/AT
S. Skehan, Dublin/IE
M. Staunton, Toronto, ON/CA
Z. Tarján, Budapest/HU
S.A. Taylor, London/UK
J. Venancio, Lisbon/PT
C.J. Zech, Munich/D



ABDOMINAL MDCT

09:05 - 10:30

Anadolu Auditorium

Postgraduate Course 1 All you need to know

PG 1.01

From 4 to 256-slice MDCT: capabilities, post-processing and PACS issues

P. Rogalla; Berlin/DE

Learning objectives: To compare the quality of MDCT images obtained with different detector configurations and the clinical capabilities of each configuration. To describe post processing methods, address PACS issues (data management, image transfer and storage etc) and to introduce 3D applications.

Abstract: A major step in CT imaging was taken when the first 4-slice CT became available for clinical imaging. For the first time, nearly isotropic image geometry could be achieved allowing for multiplanar reformations without dramatic reduction of spatial resolution. Meanwhile, with further technological improvements, up to 320 slices can be simultaneously obtained, making perfusion imaging possible without table movement. Along with the nominal number of detector rows, the amount of data rose up to several Gigabytes per patient. This fact has strong implications for the network design, the necessary calculation power of workstations and capacities in long-term archives. In order to avoid bottlenecks for the workflow, all components have to be adjusted to the increasing demands in CT imaging. Newer compression techniques as well as the new enhanced DICOM image transfer standard will play a major role in radiology departments in the future.

PG 1.02

Management of radiation dosage in MDCT

J. Damiak; Heraklion/GR

Learning objectives: To describe the basic physical parameters of MDCT which impact on patient radiation dosage. To discuss radiation dosage of MDCT vis-à-vis other imaging modalities. To review established methods of dose reduction in MDCT, put radiation exposure from MDCT into a clinical perspective and to propose simple strategies for dose reduction.

Abstract: The introduction of multi-detector CT (MDCT) has turned out to be the main factor responsible for the rapid growth in the use of CT imaging. Offering fast acquisition and isotropic resolution, MDCT has expanded the range of applications for CT imaging. As a result, the number of CT examinations has increased over the past few years considerably. Apart from the obvious clinical benefits, the use of MDCT also bears the potential of causing radiation burden to patients. Radiation doses from CT scanners are already high and are trending higher. Therefore, the need for increased awareness regarding radiation dose issues is imperative. The purpose of this presentation is to outline the parameters that affect CT dose, explain the effect of different CT protocols on radiation dose and discuss the strategies that can be used to optimize MDCT examinations. Patient doses in CT are much higher than those associated with many other common types of diagnostic X-ray examinations. The most important factors that affect CT dose are the number of scans, the exposure parameters, the scanning length and the body size of the patient. If helical scanning is used, additional dose will result from z-overscanning. The additional dose depends on the reconstruction slice width, beam collimation and the pitch settings. When a radiosensitive organ such as the thyroid gland is marginally included in the examination field, proper selection of scanning parameters is needed to restrict z-overscanning. Moreover, the relative contribution of the extra exposure due to z-overscanning may be considerable especially when the planned image volume is limited, for example in paediatric studies. MDCT scanners have new technical features that affect patient dose. Furthermore, every type of MDCT scanner has its own dosimetric characteristics. Dose-effective use of modern scanners can be established only with onsite dose measurements and deep knowledge of MDCT technology. Proper selection of scanning parameters, use of technologic innovations and protection of radiosensitive organs would all contribute to the reduction of dose. Patients undergoing CT examinations can range from newborns to oversized adults. Efforts should be undertaken to optimize CT examinations using imaging protocols that take into account the body characteristics of the patient being examined. Automatic exposure control (AEC) is an effective means of dose reduction. However, operators should fully understand the operation characteristics of the AEC system prior to its application in the clinical environment.

PG 1.03

Dual energy CT: does it signify progress?

H. Alkadhi; Zurich/CH

Learning objectives: To describe the basic principles of dual energy MDCT and discuss present and future applications in abdominal imaging. To address the radiation exposure and economic issues associated with dual energy MDCT.

Abstract: The recent introduction of the dual-source computed tomography (CT) scanner has brought about new opportunities in the imaging field. The scanner type is characterized by two X-ray tubes and two corresponding detectors that are mounted onto the rotating gantry with an angular offset of 90°. The two X-ray tubes of the scanner can be operated either at identical tube potentials that results in a doubling of the temporal resolution of the scanner being beneficial for cardiac examinations, or at two different tube potentials that enable the simultaneous acquisition of CT data in the dual-energy mode. The latter approach allows for an improved characterization of tissue and for the generation of virtual non-enhanced images through the identification and subtraction of iodine from contrast-enhanced data sets. The theoretical concept of the dual energy CT technique is based on the spectral properties of different materials, the atomic z-numbers, and the different photon energies that are emitted by the two tubes. These values define the "dual energy index". Based on this index, a so-called three-material-decomposition method is employed for the differentiation of material like calcium, iodine, fat, and soft tissue, depending on the application used. For most abdominal applications, the three-material-decomposition deals with iodine, soft tissue, and fat. In each voxel, there is a specific mixture of these three materials. Based on the decomposition, four different types of CT images are reconstructed: the 80 and 140 kV source images, weighted average images (a simulated 120 kV image using 30% of the information from the 80 kV image and 70% of the information from the 140 kV image) and virtually non-enhanced images that are based on a direct subtraction of iodine from the image data. Potential applications of the dual energy CT technique include the improved characterization of urinary stones, particularly with respect to the presence or absence of uric acid, that could be already demonstrated in both ex-vivo and in-vivo studies. Another potential application of dual energy CT represents the identification of iodine which can be helpful for the differentiation of lesions when no foregoing non-enhanced CT scan was performed. The pre-contrast CT number of a lesion can be determined which may help in the characterization of the pathology. On the other hand, the dual energy technique may help to reduce the radiation dose to the patient. For example, a standard non-enhanced CT scan can be omitted and instead a virtual non-enhanced data set can be reconstructed from the contrast-enhanced dual energy CT scan. In conclusion, there appear to be several potential applications for dual energy CT imaging. From these, the characterization of urinary stones and the identification of iodine with the generation of virtual non-enhanced data currently seem to be the most promising ones.

PG 1.04

MDCT: perfusion imaging

V. Goh; Northwood/UK

Learning objectives: To describe the basic principles of perfusion imaging using MDCT. To discuss the physiological and pathophysiological background of perfusion imaging and review the common applications of perfusion imaging in abdominal imaging.

Abstract: There is accumulating data of a role for perfusion imaging in addition to morphological imaging in clinical practice. Blood flow, blood volume and vascular leakage can be estimated by kinetic modelling of Hounsfield unit enhancement change following intravenous contrast injection. In abdominal imaging, such in vivo functional evaluation of the vasculature permits assessment of organ function, supplements standard therapeutic assessment in tumours, and potentially aids differential diagnosis and provides prognostic information. This presentation will examine the pathophysiology and basic principles of perfusion imaging using MDCT. The different methods of kinetic modelling will be compared and what the vascular parameters reflect discussed. Validation of perfusion imaging including histopathological correlation and limitations will be discussed. Common applications of perfusion imaging in abdominal imaging will be reviewed along with potential applications. Following this presentation, the audience will be familiar with the principles of perfusion imaging using MDCT, the applications in abdominal imaging, and be able to implement such techniques in their practice.

PG 1.05

Positron emission tomography-MDCT: how to handle hybrid imaging

P.R. Ros; Barcelona/ES

Learning objectives: To describe the different imaging strategies in PET-MDCT of abdominal diseases and to particularly address acquisition parameters, contrast media usage, and radiation dosage. To explain post-processing methods. To discuss the management of reporting and address the challenges of follow-up studies performed using MDCT alone.

Abstract: Positron emission tomography (PET) combined with Multi-detector computed tomography (MDCT) or PET-MDCT imaging has become, in the last five years, the first commercial hybrid-imaging tool and an invaluable clinical diagnostic modality. It has grown steadily because combined PET-MDCT is a more accurate test than either of its individual components and better than side-by-side viewing of images from both modalities. PET-MDCT has considerable utility in assessing the abdomen and GI tract. Abdominal PET-MDCT scans are optimized when intravenous and oral contrast agents are administered. Intravenous contrast artifacts are generally modest and do not require deviation from standard MDCT practice. Positive oral contrast agents can generate focal artifacts, particularly in patients with GI stenoses and compromised GI motility. The use of a low Hounsfield value (LHV) or neutral oral contrast solves this problem and it is indicated specially in patients with known or suspected GI pathology. The major clinical applications for PET-MDCT in the abdomen are - colorectal carcinoma: PET-MDCT is rarely used for the diagnosis of colorectal cancer. It is however an efficient tool for preoperative staging, with a high sensitivity for detecting distant metastases, in particular to the liver. The greatest impact of PET-MDCT imaging in patients with colorectal cancer is the detection of extrahepatic metastases that would preclude a curative surgical procedure. Esophageal cancer: PET-MDCT is currently used as the imaging modality of choice for staging, restaging, and diagnosing of recurrence of esophageal cancer. Lymphoma: This is one of the main applications of PET-CT. GI and extraintestinal manifestations of lymphoma can be studied with this technique that has established itself as the primary modality in the staging and restaging. It is the standard to evaluate individual response to therapy. Gastrointestinal stromal tumor (GIST): GISTs are mesenchymal tumors that most frequently originate in the stomach and small intestine. PET-MDCT shows early effects in patients undergoing treatment with imetinib mesylate. PET-MDCT has the unique advantage to combine functional and anatomic imaging in an integrated scanner; it allows a thoroughly evaluation of patients. PET-MDCT is the primary imaging tool in many patients with abdominal malignancies.

11:00 - 12:30

Anadolu Auditorium

Postgraduate Course 2

Added value in hepatic, pancreatic and biliary imaging

PG 2.01

Incidental lesions of the non-cirrhotic liver

V. Vilgrain; Clichy/FR

Learning objectives: To understand the role of MDCT in the diagnostic work-up of such lesions. To be aware of the features of MDCT that give added value over spiral CT and other modalities (e.g. MR, CE-US etc.). To comment on the relative roles of these different modalities in this indication.

Abstract: Liver incidentalomas or incidentally found liver lesions are asymptomatic lesions that are clinically silent and discovered „incidentally“ in patients. The widespread use of modern imaging modalities has led to an increase in the frequency of detecting those lesions. Most of the incidentally found lesions are benign and among them cysts, hemangiomas, focal nodular hyperplasia, adenoma, and focal fatty sparing and infiltration represent the vast majority of the cases. The malignant tumors that can be detected incidentally are mainly HCC, cholangiocarcinoma, and endocrine metastases. In the absence of a cancer history, the probability of a malignant liver lesion is low. But even in the presence of a history of extrahepatic cancer, about half of the detected small liver lesions are benign. In this context, it is important to avoid unnecessary interventions for benign lesions, while at the same time ensuring accurate diagnosis of hepatic malignancies. This presentation will review the clinical and biological factors that

are predictive for malignant diseases and will discuss the role of imaging in characterizing those lesions. In particular, the role of real-time contrast-enhanced US imaging has changed the strategy in patients in whom incidentalomas have been discovered at conventional sonography. On the other hand, MR plays a crucial role in characterizing small lesions in oncologic patients. Finally, the role of liver biopsy will be discussed.

PG 2.02

Surveillance of the cirrhotic liver

C. Bartolozzi; Pisa/IT

Learning objectives: To understand the optimal imaging protocol for this indication. To be aware of the features of MDCT that give added value over spiral CT and other modalities (e.g. MR, CE-US etc.). To comment on the relative roles of these different modalities in this indication.

Abstract: MDCT offers a marked reduction in the time required for thin-section imaging of the entire liver relative to standard single-detector spiral CT. In addition, the increased temporal resolution permits hepatic imaging during two distinct arterial phases: the early arterial phase and the late arterial phase. The early arterial phase is a true CT arteriography and can be used to assess vascular anatomy. The standard MDCT examination protocol for detection and characterization of hepatocellular carcinoma (HCC) should include unenhanced and contrast-enhanced images obtained in the arterial, portal venous and delayed phases, scanning, respectively, about 25–30 seconds, 70–80 seconds and 180–210 seconds after the start of contrast injection. At MDCT, typical HCC lesions show clear-cut enhancement in the arterial phase and rapid wash-out in the portal venous and delayed phases. In contrast, large regenerative nodules and dysplastic nodules usually fail to exhibit this feature and appear isoattenuating or hypoattenuating to surrounding liver parenchyma. Identification of morphological features of HCC, such as tumor capsule and internal mosaic architecture, may support the diagnosis of HCC in questionable cases. Using histopathology of the explanted liver as standard of reference, the reported sensitivity of spiral CT in detection of HCC lesions ranges 52–79%. Of interest, 89–100% of HCC lesions greater than 2 cm are detected, while only 10–47% of lesions smaller than 1 cm and 44–67% of lesions of 1–2 cm are identified. In a recent series in which MDCT was used, the sensitivity in diagnosing HCC of 1–2 cm was of 67%, with a positive predictive value of 61%. US is the imaging technique most commonly used worldwide for early detection of HCC in surveillance programs and CE-US may be a tool to show arterial neoangiogenesis of HCC. Intrahepatic staging of the disease, however, relies on MDCT or dynamic MR imaging. MR imaging in combination with liver-specific contrast agents may be useful to clarify questionable cases owing to the ability to show the changes in hepatobiliary function or Kupffer cell content associated with malignancy. MDCT is an appropriate tool to evaluate cirrhotic liver and in most instances it allows the correct characterization of liver nodules.

PG 2.03

Evaluation of biliary malignancies

M.J. Kim; Seoul/KR

Learning objectives: To understand the optimal imaging protocol for this indication, including a summary of the potential role of biliary contrast media. To be aware of the features of MDCT that give added value over spiral CT and other non-invasive modalities. To comment on the relative roles of these different modalities in the staging and management of patients with biliary malignancies.

Abstract: The purpose of this course is to define the role of MDCT examinations to evaluate extrahepatic biliary malignancies, including hilar cholangiocarcinomas, by reviewing scanning and postprocessing techniques compared to other imaging modalities. By reviewing MDCT examinations and other imaging modalities performed on patients with extrahepatic biliary malignancies and the current literature, the benefits and drawbacks of each phase scan of multiphase examinations were enumerated. The findings on MDCT examinations and other imaging modalities, such as sonography, direct cholangiography, PET scan, and MRI, were compared for preoperative assessment of extrahepatic cholangiocarcinomas. MDCT examinations can be performed with biphasic or triphasic scans in addition to precontrast scans. Precontrast scans are useful for differentiation of intraductal papillary tumors and stones. Early arterial scans may not be always necessary but provide the best arteriographic images for assessment of anatomical variation. Arterial encasement by tumor can be assessed on early arterial phase images but it may be easier to appreciate on the late arterial phase that enables equally delineate tumor and venous anatomy as

well as arterial structures. CT cholangiography (CTC) images using minimum intensity projection techniques can be best obtained at the hepatic venous phase because of highest liver-to-duct contrast. Venous anatomy is also most clearly depicted in this phase. Various postprocessing techniques, such as multiplanar or curved reformations, maximum and minimum intensity projections, and volume rendering, are useful for demonstration of the primary tumor and its relationship with the surrounding structures. CTC using oral or intravenous administration of a biliary excreting agent may play a role in the evaluation of nonobstructed bile duct anatomy or diagnosis of choledocholithiasis, but its role in the evaluation of biliary malignancy is doubtful. CTC via biliary drainage catheter may be useful in cases where biliary decompression is already done. MDCT cholangiography is useful to demonstrate extraductal pathology and missing ducts that are difficult to assess on direct cholangiography. PET-CT scan is useful to depict unsuspected metastases, but the sensitivity for the diagnosis of the primary lesion is not better than MDCT. MDCT may be better than MRI with MRCP for depiction of vascular anatomy for its higher spatial resolution; however, the assessment of vascular invasion also depends on the delineation of the tissue plane between the vascular anatomy and the tumor, which may be better appreciated on the MRI because of its higher tissue contrast. Both MDCT and MRI may have limitations for defining longitudinal spread, especially when the tumor spreads along the mucosal plane instead of the periductal plane. Multiphase MDCT combined with useful postprocessing techniques is helpful in improving diagnostic accuracy for the detection and preoperative staging of biliary malignancies but a multimodality approach is necessary for the interpretation of subtle abnormalities that are occasionally difficult to define even using a combination of all available imaging studies.

PG 2.04

Pancreatic carcinoma: detection and resectability

J. Heiken; St. Louis, MO/US

Learning objectives: To summarise MDCT scanning protocols used in detection and pre-operative assessment of pancreatic adenocarcinoma. To discuss the value of post-processing and the role of MDCT vis-à-vis state-of-the-art MRI. To review the pitfalls of MDCT evaluation.

Abstract: Purpose: To: 1) review the MDCT scanning protocols for detection and staging of pancreatic adenocarcinoma, 2) assess the value of image postprocessing in staging pancreatic cancer, 3) evaluate the role of MDCT versus MRI in detecting and staging pancreatic carcinoma, and 4) review the pitfalls of MDCT evaluation. Materials and Methods: Review published studies evaluating the optimal MDCT technique for imaging pancreatic cancer, and review published studies assessing the diagnostic performance of MDCT and MRI for the detection and staging of pancreatic adenocarcinoma. Results: MDCT is the preferred imaging method for detecting and staging pancreatic adenocarcinoma at most institutions. MDCT studies for assessing pancreatic cancer should be performed with narrow detector collimation, rapid intravenous contrast medium administration (e.g., 4 mL/sec), and dual phase imaging including both the pancreatic parenchymal and portal venous phases. Although most radiologists use a fixed scan delay of 40–50 seconds, accurate timing of the pancreatic parenchymal phase is best achieved using bolus tracking, with a scan delay of aortic transit time plus 20–30 seconds, depending upon the type of MDCT scanner being used. Accuracy of MDCT for determining nonresectability is approximately 95%, whereas accuracy for determining resectability is approximately 70–80%. Overall accuracy of MDCT for staging pancreatic carcinoma is approximately 80–90%. Review of CT angiographic images and multiplanar reconstructions improves assessment of vascular involvement compared with evaluation of transaxial images alone. Comparative studies have shown contrast enhanced MRI to be equivalent or superior to helical CT for detecting pancreatic cancer. However, recent comparisons between MDCT and state-of-the-art MRI are lacking. Limitations of MDCT include: 1) approximately 10% of pancreatic adenocarcinomas are isoattenuating to normal pancreatic parenchyma and may be very difficult to identify, 2) a number of benign abnormalities can mimic pancreatic cancer including focal pancreatitis and focal lipomatosis, 3) pancreatic cancer can be difficult to identify in patients with chronic pancreatitis, and 4) MDCT is limited in its ability to demonstrate small liver and peritoneal metastases. Conclusion: Although MDCT has some limitations and potential pitfalls, it is the preferred initial imaging method for detecting and staging pancreatic adenocarcinoma at most institutions. Proper contrast medium administration and scan timing are critical for optimal results. CT angiographic images and multiplanar reconstructions can improve staging accuracy. MRI is

comparable to CT for detecting and staging pancreatic cancer and can be used when contrast enhanced MDCT is contraindicated. MRI is also useful for problem solving when MDCT evaluation is indeterminate.

14:15 - 15:45

Anadolu Auditorium

Postgraduate Course 3

Gastrointestinal tract imaging: evolution or revolution?

PG 3.01

Oesophagus, stomach and duodenum

A. Ba-Ssalamah; Vienna/AT

Learning objectives: To describe optimized MDCT protocols for the diagnosis of oesophageal, gastric and duodenal pathology. To describe and illustrate the T and N staging protocols for upper GI tract tumours and discuss the role and limitations of MDCT for this purpose. To address the added value of MDCT virtual gastroscopy.

Abstract: The introduction of MDCT, along with the continued advancements in 3D technology, has renewed clinical interest in utilizing CT for the evaluation of disorders of the upper GI tract. The collapse of hollow viscera during CT may hide large lesions and may even mimic pseudo lesions. Thus, an optimal distension of the oesophagus, stomach, and duodenum is a necessary prerequisite for achieving good diagnostic imaging. When water is used as oral contrast, subtle pathology is easier to visualize. Gas or CO₂, after administration of effervescent granules, can be used for hollow organ distension alone or in combination with water. Using these negative contrast agents is preferable to the use of positive contrast media, especially if CT angiography images are needed. Subtle pathology is easier to visualize, especially when a good IV contrast bolus is administered. Three-dimensional reconstructions of the CT data sets with MPR, CPR, etc., are mandatory to exploit the full potential of MDCT. Three-dimensional virtual gastroscopy provides an endoluminal image, similar to conventional fiberoptic gastroscopy, but 3D virtual gastroscopy can detect even subtle mucosal abnormality that could be indicative of early gastric cancer. The most common clinical indication for MDCT imaging of the upper GI tract is the staging of oesophageal, gastric, and duodenal tumors. Endoscopic US is a complementary method, but suffers from a limited field-of-view and imaging of stenotic tumors is problematic.

PG 3.02

Small bowel

D. Maglinte; Indianapolis, IN/US

Learning objectives: To present protocols for MDCT evaluation of the small bowel. To review the indications for MDCT enterography and MDCT enteroclysis. To describe enhancing patterns of the small bowel wall in characterizing inflammation and neoplasia. To discuss the advantages and limitations of each of the techniques and address their current and future clinical roles.

Abstract: Small bowel (SB) imaging has changed dramatically in the last two decades. There was a time when barium examinations were the dominant method of investigation of small bowel diseases. The introduction of multidetector CT (MDCT) technology has changed the workup algorithm. Abdominal CT, CT enterography and CT enteroclysis are now more commonly performed than barium examinations in many leading centers all over the world for small bowel investigations. Unfortunately, this has contributed to the increasing number of CT examinations used today. Concerns regarding excessive exposure to ionizing radiation because of increased utilization of CT have gained momentum through recently published studies and media coverage. The repetitive use of CT studies including abdominal CT may lead to a significant increase in the number of future cancer cases. Progress in endoscopy has paralleled the advances of CT technology. The introduction of wireless capsule endoscopy and double balloon endoscopy has changed small bowel imaging in the 21st century as well. The SB remains to be the most difficult part of the alimentary tube to examine. Because of the low prevalence of SB disease and its nonspecific clinical presentation, effective clinical imaging of the SB should provide reliable evidence of normality or provide documentation of small structural abnormalities. In the past, it was not infrequent to see multiple SB follow-through examinations before barium

enteroclysis was performed. Currently, it is not infrequent to see patients with multiple abdominal CTs before a SB abnormality is diagnosed. The use of methods of SB examination with a poor sensitivity for showing small structural abnormalities and a low negative predictive value in ruling out SB disease will undoubtedly increase patients' exposure to ionizing radiation and increase the cost of workup of SB diseases. This session will present an overview of why we should utilize enteral volume challenged SB examinations (both barium and CT modifications) when SB disease is suspected and how it should be used in conjunction with capsule endoscopy and double balloon endoscopy. Radiologists must understand the role of imaging in the diagnosis of SB diseases and should educate clinicians in order to decrease exposure of patients to ionizing radiation and decrease cost in the evaluation of SB diseases.

PG 3.03
CT colonography
 A. Laghi; Latina/IT

Learning objectives: To describe the procedural and reconstruction techniques of CT colonography (CTC) and outline the strengths and weaknesses. To discuss strategies to optimize the interpretation of studies and illustrate the most commonly seen pathologies and pitfalls.

Abstract: Computed tomography colonography (CTC), also known as virtual colonoscopy, is an imaging modality for the evaluation of the colonic mucosa in which thin-section spiral CT provides high resolution two-dimensional (2D) axial images and CT data sets are edited off-line in order to produce multiplanar reconstructions as well as three-dimensional (3D) endoscopic-like views. Bowel preparation is critical and different regimens are used, with the final goal of developing minimally-invasive preparation, more comfortable for patients. The use of faecal tagging (i.e. the oral administration of a positive contrast agent, either barium or iodine) may improve specificity for small polypoid lesions. Patient preparation for scanning consists of air or CO₂-insufflation, administration of an antiperistaltic drug (preferably, Buscopan), and i.v. injection of iodinated contrast medium, if required. Data acquisition protocols for CTC are in continuous evolution, paralleling the progress of CT scanners; the trend is towards the reduction of patient's radiation exposure by using automatic tube current reduction devices. Image analysis, obtained on dedicated off-line workstations, is performed with either primary 2D or primary 3D approach. Three different large meta-analyses offer a good perspective of the performance of CTC, showing excellent sensitivity for colorectal cancer (over 95%) and clinically significant polyps (>10 mm: over 85%) and making this technique as the second best imaging test for the detection of colorectal lesions. Based on these results, an officially accepted clinical indication for CTC is represented by the cases of incomplete or unsuccessful colonoscopy, which may be the result of redundant colon, patient intolerance to the procedure, spasm not resolving even with the use of spasmolytics and obstructing colo-rectal cancer. CTC is also suitable for studies in elderly and frail patients, where reduced bowel preparation can be coupled with fast scanning. And it is an interesting method for a noninvasive evaluation of diverticular disease. Several new evidences of the performance in asymptomatic subjects also propose CTC as a method for colorectal cancer screening. There are multiple advantages: high accuracy, similar to conventional colonoscopy; full evaluation of the colon in virtually all the patients; invasiveness; patient comfort (reduced bowel prep; no sedation); safety (virtually no complications). And recent analysis on simulated models also demonstrates cost-effectiveness of CTC in comparison with other screening methods (i.e. sigmoidoscopy; colonoscopy). Therefore, the introduction of CTC in the list of screening options proposed by the major scientific societies is expected in the next future.

PG 3.04
Computer aided detection: a new companion?
 S. Halligan; London/UK

Learning objectives: To describe the basic principles of CAD and discuss its role in current radiology practice. To outline the different types of CAD software currently on the market. To review the literature on the the clinical utility of CAD and try to predict its future prospects.

Abstract: Computer-assisted-detection (CAD) for CTC is increasingly commercially available, especially in Europe where regulatory stipulations have been satisfied. The current role of CAD is necessarily limited because systems are only just beginning to penetrate the market. A variety of different software packages are available, but all essentially do the same thing – they aim to detect

colonic polyps and then alert the reader to their presence via a visual prompt, just as it happens in mammographic practice where CAD is well established. While this sounds simple and straightforward, in reality the scenario is complex: CAD seems to have a different effect on the ultimate diagnosis ascribed to the patient depending on when it is initiated by the reader. For example, if CAD is activated from the outset (the "first-reader" paradigm), the human observer may pay undue attention to the prompts and neglect the apparently normal colon. Because no CAD system is 100% sensitive, this may result in missed lesions. At the same time, no CAD is 100% specific – all systems make false-positive diagnoses and the effect that these have on ultimate diagnosis is also uncertain. Perhaps the major difference between commercially available systems (apart from price!) is the individual balance adopted between sensitivity and specificity. These two parameters are inextricably linked – for any given system sensitivity can only increase at the expense of specificity, and vice-versa. The different reading paradigms (first-, second-, and concurrent-readers) will be discussed. A major barrier to our understanding of the real effects of CAD in clinical practice is the fact that most research studies have determined the performance characteristics of CAD in isolation, assuming that the observer will react accordingly to prompts. In reality, there is no guarantee that an observer will classify prompts appropriately. What is needed are studies whose outcome measures revolve around the effect that CAD exerts on patient classification by the reader. Thankfully, such studies are becoming more common and it is already clear that human observers often misclassify true-positive CAD prompts as false-positive and vice-versa, diminishing the expected performance metrics. More studies of increasing complexity are needed in order to provide data for clarification but sensible and appropriate statistical analysis of such studies is exceedingly complex and at the cutting-edge of statistical methodology. Inevitably, these problems will be overcome and it is highly likely that ultimately CAD will become integrated into everyday clinical practice.

16:15 - 17:45

Anadolu Auditorium

Postgraduate Course 4
Abdominal vascular imaging: a success story

PG 4.01
Vascular evaluation with MDCT: technical considerations
 N. Elmas; Izmir/TR

Learning objectives: To review the techniques of MDCTA including protocols for contrast injection, timing of data acquisition and image reconstruction strategies. To review detector technology-related capabilities of MDCTA.

Abstract: Advances in CT technology have improved CT angiographic studies. These improvements were obtained by both high spatial resolution and the development of multi-detector scanners. Image quality depends on optimal vessel opacification, total contrast volume and injection flow rate, image quality, range of images, data acquisition and post processing procedures. Visualization of abdominal vessels by MDCT angiography may be summarized in three parts: (I) Indications of abdominal angio studies by MDCT; (II) MDCT Angio techniques and factors affecting their optimal use and (III) Parameters of detector technology-related capabilities of MDCT. (I) Indications of abdominal MDCT Angio studies: 1) Abdominal Aortic aneurysm, 2) Mesenteric ischemia, 3) Portal hypertension and liver cirrhosis, 4) Liver transplantation (pre and post), 5) Neoplastic diseases (pancreas, liver, etc.), 6) Upper gastrointestinal bleeding and 7) Hypertention. (II) MDCT Angio techniques and factors affecting their optimal use: Optimal vessel opacification remains one of the most crucial aspects of CT angiography. Correct synchronization of the scan with contrast material injection flow and timing is vital. In order to visualize the abdominal vasculature map, it is necessary to scan during all phases of the arterial, portal venous and hepatic venous phases. Correct timing of the scan delays throughout all the phases, starting from the scanning should be adjusted correctly to the contrast travel time. A total of 100–150 ml (350–400 mg/ml concentration) contrast agent has to be delivered with 3–4 ml/sec flow rate (best achieved by using a power injector). An arterial phase image should be obtained prior to significant portal venous enhancement. Optimal period for hepatic CTA imaging is approximately 20–40 sec and portography 50–70 sec after the administration of contrast material. In addition, other key factors in image acquisition protocol include: scan range, table speed and reconstructed slice thickness. During the abdominal CTA, the field of view (FOV) has to include the diaphragm and pubic symphysis. Parameters of detector technology-

related capabilities of MDCT. Some parameters may have to be adjusted according to the number of rows. Detector collimation should be 2.5 mm for 4 channel and 1.5 mm for 16 channel CT machines. Slice thickness must be 3–5 mm for 4 channel and 2–5 mm for 16 channel, respectively. 3D rendering techniques such as Shaded Surface Display (SSD), Maximum Intensity Projection (MIP) and Volume Rendering (VR) are used in determining source images.

PG 4.02 Haemorrhage

A.J. Aschoff; Ulm/DE

Learning objectives: To understand how to perform and interpret MDCT examinations in patients with acute and chronic GI tract bleeding and in the assessment of bleeding from solid organ trauma.

Abstract: Purpose: Acute gastrointestinal (GI) bleeding, as well as bleeding from solid organ trauma, is an emergency situation with high mortality rates. Fast detection and localization of the bleeding site is required for effective haemostatic therapy. Recently, contrast-enhanced MDCT has established itself as the primary imaging modality for this indication. Materials and Methods: An analysis of current studies on the detection and localization of intraabdominal haemorrhage will be offered and discussed together with our own clinical experience. Results: The availability of fast MDCT with high temporal and spatial resolution seems to eliminate the need for intraarterial contrast application, and promising results have been recently published on this emerging technique. In an experimental study, GI haemorrhage could be detected on MDCT at bleeding rates of 0.5 ml/min or even less, and in another experimental study MDCT proved to be more sensitive than first-order aortic branch selective DSA. In an own study on 36 consecutive patients with clinical signs of acute bleeding, the correct site of bleeding was identifiable on MDCT in 24/26 patients with GI bleeding and in the 9/10 patients with intraperitoneal haemorrhage. Active GI bleeding on CT depicts as focal areas of high attenuation within the bowel lumen or peritoneal cavity. Potential false-positive MDCT findings might occur from calcifications, suture material after previous bowel surgery, high-density structures within the bowel lumen such as foreign bodies, oral pharmaceutical drugs, haemostatic clips or retained contrast material in diverticula. A potential misinterpretation of these hyperdensities mimicking acute bleeding may be avoided performing additional un-enhanced scans, but we do not routinely perform these to minimize radiation exposure. Conclusion: In conclusion, our own findings and results from others suggest that an accurate localization of acute gastrointestinal and intraperitoneal bleeding is reliably achievable with contrast enhanced MDCT. Advantages of MDCT for the diagnostic work-up of patients with suspected acute abdominal haemorrhage include widespread availability, speed, reproducibility and minimal invasiveness. Moreover, CT scanning of the abdomen can be performed immediately during the hemorrhagic episode and bleeding can be depicted within the small bowel, an anatomic region not readily accessible to endoscopy. In emergency situations, invasive selective interventional angiography or surgery can be performed immediately after MDCT has identified the bleeding site. This diagnostic algorithm may lead to a significant reduction in time and may substantially decrease the rate of negative angiographies in the future.

PG 4.03 Thrombosis

O. Matsui; Kanazawa/JP

Learning objectives: To understand the pathology of intravascular thrombotic disease in the abdomen. To review the indications for MDCT in these conditions. To present imaging features of different intravascular thrombotic diseases and to discuss pros and cons of MDCTA vis-à-vis alternative modalities.

Abstract: Splanchnic thrombosis comprises a relatively infrequent but important cause of organ ischemia including mesenteric ischemia and gastrointestinal bleeding due to varices. The signs and symptoms of these visceral thrombosis are variable according to the site and etiology, and often nonspecific but occasionally serious and lethal. Therefore, the early detection of visceral thrombosis and diagnosis of etiology and associated organ changes by imaging is important clinically. The application of rapid, non- or minimally invasive imaging strategies has facilitated earlier recognition and detection of a disease process. Earlier noninvasive imaging may improve the prognosis of this disease by permitting patients to be managed more effectively. A variety of methods, including conventional arteriography, Doppler ultrasound, CT/CTA, and MRA, are currently used for evaluation of thrombosis. Among them, multi-detector row computed tomography (CT) offers important advantages in the evaluation of the

mesenteric vasculature including thrombosis. It allows faster scanning, which practically eliminates motion and breathing artifacts, as well as thinner collimation. This improves the quality of the three-dimensional (3D) data sets, which in turn leads to improved 3D vascular maps. In addition, it visualizes surrounding organs and various pathologic processes clearly. MDCT during selective arteriography offers most accurate pictures, but is invasive. Etiology of splanchnic thrombosis can be classified as follows; abdominal surgery including transplantation of the liver, interventional therapy such as radiofrequency ablation for liver cancer, vasculitis such as Bachel's disease and polyarteritis nodosa, phlebitis of portal vein, inflammation such as pancreatitis and inflammatory bowel diseases, blunt abdominal trauma, post, hypercoagulable state, portal hypertension, invasion of neoplasm and oral contraceptive use, so on. In addition, embolism and atherosclerotic stricture are one of the major causes in arterial thrombosis. CT findings of arterial or venous thrombosis include persistent, well-defined intraluminal filling defects with central low attenuation, which may be surrounded by well-defined, rim-enhancing vessel walls. Accompanying collateral circulation, engorgement of mesenteric veins and arteries may be present. To evaluate precisely the etiology and anatomical site of thrombus with possible collateral pathway is extremely important for expecting the progress of the disease and for deciding the appropriate treatment. In addition, imaging diagnosis of associated infarction or ischemic changes of the organs is also extremely important. The imaging features and their importance in patient care in major splanchnic thrombosis will be discussed.

PG 4.04 MSCT in liver transplantation

C.D. Becker; Geneva/CH

Learning objectives: To outline the role of MDCT in the pre-operative assessment for orthotopic and living-related donor liver transplantation. To discuss the pros and cons of MDCT compared to MRI and introduce computer software commonly used in these circumstances.

Abstract: Contrast-enhanced multislice computed tomography (MSCT) with multiplanar and 3D reconstructions plays a key role in the diagnostic workup before and after orthotopic liver transplantation (OLT). In the OLT recipient, contrast-enhanced MSCT is suitable to evaluate the arterial, portal, and hepatic venous anatomy and to detect anatomic variants, and also to detect hypervascular parenchymal nodules which may influence the therapeutic decisions. Workup of the living donor includes, besides assessment of vascular variants, volumetric assessment and screening for bile duct variants. Iodinated hepatobiliary contrast agents have been used for MSCT-cholangiography in some centres, but are now unavailable in many countries. Morphine-enhanced MSCT with minimum-intensity reconstructions may enable adequate visualisation of the bile ducts in many instances. Otherwise, magnetic resonance cholangiography (MRCP) may be used to visualise the nondilated bile ducts in living donors. MSCT is very well suited to detect complications after OLT: these include acute arterial and venous thrombosis or iatrogenic vessel injury, and delayed anastomotic vascular stenosis. Biliary complications include leakage (early) and stenosis or obstruction (late). Although these may be detected with MSCT, they are best delineated with MRCP or direct percutaneous or retrograde cholangiography.



12:45 - 13:45

Marmara Hall

Lunch Symposium 1**What am I going to do with CAD? A practical clinical approach and other considerations**

Sponsored by: im3D

SY 1.01**What is computer aided diagnosis and how it works in CTC**

D. Regge; Candiolo/IT

SY 1.02**CTC: benefits and pitfalls! life without computer aided diagnosis**

P.R. Ros; Barcelona/ES

SY 1.03**Using computer aided diagnosis: a little hand from a reliable friend**

M. Morrin; Dublin/IE

Computer Aided Diagnosis (CAD) is for the first time being proposed in GI radiology, applied the colon. The interest in this new diagnostic tool is overwhelming as its use may impact significantly on the diagnosis of colorectal cancer, a very common and therefore socially important disease. The aim of the symposium is to present the concept of a fully integrated colon platform conceived for diagnosis of colorectal cancer and to show how it may make a difference in the work-flow of a busy radiology unit. Information will be given on how CAD schemes are designed and integrated on workstations and on how they can positively influence everyday practice.

12:45 - 13:45

Haliç Hall

Lunch Symposium 2**Higher resolution images in oncology**

Sponsored by: GE HEALTHCARE

SY 2.01**Technology improvements in CT and MRI and their impact on abdominal radiology practice**

V. Laurent; Vandoeuvre les Nancy/FR

Latest technology breakthroughs in CT, MR and image post processing have improved patient comfort as well as lesion detection and characterization in abdominal radiology. Regarding the stomach, small bowel or colon, a higher resolution in CT provides a non-invasive alternative to conventional procedures. CT permits visualization of the wall, lumen and also extra-enteric complications with ingested neutral contrast material. For solid abdominal organs such as pancreas or liver the high resolution delivered by CT technology can now improve the sensitivity of lesion detection and leads to a better diagnosis quality. New 3D approaches in dynamic MR techniques have also brought the spatial resolution at an unprecedented level to enhance lesion characterization. These techniques can be complemented by diffusion sequences which improve dramatically lesion detection. In addition to anatomical investigations, perfusion techniques in CT and MR have revolutionized the assessment of treatment efficiency in tumors. Recent studies have shown the potential of new anti-angiogenic treatments based on quantitative perfusion measurements.

SY 2.02**Higher resolution with contrast-enhanced US and volume imaging for pancreatic tumours**

M. D'Onofrio; Verona/IT

Ultrasound (US) examination is a simple imaging method considered in the work-up of pancreatic lesions in numerous reference institutions for abdominal pathologies. Very often, US examination is the first imaging method used. The main advantage of US is the real time examination and the high contrast and spatial resolution of the state of the art technology. Moreover, US examinations enable the possibility of accurate flow analysis of the peri-pancreatic vessels at Doppler studies. Contrast-enhanced ultrasound (CEUS) has been revolutionized by the development of micro bubble contrast agents. The study of the pancreas is a relatively new application of CEUS. CEUS is different from dynamic CT and MRI in terms of technology and contrast media. In particular, CEUS is the only imaging technique which allows a continuous observation of the contrast-enhanced phases, making the identification of fast flow tumoral circulation easier. The high temporal resolution of CEUS is one of the most important characteristics of this new imaging modality. The enhancement of a pancreatic lesion can be followed up during the whole study. Contrast-specific harmonic softwares allow maximum contrast resolution during CEUS studies. Moreover, nowadays, the spatial resolution of US imaging is very high also once detailed contrast-enhanced images are obtainable. These typical features of this imaging method make CEUS very accurate in perfusional studies. Microbubbles are "blood pool" contrast agents so that CEUS images of pancreatic tumoral vessels (macrocirculation and microcirculation) are reported to have a very good correlation with the pathologic mean vascular density. Volume ultrasound imaging (VUI) is a relatively new technique based on the acquisition of volume dataset of anatomical structures. VUI has been changed by the introduction of automated 3D sweep acquisitions. Automated VUI allows overcoming the low reproducibility of the previous volume freehand sweep acquisition. Automated VUI allows introducing in the field of US the extremely important concept of reproducibility thanks to the possibility of a standardised and objective acquisition during the study.

12:45 - 13:45

Haliç Hall

Lunch Symposium 3 CAD – Help or Hindrance?

Sponsored by: MEDICSIGHT

SY 3.01

Colon computer-assisted-detection: does it work and how should we use it?

S. Halligan; London/UK

Computer-assisted-detection (CAD) for CTC is increasingly commercially available, especially in Europe where regulatory stipulations have been satisfied. CAD aims to detect colonic polyps and then alert the reader to their presence via a visual prompt, just as it happens in mammographic practice where CAD is well established. While this sounds simple and straightforward, in reality the scenario is complex: Depending on when it is initiated, CAD exerts different effects on patients' ultimate diagnosis. For example, if activated from the outset (the "first-reader" paradigm), the human observer may pay undue attention to CAD prompts and neglect an apparently normal colon. Because no CAD system is 100% sensitive, this may result in missed lesions. At the same time, no CAD is 100% specific – all systems make false-positive diagnoses and the effect of these on ultimate diagnosis is also uncertain. These different reading paradigms (first-, second-, and concurrent-readers) will be discussed. The fact that most research studies have determined the performance characteristics of CAD in isolation, assuming that the observer will react accordingly to prompts, is also a major barrier to understanding the effects of CAD in clinical practice, not least because observers frequently misclassify prompts in real-world practice. We urgently need studies whose outcome measures revolve around the effects exerted by CAD on patient classification by readers, but their analysis is exceedingly complex.

SY 3.02

Implementation of computer-aided detection into clinical practice

P.J. Pickhardt; Madison, WI/US

Computer-aided detection (CAD) will likely play an important role in CT colonography (CTC) interpretation in clinical practice. However, there are a number of challenges and unanswered questions with regard to implementing CAD into a large-volume CTC screening practice. The main potential benefit of incorporating CAD is to increase the sensitivity for lesion detection among less inexperienced or less skilled readers. However, depending upon how CAD is actually employed in the screening setting, this increase in sensitivity may be offset by decreased specificity and increased interpretation time. Instead of simply trying to maximize lesion detection rates and limit the number of false positive "hits", CAD systems should go one step further by assigning priority scores or confidence levels for suspected abnormalities rather than an unsorted list of polyp candidates. Additional challenges for CAD in clinical practice that will be discussed include the ability to handle cases with oral contrast tagging, deriving automated polyp measurements (including volumetry), and issues related to cost and reimbursement.

SY 3.03

Colon CAD in reduced laxative CTC: does it work?

P. Lefere; Roeselare/BE

The possibility to reduce cathartic cleansing in virtual CT Colonoscopy (CTC) is one of the major opportunities as well as challenges in CTC. Reduced laxative CTC applies fecal tagging to opacify residual materials (ftCTC). The presence of opacified materials complicates matters for radiologists performing the examination and for scientists struggling with the problems of CAD in ftCTC. Besides the difficulties in characterisation, radiologists are confronted with increased difficulties in detection. The presence of tagged fecal material may reduce the conspicuity of both sessile and pedunculated polyps. Flat lesions and constricting cancers may be covered by tagged material, possibly improving but sometimes reducing conspicuity. ftCTC introduces challenges to CAD. Polyps submerged in tagged materials can be CAD false-negative (FN), and partially tagged semi-solid stool can be CAD false-positive (FP). Polyps affected by

pseudo-enhancement, due to the presence of adjacent tagged material, can be identified incorrectly as tagged materials and thus missed by CAD. The following questions will be addressed: For the CAD software: 1/ What is the influence of ftCTC on the number of CAD FPs and FNs? 2/ Can we improve the accuracy of CAD by changing the sphericity or applying the adaptive density correction and density mapping? For radiologists: 1/ How does CAD in ftCTC influence the reading time? 2/ Does ftCTC affect the optimal reader paradigm of CAD?

12:45 - 13:45

Marmara Hall

Lunch Symposium 4

MR abdominal imaging in patients at risk

Sponsored by: GUERBET

SY 4.01

Double contrast MRI in the evaluation of the small and large bowels

F. Maccioni; Rome/IT

The term "double contrast MRI" does not only refer to the contemporary use of two different contrast agents (intravenous paramagnetic and oral superparamagnetic) for bowel evaluation, this term is also used to outline the white-and-black (or "double contrast") effect that can be obtained, on both T1 and T2-weighted images, by using this specific contrast association. Superparamagnetic (SPIO) oral contrast agents produce - in other terms - a very dark lumen effect both on T1 and T2-weighted images. This effect, if properly associated with fat-suppressed sequences and Gadolinium i.v. injection, outlines the bowel wall oedema (on T2-weighted fat-suppressed images) and wall hypervascularity (on post-Gadolinium T1-weighted images) in inflammatory bowel diseases (IBD), more than any other contrast agent association. In particular, SPIO oral contrast agents, if associated with fat-suppressed T2-weighted sequences, allow visualizing the intestinal wall oedema and perivisceral fluid in IBD, not otherwise detectable. Bowel wall oedema and wall hypervascularity are both sensitive parameters of disease activity. Moreover, the negative contrast produced by the superparamagnetic oral agent determines a very homogeneous dark lumen effect throughout the small and large intestines, since the intestinal air and the intestinal agent add their signal on both T1 and T2-weighted sequences, differently from biphasic contrast agents. This allows an accurate evaluation the main intestinal abnormalities of IBDs, including the diagnosis of lesion's site and length, of strictures, adhesions, abscesses and fistulas, particularly in Crohn's disease. The main MRI patterns of mural and transmural wall inflammation in Crohn's disease and ulcerative colitis, as well intestinal and extraintestinal complications, will be shown. The clinical impact of this MRI technique in the evaluation of IBD will be finally discussed.

SY 4.02

Dynamic MRI of the liver

R. Hammerstingl; Frankfurt/DE

Over the past few years, magnetic resonance imaging (MRI) of the liver has progressed significantly. Technical advances in hardware and software have allowed the acquisition of images with excellent anatomic detail, largely free of artifacts secondary to respiratory motion. Contrast-enhanced MRI has become an essential part of a liver examination in a number of circumstances. Extracellular fluid space contrast agents are safe compounds in handling and provide information on vascularization and perfusion of focal liver tumors. A dynamic contrast-enhanced study of the liver is performed with a timing scheme that enables selective imaging during the arterial phase, the portal venous-phase, and the delayed phase of enhancement, the equilibrium phase. Fast spoiled gradient echo technique allows thin-section imaging of the entire liver during a single breath-hold. New volumetric sequences have enabled 3D serial dynamic imaging of the liver with a very high spatial and temporal resolution. The key issue of contrast agents in hepatic imaging is to discriminate between tissues that cannot be adequately differentiated on unenhanced MRI. Excellent contrast is needed for two purposes: delineation of at least one malignant lesion or exclusion of malignancy in the liver as well as precise characterization of benign liver tumors. For the detection of focal liver lesions, MRI using breath-hold sequences has been shown to be equivalent or even better than dual-phase CT. Particularly, hypervascular liver tumors show high contrast uptake in the early

dynamic imaging, the arterial phase, whereas the surrounding cirrhotic liver tissue remains free of contrast agent. Information on morphology is fundamental for accurate characterization of focal liver lesions. Different characteristic features of the intravascular and extracellular spaces of the various focal liver lesions are depicted by extracellular gadolinium contrast agents. Dynamic imaging has also been shown to improve not only the distinction of malignant lesions but also to achieve the specific diagnosis for most liver tumors and to identify benign disease precisely. In addition to identifying the presence, number and type of focal lesions and the possible involvement of vascular and biliary structures, it is necessary to provide as much useful information on morphology and functionality as possible for therapeutic planning. Permeability imaging using computer assisted software solutions provides information for visualizing morphological changes and shows efficient assessment of dynamic MRI in liver tumors. It enables an adequate review of patient studies over time. Moreover, it permits easy comparison of parametric angiogenesis maps over time. Perfusion-weighted MRI allows detecting intranodular hemodynamic characteristics in different liver tumors. The time to peak, maximal relative signal enhancement, and the initial slope of signal intensity vs. time curves of the tumors and surrounding liver tissue are to be evaluated. In addition, perfusion parameters of the Gd-chelate are to be measured. Pretreatment imaging is an important and necessary step for the assessment and therapeutic planning of patients with liver disease. In this regard, dynamic contrast-enhanced MRI has an important role in diagnosing the nature of liver tumors.

SY 4.03 **MRI of pancreatic diseases** W. Schima; Vienna/AT

The most important issues in pancreatic imaging are the assessment of pancreatitis, the detection and staging of pancreatic cancer and the characterization of cystic lesions. 1.5–3.0 T MR make breath-hold imaging possible, in order to avoid motion artifacts. Standard imaging sequences are T1w GRE with and without fat saturation (which offer a very high tumor-pancreas contrast). T2-weighted imaging axial single-shot TSE with fatsat allow delineation of the pancreatic duct and peripancreatic edema in pancreatitis. MRCP pulse sequences and dynamic gadolinium-enhanced T1-weighted GRE images (preferably with fatsat) are mandatory in pancreatic imaging. They are helpful to delineate vessel infiltration by cancer and to characterize cystic masses. In case of an equivocal pancreatic mass, the presence of the “duct penetrating sign” at MRCP (i.e., the duct traversing the mass) is suggestive of an inflammatory pseudotumor. Focal fatty infiltration may mimic a tumor at CT, but in- and opposed phased T1w GRE readily depicts the fat. MDCT imaging has gained increasing popularity for pancreatic imaging because of the 3D-visualization of the peripancreatic vessels. MRI is excellent in the delineation of small pancreatic tumors. Due to its superior soft tissue contrast, MRI is also the method of choice in patients with suspected cancer and equivocal CT or compromised renal function. MRI is the technique of choice to characterize cystic lesions.

12:45 - 13:45

Marmara Hall

Lunch Symposium 5 **Pre- and postoperative liver imaging - the essentials**

Sponsored by: AGFA

SY 5.01 **Liver anatomy: segments and perihepatic space** R. Manfredi; Verona/IT

The internal lobation and segmentation of the liver is defined by the branching pattern of the structures entering and leaving its porta, with the hepatic veins coursing in the interlobar and intersegmental planes. This subdivision subdivides the liver into two lobes and eight segments, according to the Couinaud classification. At the hepatic porta, the portal vein divides into right and left portal vein branches, the proper hepatic artery divides into right and left hepatic arteries, and the common hepatic duct is formed by the junction of the right and left hepatic ducts. The right lobe of the liver is supplied or drained by the right branches of each of these structures. Likewise, the left hepatic lobe is supplied or drained by the left branches of each of these structures. Because the portal

veins are the largest and most easily imaged intrahepatic structures, they are used to identify the hepatic lobes, segments, and sub-segments. The hepatic segments are further subdivided by the intrahepatic branches of the left and right portal veins. The liver has unique peritoneal and mesenteric relationships, which cause the upper portion of the greater peritoneal sac to be subdivided into four perihepatic recesses or spaces such as the falciform ligament, the coronary ligament, the right and left subphrenic or suprahepatic recess, hepato-renal space (Morrison's pouch), and the left subhepatic recess. The common hepatic artery, in the classical pattern, arises from the celiac artery; this configuration occurs in 55% of the population. The common hepatic artery gives off the gastro-duodenal artery, which descends behind the first part of the duodenum. After the emergence of the gastro-duodenal artery, the common hepatic artery changes its name becoming the proper hepatic artery. The portal vein forms behind the pancreatic neck by the confluence of the splenic and superior mesenteric vein.

SY 5.02 **Liver volumetry: what the radiologist should know** T. Frauenfelder, B. Marincek; Zurich/CH

In order to overcome shortage of liver donors, living related liver donor transplantation as well as tissue sparing liver surgery have been established as alternative methods. For both surgical approaches, liver volumetry has become indispensable. Liver volumetry is used to estimate liver (-segment) and tumor size. This information provides a decision guidance regarding surgical strategies and preoperative interventions (chemoembolisation, occlusion of portal branch). The base of liver volumetry is a semiautomatic segmentation of liver contours on cross-section images using dedicated software. The resulting volume depends on a variety of factors, such as slice thickness, type of segmentation or imaging modality influence. In order to achieve an optimal patient outcome, liver volumetry has to be performed in close cooperation with the surgeon. The future development of preoperative 3D-simulation techniques for hepatic interventions including liver volumetry will facilitate the surgical strategy. Liver volumetry is an important preoperative planning tool for liver surgery, influencing surgical strategies and decisions. It therefore bears a great responsibility for the radiologist. The learning objectives are: (1) To describe the technique of liver volumetry; (2) To define the role of liver volumetry in clinical context; (3) To learn the limitations; (4) To outline future perspectives.

SY 5.03 **Vascular and biliary complications after liver surgery: imaging spectrum** P. Boraschi; Pisa/IT

Hepatic resection for malignant liver disease and liver transplantation for end-stage chronic liver disease, as well as for severe acute liver failure, offer the possibility of long-term cure. Imaging techniques used for post-operative work-up of patients with hepato-biliary surgery and/or liver transplantation mainly aim to identify vascular and biliary complications. A review of the literature regarding the results of post-operative complications after hepato-biliary surgery and/or liver transplantation is shown. Furthermore, the own experience on post-operative diagnostic work-up of these patients is presented. Despite the improvement and refinement of surgical techniques, the advances in organ preservation and improved immunosuppressive therapy agents, there are still significant complications after hepatic resection and/or liver transplantation. The role of imaging methods and particularly of CT and MRI consists of identifying post-operative complications, mainly including biliary strictures, stones and leakage, arterial and venous stenosis and thrombosis. The early recognition and prompt treatment of such complications improves the long-term survival of the patient and graft. Vascular and biliary complications after hepato-biliary surgery and/or liver transplantation are serious and are associated with a significant risk of morbidity and mortality. Because the clinical presentation of these patients may be subtle, imaging is extremely important in assessing and managing such complications. Knowledge and early recognition of these complications with the most suitable imaging modality is crucial for the patient.

12:45 - 13:45

Haliç Hall

Lunch Symposium 6

Further defining liver imaging: referring physician and radiologist in dialogue

Sponsored by: BAYER SCHERING PHARMA

SY 6.01

Diagnostic imaging technology in liver surgery: open questions

E. Jonas; Stockholm/SE

Purpose: Liver resection for malignant liver disease, both primary and secondary, offers the possibility of long-term cure. Imaging techniques used for pre-operative work-up of patients with suspected malignant disease aim to characterize lesions, to determine the number, size and location of tumours and to show tumour relationship to biliary and vascular structures. Materials and Methods: A review of the literature regarding the results of pre-operative work-up of patients with the most common indications for liver resection, hepatocellular cancer and colorectal cancer metastases (CRM) is presented. Furthermore, own results regarding pre-operative work-up and outcome of patients operated for CRM are shown. Results: Developments in hepatic imaging have contributed largely to the improvement in results of liver resection for malignant disease. Some challenges, however, remain. In 30-40% of patients with tumour recurrence after liver resection for CRM, the disease is limited to the liver. This is mainly due to the inability of pre-resection investigations to detect small metastases in the remnant liver. Conclusion: Major challenges in hepatic imaging remain, including extending the sensitivity of methods for lesion detection beyond current lesion size limits and increasing the sensitivity and specificity of lesion characterization. Functional imaging is likely to predict residual liver function after resection more accurately than currently used methods.

SY 6.02

Current use of Primovist liver MRI including health economic considerations

C.J. Zech; Munich/DE

Purpose: Gd-EOB-DTPA (Primovist) is a new liver-specific contrast agent for detection and characterisation of focal liver disease. The aim of the lecture is to introduce the current status of knowledge about MRI with Gd-EOB-DTPA. Materials and Methods: Based on the literature and on the own experience, the value of Gd-EOB-DTPA-enhanced MRI is evaluated with special regard to the use of Gd-EOB-DTPA as a pre-operative "one-stop-shop" examination. Results: Due to the dual pathway of excretion and, therefore, the extracellular and hepatobiliary imaging properties, Gd-EOB-DTPA-enhanced MRI can answer the usual questions arising prior to liver surgery: Where? What? How many? Also, additional questions about the liver vasculature and biliary anatomy can be addressed. In the future, even issues like liver function and prediction of the functional capacity of the remaining liver prior to resection might be resolved with the help of Gd-EOB-DTPA-enhanced MRI. Conclusion: Gd-EOB-DTPA is a versatile and safe MR contrast agent. Its imaging properties make it an ideal contrast agent for the investigation of patients with focal liver lesions, especially when liver surgery or interventional therapies are planned.

12:45 - 13:45

Marmara Hall

Lunch Symposium 7

Non-radiologists reporting CT colonography: A step too far?

Sponsored by: E-Z-EM

SY 7.01

The case for radiographer reporting

D. Burling; Harrow/UK

SY 7.02

The case for radiologist only reporting

E. Neri; Pisa/IT

SY 7.03

The case for gastroenterologist reporting

D.F. Martin; Manchester/UK

CT colonography (CTC) is rapidly disseminating into routine clinical practice and is generally regarded a safe, accurate and frequently cheaper alternative to conventional colonoscopy. Consequently, and in parallel with promotion of national bowel cancer screening programmes, demand for CTC is increasing. Although generally welcome, such demand exerts additional pressure on radiology departments already experiencing intense competition for finite CT resources. In addition, CTC requires considerable investment in training and reporting time, placing it beyond the scope of many general radiologists, and attracting non-radiologists with a subspecialty interest in the diagnosis of colorectal cancer; the American Gastroenterology Association has declared that CTC, being a technique for investigating the colon, should be controlled by gastroenterologists. This symposium tackles the controversial subject of whether non-radiologists (radiographers and gastroenterologists) should report CTC and whether this activity can be safely and accurately undertaken. In support, emerging data suggests non-radiologists can potentially report CTC as accurately as experienced radiologists but issues related to extra-colonic findings, IRMER regulations and medico-legal implications of misdiagnosis are worthy of vigorous debate. E-Z-EM have gathered together an eminent group of entertaining European speakers with a wealth of CTC experience to debate this topic, which promises to engage members of the audience by inviting their opinions and contributions to a final vote.

12:45 - 13:45

Haliç Hall

Lunch Symposium 8
Highlights in contrast imaging

Sponsored by: BRACCO

SY 8.01

Five good reasons to use contrast US during a liver US exam

P.S. Sidhu; London/UK

A US examination of the liver remains the first line investigation for patients with an abnormality attributable to the hepatobiliary system. US is cost-effective particularly if the examination precludes the need to proceed to further imaging with CT and MRI. With the advent of microbubble US contrast, the need to extend the investigative algorithm diminishes markedly with obvious cost benefits. This is particularly noticeable with characterization of the incidental benign focal liver lesion; the atypical haemangioma, areas of focal fatty sparing or focal steatosis where confidence in the findings is rapidly established. In the cirrhotic patient, microbubble contrast allows for the characterization of doubtful lesions; the typical HCC demonstrating intense enhancement in the early arterial phase allowing for differentiation from regenerative nodules. With the follow-up of patients with a known primary malignancy, any focal lesion identified may be accurately characterized; malignant lesions always demonstrate washout on the late portal-venous phase. Following detection of the metastatic liver lesion, percutaneous treatment is now widely available; instantaneous assessment of the success of treatment can be improved with the use of microbubble contrast to assess the extent of successful ablation. When liver transplantation is the only effective treatment for end-stage liver disease, the post-operative assessment of the vascular supply to the graft is markedly improved with the addition of microbubble contrast. "Doppler rescue" is particularly useful in the assessment of the patency of the hepatic artery, crucial to the viability of the transplant liver. The use of microbubble contrast in many areas of liver US is cost-effective but more importantly improves operator confidence immeasurably.



11:00 - 12:30

Marmara Hall

Scientific Session 1 CT Colonography - Clinical Impact

SS 1.01

Full preparation CTC: electrolyte and renal function disturbances in the frail and elderly patient

P. Mc Laughlin, S.E. Mc Sweeney, S. Mc Williams, M. Ryan, D. Kelly, M. Maher; Cork/IE

Purpose: The use of bowel preparation is relatively contraindicated in elderly patients with multiple co-morbidities. There are reports of fatalities secondary to electrolyte and renal dysfunction and this has prompted caution in the use of such bowel preparations. Our aim is to evaluate the metabolic safety of full mechanical bowel preparation in a subgroup of elderly patients undergoing elective CTC.

Material and methods: From a total of 613 CT Colonography (CTC) examinations performed at our centre between January 2005 and December 2006, a subgroup of 75 elderly patients (mean age=80.1) who were admitted electively for full bowel preparation and IV rehydration prior to CTC were evaluated. The bowel preparation administered was 40 mg of Sodium Picosulphate Magnesium Citrate (PSMC) over a 3 day period. Haematological and biochemical parameters were recorded 3 days prior and 1 day post CTC and patients' medical records reviewed to assess for post procedural complications.

Results: There were mild electrolyte disturbances among the group per examination. The average change in serum Na was +0.2851 mmol/L (range -6 to +8mmol/L). Importantly, changes in serum Na did not exceed 2 mmol/day in any members of the group. Renal function tests deteriorated in 24 patients per CTC. The average rise in serum urea and creatinine was also mild at 0.125 mmol/L and 10 umol/L, respectively. Renal function objectively improved in 23 patients.

Conclusion: Full mechanical bowel preparation is metabolically safe in elderly patients who are electively admitted for electrolyte monitoring and IV rehydration prior to CTC.

SS 1.02

Virtual colonoscopy: development and validation of a new patient questionnaire for assessment of experience and compliance for bowel preparation

P. Das, P. Wylie, R. Ahmad, M. Marshall, D. Burling; Harrow/UK

Purpose: Superior patient experience related to reduced laxative regimens is frequently cited as a major benefit of virtual colonoscopy (VC) but most related questionnaires are not valid or designed for endoscopy. We aimed to validate a new questionnaire for VC.

Material and methods: A 34 item questionnaire was created using expert opinion (including 2 VC researchers with relevant questionnaire-based publications), literature review and patient interview. 25 consecutive patients undergoing VC in routine practice (21 (84%) had sodium picosulphate/4 had senna 26 g and 100 mls gastrografin) were interviewed before their examination 'face-to-face' using the questionnaire. A series of open and closed questions related to ethnicity/understanding/convenience/tolerability/discomfort/anxiety/compliance were asked. Responses were evaluated for content validity (frequency of similar responses) and following statistical advice, reliability was assessed by Spearman's correlation (inter-item correlation) and Cronbach's alpha (test of overall questionnaire reliability/consistency).

Results: 25 patients (13 (52%) female; median age 70 years) undergoing VC completed the questionnaires. 22 patients (88%) were either very satisfied (32%) or fairly satisfied (56%) with the bowel preparation. 27 questions were deemed valid in content and frequency of endorsement. There was good inter-item correlation (Spearman's $\rho = -0.395 - 0.795$) with a high level of reliability (Cronbach's $\alpha = 0.904$) overall.

Conclusion: This questionnaire, developed for comparing VC bowel preparation regimens, is both valid and reliable and will be made freely available for use by ESGAR members.

SS 1.03

CTC after failed or incomplete optical colonoscopy: gender and previous hysterectomy as factors

A.S. Lev-Toaff, A. Frangos, D. Bergin;

Philadelphia, PA/US

Purpose: Evaluate gender and previous hysterectomy as contributing factors to failed or incomplete optical colonoscopy (OC) in patients referred for CT colonography (CTC).

Material and methods: Over a two-year period, 173 patients were referred for CTC; 60 were men, 113 were women. These were reviewed for: age, indications for CTC and history of hysterectomy. Prevalence of hysterectomy was compared to published prevalence in the U.S.

Results: Of 173 consecutive cases, 60 (34.7%) were men (mean age 67.3), 113 (65.3%) were women (mean age 62.5). The indication for CTC was incomplete or failed optical colonoscopy (OC) in 37/60 (62%) of men and 94/113 (83%) of women; the proportion of women referred for failed/incomplete OC was significantly more than men, $p < 0.01$, Fisher's exact test. Other indications for CTC included anticoagulation (18/173), increased sedation risk (8/173), and others (16/173). All CTC examinations were successful. Of 94 women with failed/incomplete OC, hysterectomy status is known in 85: 48 of these 85 (56.5%) women had hysterectomies. This compares to a 33% prevalence of hysterectomy by age 60 in the U.S., according to the Centers for Disease Control.

Conclusion: In our experience, women comprise a larger percent of patients referred for CTC compared to men. Female gender and history of hysterectomy are contributing factors for failed or incomplete optical colonoscopy. Our data suggests that CTC has a particularly important role in women with previous hysterectomy.

SS 1.04

Retrospective review of the introduction of CTC in a district general hospital

S. Farquhar, N. Gibbons, J. Atchley, A. Higginson; Portsmouth/UK

Purpose: CTC was introduced in Portsmouth in 2001, initially for patients with failed barium enema (BE) or colonoscopy but subsequently as a first-line investigation. Previous research has questioned the interpretative performance of CTC in UK District General Hospitals (DGH). We compared the local sensitivity of BE with CTC to determine whether CTC is superior for the detection of cancer locally.

Material and methods: All patients undergoing diagnostic BE or CTC between January 2003 and December 2005 were identified from Picture Archiving Communication System. Patients with confirmed diagnosis of colorectal cancer were identified from the local cancer registry. Patients with no cancer diagnosed on imaging were assumed true negatives if not on the cancer registry by December 2007, giving minimum 2 year follow-up. BE and CTC reports of all patients with cancer were analysed and considered positive for the detection of cancer if they stated presence of cancer or polypoid lesion.

Results: 2648 BE (mean age 65 years, range 25-96 years) and 631 CTC were included (mean age 69 years, range 28-95 years). 34 BE patients had cancer, with 27 detected (incidence 1.28%, sensitivity 79.4%). 27 CTC patients had cancer (incidence 4.33%), all detected (sensitivity 100%).

Conclusion: CTC is more sensitive for detection of cancer and its introduction in a DGH is justified. The increased incidence of cancer in the CTC group suggests more selective use by clinicians.

SS 1.05

Evaluation of CTC as triage technique for colorectal cancer in a fecal occult blood test positive screening population

M.H. Liedenbaum¹, A.F. van Rijn¹, A.H. de Vries¹, H. Dekker², P. Fockens¹, E. Dekker¹, J. Stoker¹;
¹Amsterdam/NL, ²Nijmegen/NL

Purpose: To determine whether CT-colonography (CTC) is an accurate triage technique in persons with a positive Fecal Occult Blood Test (FOBT) in a population-screening setting.

Material and methods: 200 consecutive FOBT positive individuals underwent CTC with limited bowel preparation, which was read by two independent,

experienced observers. Reference standard was colonoscopy with segmental unblinding. Per patient sensitivity and specificity were calculated for both observers ('double reading') with two cut-off points using CTC matching criteria: lesions ≥ 10 mm (category 1) and lesions ≥ 6 mm (category 2). Positive and negative predictive values (PPV and NPV) were calculated using the CTC measured size as cut-off for triage.

Results: 15 FOBT positive patients had a carcinoma; CTC sensitivity 93%. Of FOBT positives, 50% had a category 1 lesion and 70% a category 2 lesion. Per patient sensitivity for CTC was 96% (95% CI: 92–100%) and 94% (95% CI: 90–99%) in categories 1 and 2, respectively. The per patient specificity was 93% (95% CI: 88–98%) and 80% (95% CI: 72–88%) for categories 1 and 2, respectively. Regarding CTC as triage method, PPV was 88% (95% CI: 82–95%) and 88% (95% CI: 81–94%) and NPV 85% (95% CI: 78–92%) and 78% (95% CI: 70–86%) for categories 1 and 2, respectively.

Conclusion: CTC with limited bowel preparation is an accurate technique for carcinoma and polyp detection in a FOBT positive population. The use of CTC as cost effective triage technique is questionable given the high true positive FOBT rate.

SS 1.06

CTC in colorectal cancer screening

P. Della Monica on behalf of the IMPACT Study Group;
Candiolo/IT

Purpose: The aim of the study was to optimize CTC management for colorectal cancer (CRC) screening.

Material and methods: A collated archive of CTC findings in 934 subjects at high risk of CRC for personal or family history (mean age + SD 57.7+9 y; 422 F) was analysed. Data were part of IMPACT trial comparing CTC to OC (Regge et al, RSNA 2008). Neoplasia (advanced adenoma ≥ 6 mm) was in 174 patients (disease prevalence 19%), in 132 cases lesion was ≥ 10 mm (advanced neoplasia). CTC output was considered to be the diameter of the biggest lesion as measured on 2D multi-planar images. The cut-off value discriminating positive and negative CTC results was progressively increased in steps of 1 mm. Positive and negative predictive values (PPV, NPV) were calculated at each step.

Results: For CTC, cut-off progressively increased from 6 to 10 mm, PPV varied from 39 to 78% (from 50 to 74% for advanced neoplasia), NPV from 96 to 91%. Referral rate to optical colonoscopy varied from 26 to 15%. Optimum scenario was at 8 mm cut-off: PPV was 71% (62% for advanced neoplasia), NPV 94%, referral rate 20%.

Conclusion: CTC is a very promising test for CRC screening. CTC cut-off value to activate optical colonoscopy can be tailored to optimise the screening programme.

SS 1.07

A randomised comparison of CTC versus colonoscopy or barium enema for detection of colorectal cancer in symptomatic patients: the UK SIGGAR study

S. Halligan on behalf of the UK SIGGAR investigators;
London/UK

Purpose: The potential role of CT colonography (CTC) for colorectal screening has been stressed repeatedly but CTC also shows great promise for the diagnosis of established cancer in symptomatic patients, possibly preferable to standard alternatives. The SIGGAR trial is a randomised controlled study of CTC versus colonoscopy or barium enema via two parallel sub-trials and is the only randomised study of CTC. This presentation is the first international presentation of results.

Material and methods: Adult patients with symptoms suggesting colorectal cancer and judged clinically as needing a whole-colon examination by colonoscopy or barium enema (default) were subsequently randomised to default or CTC (ratio 2:1, default: CTC). Colonoscopy was performed by experienced practitioners and enema/CTC interpreted by trained radiologists. The primary outcome measures were detection rates for colorectal cancer and significant colorectal neoplasia, defined as colorectal polyps 1 cm or larger. Analysis was by multivariable logistic regression with randomised procedure as the primary explanatory variable.

Results: Interim analysis of the colonoscopy and enema sub-trials revealed a prevalence of abnormality of 12 and 4%, predicting respective sample sizes of 1,422 and 3,402 to achieve 80% power. 9,072 patients were registered and 5,438 ultimately randomised: 1,610 to the colonoscopy sub-trial (539 CTC; 1071

colonoscopy) and 3,828 to the enema sub-trial (1,283 CTC; 2,545 enema). Detection rates by each procedure for primary outcome measures will be presented orally.

Conclusion: CTC may have utility for the diagnosis of symptomatic colorectal cancer.

SS 1.08

Small and diminutive polyps detected at screening CTC: a decision analysis for referral to colonoscopy

E. lafrate¹, C. Hassan¹, A. Stagnitti¹, P.J. Pickhardt², A. Pichi¹, R. Ferrari³, A. Laghi³; ¹Rome/IT, ²Madison, WI/US, ³Latina/IT

Purpose: To assess the clinical and economic impact of colonoscopic referral for small and diminutive polyps detected at CTC screening.

Material and methods: A decision analysis model was constructed incorporating the expected polyp distribution, advanced adenoma prevalence, colorectal cancer risk, CTC performance, and costs related to CRC screening and treatment. The model assumed that CRC risk was independent of advanced adenoma size. The number of diminutive (≤ 5 mm), small (6–9 mm), and large (≥ 10 mm) CTC-detected polyps needed to be removed to detect one advanced adenoma or prevent one CRC over a 10-year time horizon were calculated.

Results: The estimated 10-year CRC risk for unresected diminutive, small, and large polyps was 0.08, 0.7, and 15.8%. The number of diminutive, small, and large polyps needed to be removed to avoid leaving behind one advanced adenoma was 562, 71, and 2.5, respectively; 2,352, 297, and 10.7 polypectomies would be needed to prevent one CRC over 10 years. The incremental cost-effectiveness ratio of removing all diminutive and small CTC-detected polyps was \$464,407 and \$59,015 per life-year gained.

Conclusion: For diminutive polyps, the very low likelihood of advanced neoplasia and the high costs associated with polypectomy argue against colonoscopic referral, whereas removal of large CTC-detected polyps is highly effective. The yield of colonoscopic referral for small polyps is relatively low, and so CTC surveillance may be a reasonable management option.

SS 1.09

Colorectal cancer screening by colonoscopy or CTC: qualitative data from semi-structured focus groups and thematic analysis

C. Robinson, C. von Wagner, S. Halligan, W. Atkin, J. Wardle;
London/UK

Purpose: It is widely believed by radiologists that CT colonography (CTC) is preferred by asymptomatic individuals for colorectal screening. We determined whether this is true by establishing the information needs and preferences of asymptomatic individuals via semistructured focus groups and thematic analysis.

Material and methods: 26 asymptomatic volunteers participated in one of 7 semi-structured focus groups, split by gender. Demographic information was collected. Structured topic-guide information about colorectal cancer, benefits of screening, physical characteristics of colonoscopy and CTC and their performance characteristics were introduced to participants in a step-wise fashion. Group discussion followed each section and participants noted their beliefs and preferences on a questionnaire before moving to the next topic. Transcripts of the interviews were made subsequently, questionnaire data collated, and a qualitative thematic analysis performed.

Results: On the basis of minimal initial information, most participants preferred CTC to colonoscopy (65 vs 11%), with 24% having no preference. However, by the end of the topic guide session, this finding was dramatically reversed, with 80% preferring colonoscopy and only 8% CTC. Thematic analysis revealed that this was due almost completely to participants' concerns about sensitivity, which was ranked the most desirable test attribute overall. Specificity and personal inconvenience/discomfort were rated less important by participants.

Conclusion: Test sensitivity is rated highest by asymptomatic screens. The assumption that CTC dominates colonoscopy by virtue of its acceptability may be incorrect.

SS 1.10**Data reporting in CTC: different methods of data analysis result in significantly different outcomes**

M.H. Liedenbaum¹, A.H. de Vries¹, A.F. van Rijn¹, S. Bipat¹, H. Dekker², P. Fockens¹, E. Dekker¹, J. Stoker¹;
¹Amsterdam/NL, ²Nijmegen/NL

Purpose: To investigate if different methods of CT colonography (CTC) data analysis result in different outcomes on per patient sensitivity, specificity, positive and negative predictive value (PPV and NPV).

Material and methods: CTC examinations of 200 FOBT positive patients who had colonoscopy with segmental unblinding were evaluated. CTCs were examined by 2 experienced, independent observers and results were added ('double reading'). Per patient sensitivity, specificity, PPV and NPV for polyps ≥ 10 mm were calculated using 2 methods: 1. by using matching criteria (matching based on size (with 50% margin of error), morphology and segmental location) and 2. by using the CTC lesion size measurement as cut-off value for colonoscopy indication. Significant differences were calculated using the Chi square test.

Results: 136 polyps of ≥ 10 mm were found in 99 patients. The sensitivity was 96% for method 1 and 84% for method 2 ($p < 0.05$). The specificity was 89 and 93% ($p > 0.05$) for methods 1 and 2, respectively. PVV was 93 and 88% ($p > 0.05$) and NPV was 96 and 85% ($p < 0.05$) for methods 1 and 2, respectively.

Conclusion: Performing CTC data analysis by using the matching criteria commonly used in literature results in significant different outcomes for sensitivity and NPV compared to using CTC lesion size as cut-off value. This last method however would be applied in lesion size based triage for colonoscopy.

11:00 - 12:30

Haliç Hall

Scientific Session 2**Focal liver lesions - Multimodality approach****SS 2.01****Hypervascular liver lesions on contrast-enhanced US: the importance of washout**

D. Bhayana, T.K. Kim, H. Jang, P.N. Burns, S.R. Wilson;
 Toronto, ON/CA

Purpose: To evaluate the value of presence and timing of negative enhancement (washout) in the differential diagnosis of hypervascular liver lesions on contrast-enhanced ultrasound (CEUS).

Material and methods: One-hundred fifty-three hypervascular liver lesions (1.0–17.0 cm, mean 3.89 cm) were evaluated with CEUS over a 6-month period. 81 were benign (34 hemangiomas, 33 FNH, 7 adenomas, 7 other) and 72 malignant (41 HCC, 25 metastases, 6 other). Two independent, blinded reviewers retrospectively determined timing of washout in the portal-venous phase, up to at least 4 minutes after injection of microbubbles (Definity). Diagnoses were confirmed by histopathology or clinicoradiological follow-up. Timing of washout was compared between different types of lesions using Fisher's exact test.

Results: Washout occurred in both benign (28/81, 35%) and malignant lesions (70/72, 97%), but more frequently in malignancy ($P < .001$) ($\kappa = .94$). Metastases showed more rapid washout than HCC ($P < .001$); 20/25 metastases by 30 seconds, and 23/41 HCC later than 75 seconds. All malignant lesions without washout were HCC (2/41). Among benign lesions, all 5 inflammatory lesions showed rapid washout and 6/7 adenomas showed washout, mostly later than 75 seconds (5/6). Unexpected washout also occurred in hemangiomas (6/34) and FNH (10/33).

Conclusion: Malignant lesions show washout, except infrequent cases of HCC. Rapid washout characterizes metastases whereas HCC show variable, often slow washout. However, washout is not unique for malignancy and may be seen in benign lesions.

SS 2.02**Quantification of wash-out of malignant liver lesions at contrast enhanced US: usefulness of a semi-quantitative index in the differential diagnosis**

E. Gavazzi, P. Cabassa, E. Orlando, R. Monesi, E. Fogari, R. Maroldi; Brescia/IT

Purpose: Determine the efficacy of a semi-quantitative index in differential diagnosis of focal liver lesions during portal phase with contrast enhanced ultrasonography (CEUS).

Material and methods: 58 consecutive histologically proven malignant lesions studied with CEUS were retrospectively analysed. CEUS was performed with 2.4 ml of SonoVue with dedicated software (contrast coherent imaging). One significant frame (in bitmap format) of portal phase was chosen for each lesion and analysed by software (AdobePhotoshop 7.0). Two circular defined regions of interest (ROI) for each image were drawn encompassing the lesion and the adjacent normal parenchyma. Sonography videotape intensity (VI) was measured in gray-scale levels (0–255) through histogram analysis for each ROI. Background VI was set at the same level for each image. A semi-quantitative index (VI_{tumor}-VI_{liver}/VI_{liver}) was calculated. Results were divided according to histologic type and also compared with 15 benign lesions.

Results: HCC showed a median index value of -0.42 , colangiocarcinomas of -0.62 , metastases of -0.61 and benign lesions of 0.15 . Well differentiated HCC showed a median index value of -0.09 . Metastases were divided according to classical vascularization in hypo and hypervascular, the former showing a median index value of -0.65 , the latter of -0.52 .

Conclusion: We quantified hypoechogenicity of different focal liver lesions by a semi-quantitative index which can be useful in characterisation. In our series, CEUS correlates with pathology.

SS 2.03**Imaging efficacy versus diagnostic efficacy of contrast enhanced US in focal liver lesions**

K. Chatzimichail, C. Karanikas, E. Mainta, A. Pomoni, N. Ptohis, S. Tanteles, S. Kampanarou, G.P. Economou, D.A. Kelekis; Athens/GR

Purpose: Impact of imaging efficacy of Contrast Enhanced Ultrasound (CEUS) on diagnostic work-up and treatment plan of the referring physician.

Material and methods: This is a retrospective study of patients who underwent CEUS in our department due to incidental US finding or in the process of monitoring them due to known cirrhosis or primary non-hepatic neoplasm. We characterized 198 focal liver lesions in 156 patients. US contrast was achieved with Sonovue (Bracco) under CPS imaging mode (Siemens). All patients underwent CE-CT and MRI (occasionally biopsy) and the results were compared with MRI/biopsy as reference diagnosis. CEUS findings were analyzed by two radiologists blinded to CE-CT/MRI results and vice versa.

Results: MRI/biopsy diagnosis included: 46 HCCs, 24 metastases, 78 hemangiomas, 20 FNHs, 22 regenerative/dysplastic nodules, 4 adenomas and 4 focal steatoses. CEUS characterization coincided with reference diagnosis in 180/198 lesions while corresponding number for CE-CT was 176/198. Statistical processing of the results for malignancy of a lesion rendered sensitivity 91% (CI 95% 84.9–98.0), specificity 97% (CI 95% 93.9–99.9), PPV 94%, NPV 95% with LR+ 29.25 and LR- 0.088 for CEUS while the respective values for CE-CT were 88% (CI 95% 81.1–96.0), 93% (CI 95% 89.6–97.9), 88%, 93% with LR+ 14.171 and LR- 0.122.

Conclusion: Apart from the proven imaging efficacy of CEUS in the diagnostic armamentarium of focal liver lesions, it appears that it possesses equivalent, if not superior than CE-CT, diagnostic efficacy.

SS 2.04**Early and late tumour vasculature changes following the vascular disruptive agent combretastatin-A4-phosphate using dynamic contrast enhanced MRI and perfusion CT**

A. Gaya, N.J. Taylor, J.J. Stirling, G. Rustin, A. Padhani, V. Goh; Northwood/UK

Purpose: To prospectively assess early and late anti-vascular effects of the vascular disruptive agent combretastatin-A4-phosphate (VDA CA4P) on hepatic metastases using dynamic contrast enhanced MRI (DCE-MRI) and Perfusion CT.

Material and methods: Following institutional review board approval, twelve patients (seven male, five female; mean age 63 years) with colorectal hepatic metastases were studied at baseline and 4 h after administration of 45–54mg/m² CA4P using DCE-MRI following IV injection of Gd-DTPA (0.1 mmol/kg). Tumour transfer constant (Ktrans) and IAUGC60 were calculated pixel-by-pixel using Tofts' method. Four of the twelve patients also underwent perfusion CT at baseline, 4 and 8 weeks following intravenous contrast (40 ml 350 mg/ml iodine). Arterial (ALP) and portal venous hepatic perfusion (PVP) and the hepatic perfusion index (HPI) were calculated using compartmental analysis. Mean tumour values were recorded for each patient and compared by t-testing.

Results: In 9/12 patients (including all four CT patients), falls in Ktrans and IAUGC60 were seen at 4 h with DCE-MRI consistent with acute vascular shutdown (Ktrans mean percentage fall -24.3%; range -76.2–+63.5% ; IAUGC60 mean percentage fall -20.5%; range -77.4–+31.8%). For three of these nine patients (not CT patients), falls in Ktrans and IAUGC60 were statistically significant (p<0.05). No significant late changes in ALP, PVP or HPI were observed with perfusion CT.

Conclusion: The anti-vascular effects of CA4P demonstrated acutely do not appear to be sustained in the longer term.

SS 2.05

CT evaluation of response to transcatheter arterial radioembolization of hepatic tumors: volumetry, RECIST and density measurements

S.M. Berggruen, A. Korutz, R. Salem, V. Yaghmai; Chicago, IL/US

Purpose: The purpose of our study was to compare volumetry, RECIST and density measurements for response evaluation of hepatic metastases undergoing transcatheter arterial radioembolization.

Material and methods: Twenty-four solid hepatic metastases (8 left and 16 right hepatic lesions) in ten patients were evaluated on baseline and post-treatment contrast-enhanced multislice CT. The average time interval between CT exams was 4.9 weeks (range 3–10 weeks). Two radiologists evaluated the hepatic masses using automated software (Siemens Medical Solutions, Forchheim, GER) to obtain RECIST, volume and density of each lesion before and after treatment. Paired T test was used to evaluate percentage change of volume, RECIST, and density measurements. P<0.05 was considered significant.

Results: The mean RECIST change for the treated hepatic lesions was minus 5.99% (P=0.04) while the volumetric percent change was minus 13.73% (P=0.53). The mean HU change was minus 18.75, with a calculated two-tailed P value of 0.0010, which is very statistically significant.

Conclusion: For treated hepatic metastases, automated volumetry does not produce better approximation of tumor bulk versus RECIST measurements. However, the decrease in Hounsfield units of hepatic metastases post treatment is significant in monitoring therapy response.

SS 2.06

The value of diffusion-weighted imaging in characterizing focal liver masses

K. Sandrasegaran, F. Akisik, A.M. Aisen, C. Lin; Indianapolis, IN/US

Purpose: To determine if focal liver masses (FLM) could be differentiated as benign or malignant on the basis of diffusion-weighted imaging (DWI).

Material and methods: 104 patients with FLM were scanned using 1.5 T MRI (Magnetom Avanto, Siemens, Erlangen, Germany). DWI was performed with b values of 0 and 500 s/mm². Of these, 76 patients had: i) lesions larger than 2 cm diameter, ii) radiological or pathological characterization of the lesion, and iii) diagnostic quality DWI. The apparent diffusion coefficient (ADC) of the largest liver lesion was measured. Some liver masses were diagnosed on histology: HCC (n=18), adenoma (n=1), FNH (n=4), and metastases (n=2). Others had characteristic CT and/or MRI findings and follow up imaging >6 months: HCC (n=23), hemangioma (n=17), cysts (n=5), FNH (n=2), adenoma (n=2), and metastases (n=2).

Results: The mean ADC values (10–5 mm²/s) of hemangiomas, cysts, FNH, and HCC were 1578, 190, 130, and 108, respectively. The ADC of cysts and hemangiomas were significantly higher than that of other lesions (p=0.0003). There was no significant difference between ADC values of solid, benign liver lesions and malignant lesions (p=0.62). In 4 of the 41 cases of HCC, DWI showed the lesion better than the standard pre and post-gadolinium sequences.

Conclusion: Solid liver lesions have a lower ADC than cysts and hemangiomas. However there is no significant difference in ADC between solid benign and

malignant lesions. DWI appears to have only minimal additional value over currently used MRI sequences in characterizing liver masses.

SS 2.07

Primovist MRI in patients with colorectal liver metastases being considered for hepatic resection: comparison with PET/CT and 64-slice MDCT

V.O. Chan, S. Mc Dermott, J.P. Das, T.A. Bangash, A. Latif, J. Geoghegan, C.D. Collins, S. Skehan, D.E. Malone; Dublin/IE

Purpose: To compare the diagnostic performance of Primovist MRI, PET/CT and 64-slice MDCT in the pre-resection workup of colorectal liver metastases.

Material and methods: Retrospective study. Eighteen months consecutive colorectal liver metastases (CRLM) referrals to 31.12.07. Workup included portal venous phase 64-slice MDCT, PET/CT and Primovist MRI (P-MRI) within 3 months of each other. Group A: Proceeded to liver resection and pathology. Gold standard for data calculation was pathology. Sensitivity, 95% confidence intervals (CI) and positive predictive values (PPV) were calculated. Group B: Unresectable by imaging criteria or awaiting surgery. Per patient data is reported.

Results: Group A (n=10). Sensitivity (95% CI) and PPV were: MDCT = 0.76 (0.57–0.95) and 0.97. PET/CT = 0.87 (0.74–0.98) and 0.90; P-MRI 0.98 (0.93–1.0) and 0.91. PET/CT missed subcentimetre lesions in 2 patients. Specificity and NPV cannot be calculated as all patients had CRLM. Group B (n=7). P-MRI found more subcentimetre lesions than PET/CT in 6 patients, precluding surgery. One patient had a solitary CRLM on both studies and awaits surgery.

Conclusion: Diagnostic performance of P-MRI exceeds that of MDCT and PET/CT for CRLM, especially for subcentimetre metastases. These preliminary data suggest it should be part of the routine pre-resection workup for CRLM pending results of larger trials.

SS 2.08

Detection of malignant hepatic lesions: value of adding ferucarbotran-enhanced MRI to gadobenate dimeglumine enhanced MRI

J. Choi, M.J. Kim, J.S. Lim, J.H. Kim, M. Park, J. Chung, H. Hong, K.W. Kim, H.S. Yoo; Seoul/KR

Purpose: To evaluate whether ferucarbotran-enhanced MRI provides additional value for the detection of malignant hepatic lesions compared with gadobenate dimeglumine (Gd-BOPTA)-enhanced imaging.

Material and methods: Forty five patients with known malignant hepatic lesions underwent gadobenate dimeglumine- and ferucarbotran-enhanced MRI. Fifty metastases and 28 hepatocellular carcinoma (HCC) were confirmed by histopathology or intraoperative US. Two radiologists independently reviewed the Gd-BOPTA-enhanced dynamic and hepatobiliary phase images and then evaluated the combined Gd-BOPTA and ferucarbotran-enhanced images. The accuracy of lesion detection was compared by the areas (Az) under the receiver operating characteristic (ROC) curve. Sensitivity and specificity for detection of malignant lesions were also calculated.

Results: The overall accuracy for detecting malignant lesions was not significantly different between the Gd-BOPTA (Az=0.977 and 0.947 for reviewers 1 and 2, respectively) and combined Gd-BOPTA and ferucarbotran-enhanced images (Az=0.973 and 0.947). The mean sensitivities and specificities of Gd-BOPTA were 94.2 and 95.7%, respectively, and those of combined Gd-BOPTA and ferucarbotran-enhanced images were 94.2 and 94.3%, respectively. When metastases and HCC were considered separately, the detection rate was similar with the two image sets (P>0.05). No statistically significant differences in the mean sensitivity were seen between the two image set in the detection of small metastasis (≤1 cm) (84.4% for Gd-BOPTA and 81.3% for combined Gd-BOPTA and ferucarbotran-enhanced images).

Conclusion: The addition of ferucarbotran-enhanced MR images to the Gd-BOPTA did not significantly improve the detection rate of malignant hepatic lesions.

SS 2.09**Diagnostic value of diffusion-weighted MRI in focal hepatic lesions**

R. Maksimovic, M. Dunjic Kratovac, G. Lilic, D. Masulovic, R. Milenkovic, L. Lazic; Belgrade/RS

Purpose: The study was designed to determine if there is a difference between apparent diffusion coefficient (ADC) values using MRI with different b factors and to compare ADC values of hepatic lesions.

Material and methods: The study included 63 patients with focal hepatic lesions, 52 men (82.5%), age 62.1±9.8 years. Fourteen patients (22.2%) had hepatocellular carcinoma (HCC) confirmed on surgery, 16 patients (25.4%) were with hepatic metastatic colorectal tumours confirmed on previous surgery, 17 patients (26.9%) with cavernous haemangioma and 16 patients (25.4%) with hepatic cysts based on clinical manifestation, US/CT/MRI and follow-up results. MRI was performed with 1.5 T scanner, with a body coil using EPI sequence with tree b values 0, 400, 800 s/mm². ADC values were measured in all the lesions and assessed among the groups.

Results: ADC values were statistically different among the groups (F=70.7, p<0.01), with the following values: HCC patients 1.11±0.29, metastatic tumours 2.18±0.15, haemangioma 2.22±0.32, cysts 3.08±0.03 (3.1±0.03) s/mm². Further comparison revealed statistically significant difference among HCC, haemangioma and cysts patients (p<0.05), while there was no significant difference among haemangioma and secondary tumors (p>0.05). Furthermore, there was a difference between benign conditions (haemangioma and cysts, 2.36±0.43) and malignant diseases (HCC and secondary tumors, 1.52±0.58), t=5.6, p<0.01.

Conclusion: ADC values based on three b values can be helpful in differentiating focal liver lesions, in particular between benign and malignant conditions.

SS 2.10**Respiratory-triggered echo-planar diffusion-weighted MRI for the differentiation between benign and malignant focal liver lesions smaller than 10 mm: experience in 95 patients**

K. Holzapfel, M. Bruegel, C. Ganter, M. Eiber, E.J. Rummeny, J. Gaa; Munich/DE

Purpose: To evaluate diffusion-weighted MR imaging (DWI) using a respiratory-triggered single-shot echo-planar imaging (SSEPI) sequence in the characterization of liver lesions with a diameter of up to 10 mm.

Material and methods: 95 patients with focal liver lesions (45 cysts, 37 metastases, 21 hemangiomas and 5 HCCs) underwent MRI at 1.5 T using a body-phased array coil. DWI was performed by a non breath-hold SSEPI sequence (TR=∞, TE=69 ms, matrix 144x192, slice thickness 5 mm, GRAPPA2, b-values 50/300/600 sec/mm²) combined with navigator echo technique (PACE). Lesion-to-liver contrast-to-noise ratio (CNR) was determined at b=50 and 600 sec/mm² and the ratio of these CNRs (CNR50/600) was calculated for each lesion. Additionally, ADC-values were obtained. Imaging results were correlated with histopathologic findings and imaging follow-up. Mann-Whitney test was used for statistical analysis and a ROC analysis was performed.

Results: The mean ADC-values (x 10⁻³ mm²/sec) were 1.01±0.14 for HCCs, 1.10±0.21 for metastases, 1.80±0.20 for hemangiomas and 2.51±0.43 for cysts. CNR~50/600~-ratios were 0.97±0.08 for metastases, 1.02±0.22 for HCCs, 1.43±0.18 for hemangiomas and 2.22±0.53 for cysts. CNR~50/600~-ratios and ADC-values of hemangiomas and cysts were significantly higher than those of HCCs and metastases. 97.2% of lesions were correctly classified as benign or malignant using a threshold ADC-value of 1.53.

Conclusion: DWI using the respiratory-triggered SSEPI sequence allows reliable differentiation between benign and malignant focal liver lesions, even when the diameter of lesions is 10 mm or less.

11:00 - 12:30

Topkapi A

Scientific Session 3**GI / Tube / Morphology and function****SS 3.01****High-resolution MRI offers an accurate method for predicting operability in oesophageal cancer**

A.M. Riddell¹, G. Brown¹, A.C. Wotherspoon², Y. Barbachano¹, C. Richardson², W.H. Allum²; ¹Sutton/UK, ²London/UK

Purpose: The presence of a positive circumferential resection margin (CRM) is considered to confer a poor prognosis in patients with oesophageal cancer. The aim of this study was to establish whether high resolution MRI can accurately predict operability, based on achieving a negative CRM, and thus improve patient selection for surgery.

Material and methods: In this prospective study, 60 patients with biopsy proven adenocarcinoma, median age 64 yrs (range 43–81), M:F - 7.5:1 underwent MRI using an external surface coil in addition to CT and endoscopic ultrasound (EUS) staging. Two radiologists independently reviewed the MRI studies blinded to results of conventional staging, surgery and pathology. MRI operability was predicted based on achieving a negative CRM. MRI prediction was compared with histopathology as the gold standard to establish the accuracy of the technique. MRI prediction was compared with EUS (McNemar's test). A positive CRM was defined as tumour at or within 1 mm of the CRM. The level of agreement between radiologists was determined using a kappa score.

Results: CT and EUS considered all patients bar 1 'borderline' case, as operable. All resections were performed with curative intent. At laparotomy, 5/60 (8.3%) patients were inoperable, all predicted by MRI. 16/60 (27%) had an R1 resection. There were 4 false positive and 7 false negative predictions with MRI, giving a sensitivity, specificity and accuracy for predicting margin status of 67, 90 and 82%, respectively. The MRI accuracy was higher than EUS 67% (p=0.078). There was a good agreement between the radiologists for margin prediction: kappa score 0.7 (CI 0.51–0.89).

Conclusion: High resolution MRI using an external surface coil offers an accurate, non-invasive method for predicting operability in patients with oesophageal cancer. Its use could help refine patient selection for surgical resection.

SS 3.02**Post-op tumor recurrence in stomach carcinoma: analyses of preoperative status and recurrence pattern**

K.N. Jee, I.H. Jeong, Y.S. Lee, Y. Kim; Cheonan/KR

Purpose: We evaluated the post-op tumor recurrence pattern in stomach carcinoma (SC) on MDCT findings and also assessed the primary pathology, location, and staging in the recurred cases after curative resection.

Material and methods: From July 2003 to June 2007, 450 had CT scans for the evaluation of tumor recurrence after curative resection of stomach cancer. Among them, 46 patients were diagnosed with recurrence of stomach cancer after curative resection but 38 patients had available preoperative information. All recurred cases were clinicopathologically confirmed. Their mean age was 62.3 year-old (range, 33–81) and male to female ratio was 31 to 8. We analyzed and correlated the recurred cases about primary location in stomach, post-op staging and gross and microscopic pathologies. We also evaluated the MDCT findings and medical records when the tumor recurrence had been diagnosed

Results: Location: cardia/fundus (3), body (8), antrum (21), or both (6). EGC (2), AGC (36). Well - (4), moderately - (14), or poorly differentiated/signet ring cell/mucinous (14) and combined neuroendocrine differentiation (2). Staging: IA (2), IIB (5), II (4), IIIA (13), IIIB (15). Pattern: local recurrence (3), lymphatic - (17), hematogenous - (24), and peritoneal metastasis (17), more than one (16).

Conclusion: More recurrence was noted in advanced gastric cancer, initially young age, histology of poorly differentiated or signet-ring cell type, and there is no difference of recurrence rate between the primary locations.

SS 3.03**MRI assessment of GI dysfunctions after a standardized meal**

V. Garbarino, F. Maccioni, B. Ciccantelli, M. Martinelli, F. Carozzo, M. Marini; Rome/IT

Purpose: To evaluate with MRI the values of gastric emptying in adult dyspeptic patients.

Material and methods: Five healthy volunteers and 14 patients with functional dyspepsia underwent MRI before and after 2 hours -30 minutes from a standardized meal (350 ml of water, 250 ml, 600 ml total). MRI was performed at 1.5 Tesla, on axial-coronal planes using T2-weighted HASTE (Half-Fourier SnapShot Turbo Spin-Echo) sequences. The fundic and overall gastric volume, the fundus/overall gastric volume ratio, the amount of gastric air before and after meal, the initial gastric volume were calculated; the gastric emptying curves and entero-colic variations of air-fluid content were assessed.

Results: In healthy volunteers, the mean residual volume and mean final fundic volume were 213 and 62.6 ml, whereas in dyspeptic patients they were, respectively, 251.4 and 82.5 ml. In pathologic patients, the mean fundus/stomach ratio was 0.46 before and 0.38 after the meal. In healthy volunteers, it was 0.75 before and 0.41 after the meal. In pathological subjects, the mean amount of gastric air before was 1.9 ml; in pathological subjects, it was 11.26 ml. In dyspeptic patient, the gastric emptying time at 2.5 hours was delayed in 2 patients (21-37%); in 12 it was within normal limits (57-70%). MRI data were correlated with clinical findings.

Conclusion: Preliminarily, MRI seems a promising modality to assess gastric dysfunctions in dyspeptic patients.

SS 3.04**Evaluation of bowel motility by cine-MRI to detect bowel stenosis, adhesions or disturbances of peristalsis**

T. Heye, W. Hosch, G.W. Kauffmann, H.U. Kauczor, B. Radeleff; Heidelberg/DE

Purpose: Implementation of a cine-MRI sequence to enhance diagnostic performance of hydro-MRI studies to identify relevant stenosis or adhesions of the small/large bowel.

Material and methods: In this ongoing study, a total of 37 patients (median 45 yrs, age range 0-76, 14 m, 23 f) were examined in a 1.5 Tesla MRI scanner by trufisp cine-MRI (10-12 slices, 10 measurements/slice, 7-10 mm slice thickness) to display real time bowel movement after oral intake of water and rectal filling with methyl cellulose. A standard hydro-MRI of the bowel was then added. 23 patients were referred for adhesions, 12 patients for inflammatory bowel disease, 1 patient for evaluation of a bowel stenosis and 1 patient for evaluation of bowel motility.

Results: 9 patients underwent surgery: in 6 patients with adhesions by MRI and relevant bowel obstruction surgery confirmed the diagnosis. 2 patients without adhesions by MRI underwent surgery for other reasons which showed no adhesions. In one patient, a relevant bowel stenosis was found by MRI and confirmed by surgery. In one patient, stenosis of bowel anastomosis was diagnosed by MRI and confirmed by fluoroscopy. 27 patients without findings by MRI were followed up without signs of bowel impairment so far.

Conclusion: Dynamic cine-MRI of the bowel is beneficial by directly visualizing bowel motility to assess the functional relevance of a suspected bowel stenosis or impairment of bowel peristalsis.

SS 3.05**CT enteroclysis: role in diagnosis and management of low grade small bowel obstruction**

J. Nair, D.U. Kakde, V. Rathi; Nagpur/IN

Purpose: To demonstrate clinical feasibility and combined advantages of enteral challenge, cross sectional imaging and MDCT in the diagnosis and management of low grade small bowel obstruction (SBO).

Material and methods: Thirty patients with clinical suspicion of SBO were subjected to CT enteroclysis from September 2006 to September 2007. With informed consent, a 12 CH/FR Frekatube 120 cm gastroduodenal tube was positioned into the duodeno-jejunal junction under fluoroscopic guidance. Methyl cellulose preparation was infused @ of 150-200 ml/min. In all patients, CT enteroclysis was performed with dual slice helical CT scanner. Using 2 x 5 mm collimation, 120 kvp, 165 mA and 12.5 mm table speed, images were obtained.

1-2 ml IV buscopan was administered to the patient. Non-ionic contrast media was injected @ 2.5 ml/sec. Plain, arterial phase and venous phase (60 sec delay) images are obtained using 2 x 3 mm collimation. Soft tissue windows (WW=360 HU, WL= 40 HU) for viewing and 3D MPR reformation was done with thin 3 mm sections in spiral protocol.

Results: CT enteroclysis was well tolerated in all patients. Out of 30 patients, the order of occurrence of causes of SBO were adhesions 43%, strictures 27%, neoplasm 10%, vascular 7%, and others 13%.

Conclusion: The combination of multiplanar reformatting, volume challenges of enteroclysis provides accurate assessment of overlapping loops making CT enteroclysis an important tool in the diagnosis and management of low grade SBO.

SS 3.06**MDCT evaluation of the small bowel pathologies using oral administration of hypodense isotonic solution**

S. Mazzeo, V. Battaglia, C. Cappelli, F. Forasassi, L. Novaria, A. Belcari, C. Bartolozzi; Pisa/IT

Purpose: To assess the role of MDCT in the evaluation of small bowel in different pathologic conditions.

Material and methods: CT examinations of 106 patients with suspected/certain small bowel diseases were retrospectively analysed. CT protocol included oral administration of 2 L of polyethylene glycol solution and scans before and 50" after i.v. contrast medium administration. Patients were divided into four groups: suspected/certain chronic inflammatory disease (A), suspected neoplastic lesion (B), malabsorption (C), aspecific abdominal pain, and occult bleeding or fever of unknown origin (D). Wall thickening, parietal contrast enhancement, valvular distribution, extraparietal involvement and abnormalities of the abdominal organs were analysed. CT findings were compared to clinical/laboratory findings, results of barium follow-through, ileo-colonoscopy findings and surgery.

Results: CT examination allowed a correct diagnosis in 86/106 cases; 20 patients were not included in the study because of inadequate bowel distention. At histopathology, patients resulted to be affected by: Crohn's disease of the small bowel (38), duodenal Crohn (1), granulomatous colitis (3), malabsorption (8), neoplastic lesion (4), post-actinic conglomeration of ileal loops (1), lymphangiectasia (1) and ulceration of the last ileal loop (1). CT showed a sensitivity, specificity and diagnostic accuracy of 91, 93 and 92%, respectively.

Conclusion: MDCT of the small bowel represents a valid alternative to conventional radiographic studies and to small bowel methylcellulose enteroclysis spiral CT examinations.

SS 3.07**Influence of temporal resolution on tumour perfusion CT measurements: implications for helical perfusion CT techniques**

V. Goh¹, J.V. Liaw¹, D. Wellsted², S. Halligan²; ¹Northwood/UK, ²London/UK

Purpose: Helical perfusion CT techniques are being developed to enable a greater tumour volume to be assessed, yet scan temporal resolution achievable currently may preclude accurate measurement. Our purpose was to determine how scan temporal resolution influences ultimate colorectal cancer vascular parameters.

Material and methods: Following institutional review board approval, 45 patients with colorectal adenocarcinoma underwent a 65-second CT perfusion study: blood flow, volume and permeability surface area product were determined using commercial software based on distributed parameter analysis for three different temporal intervals between acquisitions (1, 2, 3 seconds, respectively). Mean blood flow, volume, and permeability surface area product measurements obtained for these three different intervals were compared using analysis of variance; statistical significance was at 5%.

Results: Mean (SD) for blood flow, volume and permeability surface area product were 71.5 ml/min/100g tissue, 6.33 ml/100g tissue, and 14.9 ml/min/100g tissue; 86.6 ml/min/100g tissue, 6.30 ml/100g tissue and 14.5 ml/min/100g tissue; and 97.8 ml/min/100g tissue, 5.98 ml/100g tissue and 14.5 ml/min/100g tissue for 1, 2 and 3 second intervals, respectively. Blood flow rose significantly as the temporal interval increased (p=0.008).

Conclusion: Increasing the interval between acquisitions overestimates tumour blood flow, but not blood volume or permeability surface. Unless a temporal resolution better than 3 seconds can be achieved, helical perfusion CT techniques will inaccurately estimate blood flow.

SS 3.08**Ionizing radiation exposure from CT in patients with Crohn's disease: which patients are most at risk?**

K. O'Regan, C. Curran, A. Desmond, S. Mc Williams, S.E. Mc Sweeney, F. Shanahan, M. Maher; Cork/IE

Purpose: CT has become the first line imaging tool for the evaluation of patients with Crohn's Disease (CD). The most severely affected patients often undergo multiple imaging studies due to the chronic relapsing and remitting nature of the condition. We investigated the clinicopathological features of patients with CD that may influence which patients are most likely to undergo multiple CT examinations.

Material and methods: From a local database of 390 patients (Mean age 38.9 yrs; range 16–84; 206 F: 184 M) with CD at a single tertiary referral centre, patients who had undergone CT during the period 1998–2006 were selected. CTDIw and DLP were calculated using standard CT phantoms for all head, chest and abdominal CT studies. Effective Dose was subsequently calculated using standard conversion factors. Patient characteristics, Montreal classification, medications and surgeries were documented.

Results: A total of 130 patients underwent 325 CT examinations at our institution (Mean 2.5 scans per patient, range 1–11). Of these, 52.3% (n=68) underwent more than one CT examination. A cumulative effective dose of >20 mSv was found in 22.3% of patients from CT alone. We examine the influence of surgery, medications and disease severity score on total cumulative effective dose from CT.

Conclusion: Subsets of patients with CD are at risk of potentially harmful doses of ionizing radiation. Low dose CT protocols or alternative modalities such as MRI should be considered.

SS 3.09**Dynamic contrast enhanced MR of the bowel wall in celiac disease**

G. Masselli, E. Casciani, E. Poletti, A. Picarelli, A. Piermattei, P. Palumbo, G.F. Gualdi, A. Pittalis, D. D'Amico, S. Caprasecca; Rome/IT

Purpose: To prospectively evaluate the role of contrast-enhanced MR for dynamic evaluation of the enhancement kinetics of bowel wall in celiac patients.

Material and methods: Forty-five patients with celiac disease and 10 healthy volunteers were examined with MR. 22 patients were untreated and 23 patients were treated with a gluten-free diet at the time of examination. Coronal dynamic 3D GRE T1-weighted sequences were performed every 20 sec for a total duration of 5 minutes after contrast administration. Quantitative analysis of bowel wall enhancement kinetics was performed evaluating the slope of enhancement, enhancement ratio and thickness of the small-bowel wall at the level of duodenum. These MR dates were compared with laboratory studies and endoscopy findings.

Results: Untreated patients with flat mucosa showed a higher enhancement ratio, followed by untreated patients with mucosal subatrophy, treated patients and healthy volunteers. A statistically significant difference was noticed between the enhancement ratio of healthy volunteers and both those of untreated patients with subatrophy (p=.018) and of the patients with complete atrophy (p=.012) as well as between the enhancement ratio of the treated patients and both those of the untreated patients with subatrophy (p=.030) and of the patients with complete atrophy (p=.025).

Conclusion: The enhancement ratio of bowel wall can be an effective and reproducible way of expressing the severity of celiac disease.

SS 3.10**MR-colon transit time examination and MR-defecography results in chronic constipated patients**

S. Kirchhoff, C. Kirchhoff, M. Kreis, K.W. Jauch, M.F. Reiser, A. Lienemann; Munich/DE

Purpose: The aim of this study was to determine the value of MR- colonic (MR-C) transit time in comparison to MR-defecography (MR-D) in patients suffering from chronic constipation.

Material and methods: 10 patients suffering from chronic constipation following "Rome II criteria" were examined using MR-visible markers for the assessment of the colonic transit time. In all patients, a dynamic MR-D examination was performed as well. For comparison reasons, 10 healthy volunteers also underwent the MR-transit time examination.

Results: Regarding the assessed total colon transit time, the healthy volunteers showed a mean transit time of 42±9.3 hrs. In comparison, the 10 female patients with chronic constipation presented with a significantly prolonged transit time throughout the entire colon of 68.5±7.8 hrs. The most common findings in MR-D was an intussusception and rectoceles of different extent.

Conclusion: To differentiate between chronic constipation and anorectal disorders or a combination of both, an MR-C transit time examination should be performed as well as an MR-D.

11:00 - 12:30

Topkapi B

Scientific Session 4**Pancreatic tumours: detection, differential diagnosis and follow up****SS 4.01****Resectable ductal adenocarcinoma: enhancement pattern at contrast-enhanced US as preoperative prognostic factor**

M. D'Onofrio, R. Malago, G. Zamboni, N. Faccioli, F. Principe, R. Pozzi Mucelli; Verona/IT

Purpose: To determine whether enhancement pattern of ductal adenocarcinoma (DA) of the pancreas at contrast-enhanced ultrasonography (CEUS) is related to patients prognosis after surgery.

Material and methods: CEUS of 42 resected DAs of the pancreas were retrospectively reviewed. The lesion enhancement at CEUS was scored as: 1=poorly vascularized (presence of avascular areas) or 2=well vascularized (absence of avascular areas). All the lesions were resected and underwent pathological examination assessing tumor differentiation as: 1=undifferentiated (poorly differentiated) or 2=differentiated (moderately and well differentiated). The results of CEUS enhancement and pathology were correlated by using Spearman's test. Survival analysis during four years was made by Kaplan-Meier method.

Results: There were 30 differentiated and 12 undifferentiated adenocarcinoma at pathology. CEUS revealed poor vascularization in 9 tumors; while 33 adenocarcinomas resulted well vascularized. Moderate correlation was found between vascular pattern at CEUS and tumor differentiation (rs=0.70; p<0.0001). At CEUS 29/30 (97%) differentiated adenocarcinoma were well vascularized while 8/12 (67%) undifferentiated adenocarcinoma were poorly vascularized. Survival rate in group 1 of CEUS was significantly lower than that of group 2 (p=0.0011). Survival rate in group 1 of pathology was not significantly lower than that of group 2 (p=0.2892).

Conclusion: Correlation between vascular pattern of DA at CEUS and tumor differentiation was found. Vascular pattern of enhancement of DA seems to be a prognostic indicator.

SS 4.02**A new invasion score for determining the resectability of pancreatic carcinomas with MDCT**

L. Grenacher, M. Klaus, H. Tengg-Koblik, G.M. Richter, G.W. Kauffmann, H.U. Kauczor; Heidelberg/DE

Purpose: To evaluate a new vessel infiltration score to determine the resectability of pancreatic carcinomas in preoperative planning.

Material and methods: Eighty patients with suspected pancreatic tumor were examined prospectively using 16-row multidetector-spiral CT. The scans were evaluated with regard to the presence of pancreatic carcinoma, peripancreatic tumor extension, and vascular invasion using a standardized questionnaire. Invasion of the surgically relevant vessels was evaluated using a new invasion score. The operative and the histological findings and the clinical follow-up served as the gold standard.

Results: Forty patients had a pancreatic carcinoma, five had a metastasis of a different primary tumor, and in 35 patients there was no malignant pancreatic disease. The sensitivity for tumor detection was 100%, with a specificity of 88% for differentiating between malignant and benign pancreatic tumors. Invasion of the surrounding vessels was evaluated correctly using the invasion score with a sensitivity of 89% and a specificity of 99%. In evaluating resectability, a sensitivity of 94% and a specificity of 89% were achieved.

Conclusion: The invasion score could be a helpful tool for correctly assessing invasion in relevant vessels in cases of pancreatic carcinoma and for determining resectability.

SS 4.03**Evaluation of 320 slice CT in patients with pancreatic cancer**

S. Kandel, C. Kloeters, H. Meyer, F.J.F. Engelken, L. Krug, A. Lembcke, P. Rogalla; Berlin/DE

Purpose: Perfusion information may improve detection of pancreatic cancer (PC). Dynamic volume CT with 16 cm detector width covers the pancreas without patient movement. The aim was to develop a dynamic scanning protocol for pancreatic perfusion imaging in order to detect lesions with abnormal perfusion.

Material and methods: The 320-slice CT unit was used for evaluation of 7 patients with suspected cancer of the pancreas. Scanning was performed with 0.5 mm slice thickness and 0.25 slice interval. Patients were prepared with oxygen hyperventilation before scanning. Scanning was started manually after contrast injection (6–8 ml/s, 350 mg iodine/ml) and dynamic density measurements in the right ventricle. Datasets were acquired over 180 seconds. After image registration, ROIs were defined for perfusion measurements. Perfusion maps were generated for visualization. The study had ethics committee approval.

Results: Registration of datasets enabled successful generation of perfusion information and required 2 min of calculation time. Perfusion differences between PC and normal tissue could be visualized using postprocessed colour maps. Total radiation exposure was comparable to the dose deposited by standard triphasic pancreas CT scans.

Conclusion: Perfusion imaging of the pancreas is feasible using dynamic volume CT technology. To avoid high radiation exposures, low-dose acquisition is mandatory and does not hinder perfusion analysis. Perfusion imaging carries the potential to facilitate differentiation of cancerous and normal pancreatic tissue.

SS 4.04**64-row MDCT versus gadobenate-enhanced 3.0 T MRI for detection and classification of pancreatic tumors**

C. Koelblinger, A. Ba-Ssalamah, C. Kulinna-Cosentini, G. Schueller, P. Goetzinger, W. Schima; Vienna/AT

Purpose: To prospectively compare the diagnostic performance of 64-row MDCT and gadobenate-enhanced 3.0 T MR imaging for detection and classification of pancreatic masses.

Material and methods: 44 patients were prospectively examined within one week with 64-row MDCT (Sensation 64, Siemens) and gadobenate-enhanced 3.0 T-MRI (Trio, Siemens). The CT protocol consisted of unenhanced, pancreas-parenchymal and portal-venous phase images acquired after injection of 150 ml Iomprol® (300 mg iodine/ml; flow-rate 5 ml/s). MRI included T1w-GRE, T2w-TSE with and without fatsat, MRCP, dynamic and 60 min-delayed gadobenate (MultiHance®, @0.1 mmol/kg)-enhanced T1w-3D-VIBE sequences. The standard-of-reference (surgery, n=21; biopsy, n=16; follow up, n=7) revealed 28 adenocarcinomas, 7 metastases, 1 neuroendocrine tumor and 6 benign lesions. Images were evaluated by one blinded reader.

Results: CT detected 38/41 (93%) and MRI detected 40/41 (98%) of the pancreatic tumors. All 28/28 adenocarcinomas were shown by MRI whereas CT failed to show two adenocarcinomas (n.s.). One inflammatory mass was depicted with MRI only, and another mass was incorrectly identified with MRI (false-positive). One gastric cancer metastasis was only detected with CT. One focal steatosis was incorrectly classified with CT. Accuracy for lesion classification was 90% with CT and 93% with MRI. Accuracy for neoplastic vessel infiltration was 95% for CT and 98% for MRI (n.s.).

Conclusion: Gadobenate-enhanced 3.0 T-MRI seems to be slightly superior (not significant) to 64-row MDCT regarding detection and classification of pancreatic tumors.

SS 4.05**Follow-up examinations in patients with inoperable pancreatic cancer using multislice-CT**

M. Klaus, C. Alt, T. Welzel, G.M. Richter, G.W. Kauffmann, H.U. Kauczor, L. Grenacher; Heidelberg/DE

Purpose: To evaluate the value of multislice-CT (MSCT) in follow-up examinations of patients with inoperable pancreatic cancer during neoadjuvant therapy.

Material and methods: 26 patients with inoperable pancreatic cancer underwent MSCT before and after neoadjuvant therapy. Tumor extension, infiltration and resectability were evaluated by two radiologists independently; vascular invasion was described using a score system. Staging was done in 10 patients by surgery, in 16 patients by biopsy or clinical follow-up. Kappa-analysis was used to evaluate the consensus of the readers.

Results: Sensitivity for the assessment of irresectability was 100%. In 54% of the carcinomas, tumor volume decreased after therapy (14/26), 42% increased (11/26) and one carcinoma remained stable. Infiltration of portal vein changed in 9 patients (5 higher, mean score 10.4/16.2; 4 lower score, mean score 17.5/11.5). Superior mesenteric vein infiltration changed in 17 patients (12 higher, mean score 11/14.4; 5 lower score, mean score 16.2/14.6 - p=0.026). Hepatic artery infiltration changed in 7 patients (4 higher, mean score 5.7/10.2; 3 lower score, mean score 11.6/10.3 - p=0.182). In 3 cases, score for the celiac trunk increased during therapy (score 3.3/10) (p=0.066). The results of the Kappa-analysis were between 0.56 and 0.87.

Conclusion: MSCT is adequate to evaluate the progression of irresectable pancreatic carcinoma during therapy. The infiltration score is useful to assess changes of vessels invasion.

SS 4.06**Radiological diagnosis of recurrence after pancreatic cancer: is there a pattern?**

T. Heye, N. Zausig, W. Hosch, G.W. Kauffmann, H.U. Kauczor, B. Radeleff, G.M. Richter; Heidelberg/DE

Purpose: Definition of radiomorphological criteria to differentiate unspecific postoperative changes from true relapse in the follow-up of pancreatic cancer after surgery.

Material and methods: In this ongoing study, all patients (since 2002) with operative therapy due to a malignant primary tumor of the pancreas (n=511) were included if they had frequent follow-up hydro-CT exams (n=245). The operative technique, R-status, T-stage and development of tumor markers were evaluated. Two radiologist analyzed CT data independently. Local recurrence, lymph node recurrence and organ metastasis have been distinguished by previously established criteria's. Surgery and progression of findings on follow-up CT exams were considered as gold standard.

Results: Follow-up CT exams demonstrated tumor recurrence in 42 patients. The mean follow-up interval was 3.7±1.9 months, the mean relapse free time period 12±6.2 months. In 25 patients with a local recurrence, 11 patients showed recurrence along the superior mesenteric artery and 10 patients laterally the celiac trunk. In 12 patients with lymph node recurrence, 7 patients showed recurrence left laterally the aorta and 5 in the mesenteric root. Surgery confirmed these findings in 12 patients and follow-up CT in 30 patients, tumor markers increased simultaneously by a mean factor of 5.8±9.2 in 72% of the cases.

Conclusion: Our experience so far shows that specific changes of recurrence are found especially in the run of the peripancreatic cardinal vessels indicating a pattern of recurrence for local relapse and lymph node recurrence.

SS 4.07**Prospective evaluation of cystic pancreatic lesions: MDCT with pathological correlation**

D. Sahani, N. Sainani, S. Fritz, S. Crippa, V. Deshpande, C. Fernandes-del Castillo; Boston, MA/US

Purpose: Categorization of cystic pancreatic lesions into mucinous and non-mucinous on MDCT. Accuracy of MDCT in characterizing lesions and differentiating benign from malignant. Evaluation of MDCT features that are predictors of malignancy. Determine whether cyst size impacts accuracy.

Material and methods: In this prospective study, 73 consecutive patients (27 M: 46 F, age 23–89 years) with 93 cystic lesions (size 7–100 mms) underwent a dedicated thin-section pancreatic protocol 16-MDCT. Morphological features of the lesions were recorded on a template. All patients underwent surgical exploration and pathological features served as reference standard.

Results: Pathologically, 64/93 lesions were mucinous, 29/93 non-mucinous. 31/93 lesions were malignant, 50/93 benign, 12/93 borderline. 22/31 malignant lesions were mucinous. Among 29 non-mucinous lesions, 14 were benign cysts, 4 SCAs, 9 adenocarcinomas and 2 SPPNs. MDCT accuracy for mucinous v/s non-mucinous and various subtypes was 80 and 70%, respectively; sensitivity and specificity for malignancy and benignity was 65 and 80%. Features favoring malignancy were mural nodules, MPD dilatation and biliary obstruction with PPV of 80, 88 and 100%, respectively. Borderline lesions could not be distinguished on MDCT. MDCT accuracy was better for larger lesions (>30 mm).

Conclusion: Thin-section MDCT allows reliable differentiation of mucinous and non-mucinous cysts. MDCT features can characterize malignant from non-malignant lesions with moderate accuracy. MDCT accuracy for characterization and detection of malignancy is superior for lesions larger than 30 mm.

SS 4.08**Solid pseudopapillary carcinoma of pancreas: CT and MRI differentiation from benign solid pseudopapillary tumor**J.H. Lee¹, J. Yu², H.K. Kim², J.K. Kim¹, T.H. Kim¹, M. Park², K.W. Kim², J.H. Kim¹, Y.B. Kim¹; ¹Suwon/KR, ²Seoul/KR

Purpose: The purpose of this study was to describe the CT and MRI findings that differentiate solid pseudopapillary carcinoma (SPC) from benign solid pseudopapillary tumor (SPT) of the pancreas.

Material and methods: Preoperative CT (n=23) or MR (n=16) images for histopathologically confirmed 26 patients (8 with SPC and 18 patients with benign SPT) were retrospectively reviewed, blinded either malignant or benign. In addition to the general morphologic features and contrast-enhancement patterns, the presence of pancreatic duct dilatation, vascular invasion, and extrapancreatic metastases were comparatively assessed.

Results: There were no significant differences between SPC and benign SPT with respect to the tumor size, location, capsule thickness, internal composition, and pattern of calcification, nor was there any correlation with the age and sex of the patients. Pancreatic duct dilatation was present in 4 of 8 (50%) SPC patients, while absent in all benign SPT patients (P=.005). Vascular encasement by the tumor (n=2, P=.086) and hepatic metastases (n=2, P=.086) were also exclusively demonstrated in SPC patients.

Conclusion: In conclusion, SPC could be differentiated from benign SPT using the imaging features of aggressive behavior of pancreatic duct dilatation, vessel encasement with or without metastases. And, if these imaging features are present, aggressive surgical approach is mandatory rather than laparoscopic pancreatectomy.

SS 4.09**Comparison between MDCT findings and histopathologic reports in assessing neuroendocrine pancreatic neoplasms nature**

S. Mazzeo, V. Battaglia, C. Cappelli, D. Caramella, G. Caproni, B. Pontillo Contillo, D. Campani, U. Boggi, C. Bartolozzi; Pisa/IT

Purpose: To evaluate the role of MDCT in assessing the nature of neuroendocrine pancreatic neoplasms (NPN).

Material and methods: We evaluated 30 patients with 49 pancreatic lesions (3 patients had, respectively, 15, 5 and 2 lesions). CT exams were performed before and after contrast medium administration in early arterial (20"), pancreatic (35"), venous (70") and delayed (180") phases. At CT, two different post-contrastographic patterns were identified: pattern A-lesions with early enhancement (arterial/pancreatic phase) and early wash-out (compared to pancreatic parenchyma); pattern B- lesions with early wash-in and absent/slow wash-out (B1) and lesions with enhancement only in venous phase (delay wash-in) (B2). For each lesion, the greatest diameter was also considered. CT results were compared with pathological results after surgery.

Results: Histopathology classified 23 as benign lesions, 18 as malignant and 8 borderline. At CT, 27/49 lesions showed pattern A (average dimension-a.d: 13 mm); at histopathology, 22/27 neoplasms resulted to be benign (a.d: 8 mm), 4 borderline and 1 malignant. Patterns B included 22/49 lesions (a.d: 41 mm); at histopathology 17/22 were malignant (a.d: 39 mm), 4 borderline and 1 benign. Pattern A showed a PPV of 82% in predicting lesions benignancy, while pattern B showed a PPV of 77% in predicting malignancy.

Conclusion: MDCT may suggest the nature of NPN basing on their enhancement pattern; lesion dimension >2 cm must be considered as the cut off for suspecting malignancy.

SS 4.10**The utility of diffusion-weighted MRI with secretin enhancement in the assessment of chronic pancreatitis**

F. Akisik, A.M. Aisen, K. Sandrasegaran, C. Lin, S. Sherman; Indianapolis, IN/US

Purpose: To compare the changes in pancreatic apparent diffusion coefficient (ADC) following secretin administration in symptomatic patients with and without chronic pancreatitis who underwent MRCP with diffusion-weighted imaging (DWI).

Material and methods: Patients were categorized as normal (no chronic pancreatitis), mild or severe chronic pancreatitis according to ERCP or endoscopic US criteria. MRCP (1.5 T) was performed with serial DWI (b values of 0, 100, and 400 sec/mm²) for 10 minutes after secretin injection. ADC values

before and after secretin were compared for the 3 groups.

Results: 89 patients were included (37 normal, 33 mild and 19 severe chronic pancreatitis). Mean pre-secretin and maximum post-secretin ADC values were higher in normal than mild or severe chronic pancreatitis patients, but did not differ significantly between the chronic pancreatitis patients. The percent increase in ADC post-secretin and the time to peak ADC did not differ among the three groups. Using ROC analysis, the ADC values that separates normal from chronic pancreatitis patients were 169 and 210 X 10⁻⁵ and mm²/s, for pre and post-secretin acquisitions.

Conclusion: Pancreatic pre- and post-secretin ADC may aid in the diagnosis of chronic pancreatitis.

11:00 - 12:30

Dolmabahçe A

Scientific Session 5**Imaging acute abdomen****SS 5.01****Split iv-bolus technique in abdominal CT of emergency room patients with acute abdominal pain**G.A. Zamboni¹, S. Gourtsoyianni², J. Romero³, V. Raptopoulos³; ¹Verona/IT, ²Heraklion/GR, ³Boston, MA/US

Purpose: To evaluate the routine use of split iv-bolus technique in emergency room (ER) patients undergoing abdominal CT for non-traumatic acute abdominal pain.

Material and methods: We reviewed retrospectively 157 consecutive ER patients with acute abdominal pain who underwent abdominal CT with split iv-bolus of 130-150 ml of contrast as follows: 1st 50 ml bolus; 3 minute pause; 2nd 80 ml bolus (100 ml for patients >55 Kg). Patients were scanned 65 sec after initiating the 2nd bolus. 64-row MDCT was used with 0.625 mm collimation acquisition, reconstructed at 5 mm axial, coronal and sagittal consecutive image display. Two radiologists reviewed the studies, graded parenchymal and vascular enhancement by consensus on a 5-point scale (1=none to 5=excellent) and measured attenuation in liver and spleen parenchyma, renal pelvis, aorta and porta to objectively assess contrast enhancement.

Results: A combined nephrographic+excretory phase was achieved (medians 4 and 5, respectively). The nephrogram had a late cortico-medullary pattern in most cases. Mean renal pelvis attenuation was 722 HU. The great vessels were well opacified (mean attenuation: aorta 191 HU, porta 169 HU) allowing for vascular evaluation (median=5). Enhancement of abdominal organs was satisfactory (mean liver and spleen attenuation: 116 HU and 130 HU, respectively). In no case the need was felt for additional early-parenchymal or delayed-excretory phase scanning.

Conclusion: Routine use of split-bolus iv-contrast administration is feasible in acutely sick patients, and results in an effective noninvasive exam informative of organ and vessel pathology.

SS 5.02**Radiological features of the diagnosis acute appendicitis on ultrasonography and CT**A. van Randen¹, W. Laméris¹, W.H. van Es², W. ten Hove³, E.M. van Keulen⁴, O.D. Henneman⁵, M.S. van Leeuwen⁶, P.M.M. Bossuyt¹, M.A. Boermeester¹, J. Stoker¹; ¹Amsterdam/NL, ²Nieuwegein/NL, ³Apeldoorn/NL, ⁴Hilversum/NL, ⁵Den Haag/NL, ⁶Utrecht/NL

Purpose: Evaluation of features on ultrasonography (US) and CT contributing to the diagnosis appendicitis in non-selected patients with acute abdominal pain at the emergency department (ED). Evaluation of features on US and CT contributing to the diagnosis appendicitis in non-selected patients with acute abdominal pain at the emergency department (ED).

Material and methods: US and CT were performed in consecutive patients with acute abdominal pain at the ED. Imaging features and diagnoses were prospectively recorded by independent radiologists for US and CT. Reference standard was the final diagnosis after 6 months of follow-up. Imaging features resulting in appendicitis or false-positive (FP) appendicitis for US and CT were evaluated with logistic-regression.

Results: 1021 patients were evaluated, 565 woman; mean age 47.4 years.

Observed probability of 100% of appendicitis at US had the combination: thickened appendix/ transducer tenderness and moderate appendiceal fat infiltration, and at CT 98%: visualized, thickened appendix/ increased appendiceal vascularity/ mild or moderate peri-appendiceal fat infiltration. Imaging features, significantly resulting in FP diagnoses of appendicitis were the single features: transducer tenderness ($p < 0.01$), thickened appendix ($p < 0.01$), and intact appendiceal layered wall ($p = 0.05$) for US, and thickened appendix ($p < 0.01$), mild ($p = 0.02$) or moderate ($p = 0.02$) peri-appendiceal fat infiltration for CT. Highest observed probability of FP was moderate peri-appendiceal fat infiltration on CT (13.1%) and transducer tenderness with intact appendiceal layered wall on US (50%).

Conclusion: Multiple positive imaging features increase the probability of appendicitis. Single findings as mild or moderate fat infiltration at CT or painful compression at US make appendicitis less likely.

SS 5.03

Feasibility of low-dose unenhanced MDCT in patients with suspected acute appendicitis: comparison with sonography

N. Karabulut¹, Y. Kiroglu, B. Koçak, B. Erdur, i Türkücüer; Denizli/TR

Purpose: To prospectively compare the accuracy of ultrasonography (US) and unenhanced low-dose multidetector row computed tomography (CT) in patients with suspected acute appendicitis by using surgery or clinical follow-up as the reference standard.

Material and methods: Fifty-four patients (26 males, 28 females) with suspected acute appendicitis underwent both US and unenhanced (without oral, rectal, or IV contrast) low dose CT of the lower abdomen using 50 effective mAs. The US and CT images were prospectively and independently reported by two different radiologists for acute appendicitis and an alternative diagnosis. Data from US and CT were compared, and the definite diagnosis was established by surgical findings ($n = 21$) or results of clinical follow-up ($n = 33$) as the reference standard.

Results: Twenty-one patients underwent surgery and had definite appendicitis. The sensitivity of CT and sonography was 91 vs. 91%, respectively; the specificity was 85 and 76%; the positive predictive value was 79 and 70%; the negative predictive value was 93 vs. 92%, and the accuracy was 87 vs. 81%, respectively. Alternative diagnoses were provided at CT in 10 of 33 (30%) cases without appendicitis. The mean outer diameters of the visualized appendices in patients with and without acute appendicitis, respectively, were 12 ± 4.1 mm vs. 6.7 ± 2.1 mm at CT ($p < 0.001$). The calculated mean effective radiation dose was 1.2 mSv for male and 2.1 mSv for female patients.

Conclusion: Eliminating the potential risks of contrast media and reducing hazards of radiation, low-dose unenhanced CT using 50 mAs is feasible for the evaluation of suspected appendicitis producing comparable diagnostic performance with US.

SS 5.04

Accuracy of the clinical diagnosis, a clinical prediction model, and imaging for the diagnosis of acute diverticulitis in patients with abdominal pain

W. Laméris¹, A. van Randen¹, B. van Ramshorst², E.J. Hesselink³, H.G. Gooszen⁴, J.W. Juttman⁵, P.M.M. Bossuyt¹, M.A. Boermeester¹, J. Stoker¹; ¹Amsterdam/NL, ²Nieuwegein/NL, ³Apeldoorn/NL, ⁴Utrecht/NL, ⁵Hilversum/NL

Purpose: To compare the accuracy of clinical diagnosis, a clinical prediction model, and US and CT for acute diverticulitis (AD).

Material and methods: Consecutive emergency department patients with non-traumatic acute abdominal pain underwent US and CT. Clinical findings and most likely clinical diagnosis were recorded prospectively. A prediction model, based on clinical variables, was built and accuracy of the model was calculated for the most optimal probability cut-off value. Accuracy of the model was compared with that of the clinical diagnosis, US, and CT.

Results: This study included 1021 patients (55% female; mean age 47 years (19–94)). AD was suspected in 126 patients and was present in 119 (prevalence: 12%). Sensitivity was 67% (95% CI: 59–76%) for clinical assessment and 76% (95% CI: 68–83%) for the prediction model, not significantly different ($p = 0.08$). Specificity was significantly higher for clinical diagnosis, 95% (95% CI: 93–96%) versus 89% (95% CI: 87–91%) ($p < 0.001$). Of US and CT, only CT had a significantly higher sensitivity, 94% (95% CI: 90–98%; $p = 0.01$), compared to the

clinical diagnosis. US in all patients gave a 35% missed rate, whereas this was 6% for CT with less false positives than clinical assessment only.

Conclusion: The accuracy of the clinical diagnosis of AD is moderate and is not significantly improved by a clinical prediction model. Therefore, CT imaging is warranted when AD is considered as a clinical diagnosis.

SS 5.05

Imaging integration in the evaluation of acute cholecystitis in a modern emergency department: role of US, MDCT and MR

M. de Vargas Macciucca, S. Lanciotti, M.L. de Cicco, G. Marcelli, G. Avventurieri, E. Casciani, G.F. Gualdi; Rome/IT

Purpose: To assess a new diagnostic guide-line in the US, MDCT and MR integration for the evaluation of acute cholecystitis (AC).

Material and methods: 35 patients (23 male; 12 female; median age 66.6 years) presenting AC were evaluated by US (Toshiba Aplio), 16-slice MDCT (Siemens Somatom Sensation 16) with i.v. cm and 1.5 MR (Siemens Avanto) in case of complications. Signs were considered major (stratified wall thickening, distention and US Murphy' sign), minor (bile stones, sludge and biliary dilatation) and specific for complication (pneumobilia, pericolecistic fluid or air, wall emphysema, intracholecystic air and missed identification of the gallbladder). Patients underwent surgery in emergency. The US findings were compared to MDCT and MR features; histologic results represented the gold standard.

Results: Concordance with histology was 70% for US and 100% for MDCT and MRI. US accuracy was 70%, sensitivity 42.8%, specificity 93.7%, PPV 85.7% and NPV 65.2%. In 3 cases, the gallbladder was not identified (abscessualization or perforation). MDCT and MR presented high accuracy, sensitivity and specificity for the diagnosis and stadiation of complications. MR presented better results than MDCT in the identification of causes of jaundice in presence of biliary dilatation.

Conclusion: If US shows complication signs, a II level exam is mandatory to indicate the correct therapeutic approach. This role is generally assessed by MDCT, but in case of biliary dilatation MR is recommended.

SS 5.06

Comparison of accuracy of US and CT in patients with acute abdominal pain at the emergency department

A. van Randen¹, W. Laméris¹, W.H. van Es², J.P.M. Heesewijk², B. van Ramshorst², W. ten Hove³, W.H. Bouma³, M.S. van Leeuwen⁴, E.M. van Keulen⁵, P.M.M. Bossuyt¹, M.A. Boermeester¹, J. Stoker¹; ¹Amsterdam/NL, ²Nieuwegein/NL, ³Apeldoorn/NL, ⁴Utrecht/NL, ⁵Hilversum/NL

Purpose: Head-to-head comparison of ultrasonography (US) and computed tomography (CT) in non-selected patients with acute abdominal pain (AP) presenting to the emergency department (ED).

Material and methods: Prospective evaluation of US and CT in all patients with acute AP >2 hours and <5 days at the ED. Excluded were patients to be discharged home from the ED without diagnostic imaging. Reference standard was final diagnosis after 6 months follow-up. Sensitivity, specificity, positive predictive value (PPV) and negative predictive value (NPV) of US and CT were measured for urgent versus non-urgent diagnoses and specific diagnoses causing acute AP.

Results: In total, 1021 consecutive patients were included: 565 females (mean age 47.4 yr); 661 patients (64.7%) had an urgent diagnosis, including 284 appendicitis and 118 diverticulitis. Sensitivity of urgent diagnoses was 0.70 for US versus 0.89 for CT ($p < 0.01$), while specificity was 0.85 and 0.77 ($p < 0.01$), respectively. PPV was 0.89 (95% CI: 0.87–0.92) for US and 0.88 (95% CI: 0.85–0.90) for CT, NPV was 0.61 (95% CI: 0.57–0.65) and 0.80 (95% CI: 0.75–0.84) ($p < 0.01$), respectively. CT had more false positive urgent diagnoses (8.2%; 84/1021) than US (5.4%; 55/1021) ($p < 0.01$). US had more false negative urgent diagnoses (11.3%; 115/1021) than CT (7%; 71/1021) ($p < 0.01$).

Conclusion: In non-selected ED patients, CT was overall better in detecting (urgent) disease than US. US missed significantly more urgent diagnoses, while CT overestimated urgent disease.

SS 5.07**Imaging the small bowel obstruction with MDCT: how to really help the surgeon, beyond the conventional search for the point of intestinal occlusion**

S. Romano, C. Stavolo, P. Lombardo, N. Gagliardi, L. Romano; Naples/IT

Purpose: Rivers of ink have been used to magnify the role of the MDCT in detecting the exact point of obstruction using multiplanar reformatting processing. However, poor interest appears to have had the evaluation of degree of the intestinal occlusion in order to answer the frequent question of the surgeons in emergency about the need to submit the patient to immediate intervention. In our study, we report the role of the MDCT in patients with small bowel obstruction (SBO) regarding the evaluation of the cause and various stages of disease.

Material and methods: A retrospective evaluation of the imaging findings of 220 adult patients with proven small bowel intestinal obstruction priorly submitted to emergency abdomen MDCT examination was made. Correlation between the clinical results and the imaging findings (small bowel dilation, transition point evidence, suggestive or evident cause of obstruction, feature of the intestinal wall, alterations in bowel enhancement) was made.

Results: Common and uncommon causes of SBO have been observed in our patient population. Appearance of the intestine was correlated to the definitive diagnosis. Complications with segmental infarction were mostly observed in patients with intestinal obstruction caused by volvulus.

Conclusion: MDCT examination could be considered of critical clinical usefulness in the assessment of the intestinal obstruction spectrum of findings in developing criteria for diagnosis and prognosis and to plan an effective surgical therapy.

SS 5.08**Role of 64-slice CT multiplanar reconstructions in acute mechanical bowel obstruction**

M. Galia, G. Lo Re, L. La Grutta, G. Brancatelli, T.V. Bartolotta, M. Midiri, R. Lagalla; Palermo/IT

Purpose: To illustrate the role of 64-slice CT in the diagnostic work-up of mechanical acute bowel obstruction. To highlight the advantages of isotropic multiplanar reconstruction (MPR) in the diagnosis of bowel obstruction.

Material and methods: 30 patients who underwent unenhanced 64-slice CT for suspected acute bowel obstruction (13 intussusceptions, 9 volvuli, 4 adhesions, 2 coproliths, 1 incarcerated hernia, and 1 gallstone ileus, all confirmed by surgery) were reviewed by two blinded experienced radiologists. The site and cause of the obstruction and the early signs of adverse features were independently evaluated. Firstly, only axial images were assessed. Subsequently, MPR images were in addition analyzed.

Results: The first reader correctly evaluated the cause of the obstruction, the site and initial adverse signs in 22/30, 18/30, and 20/30 cases using axial images, and in 28/30, 28/30, and 27/30 cases using MPR. The second reader correctly assessed the cause of the obstruction, the site and initial adverse signs in 24/30, 19/30, and 20/30 cases using axial images, and in 29/30, 27/30, and 29/30 cases using MPR. Despite an improved diagnostic confidence, the mean time for an integrated MPR interpretation was longer (13 vs. 8 minutes).

Conclusion: 64-slice CT provides high-resolution MPR imaging that improves diagnostic confidence (site, cause, and related adverse features) in bowel obstruction as compared with standard axial images. MPR integrated interpretation relatively increases the reading time.

SS 5.09**The use of CT in the detection and characterisation of large bowel obstruction**

E.M. Godfrey, S. Armitage, S. Etkind, N. Wilson, A. Shaw; Cambridge/UK

Purpose: CT of the abdomen and pelvis has become standard practice for patients with suspected large bowel obstruction despite a lack of evidence to support this approach.

Material and methods: We interrogated the radiology database at our institution to identify patients referred for CT with a clinical history of obstruction and dilated large bowel on a prior abdominal radiograph. The CT studies of these 48 patients were reviewed by a single radiologist to determine whether there was evidence of large bowel obstruction and, if so, the aetiology. The results were compared with the final diagnosis in the clinical records and histology database.

Results: Large bowel obstruction was diagnosed at CT in 12/48 patients, with no false positive results. In a single patient, there was a discrepancy between CT and surgical findings. On further review, incomplete obstruction was probably present as air was seen in a distended rectum. The correct aetiology was determined in 9/12 cases. In all 3 incorrect cases, we were unable to differentiate diverticulitis from colonic carcinoma. These results yield a sensitivity of 93%, specificity of 100% and accuracy of 75% in the detection and characterisation of large bowel obstruction.

Conclusion: CT has a high sensitivity and specificity in determining both the presence and site of large bowel obstruction. Distinguishing between diverticular and malignant strictures is problematic.

SS 5.10**Multislice CT for the diagnosis of acute mesenteric ischemia**

O.I. Karahan, S. Senol, H.Y. Akyildiz, A. Yikilmaz; Kayseri/TR

Purpose: We aimed to use multislice computed tomography (MSCT) for the differential diagnosis of mesenteric ischemia and other conditions associated with acute abdomen.

Material and methods: A total of 100 patients were included. Initially, images of the whole abdomen were obtained from the level of diaphragm downwards with 5 mm collimation including pelvis, without administration of intravenous contrast material. Then, 100 ml of nonionic contrast material was administered at a rate of 3.5 ml/s. Arterial (collimation: 1.25 mm) and venous (collimation: 5 mm) phase images were obtained at 25 and 60 seconds, respectively. CT angiography images were reconstructed by multiplanar, maximum intensity projection (MIP) and volume-rendering techniques.

Results: Laparotomy was performed in 42 cases for mesenteric ischemia or other causes of acute abdomen. The remaining 58 cases were followed conservatively. Among 42 surgical cases, mesenteric ischemia was confirmed in 20 cases. Among 21 cases diagnosed with mesenteric ischemia by the use of MSCT, 12 (57.1%) had emboli in SMA, 2 (9.5%) had thrombus in SMV, 1 (4.7%) had stenosis due to thrombosis, 1 (4.7%) had emboli in SMA and thrombus in SMV. The remaining 5 patients (23.8%) had patent SMA and SMV, which were diagnosed with the accessory CT findings for mesenteric ischemia.

Conclusion: MSCT with CT angiography is an effective imaging method for the diagnosis of acute mesenteric ischemia.

11:00 - 12:30

Marmara Hall

Scientific Session 6 CT Colonography - Technique / CAD

SS 6.01

Quantitative assessment of colonic movement between prone and supine patient positions during CTC

S. Punwani, C. Robinson, D. Hawkes, S.A. Taylor, S. Halligan; London/UK

Purpose: Position change between prone and supine CT colonography (CTC) acquisitions confounds segmental matching. While colonic mobility has been determined for barium enema, these data have not been established previously for CTC.

Material and methods: The centreline for 20 CTCs (10 male) with adequate colonic distension was determined for both prone and supine studies using a workstation and the colon divided into five segments. The spatial co-ordinates of each segment were related to the SMA origin by triangulation and the degree and direction of displacement between prone/supine studies determined.

Results: Mean displacement of centerline points within individual colonic segments was 3.6 (0.7), 3.1 (0.3), 3.5 (1.1), 4.6 (0.5) and 3.7 (SD 0.7 cm) cm for men and 2.9 (0.4), 3.2 (0.7), 3.1 (0.8), 4.1 (0.4) and 3.7 (SD 0.5 cm) cm for women for rectum, sigmoid, descending, transverse and ascending segments, respectively. On change from supine to prone position, overall colonic displacement reflected anterior abdominal wall compression. Rectum and sigmoid preferentially moved posteriorly and to the patient's right and ascending, descending and transverse colonic segments preferentially moved posteriorly. Furthermore, a caudal displacement was found for sigmoid, transverse and ascending colonic segments. There was no significant difference in total colonic length between the prone and supine position for men ($p=0.98$) or women ($p=0.87$).

Conclusion: Our findings suggest that when distended, colonic configuration change is small and dictated primarily by changes in abdominal compression rather than gravity.

SS 6.02

CTC: who should read it?

Z. Tarján, L. Lukács, N. Mészáros, J. Koloszá, Budapest/HU

Purpose: To evaluate if medical students using a CAD system could effectively read CTC.

Material and methods: Fifty colonoscopy controlled CTC data (with high lesion prevalence) were evaluated by 5th year medical students and a radiologist skilled in CTC reading. Five reading strategies were used: a) 2D reading, b) 2D reading with CAD prompts, c) 3D virtual endoscopy based reading, d) 3D with CAD prompt, and e) CAD read alone using an academic CAD system. The reading time and diagnostic accuracies of the different strategies were compared statistically by a Yates corrected chi square test.

Results: In detecting polyps and masses >5 mm, the radiologist using CAD prompts reached 0.93 and 0.7, medical students 0.85–0.89 and 5.2–6.3, while the CAD system alone 0.87 and 4.8 (sensitivity, false positive finding/case) ($p>0.05$). 2D reading by the radiologist with CAD prompts proved to be the fastest reading strategy (average 52+34 sec SD), while the students needed 267+123 sec SD for the same. Using 3D virtual endoscopy, the reading time was significantly longer ($p<0.05$), and yielded higher sensitivity, but less specificity ($p>0.05$) for all readers compared to 2D+CAD.

Conclusion: CAD prompts bring the sensitivity of medical students close to that of a skilled radiologist in reading CTC data, but the CAD or students with CAD could not rule out false positives effectively.

SS 6.03

Validating virtual colonoscopy training in the United Kingdom

P. Wylie, J. Muckian, A. Haycock, A. Gupta, M. Marshall, D. Burling; Harrow/UK

Purpose: Validation of virtual colonoscopy (VC) training supports uptake and may attract funding for national training initiatives. This study evaluates our radiographer course using Kirkpatrick's educational methods.

Material and methods: A 5-day 'hands-on' course designed to train small teams of subspecialist radiographers VC technique and interpretation was evaluated by assessment of knowledge, skills and performance outcomes via feedback, pre and post course MCQs, and pre and post test datasets (5 validated examinations each). Interim basic data (%/Mean/Median) is provided but five additional

courses (20 delegates) will be completed by ESGAR 2008, providing sufficient data for analysis (statistical advice sought): Paired t-tests for assessment of change in performance (MCQs/Interpretation accuracy/report times).

Results: Two courses (group 1 and 2; four delegates/group) were evaluated. Mean feedback satisfaction scores were 88%/98% for groups 1/2, respectively. Mean MCQ scores for group 1 decreased from 62 to 58% at the start/end of course; delegate fatigue was considered a contributing factor and therefore course timetable was revised. Mean MCQ scores for group 2 increased from 54 to 67%. Correct examination classification (all delegates) ranged from 20–100% (Mean/Median; 55%/50%) at start to 20–100% (Mean/Median; 65%/70%) at the end with large polyp (10 mm+) detection rates ranging from 0 to 78% (Mean/median; 33%/28%) and 22 to 67% (Mean /median; 53%/61%) at the start/end.

Conclusion: Interim evaluation demonstrates that our VC training course can improve radiographer performance.

SS 6.04

Impact of CAD on 27 CTC inexperienced readers

F. Turini¹, E. Neri¹, D. Regge², F. Cerri¹, G. Carmignani¹, C. Bartolozzi¹; ¹Pisa/IT, ²Candiolo/IT

Purpose: The goal is to determine whether CAD systems applied to CTC can be useful in supporting inexperienced radiologists in recognizing colorectal polyps and whether sensitivity increases when dealing with clinically significant lesions.

Material and methods: A hands-on training course on CTC, based on the direct teaching on workstations, has been carried out in Italy. Three groups of workstations were used: CADCOLON (Im3D, Italy), Voxar Colonscreen with Medicsight CAD (UK) and ColonVCAR (GE/Healthcare, US). Twenty-seven inexperienced radiologists (no CTC performed before the course) were involved in the study. The used dataset included 26 cases with different kind of lesions: 12 diminutive lesions (<6 mm), 12 medium size polyps (6–9 mm), 9 large polyps (>10 mm) and 6 masses (>3 cm). Participants had 20 minutes to assess each CTC dataset without CAD and then with CAD. They were asked to recognize the lesion, determine the morphology, size and location.

Results: The overall sensitivity for the detection of polyps of all sizes increased from 35 without CAD to 42% when using CAD (p -value<0.05). In particular, the sensitivity for the detection of small polyps moved from 18 to 27%, for medium size polyps from 33 to 36% and for large polyps from 60 to 68%.

Conclusion: CAD increases the performance of inexperienced radiologists in detecting colorectal lesions of all sizes. The readers judged the use of CAD helpful as a self-assessment tool.

SS 6.05

Computer aided detection in CTC: evaluation of benefit to the readers in a second reader paradigm

P. Braude¹, M. Zalcman², S. Virmani³; ¹Geneva/CH, ²Brussels/BE, ³Highland Heights, OH/US

Purpose: To assess the performance of readers without and with colon computer aided detection (CAD) assistance in second reader paradigm.

Material and methods: The study cohort included 29 CTC cases independent of the training cases used for algorithm development. Optical Colonoscopy (OC) results were considered the ground truth for polyp presence, size, type and location. A total of 66 polyps were identified by OC (31 <6 mm, 16 6–9 mm, and 19 ≥10 mm diameter). Two readers interpreted all cases (in random order) without and with CAD in a second read paradigm using 2D and 3D visualization (Perspective Filet View) techniques. Per-polyp sensitivity and per-patient false positive (FP) rate were calculated based on the combined results of the prone and supine CT datasets.

Results: Both readers showed an improvement in the polyp detection sensitivity with CAD assistance. Reader 1's sensitivities without CAD assistance for lesions 6–9 mm and ≥10 mm were 75.0% (12/16) and 73.7% (14/19), respectively, with 0.72 FP/patient. With CAD assistance, Reader 1's sensitivities for lesions 6–9 mm and ≥10 mm increased to 93.8% (15/16) and 89.5% (17/19), respectively, with 0.62 FP/patient. Reader 2's sensitivities without CAD assistance for lesions 6–9 mm and ≥10 mm were 43.8% (7/16) and 68.4% (13/19), respectively, with 0.55 FP/patient. With CAD assistance, Reader 2's sensitivities for lesions 6–9 mm and ≥10 mm increased to 68.8% (11/16) and 94.7% (18/19), respectively, with 0.41 FP/patient.

Conclusion: Both readers benefited from CAD. Increase in sensitivity and lower false positive rate were achieved.

SS 6.06**CTC: computer-aided detection of morphologically flat early (T1) colonic carcinoma**S.A. Taylor¹, G. Iinuma², J. Zhang³, S. Yutaka², S. Halligan¹;
¹London/UK, ²Tokyo/JP, ³Beijing/CN**Purpose:** To retrospectively evaluate the ability of computer-aided detection (CAD) software to detect morphologically non-polypoidal (flat) early colonic carcinoma using CTC.**Material and methods:** Twenty-four consecutive early (stage T1) carcinomas endoscopically classified as non-polypoidal (flat), [Paris classification-stage 0-II] were collected from a symptomatic population undergoing staging with multi-detector row CT colonography (CTC). The location of each tumour within CTC datasets was noted by three experienced radiologists in consensus aided by the endoscopic report. CAD software (ColonCAD 4.0, Medicsight PLC) was then applied at 3 settings of sphericity (0, 75 [default], and 100). Computer prompts for each patient were categorized as either true positive if the mark overlapped tumour boundary, or false-positive if located elsewhere. True positive CAD prompts were subclassified as focal (overlying a focal elevation beyond the contour of the main lesion) or non focal.**Results:** The 24 cancers were endoscopically classified as type IIa [n=11] and type IIa-IIc [n=13]. The mean size (range) was 27 mm (7–70 mm). CAD detected 20 (83.3%), 17 (70.8%), and 13 (54.1%) of the 24 cancers at filter settings of 0, 75, and 100, respectively. Most missed cancers were type IIa lateral spreading. The mean total number of false-positive CAD marks per patient at each filter setting was 36.5, 21.1, and 9.5, respectively, excluding polyps. At all settings, >96.1% of CAD true positives were classified as focal.**Conclusion:** CAD is effective for the detection of morphological non polypoidal (flat) cancer, although minimally raised lateral spreading tumors remain problematic.**SS 6.07****Virtual colonoscopy: assessment of computer aided detection assisted radiographer performance in routine clinical practice**D. Burling¹, P. Wylie¹, J. Muckian¹, R. Ahmad¹, A. Gupta¹, A. Moore¹, C. Gillen¹, R. Baldwin¹, J. Weldon¹, K. Sayedee¹, L. Honeyfield², M. Marshall¹, S.A. Taylor³;
¹Harrow/UK, ²London/UK**Purpose:** To validate computer aided detection (CAD) assisted radiographer reporting of virtual colonoscopy (VC) and investigate the effect of reading method and experience.**Material and methods:** 304 consecutive patients underwent VC as part of routine clinical care. Examinations were double read by 2 of 5 trained (>50 cases) radiographers using either primary 2D or 3D analysis (randomly assigned) supplemented by 'second-reader' CAD. Radiographers recorded colonic neoplasia/interpretation times and proposed a patient management strategy code for each examination (S0-5; inadequate/normal/6–9 mm polyp/10 mm+polyp/cancer/benign stricture). Findings were compared to experienced radiologist supplemented by colonoscopic findings (if undertaken). Following statistical advice, strategies were compared using Kappa; effect of 2D/3D analysis using Fischer's exact test; learning curve over time using logistic regression (strategy)/Pearson's correlation coefficient (reporting time), respectively.**Results:** Of 304 examinations (119 male/185 female; Mean/Median age 69/69 yrs), 78 (26%) were abnormal containing 109 significant polyps/cancers. CAD assisted radiographers detected 17/17 (100%) cancers; 21/29 (72%) 10 mm+polyps; 42/63 (67%) 6–9 mm polyps. There was agreement with reference strategy S1 in 187/211 (89%) examinations; S2 19/28 (70%); S3 12/19 (63%); S4 17/17 (100%). Overall agreement (S0-5) was good (Kappa 0.72; CI: 0.65, 0.78). There was no significant difference in strategy accuracy between primary 2D and 3D analysis (P=0.42), or over time (OR 0.88; CI: 0.76, 1.0; p=0.12). Mean interpretation time with CAD was 17 mins (SD 11) decreasing over study duration (14 mins last 50 examinations); correlation coefficient -0.46; p<0.001.**Conclusion:** Routine primary reporting of VC by CAD assisted radiographers is effective in triaging initial patient management following VC.**SS 6.08****Influence of CAR software on different experienced readers: primary 3D flythrough approach versus 3D + CAR approach**M. Rengo¹, F. Vecchietti¹, R. Ferrari¹, F. Iafrate², P. Paolantonio¹, A. Laghi¹; ¹Latina/IT, ²Rome/IT**Purpose:** To compare the performances of different experienced readers using a primary 3D fly through approach with and without the use of CAR analysis.**Material and methods:** Three readers evaluated 50 patients with 100 endoscopically proved polyps (ranging from 3 to 40 mm) and different colonic preparations (18 fluid tagging, 32 full cathartic preparation). Datasets analysis was performed on a VIATRONIX workstation equipped with V3D colon (version 1.3) software and with Medicsight Colon CAR 1.3 software. Per-polyp sensitivity, inter-reader agreement, mean reporting time and false positive were evaluated for each approach.**Results:** Less experienced readers increased per-polyp sensitivity respectively from 75 and 64% for 3D analysis to 86 and 74% for primary 3D+CAR analysis with a significant difference (p=0.001 and p=0.04) while no significant differences were found for the expert one (p=0.06). Less experienced readers were faster when assisted by CAR but no significant differences were found on mean reading time for all readers (p= 0.5/0.07/0.1). Mean false-positive findings for CAR analysis were 12 (SD.13). All readers decrease false positive when assisted by CAR especially less experienced ones. Inter reader agreement was higher among all readers when assisted by CAR (0.33 to 0.63/0.39 to 0.62/0.58 to 0.65).**Conclusion:** Our study demonstrated that if less experienced readers were assisted by CAR, they increase their sensitivity significantly. They have other not significant advantages like the reduction of false positive rate and mean reporting time.**SS 6.09****Non laxative PET CTC: do patients really prefer it to conventional colonoscopy?**

S.A. Taylor, R. Greenhalgh, J. Bomanji, G. Cattani, A. Groves, J. Dickson, S. Halligan, P. Ell; London/UK

Purpose: To investigate whether patient tolerance of combined PET CT colonography (PET-CTC) is superior to conventional colonoscopy.**Material and methods:** Non laxative PET-CTC [24 hour low residue diet, 3 oral doses of 40%w/v barium sulphate] was performed in 22 symptomatic patients (12 female, mean age 65) post injection of 130 MBq FDG in the supine and prone position using C0-2~ insufflation. Patients underwent conventional colonoscopy within 2 weeks. A validated patient satisfaction questionnaire with 22 items (marked from 1 [best] to 7 [worse]) grouped into 3 principal-components (discomfort, satisfaction and worry) was administered after both PET-CTC and colonoscopy. Overall preference was canvassed 2-weeks after colonoscopy. On statistical advice, data were compared using Mann U Whitney statistic.**Results:** There was no significant difference in responses to questionnaire items either individually or when grouped by principal component. In particular, patients reported no differences in satisfaction (p=0.4), pain (p=0.8), weariness (p=0.9), comfort (p=0.4) or embarrassment (p=0.4). However, of those 14 expressing a preference, 11 (79% CI 57–100%) would prefer PET-CT over colonoscopy in the future (p<0.001) and 8 (57% CI 31–83%) found PET-CTC the most acceptable compared to 1 (6%, CI 0–19%) for colonoscopy (p<0.01), all stating improved tolerance of the preparation.**Conclusion:** Patients tolerate colonoscopy just as well as PET-CTC, but in general prefer the latter. Recruitment continues and full data will be presented.**SS 6.10****Radiation dose in CTC: trends in time and differences between daily practice and screening protocols**

M.H. Liedenbaum, H.W. Venema, K. Boon, J. Stoker; Amsterdam/NL

Purpose: To evaluate the currently used effective doses in CT colonography (CTC) for daily practice and screening protocols and to search for trends in time in CTC radiation dose.**Material and methods:** A Pubmed search for articles and a search for congress abstracts concerning CTC were performed. Research institutions were sent a CTC dose questionnaire concerning scanner type, number of detector rows and scan parameters. With the ImPACT CT Dosimetry Spreadsheet, effective doses

for the CTC examinations were calculated. Doses for daily practice and screening protocols were compared and the present results were compared with results of a CTC dose evaluation study in 2004.

Results: Of 82 institutions, 34 returned a complete questionnaire; 20 (59%) used 64-detector row CT and 17 (50%) used dose modulation. The median effective dose was 5.7 mSv (3.6 mSv supine and 2.1 mSv prone) for screening protocols and 9.1 mSv (5.2 and 3.0 mSv, respectively) for daily practice protocols ($p < 0.05$). Doses did not differ significantly between different detector row scanners. In 17 institutions incorporated in the former study as well, the median dose changed from 11 mSv to 9.7 mSv (n.s.).

Conclusion: Median effective dose for CTC is significantly lower for screening than for daily practice protocols. Although the number of CTC-protocols with dose modulation increased substantially since 2004, no significant decrease in effective dose was found.

11:00 - 12:30

Haliç Hall

Scientific Session 7

HCC: detection and characterisation

SS 7.01

Small hepatic nodules in patients with chronic liver disease: characterization with contrast enhanced ultrasonography, a receiver operating characteristic analysis

P. Cabassa, S. Carizzoni, E. Gatti, S. Mombelloni, P. Narbone, R. Maroldi; Brescia/IT

Purpose: To evaluate the capability of CEUS in the characterization of small hepatic nodules in patients with chronic hepatitis or cirrhosis.

Material and methods: 105 nodules in 82 consecutive patients with chronic hepatitis (n=30) or cirrhosis (n=52) were prospectively studied with Sonovue. Exclusion criteria were: previous treatments with chemoembolization, alcohol injection or radiofrequency ablation during the last three months; patients with more than three nodules; known extrahepatic malignancy; Child-Pugh class C. All lesions were therefore examined with CEUS by using continuous real-time scanning at low MI (MI: 0.1–0.2). The standard dose of 2.4 ml was administered in all patients. Enhancement patterns were assessed lesion by lesion during arterial, portal and late phases. The area under the receiver operating characteristic (ROC) curve, sensitivity, and specificity were estimated. The standard of reference was CT/MR with at least a six-month follow-up and histology (biopsy or surgery).

Results: Final diagnoses were: HCC (n=58), haemangioma (n=11), regenerative nodule (n=23) and other lesions (n=13). CEUS correctly characterized 101/105 (96.2%) lesions (sensitivity 98.6%, specificity 91.4%, PPV 95.8%, NPV 97%). The area under the ROC curve showed a value of 0.978 (95% CI: 0.9587–0.9975).

Conclusion: CEUS is an effective tool in the characterization of small focal liver lesions in the periodic screening of patients with chronic hepatitis and cirrhosis.

SS 7.02

The combined assessment of hepatocellular nodule vascularity at 64-row multidetector-row CT and at contrast-enhanced US: value in malignancy diagnosis in patients with liver cirrhosis

E. Quaia¹, V. Alaimo², R. Pizzolato¹, E. Baratella¹, M.A. Cova¹; ¹Trieste/IT, ²Palermo/IT

Purpose: To assess the diagnostic value of 64-row multidetector-row CT (MDCT) combined to contrast-enhanced US (CEUS) in the assessment of hepatocellular nodule vascularity in patients with liver cirrhosis.

Material and methods: 40 cirrhotic patients (27 male, 13 female; mean age \pm SD, 71 \pm 7 years) with 56 biopsy-proven hepatocellular nodules detected by US surveillance were prospectively examined both by CEUS and 64-row MDCT. CEUS was performed after sulfur hexafluoride-filled microbubble injection during arterial (10–40 secs) and extended portal venous phase (from 45–300 secs after microbubble injection). Multiphasic MDCT consisted in arterial, portal venous, and delayed equilibrium phases (iodine 400 mg/mL at 5 mL/sec; 50 mL of saline chaser; bolus tracking with one ROI on superior abdominal aorta with 140 HU

threshold). Nodule vascularity and enhancement pattern at CEUS (arterial and extended portal venous phases), MDCT (arterial and delayed equilibrium phases), and combined CEUS/MDCT were evaluated side-by-side by 2 independent blinded readers who classified nodules as benign or malignant.

Results: Final diagnoses comprised 44 HCC, 7 macroregenerative and 4 dysplastic nodules, and 1 necrotic nodule. The combined assessment of CEUS/MDCT provided a higher diagnostic accuracy (reader 1 and reader 2: 98 and 94%, respectively) than the separate assessment of CEUS and MDCT (91% for both readers; $P < 0.05$).

Conclusion: The combined assessment of hepatocellular nodule vascularity at MDCT and CEUS improved the diagnostic performance in malignancy diagnosis in liver cirrhosis.

SS 7.03

Evaluation of Sunitinib antitumor activity with MDCT scan in patients with unresectable HCC

M. Zappa, S. Faivre, G. D'Assignies, E. Raymond, V. Vilgrain; Clichy/FR

Purpose: Solitary necrotic nodule (SNN) of the liver is a rare benign lesion, typically incidentally found at imaging. The aim of our study is to correlate imaging findings with histopathological examination.

Material and methods: 26 patients with proven HCC treated with Sunitinib had assessable MDCT scans before and each month after treatment. Tumor response was first evaluated according to RECIST criteria. Furthermore, we evaluated changes in tumor by measurement of the tumor density and tumor necrosis volumetry in all patients and intratumoral blood perfusion changes in 9 patients.

Results: Most significant tumor changes were observed after the first treatment. According to RECIST criteria, 1 patient (3.8%) had partial response, 22 patients (84.6%) had stable disease and 3 patients (11.5%) had progressive disease. After treatment, 21 patients (80.7%) had at least 15% decrease in tumor density, including 16 patients (61.5%) with 30% decrease in tumor density. In the 21 patients assessable for volumetric measurement of tumor necrosis, 13 patients (62%) had at least 15% of tumor volume necrosis, including 10 patients (48%) with 30% of necrosis. Perfusion CT showed a median decrease in blood flow and in blood volume of 56.3 and 59.3%, respectively.

Conclusion: Most patients were considered stable with RECIST criteria whereas significant tumor changes were observed (decreased tumor density and increased tumor volume necrosis) in the majority of them. Changes were also observed in patients in whom CT perfusion was performed.

SS 7.04

Perfusion CT for monitoring anti-angiogenic treatment by thalidomide in HCC: correlation with clinical response and with surrogate biomarkers of angiogenesis

G. Petralia, N. Fazio, P. Mancuso, G. D'Andrea, D. Radice, M. Bellomi; Milan/IT

Purpose: To assess potential of perfusion CT (CTp) for monitoring therapy and for predicting outcome, in patients with hepatocellular carcinoma (HCC) undergoing thalidomide. To verify any correlation between CTp parameters and surrogate biomarkers of angiogenesis (SBA).

Material and methods: 23 patients with HCC, undergoing oral thalidomide (200 mg/die), underwent pre-therapy and follow-up CTp, every 8 weeks; 10 of them underwent simultaneous CTp and SBA assessment at baseline, 15 days and 8 weeks. CTp parameters (BF, blood flow; BV, blood volume; MTT, mean transit time; PS, permeability-surface) of HCC, obtained by CT perfusion 3 software (GE), were correlated with clinical response and SBA [circulating endothelial cells (CECs), progenitor cells (CEP), apoptotic CECs], measured by flow cytometry.

Results: 18 patients were assessable for response. BF and BV of HCC significantly increased after 8 weeks ($p < 0.04$) in the 6 patients with PR or SD at 6 months and were almost stable in the 12 patients with PD. Significantly lower BF, BV, PS ($p < 0.04$) of HCC were found at pre-therapy CTp in patients with PR or SD at 6 months than ones in patients with PD. Weak correlation was found between CTp parameters and SBA.

Conclusion: CTp showed potential for monitoring therapy with thalidomide in HCC patients and predicted therapy outcome in our cohort. Larger studies may better evaluate correlation between CTp parameters and SBA.

SS 7.05**Significance of fat-containing nodules on MRI detected in a screening population for HCC**

H. Jang, K. Khalili, M.A. Haider, M. Guindi, M. Sherman, T.K. Kim; Toronto, ON/CA

Purpose: To determine the significance of the presence of fat on MRI within nodules detected in a screening population for HCC.

Material and methods: The study included 126 newly detected liver nodules (0.5–5.2 cm, mean=1.6 cm) other than hemangioma in 85 patients who were enrolled in Toronto HCC Screening Protocol and underwent MR examination over an 18-month period. Presence or absence of fat within the nodules was assessed prospectively on subtraction images of chemical shift dual-echo MR. Final diagnosis was made by histopathology or clinico-radiological follow-up over a year. Echogenicity on US of fat-containing nodules on MRI was also assessed.

Results: 34/126 (27%) liver nodules (0.7–4.5 cm; mean, 1.5 cm) in 25 patients were found to contain fat on MR; 12/34 (35%) were HCC (mean, 1.8 cm) and the remaining 22/34 (65%) were benign lesions (mean, 1.3 cm) including 5 dysplastic nodules, 2 regenerative nodules, 2 FNH, 1 angiomyolipoma, and 12 stable indeterminate lesions. The majority (25/34, 74%) was hyperechoic on US, but the remaining 9/34 (26%) were either hypoechoic or isoechoic. Among 43/126 (34%) confirmed HCC, 12/43 (28%) showed fat on MR.

Conclusion: Intralesional fat is occasionally (28%) seen in HCC. However, the presence of fat on MR within nodules detected in a screening population may not be a reliable predictor of HCC as about two-thirds of fat-containing lesions are benign.

SS 7.06**Usefulness of the hepatobiliary phase for the characterization of small (≤ 20 mm) hepatic nodules seen on arterial phase on gadobenate dimeglumine (Gd-BOPTA) enhanced MRI**

A. Guerrisi, M. Di Martino, C. Catalano, D. Marin, M. Baski, D. Geiger, F. Galati, R. Passariello; Rome/IT

Purpose: To retrospectively assess whether gadobenate dimeglumine (Gd-BOPTA) enhanced MRI during the hepatobiliary phase can improve the characterization of small (≤ 20 mm in diameter) hepatic arterial phase-enhancing (HAPE).

Material and methods: This study was approved by the institutional review board and a waiver for informed consent was obtained. Two-hundred and fifty patients who underwent Gd-BOPTA enhanced MRI were evaluated with breath-hold T2-weighted images and volumetric three-dimensional Gd-BOPTA-enhanced T1-weighted GRE MR images were acquired in the arterial (25 s), portal venous (60 s), equilibrium (180 s), and hepatobiliary phases (180 min). Two readers retrospectively reviewed the MR images in consensus for small HAPE-only nodules. The final study group included 40 patients with a total of 55 HAPE-only lesions. Qualitative analysis of MR enhancement features during the hepatobiliary phase was related to pathology reports or imaging follow-up. Sensitivity, specificity, and positive and negative predictive values with corresponding 95% confidence intervals were determined.

Results: Of the 55 HAPE-only lesions, 25 (45%) were hepatocellular carcinomas (HCC). The remaining 30 (55%) lesions were considered definite pseudolesions. The sensitivity and specificity of Gd-BOPTA MR imaging during the hepatobiliary phase for depicting HCCs was 52 (13 of 25) and 90% (27 of 30), respectively. The positive and negative predictive values of Gd-BOPTA MR imaging were 81 (13 of 16) and 70% (27 of 39), respectively.

Conclusion: Gd-BOPTA-enhanced MRI during the hepatobiliary phase has high specificity, but low sensitivity for the characterization of small HAPE-only lesions in patients with cirrhosis.

SS 7.07**Benign and malignant hepatic nodules detected in a screening population for HCC: findings on delayed-phase MRI with gadobenate dimeglumine**

T.K. Kim, H. Jang, M.A. Haider, M. Guindi, M. Sherman, K. Khalili; Toronto, ON/CA

Purpose: To describe the enhancement pattern of benign and malignant nodules in cirrhotic liver on 2-hour delay gadobenate dimeglumine (Gd-BOPTA) enhanced MRI.

Material and methods: Subjects included 96 newly detected hepatic nodules (size, 0.7–4.5 cm; mean, 1.7 cm) other than hemangiomas in 67 patients who were enrolled in Toronto HCC Screening Protocol and underwent Gd-BOPTA-enhanced MRI over a 20-month period. There were 44 benign lesions and 52 HCC, based on histopathology (n=39) or clinico-radiological follow-up (n=57). Signal intensity relative to normal liver in the arterial-phase, portal-phase, 5-minute, and 2-hour delayed imaging was prospectively assessed. Enhancement patterns were compared between benign and malignant lesions using Fisher's exact test.

Results: HCC were hypointense in 42/52 (81%), isointense in 9/52 (17%), and hyperintense in 1/52 (2%) at 2-hour delay, whereas benign lesions were hypointense in 11/44 (25%), isointense in 26/44 (59%), and hyperintense in 7/44 (16%) (P<.001). Of 44/52 HCC that were hyperintense in the arterial-phase; 32/44 showed washout (hypointensity) to 5 minutes. Of the remaining 12/44 that did not show washout to 5 minutes, 11/12 were hypointense at 2-hour delay. Among 8 well-differentiated HCC, 4 were hypointense and the remaining 4 were isointense at 2-hour delay.

Conclusion: Hypointensity at 2-hour delay post-Gd-BOPTA MRI is seen in a majority of HCC but also occasionally in benign lesions. Two-hour delay imaging may help to characterize hypervascular HCC which do not show washout to 5 minutes.

SS 7.08**Detection of HCC in patients with cirrhosis: intraindividual comparison of gadobenate dimeglumine (Gd-BOPTA) enhanced MRI and multiphasic 64-slice CT; correlation with explanted liver**

M. Di Martino, A. Guerrisi, C. Catalano, D. Marin, F. Galati, D. Geiger, G. de Filippis, R. Passariello; Rome/IT

Purpose: To intraindividually compare gadobenate dimeglumine (Gd-BOPTA) enhanced MRI and 64-slice CT for the detection of HCC in patients with cirrhosis.

Material and methods: Thirty-six consecutive patients with 46 HCC nodules underwent MRI at 1.5 T (Avanto, Siemens) and 64-slice CT (Sensation 64, Siemens). All patients underwent transplantation within 60 days. MR acquisitions comprised unenhanced breath-hold T2W images and volumetric 3D Gd-BOPTA-enhanced (MultiHance, Bracco) T1W GRE images acquired at 25 s, 60 s, 180 s and 120 min. 64-slice CT was performed with 0.6 x 64 mm collimation, 3-mm section thickness, 250 mAs, 120 kVp. A triple-phase protocol was started 18 s, 60 s and 180 s after reaching a trigger threshold of 150 HU above baseline CT number of the aorta. Image analysis was independently performed by three observers in two sessions separated by 4 weeks. Findings were compared directly with explanted liver pathologic results. Diagnostic accuracy was evaluated using the AFROC method. Sensitivity and specificity with corresponding 95% confidence intervals were determined.

Results: The mean area under the AFROC curve for Gd-BOPTA MRI (0.92) was significantly higher than that of CT (0.84) (P<.05). On a lesion-by-lesion basis, the mean sensitivity (77%, 91/138) of Gd-BOPTA MRI was significantly higher than that of CT (66%, 91/138) (P<.05). Both techniques showed an equal mean specificity (90%, 133/148).

Conclusion: Gd-BOPTA-enhanced MRI is significantly more accurate and sensitive than 64-slice CT for the diagnosis of HCC in patients with cirrhosis prior to liver transplantation.

SS 7.09**Toronto HCC screening protocol: 18 months experience with systematic implementation of American Association for Study of Liver Diseases HCC practice guidelines**

K. Khalili, T.K. Kim, L.M. Khan, M.A. Haider, M. Guindi, M. Sherman, H. Jang; Toronto, ON/CA

Purpose: To describe the implementation of Toronto Hepatocellular Carcinoma Screening Protocol (THSP), a systematic protocol based on AASLD HCC practice guidelines.

Material and methods: A protocol for workup of liver lesions found at screening for HCC was developed with standard imaging criteria for benign, malignant and indeterminate lesions. Lesions <1 cm were followed; lesions ≥ 2 cm were examined with 4-phase CT; lesions 1–1.9 cm were examined with 3 contrast-enhanced scans: Contrast-US (CUS)/4-Phase CT/MR. Standardized imaging protocols were used. Results were reviewed prospectively by expert readers in consensus meeting with 4 outcomes: Treat, Biopsy, Follow, Benign (no follow-up). Lesions fulfilling criteria for malignancy on 2/3 modalities for <2 cm lesions and on single modality for >2 cm lesions were referred for treatment. From Jan

06 to Jun 07, 135 patients (210 lesions, 1.5 lesion/patient) were enrolled.

Results: Mean/Median lesion sizes were 1.6/1.4 cm (SD 0.8). 51/210 (24%) of lesions were <1 cm, 123 (59%) were 1–1.9 cm, and 36 (17%) were ≥2 cm. For the 210 lesions, consensus recommendations were: treat 49 (23%), biopsy 42 (20%), follow 66 (31%) and benign 53 (25%). In treat category (n=49), 23 were <2 cm and 26 were ≥2 cm. 40/49 (82%) were proven malignant by growth or biopsy. In biopsy category, 29/42 underwent biopsy: 7 were malignant, 7 dysplastic, 8 benign, and 7 non-lesional. Overall, 56 lesions in 39/135 (29%) patients were deemed malignant; mean/median lesion sizes were 2.2/2.0 cm (SD 0.9, range 0.5–5.2 cm).

Conclusion: THSP successfully stratified lesions found leading to detection of high number of small HCCs potentially achieving tumor down-staging.

SS 7.10

Usefulness of FDG PET/CT in detecting occult HCC in patients with high tumor markers during follow-up after interventional procedure

W.J. Lee, J.Y. Lee, Y. Park, H.J. Kim, J.Y. Choi, B. Kim; Seoul/KR

Purpose: To evaluate the usefulness of FDG PET/CT in detecting occult hepatocellular carcinoma (HCC) when high tumor markers develop during follow-up in patients treated with interventional procedure by assessing their diagnostic values of FDG PET/CT findings.

Material and methods: A retrospective search of our imaging database of January 2004 to December 2006 was performed for 112 HCC patients with suspected recurrence after interventional procedures who were evaluated with both FDG PET/CT and MDCT, and 75 patients with high tumor markers (AFP >100 ng/mL) who had no evidence of recurrence at MDCT report were identified. Among them, 31 patients were excluded due to insufficient follow-up period (<1 year), and the remaining 44 patients (M:F=25:19, mean age=57 yrs) formed our study population. The presence or absence of recurrence was proved by biopsy or follow-up imaging and were correlated with FDG PET/CT findings (the presence or absence of FDG uptake) by calculating the diagnostic values. FDG PET/CT findings were also compared with initial CT findings and histologic grades of HCCs.

Results: FDG uptake was present inside the liver in 11 patients and outside the liver in 6 patients, and all these patients proved to have intra- or extrahepatic recurrences. FDG uptake was absent in the remaining 27 patients, but 15 of these patients were proved to have recurrences. The sensitivity, specificity, positive predictive value and negative predictive value of FDG uptake for detecting recurrence were 53, 100, 100 and 44%, respectively. FDG uptake had no significant correlation with initial CT findings and histologic grades of HCCs.

Conclusion: FDG PET/CT is highly specific and predictive in detecting HCC which is occult at CT for post-procedural patients particularly when tumor markers are elevated. Moreover, FDG PET/CT may be helpful in detecting distant metastasis.

11:00 - 12:30

Topkapi A

Scientific Session 8

Rectum and pelvic floor

SS 8.01

Can US elastography help characterise anal sphincter pathology?

R. Greenhalgh¹, Y. Hu¹, D. Barratt¹, D.J.M. Tolan², S.A. Taylor¹, D. Hawkes¹, S. Halligan¹; ¹London/UK, ²Leeds/UK

Purpose: US elastography is a novel technique to assess tissue stiffness and is used for breast, liver and prostatic imaging. A role in anal sphincter imaging has not been investigated. We aimed to determine whether elastographic properties of different anal sphincter components differed, postulating a role in characterising incontinent patients.

Material and methods: 110 adult patients undergoing anorectal physiology for the investigation of incontinence were divided into those with and without normal physiologic parameters. All underwent subsequent standard anal endosonography using (Hitachi EUB R54AW–19; EUP R54AW radial anal endoprobe), followed by elastography. Tissue compression was performed in four quadrants at mid canal level and cine-loops of resultant elastographic data were obtained. Elastographic data were segmented for each sphincter component using in-house software

written specifically for the purpose.

Results: The normalised mean stiffness for the different sphincter components in 18 patients with normal physiology was 0.6161 for the internal sphincter, 0.5956 for the longitudinal muscle, and 0.6525 for the external sphincter, showing that the external sphincter was the least compliant (stiffest) tissue, the longitudinal muscle most compliant, with the internal anal sphincter intermediate. Data for patients with abnormal physiology will be presented.

Conclusion: This is the first description of anal sphincter elastography. Different sphincter components show different compliance, a finding that may have clinical potential for the characterisation of incontinent patients.

SS 8.02

Pelvic floor diseases: defecography versus cine-MRI

F. Maisto, A. Reginelli, A. Rotondo, A. Russo, R. Grassi; Napoli/IT

Purpose: To compare the value of defecography versus functional cine-MRI in the study of pelvic floor disorders.

Material and methods: We examined a total of 30 female and 10 male volunteers (mean age 53, range 26–80 years). All the volunteers were examined first with defecography and then with a functional cine-MRI. Defecography was performed using a remote controlled device (Siemens); the patients were in a sitting position, opacification of rectum and vagina (in the female) was achieved by filling them with barium paste. The rapid sequence radiographs were reordered on videotape. Functional cine-MRI was performed with a 0.22 T magnet unit open configuration (Siemens, Concerto). Static images with T2-w sequences and dynamic images with T2-Breath-hold sequences were obtained during relaxation, maximal sphincter contraction and straining. The patient rectum was filled with sonography gel and Gd-DTPA. The images thus obtained were assembled in cine-view.

Results: Cine-MRI findings were: 21 anterior rectoceles, 4 rectorectal intussusception, 2 rectal prolapse, 5 cystoceles, 7 enteroceles, and 2 cervical/vaginal vault prolapse. Defecography detected 19 anterior rectoceles, 7 rectorectal intussusceptions, 8 rectal prolapse, and 4 cystoceles.

Conclusion: The use of the fast sequences of the cine-MRI allows the morphologic study of the pelvic floor together with the dynamic evaluation of the pelvic organs with a more diagnostic accuracy and sensibility than the defecography in order to detect the different types of pelvic organ prolapse.

SS 8.03

Dynamic MRI of posterior pelvic floor disorders: comparison between lateral and supine position

F. Carozzo, F. Maccioni, M. Indinnimeo, F.I. Habib, V. Garbarino, M. Marini; Rome/IT

Purpose: Comparison between pelvic floor dynamic MRI performed in lateral and supine position, to assess pelvic floor disorders (PFD).

Material and methods: 23 patients with clinical evidence of PFD underwent conventional defecography and MRI in two different positions. The rectum was distended with air. A T2-weighted HASTE (Half-Fourier SnapShot Turbo Spin-Echo) sequence was acquired at rest, contraction and straining on sagittal planes and repeated in dynamic modality on the mid-sagittal plane two times, with no evacuation phase, in supine and lateral position. We adopted specific MRI modified values for rectoceles and ano-rectal descents, obtained by a control group of healthy volunteers. Gold standard was conventional defecography and/or surgery.

Results: MRI identified with both techniques 18 rectoceles (100%), 15/17 (88%) ano-rectal junction descents, 15/19 (79%) rectal invaginations, 2 dyskinetic pubo-rectal syndromes, 4 uterine descents, 5 cystoceles, 3 enteroceles. In 18/23 patients, the same results were obtained with both techniques, for all parameters; in 3/18 patients with rectocele and 3/5 with cystoceles, a slightly higher evidence of the disease was obtained in lateral positions. In 1/23 patients, pathologic findings were observed in lateral position only.

Conclusion: Both supine and lateral positions, although non physiologic, allow MRI assessment of the majority of posterior pelvic floor disorders. Lateral position, however, allowed better evidence of rectoceles and cystoceles in our experience.

SS 8.04**Value of MDCT in preoperative staging of rectal cancer in predicting the necessity for neoadjuvant radiochemotherapy**

A.S. Ernst, B.L. Schmitz, M. Kornmann, H.J. Brambs, A.J. Aschoff; Ulm/DE

Purpose: Neoadjuvant therapy (NT) reduces local rectal cancer recurrence after total mesorectum extirpation in patients with advanced disease. This study was performed to assess whether MDCT is capable to reliably differentiate UICC I (surgery) from UICC II to IV (NT).

Material and methods: 29 rectal cancer patients underwent preoperative contrast-enhanced MDCT (2 mm thickness, 1 mm increment) of the abdomen. Two blinded readers independently evaluated these using axial and coronal reformations for TNM/UICC staging. Findings were correlated with histology.

Results: Histologically, 9 patients were UICC I; 20 UICC >I (II: 7; III: 11; IV: 2). Reader 1 correctly identified 3/9 as UICC I, overstaged 6/9, and correctly staged 20/20 as UICC >I. Reader 2 correctly identified 4/9 as UICC I, overstaged 5/9, understaged 4/20 and correctly staged 16/20 as UICC >I. (PPV UICC I 100% (50%) reader 1 (reader 2), NPV 77% (76%), accuracy 79% (69%).) Reasons for overstaging by reader 1 (reader 2) included false-positive lymph nodes (LN) in 5 (5), overgrading T1 tumors as T3 in 1 (0), and T-overgrading in 4/5 (2/5) patients with false-positive LN. Understaging was due to false-negative LN (2) and undergrading T3 cancers as T2 (2).

Conclusion: MDCT failed to reliably identify UICC I in rectal cancer patients.

SS 8.05**Diffusion weighted imaging of the rectum: comparison of apparent diffusion coefficient measurements of rectal tumor with those of normal rectal wall using two different sequences**

S. Gourtsoyianni, N. Papanikolaou, S.D. Yarmenitis, D. Tsiftsis, N. Gourtsoyiannis; Heraklion/GR

Purpose: To assess image quality of two different diffusion weighted sequences and compare apparent diffusion coefficient (ADC) values of rectal tumors and normal rectal wall (NRW).

Material and methods: 29 consecutive patients with rectal carcinoma underwent pretreatment MRI examination of the rectum, including either a spin-echo echo planar imaging (SE EPI) sequence (n=24) or an inversion recovery (IR EPI) diffusion sequence (n=21) or both (n=16). Efficient fat saturation and presence of geometrical distortions were qualitatively assessed. Quantification of ADC values of rectal tumors, normal appearing rectal wall (NARW) was performed. 12 patients who underwent prostate MRI formed the control group.

Results: IR EPI sequences provided significantly better fat saturation efficiency ($p < 0.001$) while differences between IR and SE EPI sequences on geometrical distortions were not significant ($p = 0.999$). There were statistically significant differences between mean ADC measurements of rectal tumors as compared to either NARW of the same patients or NRW of the control group when using both sequences ($p < 0.0001$). Mean ADC values of NARW and NRW of the control group were non significant for both sequences ($p > 0.05$). All comparisons between NRW ($p = 0.184$), NARW ($p = 0.409$) and tumor ($p = 0.094$) ADC measurements, with either SE EPI or IR EPI, were non-significant.

Conclusion: IR EPI sequence provides better image quality due to more efficient fat saturation. ADC quantification based on both sequences may be used for tumor characterization.

SS 8.06**Stapled transanal rectal resection: persisting functional deficits despite anatomical correction? Correlation with dynamic MR-defecography-findings**

S. Kirchhoff, R. Lang, C. Kirchhoff, K.W. Jauch, M. Kreis, M.F. Reiser, A. Lienemann; Munich/DE

Purpose: Transanal-stapler-resection for treating obstructive defecatory disorders presents an innovative operation-technique. The aim of this study was to prospectively evaluate morphological and functional results after stapled transanal rectal resection (STARR)-surgery using dynamic MR-defecography.

Material and methods: Patients with obstructive defecation-dysfunction were interviewed pre- and postoperatively, also undergoing rectal-manometry, procto/rectoscopy and MR-defecography. Slow-transit-patients with a defecation rate

>1/week and patients with concomitant pelvic-floor-dyssynergy were excluded. All patients underwent a STARR-operation in general anaesthesia. The mean follow-up was 20 ± 6 months.

Results: 10 patients (10 f, 0 m; 62 ± 12 years) were enrolled with successful performance of the STARR-operation. Preoperatively all patients reported a fractionated defecation, only 6 patients ($p = 0.02$) postoperatively. A subjective defecatory improvement was observed in 6 patients ($p = 0.02$), 9 patients showed a preoperative intussusception, compared to only 3 patients ($p = 0.02$) postoperatively. In MRI, 9/10 patients showed preoperative intussusception versus 1/10 patient postoperatively ($p = 0.002$). The rectocele-size was assessed on MRI preoperatively with 2.6 ± 1.4 cm versus postoperatively with 1.4 ± 1.2 cm ($p = 0.05$). In patients with additional MR-findings as cystocele a significant extent-reduction was found comparing pre- with postoperative findings. During rectal manometry, the active pinch-pressure and the pressure-at-rest showed no significant difference pre versus postoperatively.

Conclusion: Whereas in almost all patients an anatomic correction of intussusception was performed, only a few report functional improvement, comparable to alternative operation-methods. Examinations such as MR-defecography are necessary to identify those patients possibly benefiting the most from the STARR-operation.

SS 8.07**Contrast enhanced MRI and PET-CT in the evaluation of patients with suspected local recurrence of rectal carcinoma**

F. Focchi, V. Iotti, G. Ligabue, G. Luppi, P. Torricelli, B. Bagni; Modena/IT

Purpose: To evaluate contrast enhanced MRI (ce-MRI) and PET-CT accuracy in the assessment of local recurrence of rectal cancer.

Material and methods: In a group of 180 patients scheduled for CT follow-up for rectal cancer, 36 patients (29 low risk; 7 high risk) were selected due to suspected local recurrence at CT study. Patients underwent within 2 weeks to ce-MRI and PET-CT. The gold standard was considered in 19 cases histological biopsy and in the remaining 17 the negative follow-up at 6 and 12 months. Specific tumour markers were also evaluated.

Results: Histological biopsy confirmed local recurrence in 9 cases (4 low risk; 5 high risk) and excluded in 27 (17 by long term follow-up and 10 by histological biopsy). Sensitivity, specificity, positive predictive value, negative predictive value and accuracy were as follows: 77.8, 66.7, 43.8, 90 and 69.4% for ce-MRI; 88.9, 66.7, 47.1, 94.7 and 72.2% for PET-CT. The presence or absence of local recurrence was not related to blood level of tumour markers; in 3 cases, the rise of tumour markers was related to pulmonary metastases without local recurrence.

Conclusion: ce-MRI and, in particular, PET-CT can help in the detection of local recurrence of rectal cancer, especially in high risk patients. However, the role of these techniques in the current surveillance protocols is still to be defined.

SS 8.08**Tumour response to neoadjuvant chemoradiation in primary rectal cancer: Can postchemoradiation USPIO enhanced MRI predict downstaging?**M. Lahaye¹, G.L. Beets¹, S.M.E. Engelen¹, A.P. de Bruïne¹, P. Post², L. Opendakker³, J. Dohmen⁴, J.M.A. van Engelshoven¹, M.F. van Meyenfeldt¹, C.J.H. van de Velde⁵, R.G.H. Beets-Tan¹; ¹Maastricht/NL, ²Venlo/NL, ³Roermond/NL, ⁴Weert/NL, ⁵Leiden/NL

Purpose: To determine the accuracy of MRI with and without USPIO for predicting T- & N-stage after chemoradiation (CRT) in locally advanced rectal cancer, and to evaluate whether patients with good response to CRT can be selected for less extensive surgery.

Material and methods: From February 2003 until August 2007, 332 patients were enrolled in a prospective multicenter study. The locally advanced tumours (CRM+/N2-status) received CRT followed by USPIO MRI (6 weeks postCRT) and surgery. The local radiologists (non-experts) and an expert MR radiologist prospectively predicted the postCRT T-stage and the postCRT N-status first on T2WTSE images (USPIO-), and then on the combined T2W and 3DT2* (USPIO+), blinded for each other's results. The expert prospectively double read each MR of the regional patients. Reference standard was histology.

Results: Histological and MR results were available for 59 locally advanced tumours (7/59 had a ypN+ status).

Table 1

| ypT0/1/2 | Non-expert | Expert |
|----------|------------|--------|
| SENS | 0.43 | 0.33 |
| SPEC | 0.93 | 0.94 |
| PPV | 0.86 | 0.82 |
| NPV | 0.64 | 0.63 |

Table 2: Nonenhanced N-status

| N-status | Non-expert | Expert |
|----------|------------|--------|
| SENS | 0.63 | 0.71 |
| SPEC | 0.75 | 0.84 |
| PPV | 0.56 | 0.60 |
| NPV | 0.80 | 0.89 |

Table 3: USPIO N-status

| N-status | Non-expert | Expert |
|----------|------------|--------|
| SENS | 0.90 | 0.88 |
| SPEC | 0.39 | 0.79 |
| PPV | 0.45 | 0.63 |
| NPV | 0.88 | 0.94 |

Conclusion: 1. MRI can predict downstaged tumours limited to the bowel wall (ypT0/1/2) with high PPV for expert and non-experts. 2. PostCRT USPIO MRI has a high NPV for predicting ypN0, for expert as well as non-expert readers. These results imply that postCRT USPIO MRI could have an impact on the selection of postCRT rectal cancer patients in whom more local treatment is an option.

SS 8.09

Accuracy of rectal MRI in restaging after neoadjuvant chemoradiotherapy for rectal cancer: comparison with 18F-FDG PET

M.J. Kim, S.J. Lee, S.H. Kim, S.H. Kim, H.K. Chun, B.T. Kim; Seoul/KR

Purpose: To investigate the accuracy of MRI and 18F-FDG PET in restaging after neoadjuvant chemoradiotherapy (CRT) for rectal cancer.

Material and methods: Between April 2006 and February 2007, 30 patients with histologically proven rectal adenocarcinoma were included. Pelvic MRI was used to stage the tumor clinically before and after CRT. One month later, the end of CRT whole body 18F-FDG PET were performed to all the patients. Surgery was performed 6–8 weeks after the end of CRT and pathologic stage defined. Two patients receiving transanal endoscopic microsurgery after CRT were excluded when N stage was evaluated.

Results: The overall predictive accuracy of MRI in T stage was 71% (overstaging 22%, understaging 7%) and 75% in N stage (overstaging 14%, understaging 11%). Good agreement between post-CRT MRI and pathologic staging was observed in both T stage ($\kappa=0.422$) and N stage ($\kappa=0.410$). The accuracy of 18F-FDG PET was 60% in T stage and 68% in N stage. 18F-FDG PET showed 75% accuracy in predicting the pathologic complete response. Good correlation of T stage was found between 18F-FDG PET and pathology ($\kappa=0.372$); however, there was poor agreement in N stage ($\kappa=0.031$). Four distant metastatic lesions (liver 1, lung 2) were detected on 18F-FDG PET. One false negative hepatic metastasis lesion was identified.

Conclusion: Rectal MRI is useful to predict both T and N stages after neoadjuvant CRT. 18F-FDG PET is helpful to predict pathologic complete response and to find possible metastasis after neoadjuvant CRT.

SS 8.10

Tailored treatment of primary rectal cancer based on MRI: does it reduce the number of incomplete resections?

M. Lahaye¹, G.L. Beets¹, S.M.E. Engelen¹, J. Konsten², H. Verkooyen³, J. Debets⁴, A.P. de Bruine¹, M.F. van Meyenfeldt¹, C.J.H. van de Velde⁵, R.G.H. Beets-Tan¹; ¹Maastricht/NL, ²Venlo/NL, ³Weert/NL, ⁴Roermond/NL, ⁵Leiden/NL

Purpose: To evaluate whether tailor-made treatment of primary rectal cancer based on USPIO MRI can reduce the number of incomplete resections.

Material and methods: From February 2003 until August 2007, 332 patients were enrolled in this prospective multicenter study. All underwent preoperative USPIO MRI to predict CRM, T- and N-stage. Patients were stratified in different treatment groups: early tumours (CRM- & N0, received TME alone/local excision), non-locally advanced (received preoperative 5x5Gy +TME) and locally advanced tumours (CRM+, N2 status; received chemoradiation therapy followed by surgery). Histopathological evaluation was the reference standard for the number of complete resections (CRM>1 mm).

Results: Histopathological evaluation of 202 patients is completed. Thirty-five tumours were treated as early tumours (14 local excisions), 85 as non-locally advanced tumours and 82 as locally advanced tumours. The number of complete resections was 192 (95%). 9/10 incomplete resections had a positive CRM. 5/10 incomplete resections were locally advanced tumours.

Conclusion: Tailor-made treatment of rectal cancer based on USPIO MRI leads to 95% complete resections. The striking finding is the high proportions of tumours defined as 'locally advanced' based on USPIO MRI. Remarkable is the higher proportion of local excisions. The NPV of USPIO MRI for nodal disease makes local excision of superficial tumours with N0-status possible. To evaluate whether this tailored treatment will also reduce the local recurrence rate, a longer follow up is necessary.

11:00 - 12:30

Topkapi B

Scientific Session 9

Diffuse liver diseases

SS 9.01

Effect of number of shots on diffusion weighted MRI of liver

M. Shiehorteza, M. Bydder, G. Hamilton, C. Kohl, C. Sirlin; San Diego, CA/US

Purpose: To show that the signal intensity (SI) varies systematically with number of shots in diffusion-weighted echo planar imaging (EPI).

Material and methods: This prospective study was performed on eleven subjects (25–55 years) two hours after fasting. Measurements were made on a 3T MRI scanner using a breath-held diffusion-weighted EPI sequence and one diffusion direction. Two protocols were used: (A) TR 3000 ms/TE 34 ms with eight consecutive shots at a fixed b-value, performed on four subjects; and (B) TR 3500 ms/TE 55 ms with seven consecutive shots at b-values 0, 1000, 750, 500, 250, 100, 0 (in that order) performed on all subjects. ADC values were calculated by non-linear fitting of the SI to an exponential decay. Comparisons were made using paired t-test and Wilcoxon signed-rank test.

Results: For protocol (A), SI decreased 22% from the first to second shot ($p<0.05$) and thereafter remained constant (coefficient of variation <2%). For protocol (B), the SI of the first and second b=0 differed significantly ($p<0.00001$). Using the first b=0 in the ADC fitting, the mean ADC was 9% higher than using the second b=0 ($p<0.0001$).

Conclusion: The observed SI varied with shot number for up to two shots. The ADC value depended on which shot was used for b=0. This suggests that a steady-state of the longitudinal magnetization should be attained to calculate ADC.

SS 9.02**Comparison of a standard and a weighted linear regression analysis method for the calculation of the apparent diffusion coefficient of the liver and spleen**

T.G. Maris, S. Gourtsoyianni, N. Papanikolaou, K. Karolemeas, S.D. Yarmenitis, N. Gourtsoyiannis; Heraklion/GR

Purpose: To compare two mathematical techniques for the calculation of apparent diffusion coefficient (ADC) of normal liver, liver focal lesions and normal spleen.

Material and methods: Forty-five consecutive patients underwent MRI examination of the liver and spleen, utilizing a spin-echo echo planar imaging diffusion sequence with four b-values (0, 50, 500, 1000). ADC calculated colour image maps were post-processed using: (a) a standard and (b) a weighted linear regression fitting model with b-values of 50, 500 and 1000. The two analytical methods (a and b) were compared in terms of their precision in the ADC calculations.

Results: Differences amongst all ADC values were considered significant (ANOVA, $p < 0.01$) using either methods. Post-hoc pair wise comparisons showed a better discrimination between normal liver and focal liver lesions when using method (b) ($p < 0.01$). ADC measurements performed with method (b) showed a better precision (mean CV=3.5%) as compared with method (a) (mean CV=8.3%). Bland-Altman plot showed a 4% increment of the mean ADC values when method (b) was used and a random statistical variation within the 95% confidence intervals indicating that both methods could be used interchangeably.

Conclusion: ADC quantification of the liver and spleen may be performed with both standard and weighted linear regression analysis methods. However, the precision is significantly improved when weighted regression analysis methods are utilized.

SS 9.03**Can diffusion weighted imaging be used to grade the severity of liver fibrosis and cirrhosis?**

K. Sandrasegaran, F. Akisik, A.M. Aisen, C. Lin; Indianapolis, IN/US

Purpose: To determine the correlation between apparent diffusion coefficient (ADC) of liver parenchyma and the grade of liver fibrosis determined by liver histology in patients with chronic liver disease.

Material and methods: 78 patients who had diffusion weighted imaging (DWI) using 1.5 T MRI (Magnetom Avanto, Siemens, Erlangen, Germany) and pathological staging of liver fibrosis were included for this study. DWI was performed with b values of 0 and 500 s/mm². Apparent diffusion coefficients (ADC) of liver were measured in the right and left lobes of the liver.

Results: The mean (standard deviation) ADC values of liver fibrosis graded as 0 (n=11), 1 (n=16), 2 (n=10), 3 (n=14) and 4 (n=27) were 118.5 (22.7), 101.1 (16.6), 102.4 (20.4), 102.3 (16.6) and 99.1 (12.0) x10⁻³ mm²/s, respectively. The correlation between the ADC values and degree of liver fibrosis was good ($r = -0.77$). There was a significant difference in ADC values between those with normal liver and cirrhosis ($p = 0.001$). No significant difference was seen in ADC values between grades 1 and 2 combined versus grades 3 and 4 combined ($p = 0.71$). The etiology of liver disease did not affect ADC.

Conclusion: ADC in cirrhotic livers is significantly lower than in normal liver. ADC values decrease with increasing hepatic fibrosis. However, we were unable to reliably classify patients as having low or high degree of fibrosis using ADC values.

SS 9.04**Diffusion-weighted MRI for the assessment of liver fibrosis is just a matter of perfusion: a study using two single-shot spin echo echo-planar diffusion-weighted MRI sequences with increasing b-values**

R. Girometti, A. Furlan, M. Bazzocchi, G. Esposito, L. Cereser, C. Zuiani; Udine/IT

Purpose: To investigate the effects of increasing b-values in evaluating liver fibrosis through the agreement of two diffusion-weighted MRI (DW-MRI) sequences.

Material and methods: 29 cirrhotic patients and 29 healthy volunteers were studied on a 1.5T system. Two single-shot spin-echo echo-planar DW-MRI sequences were acquired using sets of increasing b-values: 0, 150, 250, 400

(DW1) and 0, 150, 250, 400, 600, 800 s/mm² (DW2). Apparent Diffusion Coefficients (ADCs) of the hepatic parenchyma were calculated on ADC-maps, obtained by the processing software using a linear fitting algorithm. Noise-scaled single-point ADCs were calculated for DW1 at b=0-400 s/mm² and DW2 at 0-400, 0-600, and 0-800 s/mm².

Results: ADCs values resulted as significantly lower in cirrhotic patients compared to controls using both DW1 (mean 1.14 ± 0.20 vs $1.54 \pm 0.12 \times 10^{-3}$ mm²/s) ($p < .0001$), and DW2 (mean 0.91 ± 0.18 vs $1.04 \pm 0.18 \times 10^{-3}$ mm²/s) ($p = .0089$). DW1 and DW2 significantly differed in diagnosing fibrosis at ROC analysis ($p = .003$), showing AUCs of 0.93 (sensitivity 89.7%, specificity 100%) and 0.73 (sensitivity 62.1%, specificity 79.3%), respectively. The noise-scaled single point ADCs showed a progressive convergence in cirrhotic and healthy livers toward b=800 s/mm² (1.12 ± 0.27 vs $1.13 \pm 0.17 \times 10^{-3}$ mm²/s) ($p > .05$). Perfusion fraction for ADCs resulted in 10% (both DW1 and DW2) in cirrhotic livers and 27% (DW1) and 21% (DW2) in the normal livers.

Conclusion: A DW-MRI sequence is more accurate in assessing liver fibrosis using intermediate (400 s/mm²) rather than high (800 s/mm²) b-values. Perfusion was considered responsible for the difference in ADCs.

SS 9.05**Non invasive diagnosis of liver fibrosis in chronic hepatitis C using high resolution US and basic biochemical markers**S. Aufort¹, C. Combescure², P. Blanc¹, B. Gallix¹, J.M. Bruel¹; ¹Montpellier/FR, ²Nîmes/FR

Purpose: To assess a new diagnostic score by non invasive combination of high resolution ultrasound (HRUS) findings and basic serum biochemical markers for evaluation of clinically significant fibrosis ($\geq F2$) of the liver.

Material and methods: 122 patients with Hepatitis C virus (HCV) were prospectively involved and had HRUS, blood sample and liver biopsy within the same day. Echopatterns scores of liver parenchyma and liver surface regularity, basic biochemical markers and Fibrotest® were studied, respectively. Pathological patterns of liver fibrosis were scored according to Metavir system. The diagnosis performances of HRUS alone, biochemical markers alone and combined scores were compared to liver biopsy results, respectively, by using Receiver Operating Characteristics (ROC) curves and area under ROC (AUROC) analysis.

Results: HRUS score was not statistically different than Fibrotest®. A new combined score resulted from logistic regression analysis in three current variables: aspartate amino transferase, apolipoprotein A1 and the HRUS morphological analysis of the liver surface. AUROC for this new combined score was 0.871 CI-95%=[0.811 - 0.937], significantly better than those for the HR US score alone (0.754 CI-95%=[0.668 - 0.841], $p = 0.0028$) and for the biochemical score alone (0.749 CI-95%=[0.665 - 0.841], $p = 0.0016$), respectively.

Conclusion: A combined score based on both HRUS morphological analysis and current biological markers (aspartate amino transferase, apolipoprotein A1) allows a better evaluation of liver fibrosis than biological evaluation alone and HRUS alone.

SS 9.06*Withdrawn by authors***SS 9.07****Gradient echo sequences versus spin echo sequences in MR evaluation of non-alcoholic liver steatosis: monitoring during dietetic therapy**

E. Piccione, I. Sansoni, G. Della Longa; L. Antonelli, R. del Vescovo, B. Beomonte Zobel; Rome/IT

Purpose: To assess MR capability in evaluating fat liver variation after dietetic therapy compared with Body-Mass-Index (BMI) and Fat-Tissue (FT) thickness and to define the most accurate MR sequence for that purpose.

Material and methods: On 20 patients with non-alcoholic liver steatosis, we performed MR examination and measured BMI and FT before and three months after dietetic therapy. Based on GRE MR T1-weighted sequences (with TE in phase and out of phase) and TSE T2-weighted sequences (with and without fat saturation), hepatic fat fraction (HFF) was measured and its percentage of variation after therapy was quantitized. We compared the variation of average

HFF obtained by all the sequences with variation of BMI and FT measured at MR. Average HFF variation has been compared with HFF variation in each MR sequence.

Results: In 10 patients we found HFF reduction after diet, with a good correlation with BMI and FT. One patient with inadequate diet showed a stable value of HFF and FT but a worsening of BMI. TSE T2-weighted sequences demonstrated to be the more accurate to evaluate HFF and its percentage of reduction.

Conclusion: MR was shown to be a valid technique in liver steatosis follow-up, free from subjective interpretations and interobserver variation, in good agreement with anthropometric values. TSE T2-weighted sequences showed a better performance and accuracy than GRE T1-weighted sequences.

SS 9.08

Non-invasive quantification of hepatic steatosis with 3.0 Tesla MR spectroscopy in patients undergoing liver resection

J.R. van Werven, H.A. Marsman, A.J. Nederveen, F.J. ten Kate, T.M. van Gulik, J. Stoker; Amsterdam/NL

Purpose: Hepatic steatosis (HS) is a risk factor in liver surgery or living donor liver transplantation. Invasive liver biopsy remains the gold standard for assessment of steatosis. Proton magnetic resonance spectroscopy (1H-MRS) could be a non-invasive alternative. The purpose of this study was to quantify steatosis with 1H-MRS in patients undergoing liver resection.

Material and methods: 1H-MRS was performed preoperatively in twenty patients undergoing liver resection. Intraoperatively, liver biopsies were taken for histopathological and biochemical analysis. A ratio representing hepatic fat was calculated from CH₂ fat peak versus the reference H₂O peak, and correlated (Spearman) with histopathological steatosis and biochemical parameters in the liver. 1H-MRS measurements were compared in different grades of steatosis to investigate discriminative power (Mann-Whitney U analysis).

Results: 1H-MRS measurements of hepatic fat correlated with histopathological steatosis assessment ($r=0.86$, $p<0.001$). 1H-MRS also correlated with biochemical fatty acid concentration ($r=0.85$, $p<0.001$). Comparing the 1H-MRS in different grades of steatosis showed significant discriminative power: no versus mild ($p=0.039$), mild versus moderate ($p=0.010$), and no versus moderate HS ($p=0.002$).

Conclusion: 3.0 T 1H-MRS can accurately measure HS in patients and strongly correlates with histopathological and biochemical hepatic fat analysis. 1H-MRS can also accurately discriminate between different grades of steatosis. The assessment of steatosis with 1H-MRS is a promising modality for accurate non-invasive preoperative risk assessment in patients undergoing major liver surgery.

SS 9.09

Inhomogeneous liver in patients under surveillance for chronic liver disease: impact of contrast enhanced US in patient management

P. Cabassa, E. Gatti, S. Palmieri, M. Morone, S. Mombelloni, R. Maroldi; Brescia/IT

Purpose: To evaluate the usefulness of contrast enhanced ultrasonography (CEUS) in patients with inhomogeneous liver ecogenicity.

Material and methods: In a 1 year period, 34 patients in screening for viral chronic liver disease (chronic hepatitis n=12; cirrhosis=22) showed inhomogeneous liver at baseline B-mode US. CEUS was performed with standard doses (2.4 ml) of SonoVue with continuous scanning with specific contrast setting at low MI (0.1, 0.2). Every nodule enhancing during arterial phase with wash out at portal or late phase was considered malignant and studied with MDCT or MR. The CEUS impact was classified into 5 categories: no effect (A), benign focal liver lesions discovered (B), indeterminate lesion (C), single HCC(D); and bilateral HCCs (E). Variables like pseudonodular appearance and raised alfafetoprotein (AFP) levels were also analysed.

Results: The outcome of CEUS was A in 14 (41.2%), B in 9 (26.5%), C in 2 (5.9%), D in 4 (11.8%), E in 5 (14.7%). Therefore, patient management significantly changed (C-E) in 11/34 patients (32.6%). HCC detection was significant superior in patients with raised levels of AFP and in patients with pseudonodular appearance of liver echotexture ($p<0.05$).

Conclusion: One third of patients changed management (C-E) following CEUS. Therefore, CEUS, from these preliminary experiences, could be proposed as useful tool in these patients.

SS 9.10

Early post-operative living related liver transplant sonographic and non-contrast Doppler as a detector and predictor of vascular and parenchymal complications in recipients

H.M. Attia¹, H.M. El Gabaly¹, A.M. Hassib¹, S.S. Labib¹, K. Tanaka², R.R. Kamel¹, G.E.D. Essmat¹, A.O. Abdel Aziz¹; ¹Cairo/EG, ²Kyoto/JP

Purpose: To correlate the clinical, laboratory, sonographic and Doppler findings in the hepatic graft vasculature in living related liver transplant (LRLT) recipients in the early post-transplantation period.

Material and methods: The study enrolled 100 adult recipients of LRLT who underwent their surgery in Dar AL-Fouad Hospital over a period of four years between 2001 and 2005. All recipients received a right hepatic lobe. Clinical and radiological reports were reviewed for vascular and parenchymal including biliary complications.

Results: Hepatic vascular problems were diagnosed in 15 recipients (15%). Their total number was 17 (9 hepatic artery, 6 portal vein, and 2 hepatic venous outflow problems). Twelve (70.6%) of the reported vascular complications occurred within the first 4 weeks post-transplantation and the remaining 5 (29.4%) occurred beyond 4 weeks post-transplantation. There was no statistical significance between the group which developed vascular complications and the group that did not in the overall mortality rate, rate of rejection, number of biliary problems, recurrence of HCV hepatitis, incidence of systemic or graft sepsis. The Doppler US findings obtained from the hepatic vasculature were reliable for diagnosing the various post-transplantation vascular problems but non-diagnostic nor specific in the patients who developed other hepatic parenchymal problems.

Conclusion: Doppler US is a reliable method in the diagnosis of hepatic vascular problems occurring in the post-transplantation setting but is less sensitive in diagnosing or in follow-up of other medical or surgical complications.

11:00 - 12:30

Dolmabahçe A

Scientific Session 10

Liver tumour ablation: technique and clinical results

SS 10.01

Flat detector-based CT during hepatic chemoembolization: impact on interventional management

P. Huppert, O. Kotterer, H. Wietholtz; Darmstadt/DE

Purpose: Flat detector (FD) based digital angiography systems offer the option of detector-based CT (DBCT). This single center prospective study evaluated the impact of DBCT on interventional management of patients during hepatic chemoembolization (HCE).

Material and methods: During 65 chemoembolizations of HCC (n=21) and liver metastases (n=44), respectively, 75 DBCT acquisitions (Dyna-CT, Siemens Medical Solutions) were obtained. For chemoembolization, various cytotoxic drugs, iodized oil, drug eluting microspheres and PVA-particles were used in combinations depending on the type of tumor. DBCT scans were obtained during arterial contrast infusion (flow 0.5–2.0 ml/sec, iodine load 100 mg/ml, delay 3–4 sec, scan time 8 sec) via microcatheters in positions selected for treatment based on angiographical findings. Axial, coronar and sagittal sets of CT-images were obtained as a rule. Appropriateness of catheter position was rated before and after considering the findings of DBCT.

Results: DBCT-images clearly showed the areas of perfusion in relation to target tumor areas. Correlation of findings of DBCT during contrast perfusion with findings of baseline CT or MRI was necessary for correct localization of target tumor volumes. Considering the findings of DBCT, catheter positions were changed in 21 of 65 procedures (32%). Reasons for changing catheter position were mismatch of target volume and perfusion area, non-target extra hepatic perfusion and insufficient perfusion via collaterals. Diagnostic information obtained by DBCT during perfusion was mostly valuable during treatments of hypovascular metastases.

Conclusion: DBCT with arterial contrast perfusion is highly valuable for proper selection of catheter position during HCE, especially in treatments of hypovascular metastases.

SS 10.02**Experience with insertion of metallic markers in the liver before radiofrequency ablation in poorly visible tumours on CT**

F. Vandembroucke¹, B. Ilisen¹, N. Buls¹, B. Op De Beeck², J. de Mey¹;
¹Brussels/BE, ²Edegem/BE

Purpose: To determine the indications and the procedure, and to evaluate technical results and the safety of insertion of metallic markers in the liver before radiofrequency ablation (RFA) in poorly visible tumors on CT-fluoroscopy.

Material and methods: From January 2003 to June 2007, 30 radio-opaque markers were inserted in liver lesions of 24 patients. These vascular platinum coils were inserted through an 18-gauge needle based on prior imaging modalities (CT and/or MRI) before the RFA procedure. After contrast enhanced CT-scan, we used those radio-opaque markers for guidance of the RFA procedure during CT-fluoroscopy. Thirty-one tumours (17 HCC, 14 metastases poorly visible on unenhanced CT-scan) with mean size 2.3 cm (SD 1.1) were ablated. The outcome and complications were analyzed.

Results: The markers guided the RFA electrodes in all cases. The median follow-up time was 11.3 months (range 2–32 months). The technique effectiveness rate was 77.8%. There were no direct complications after marker insertion. We noted 4 minor complications (subcapsular hematomas) after RFA.

Conclusion: The described technique is easy to perform and safe. This technique enables accurate guidance of RFA in poorly visible lesions on CT-fluoroscopy.

SS 10.03**Percutaneous CT-guided cryoablation of liver tumors: experience in 32 tumors**

S. Tatli, P.R. Morrison, K. Tuncali, S.G. Silverman; Boston, MA/US

Purpose: To report our experience with CT-guided percutaneous cryoablation of liver tumors.

Material and methods: Thirty-two tumors (range: 0.7–5.6 cm, mean diameter 2.7 cm) in 22 patients (12 F, 10 M; mean age 63 years, range 44–88) were treated (26 procedures; 33 total cryoablations). Of 32 tumors, 9 were hepatocellular carcinoma, and the remaining were metastases from various primaries. Using CT fluoroscopy, multiple (mean 3, range 1–7) cryoprobes were placed and intermittent CT monitoring was used to depict the growth of iceball and nearby organs. Procedures were performed under general (n=10) or monitored assisted (n=16) anesthesia. Adjacent structures were displaced away with percutaneously injected saline (n=3). All but two tumors were evaluated next day with enhanced MRI (n=29) or CT (n=1). Thirty tumors have been followed for 3 months or more (mean 6, range 3–12). Tumors were considered successfully ablated if they demonstrated no enhancement.

Results: Thirty-one (97%) of 32 tumors were successfully ablated. 31 (97%) tumors required only one treatment session. All patients but two were discharged the next day without complication. One patient developed pulmonary edema but recovered fully. An 88-year-old man experienced renal and respiratory failure the day after the procedure and died.

Conclusion: Cryoablation can be used to treat liver tumors successfully. CT scan can be used to visualize the iceball and tumor to maximize the changes of treating the tumor completely, while avoiding complications.

SS 10.04**Analysis of the use of multiple, sequentially-activated, internally-cooled electrodes for radiofrequency ablation of hepatic metastases**

J. Taylor, W.R. Lees, A. Gillams; London/UK

Purpose: To report on the use of multiple, sequentially-activated, internally-cooled radio-frequency electrodes in the treatment of hepatic metastases (HM).

Material and methods: Forty-five metastases in 26 patients, 17 male, mean age 62 years (39–82) were treated with 2 or 3 internally cooled electrodes sequentially and alternatingly activated via a switching controller (Covidien, Boulder, CO). Twenty-one patients had colorectal liver metastases, 2 breast, 2 neuroendocrine and 1 adrenal. The lesion size, location, number of electrodes, ablation zone size, completeness, complications, local recurrence, tract seeding and follow up imaging were recorded.

Results: Two electrodes were used in 26 lesions, mean diameter 2.8 cm, and 3 electrodes were used in 19 lesions, mean diameter 5.0 cm ($p < 0.05$). The mean ablation zone with 2 electrodes was 4.6 x 3.8 x 4 cm and with 3 electrodes was

5.6 x 4.8 x 4.8 cm ($p < 0.01$). Complete ablation at 24 hours was successfully achieved in 33 of 35 (94%) lesions being treated with curative intent and 73% of all lesions. There were 6 complications, one delayed abscess in a patient who was Cushingoid, 1 chest infection and four minor complications. There was no tract seeding.

Conclusion: Multiple switching electrodes can create large ablation volumes permitting treatment of patients with larger HM.

SS 10.05

Withdrawn by authors

SS 10.06**Pre-liver transplant transarterial chemoembolization for HCC beyond Milan criteria**

C. Vignali, I. Bargellini, P. de Simone, D. Campani, P. Petruzzi, R. Cioni, F. Bonvin, F. Filippini, C. Bartolozzi; Pisa/IT

Purpose: To report our experience with transarterial chemoembolization (TACE) before liver transplantation (LT) in patients with hepatocellular carcinoma (HCC) exceeding Milan selection criteria.

Material and methods: The study included 26 HCC patients (M:F=24:2, mean age 53.8 years) beyond Milan selection criteria (1–10 tumor nodules, 32–126 mm axial diameter) who underwent LT 32–381 days (mean 146) after TACE. Tumor response to TACE was evaluated by CT 1 month after treatment, according to WHO-modified criteria. Tumor necrosis on explants histology was graded as nil, minimal ($\leq 25\%$), partial ($\leq 50\%$), subtotal ($\leq 75\%$), and total (75–100%).

Results: After TACE, 1-month CT control showed complete tumor response (CR) in 12 patients (46%); total/subtotal necrosis was histologically proven in 16 (61.6%) cases on the explanted liver. At a mean follow-up of 53 months after LT (range 1–109), 9 (34.6%) cases of tumor recurrence were observed. The post-LT 5-year cumulative and recurrence-free survival rates were 64.5 and 60%. The 5-year recurrence-free survival was higher in patients with histologic total/subtotal necrosis (63.6 versus 54.5%), although the difference was not statistically significant ($p=0.3$); on the contrary, survival was significantly ($p=.004$) associated with the tumor response according to the WHO-modified criteria (83.3, 53.3 and 33% in CR, SD and PR, respectively).

Conclusion: In HCC patients beyond Milan criteria, CR assessed 1 month after TACE by CT can represent selection criteria for LT.

SS 10.07**Transarterial chemoembolization in down-staging program for HCC prior to liver transplantation: the Bologna work-in-progress experience**

A. Cappelli, E. Giampalma, A. Bazzocchi, R. Golfieri; Bologna/IT

Purpose: To assess the efficacy and the safety of transarterial chemoembolization (TACE) on long-term survival and tumor recurrence rate in down-staging patients (pt) with hepatocellular carcinoma (HCC) listed for liver transplantation (LT); a new allocation policy still under evaluation.

Material and methods: We prospectively analyzed the outcome of 173 pt listed for LT with a diagnosis of HCC. HCCs were divided in 3 groups: single nodule <3 cm (T1, 38 pts), single nodule <5 cm or multiple nodules <3 with a diameter <3 cm (T2, 94 pts) meeting the conventional Milan criteria, and the down-stage group (T3, 41 pts): single HCC <6 cm or multiple nodules <6 with a total tumor diameter <12 cm. TACE was performed in 114 pt (65.9%): 15 in T1 (39.5%), 61 in T2 (64.9%), 38 in T3 (92.7%).

Results: The rate of LT was equally distributed among the 3 groups and after a median follow-up of 21 months, the overall tumor recurrence rate was 12% and the overall patient survival was 83%. The HCC recurrence rate was comparable among the 3 groups and the presence of HCC recurrence did not affect significantly the patients' survival.

Conclusion: The pre-operative tumor stage did not affect the pt survival and the down-stage group had comparable outcome than the other groups. TACE is effective and safe as a down-staging procedure to extend selective criteria for patients waiting for LT.

SS 10.08**Doxorubicin eluting bead-enhanced radiofrequency ablation of HCC: a pilot clinical study**

R. Lencioni, L. Crocetti, E. Bozzi, P. Petruzzi, C. Vignali, M.C. Della Pina, I. Bargellin, C. Bartolozzi; Pisa/IT

Purpose: Experimental studies in animal tumour models have shown a synergy between radiofrequency (RF) ablation and adjuvant chemotherapy. The aim of our study is to assess safety and efficacy of doxorubicin-eluting bead (DEB)-enhanced RF ablation in the treatment of human hepatocellular carcinoma (HCC).

Material and methods: Twenty patients with single HCC ranging 3.3–7.0 cm (mean, 5.0±1.4 cm) showing evidence of residual viable tumor after standard RF ablation underwent intraarterial DEB administration (50–125 mg doxorubicin; mean, 60.2±21.8 mg). Follow-up period ranged 6–20 months (mean, 12±5 months).

Results: No major complication occurred. No relevant deterioration of liver function parameters was observed. The volume of treatment-induced necrosis – as measured on CT or MRI – increased from 48.1±35.7 cm³ after RF ablation alone to 75.5±52.4 cm³ after DEB administration, with an increase of 60.9 ±39%. The enhanced necrotizing effect resulted in confirmed complete response (CR) of the target lesion in 12 (60%) of 20 patients. Persistence of viable tumor mass of less than 10% of initial tumor volume was observed in the remaining 6 (40%) of 20 patients.

Conclusion: Intraarterial DEB administration substantially increases the effect of RF ablation on HCC. DEB-enhanced RF ablation is safe and results in a high rate of CR in patients' refractory to standard RF treatment.

multivariate analysis were performed using SPSS v.10.

Results: The mean number of LM was 4 (1–27) and the mean maximum diameter 3.7 cm (0.9–12). 115/309 (37%) had extra-hepatic disease. On multivariate analysis, the number and size of LM (HR 95% CI 1.9 (1.3–2.9)) and the presence of extra-hepatic disease (2.7 (1.8–4.1)) were the only significant factors to impact survival from ablation. Median, 3 and 5 yr survival in 123 patients ≤ 5 metastases, ≤5 cm with no extra-hepatic disease were 46 months, 63 and 34% from diagnosis and 36 months, 49 and 24% from ablation.

Conclusion: The number and size of LM and the presence of extra-hepatic disease were the dominant factors influencing 5 year survival.

SS 10.09**Radioembolization (yttrium 90) of liver primary and metastatic tumors: two years' experience**

A. Saltarelli, E. Notarianni, C. Urigo, M. Iozzino, R. Salvatori, R. Cianni; Latina/IT

Purpose: To evaluate liver primary and metastatic tumors radioembolization with yttrium (Y-90) in patients not responsive to chemotherapy.

Material and methods: In the last two years, we treated 110 patients suffering from liver primary or metastatic tumor. All patients arrived to our observation with disease progression, despite undergoing different major/minor surgical or micro-invasive percutaneous procedures (RFA, PEI, etc.). Patients underwent a preliminary abdominal CT and a body PET. On treatment planning, we performed a gastro-duodenal artery coiling. At the end of procedure, we injected technetium (Tc-99m) aggregated albumin through the hepatic artery. We excluded from the treatment patients with bilirubin level greater than 1.8 mg and patients with pulmonary shunt over 20% but not patients with extra-hepatic metastases. On the day of treatment, under fluoroscopy guidance, we implanted a dose of Y-90 microspheres calculated on the basis of liver tumoral involvement and BSA formula. The patients were kept under observation for 18–24 hours and discharged the day after treatment.

Results: In all cases, we obtained a reduction and/or a normalization of tumoral markers in a period of between 4 and 8 weeks. PET showed a partial and/or total remission of liver metastases. A patient with bilirubin levels of 1.7 mg died of hepatic failure, 30 days after treatment. Two patients with hepatic involvement of over 60% died during follow-up.

Conclusion: Y-90 spheres radioembolization is an effective and safe method for treating liver metastases with acceptable levels of complications and very high response rates.

SS 10.10**Analysis of the factors that impact 5-year survival following radiofrequency ablation of colorectal liver metastases**

A. Gillams, W.R. Lees; London/UK

Purpose: Radiofrequency ablation is increasingly accepted as a treatment option in patients with colorectal liver metastases (LM). We analysed the factors that impact 5-yr survival.

Material and methods: There were 309 patients, 198 male, mean age 64 years (24–92) treated at 617 treatment sessions. The standard protocol was treatment under general anaesthesia with internally water-cooled electrodes (Covidien, Boulder, CO) introduced percutaneously using US and CT guidance/monitoring. The number and size of metastases, presence and location of extra-hepatic disease, primary resection, clinical and follow-up data were recorded. Survival was calculated from the diagnosis of LM and from ablation. Univariate and

11:00 - 12:30

Marmara Hall

Scientific Session 11 Small bowel imaging

SS 11.01

Dynamic contrast enhancement: an innovative software for contrast enhancement analysis in terminal ileum Crohn's disease patients

R. del Vecovo, I. Sansoni, G. Della Longa, C. Quattrocchi, R. F. Grasso, B. Beomonte Zobel; Rome/IT

Purpose: To present an innovative tool designed for CE-analysis: Dynamic Contrast Enhancement (DyCoH).

Material and methods: 16 consecutive patients with established CD underwent serial bowel D-CE-MRI. Manual-Quantitative-Analysis (MQA) of bowel wall enhancement kinetics was performed basing on signal-to-noise ratio (SNR) of a region-of-interest (ROI). Enhancement curves were obtained at the inner (Mucosa-Submucosa, M-SM) and at the outer (Muscular-Serosa, Ms-S) parietal layers. Computer-Aided-Quantitative-Analysis (CAQA) was performed using DyCoH system developed in MATLAB environment, which produced four different inspectionable colour-maps underlying the difference in bowel wall contrast enhancement. Basing on DyCoH results, the ROI was manually positioned on the most relevant areas to obtain the dynamic evaluation. Disease activity was defined by post-colonoscopy histological features.

Results: Parietal CE-D-MRI pattern completely correlated with histologic features ($r=0.8$; $p<0.001$, Spearman test): 9 patients with active CD showed significant difference in parietal layer enhancement curves (M-SM vs Ms-S, $p<0.03$) not observed in 7 patients with inactive disease; M-SM and Ms-S enhanced curves in active patients were significantly different with respect to those of patients with inactive CD ($p<0.001$). In all tested cases, there was a complete diagnosis concordance between MQA and CAQA analysis, but DyCoH system proved to be much time-saving.

Conclusion: Clinical tests showed the effectiveness of the software and its capability to concretely support CE diagnoses, providing a simple, standardized, and rapid method of patient assessment.

SS 11.02

MR enterography for small bowel polyp surveillance in Peutz Jeghers syndrome

A. Gupta, A. Postgate, R. Illangovan, M. Marshall, C. Fraser, D. Burling; Harrow/UK

Purpose: To investigate the feasibility and patient acceptance of MR enterography (MRE) for clinically significant (10 mm+) small bowel polyps in Peutz Jeghers Syndrome (PJS).

Material and methods: Over 6 months, eligible (>16 yrs; no MRE/capsule endoscopy (CE) contraindication) PJS patients undergoing routine biennial polyp surveillance were recruited and underwent MRE followed by CE (CE=reference standard). MRE technique included oral intake 1.5 litres of 2.5% mannitol/0.2% locust bean gum; trueFISP/HASTE and pre/post contrast FLASH sequences; 20 mg iv buscopan at start of scan and prior to contrast administration. Two radiologists (limited prior MRE experience/no PJS examinations) reported examinations in consensus, blinded to CE findings, recording size (mm)/location of detected polyps. Polyp matching by comparison to CE findings was performed by study coordinator enabling calculation of performance characteristics. Patient comfort/convenience was assessed by visual analogue scale and compared using Wilcoxon signed-rank test; test preference was noted.

Results: Of 9 patients (5males/4females; Mean/Median age 34.4/36years) recruited, 6 had a total of fifteen 10 mm+ polyps (one patient was identified by CE only after reviewing MRE). MRE correctly identified all 6 patients with a 10 mm+ polyp (Per-patient sensitivity/specificity=100%/100%) and 12 of 15 polyps (sensitivity 80%; CI 0.59, 1.0) with two false positives. There was no significant difference in patient comfort/convenience ($P=0.24/1.0$, respectively) or preference between MRE/CE.

Conclusion: MRE is potentially a highly accurate and acceptable alternative imaging strategy to CE for patients with PJS undergoing polyp surveillance.

SS 11.03

MR enteroclysis in the evaluation of the small bowel neoplasm

G. Masselli, E. Casciani, E. Poletini, L. Bertini, D. D'Amico, G.F. Gualdi; Rome/IT

Purpose: The role of MR in small bowel neoplasm (SBN) has not been fully established in previous studies. The aim of this study was to evaluate the usefulness of MR Enteroclysis (MRE) in the diagnosis of SBN.

Material and methods: 100 patients (58 males and 42 females) who were suspected of having palpable abdominal mass ($n=28$), low grade small bowel obstruction ($n=36$), unexplained gastrointestinal bleeding ($n=24$), and refractory celiac sprue ($n=12$) underwent prospectively to MRE. MRE were performed on 1.5 T magnet by injection of 1.5-2 l of polyethylneglycol (PEG) solution via a nasojejunal catheter. MRE findings were analyzed by two radiologists working in consensus. Findings were compared with the results of endoscopy, enteroscopy, videocapsule endoscopy, histopathologic analysis, or clinical follow up.

Results: MRE was well tolerated in all 100 patients. In 11/100 patients (11%) that suspected of having palpable abdominal mass, MR was performed with oral administration of PEG solution. MRE of small-bowel masses allowed the diagnosis of SBN ($n=18$), small bowel lymphoma complicating celiac disease ($n=3$), and Crohn's disease ($n=27$). Negative examination included 52 patients. Tumors ranged in diameter from 0.5 to 9 cm (mean range 4 cm). Sensitivity, specificity, accuracy, positive predictive value, and negative predictive value of MRE were 94, 90, 92, 89, and 94%, respectively.

Conclusion: MRE permits visualizing luminal, parietal, and mesenteric abnormalities and is an accurate method for the depiction of SBN.

SS 11.04

Improved diagnosis of Crohn's disease by peristaltic motion assessment: a comparison of standardized MR of the small bowel with and without cine TrueFISP sequence

M.A. Patak¹, C. Waldherr¹, C. Stoupis², S.M. Erturk³, J.M. Froehlich⁴; ¹Berne/CH, ²Maennedorf/CH, ³Istanbul/TR, ⁴Winterthur/CH

Purpose: Peristaltic motion evaluation in MR enterography (MRE) of the small bowel for Crohn's disease (CD) has not been established. The aim was to evaluate the diagnostic accuracy of CD-MR by adding cine TrueFISP (cMRE) sequences for the assessment of CD.

Material and methods: 40 patients with histological proven CD ($m:22$, $f:18$) underwent standardized MRE of the small bowel (ingestion: 1000 ml of 3% Mannitol). Imaging was done by TrueFISP (cor & trans), T2w-HASTE (cor & trans) and coronal T1w-FLASH-3D 20, 60 and 90 sec after iv-contrast. Cine MRE were acquired covering the entire small bowel using cor plane 2D cine TrueFISP sequences with a slice repetition time of 500 msec. Both MRE and cMRE were evaluated by two readers for image quality, bowel distension and number of pathologic findings.

Results: MRE image quality was scored as good in 70/78/78% (upper/lower abdomen/terminal ileum). cMRE distension and motion were scored as good in 80/83% (upper abdomen), in 90/88% (lower abdomen) and in 85/90% (terminal ileum). Number of findings of cMRE compared to MRE: wall thickening 31/25 ($p=0.01$), mural or extramural masses 1/0, wall layering 17/12 ($p=0.03$), mucosal ulcers 5/2 ($p=0.09$), abscesses 1/0, enlarged lymph nodes 21/12 ($p=0.005$), fistulae 0/1, comb sign 22/16 ($p=0.006$) and stenoses 24/19 ($p=0.03$). Overall, cMRE detected additional 12 lesions in these patients, cMRE 44 lesions, MRE 32 lesions ($p=0.008$).

Conclusion: The inclusion of small bowel peristaltic motion evaluation in MR imaging of CD increases the lesion detection rate for CD related pathologic findings significantly compared to standard MRE.

SS 11.05

Prediction of angiogenesis in Crohn's disease using quantitative and semi-quantitative in-vivo dynamic contrast enhanced MRI

S.A. Taylor, S. Punwani, R. Greenhalgh, M. Rodriguez-Justo, A. Bainbridge, E. de Vita, S. Halligan; London/UK

Purpose: Increased mural angiogenesis is reported in Crohn's disease. The purpose was to assess dynamic contrast enhanced- MRI (DCE-MRI) in predicting small bowel mural microvascular density.

Material and methods: 11 consecutive Crohn's patients (>16 yrs age) undergoing small bowel surgery underwent pre-operative MRI enterography. Following 10 ml gadolinium injection (3 mls/sec), DCE-MRI was performed through the diseased segment using a 2D spoiled gradient echo sequence (TR/TE: 11/3.2 ms; flip angle 35°) every 3 seconds during a 30 s breath-hold, and then during gentle breathing (every 6 seconds) for 5 minutes. Regions of interest (ROIs) were placed in the abnormal bowel wall and corrected enhancement curves generated to calculate Slope of enhancement (SoE), ERdyn and Ktrans and ve. Post surgical resected specimens were scanned to ensure histological sections were taken through the MRI ROI placement sites. Mural microvascular density (MVD) was quantified after CD34 staining (Chalkley point method). Dates were correlated using Kendalls rank correlation coefficient.

Results: MVD ranged from 31 to 52, SoE from 0.05 to 0.50, ERdyn from 7.1 to 19.2, Ktrans from 0.02 to 0.08 and Ve from 0.04 to 0.37. SoE was strongly negatively correlated with MVD ($\tau = -0.77$, $p = 0.002$), but there was no correlation between MVD and ERdyn ($p = 0.18$) or Ktrans and Ve ($p = 0.15$ and 0.75, respectively).

Conclusion: A strong negative relationship exists between SoE and MVD in Crohn's disease. Angiogenesis may reflect a response to reduced mural blood flow.

SS 11.06

Prediction of histopathological markers of mural inflammation in Crohn's disease using quantitative and semi-quantitative in-vivo dynamic contrast enhanced MRI

S.A. Taylor, S. Punwani, R. Greenhalgh, M. Rodriguez-Justo, A. Bainbridge, E. de Vita, S. Halligan; London/UK

Purpose: To correlate in-vivo dynamic contrast enhanced MRI (DCE-MRI) parameters with histologically defined mural inflammation.

Material and methods: 11 consecutive Crohn's patients (>16 yrs age) undergoing small bowel surgery underwent pre-operative MRI enterography. Following 10 ml gadolinium injection (3 mls/sec), DCE-MRI was performed through the diseased segment using a 2D spoiled gradient-echo sequence (TR/TE: 11/3.2 ms; flip angle 35°) every 3 seconds during a 30 s breath-hold, and then during gentle breathing (every 6 seconds) for 5 minutes. Regions of interest (ROIs) were placed in the abnormal bowel wall and corrected enhancement curves generated to calculate Slope of enhancement (SoE), ERdyn, Ktrans and ve. Post surgical resected specimens were scanned to guide histological section selection. Validated histological acute and chronic inflammatory scores (AIS and CIS) were derived based on grading of mucosal ulceration, oedema, neutrophil quantity, infiltration, and depth of lymphoid aggregates, perineural inflammation and granulomas, respectively. Data were correlated using Kendalls-rank correlation coefficient.

Results: AIS ranged from 0 to 10, and CIS 0 to 7, SoE 0.05 to 0.50, ERdyn from 7.1 to 19.2, Ktrans from 0.02 to 0.08 and Ve from 0.04 to 0.37. There were no significant correlations between MRI and histopathological scores. In particular, neither SoE nor ERdyn correlated with AIS ($p = 0.3$, and $p = 0.13$, respectively) or CIS ($p = 0.94$, $p = 0.99$, respectively).

Conclusion: Mural MRI contrast dynamics in Crohn's disease do not simply reflect the severity of histological inflammation.

SS 11.07

MRI evaluation of paediatric Crohn's disease using a super-paramagnetic oral contrast agent

V. Garbarino, F. Maccioni, O. Borrelli, F. Viola, S. Cucchiara, M. Marini; Rome/IT

Purpose: To assess with MRI the main morphological changes and complications of Crohn's disease in paediatric patients.

Material and methods: 40 patients, mean age 15 years (range 6–18), underwent MRI scan following the administration of super-paramagnetic oral contrast agent at variable doses, according to patient weight and compliance, using T2-weighted HASTE (half Fourier snapshot turbo spin echo), and T1-weighted FLASH (fast low angle shot) sequences, both with or without fat saturation (FS), before and after contrast agent (gadolinium) iv injection. Two radiologists independently evaluated localization and length of the lesions, complications (stenoses, abscesses and fistulas), and peri-anal localization of Crohn's disease. MRI results were compared with ileo-colonoscopy, barium upper GI series and intestinal US examinations. Sensitivity and accuracy were estimated. Results were also compared with data obtained from an adult population sample.

Results: MRI accuracy in lesions localization in the small and large bowels was, respectively, 93 and 97%. MRI revealed 83% of stenoses, 100% of entero-enteric and peri-anal fistulas. The percentage of ileal localization was the same in children and adults, while colonic localization was more frequent in children (D: 40%).

Conclusion: MRI, as a non invasive and safe technique, has shown a high accuracy in the evaluation of intestinal lesions and complications of paediatric Crohn's disease, reporting a good correlation with the results obtained by more invasive reference examinations.

SS 11.08

Absolute value of T2-weighted sequences in Crohn's disease

M. Martinelli, F. Maccioni, A. Castorino, I. Staltari, A.R. Pino, M. Marini; Rome/IT

Purpose: To assess the accuracy of T2-weighted sequences in the evaluation of Crohn's disease.

Material and methods: Sixty-five patients with Crohn's disease underwent MRI, using T2-weighted HASTE (Half-Fourier SnapShot Turbo spin-Echo) sequences, with or without fat-saturation after oral administration of a superparamagnetic contrast agent, to optimize T2 bowel wall signal. For comparison, FLASH (Fast Low Angle Shot) T1-weighted sequences, with or without fat-suppression, before and after gadolinium injection were obtained. References examinations were: barium studies, ileocolonoscopy, US and CT, and endoscopic index of severity (CDEIS). The data obtained with T2-sequences were evaluated independently from those obtained with T1-sequences, as for: - disease localization and length of lesions, from jejunum to rectum - presence of wall fibrosis, strictures and fistulas.

Results: T2 weighted MRI was 98% sensitive and 92% specific for detection of ileal lesions; 80% sensitive, 78% specific for jejunal lesions; 67 to 88% sensitive and 96 to 100% specific for colonic lesions, at different levels. Accuracy in detecting entero-enteric fistulas was 88%, non enteric fistulas 98%; all abscesses and phlegmons were diagnosed. T2-wall signal and T2-signal of the perivisceral fat were significantly related ($p < 0.001$) to CDEIS and biological activity. Similar results were obtained for T1-weighted post-Gadolinium sequences.

Conclusion: T2-weighted MRI can be used alone for the assessment of Crohn's disease.

SS 11.09

Assessment and clinical validation of colon motility using functional cine-MRI

S. Kirchhoff, M. Nicolaus, J. Schirra, C. Kirchhoff, B. Göke, M.F. Reiser, A. Lienemann; Munich/DE

Purpose: GI functional disorders (constipation, stool-outlet-obstruction) are common symptoms. The diagnosis of functional motility-disorders especially of the colon is difficult due to non-existing adequate examination-techniques. Barostat and manometry are rarely used in routine due to duration and invasiveness. Colon-transit-time-, double-contrast-enema-examination provide only static information. Due to great soft-tissue contrast, missing ionizing radiation, MRI seems to be appropriate to depict morphology and function of the large bowel. Therefore, the aim of our study was to cholinergically stimulate the phasic colon motility under manometric control and to simultaneously identify the morphology with Cine-MRI.

Material and methods: During colonoscopy, a water-perfused-multi-luminal-probe is placed in the descending-colon, and intraluminal pressure-changes were marked over-time. After a 90-minute-equilibration-phase, an MR-exam-at-rest (HASTE-sequence, 1.5 Tesla-Avanto®, Siemens-Medical-Solutions, Erlangen) was performed. Consecutively, bisacodyl (3 ml-and-10 ml-saline 0.9%) were instilled via the probe. Cine-MRI and manometry were performed simultaneously over 24 minutes. Manometry-data were analysed for high amplitude propagated contractions using PC-based software, and MRI-data were primarily analysed visually.

Results: 18 healthy volunteers (age: 19–62 years, 8 f, 10 m) were enrolled. In correlating MRI with manometry-data, manometry showed 13 HAPCs, 12 were identified in MRI. In addition, MRI showed 7 negative-colonic-peristaltic-waves (relaxation) without correlate in manometry.

Conclusion: In this feasibility study, we could show that Cine-MRI allows for a visualisation and quantification of HAPCs using an adequate stimulus. However, our first visual evaluation of MR-data needs to be supported by the results of semi-automatic software being the focus of current investigations.

SS 11.10**MR enterography compared to CT enterography in the evaluation of bowel disease**

M.M. Amitai¹, L. Raviv-Zilka², B. Avidan², S. Apter²;
¹Tel Aviv/IL, ²Ramat Gan/IL

Purpose: The relatively high radiation exposure in CT enterography (CTE) constitutes a growing limitation when imaging the bowel. The purpose of this study was to compare the diagnostic accuracy of MR-Enterography (MRE) to CTE in the evaluation of bowel disease (BD).

Material and methods: Between November 2005 and December 2007, 69 consecutive patients were referred for MRE. Twenty four CTE examinations performed within six months after the MRE examination were available for comparison (mean age 26 years, mean interval 2 months). Fifteen of the 24 patients had Crohn's disease; four non specific abdominal pain, two celiac disease, one lymphoma, one cystic fibrosis and one patient had bowel wall vascular malformation. MRE findings were compared with CTE examinations by two radiologists in consensus for wall thickening, bowel stenosis, and presence of abscess, phlegmon and fistula.

Results: The correlation between CTE and MRE showed an accuracy of 87% (21/24) for wall thickening, 71% (17/24) for stenosis, 96% (23/24) for abscess, 91% (22/24) for phlegmon, and 66% (16/24) in the diagnosis of fistula.

Conclusion: A good correlation was found between MRE to CTE regarding the evaluation of wall thickening, abscess and phlegmon. A moderate accuracy rate was found regarding luminal stenosis and detection of fistulae. MRE is a reliable modality for the evaluation of BD, particularly in patients necessitating recurrent imaging and in populations sensitive to radiation exposure.

11:00 - 12:30

Haliç Hall

Scientific Session 12**Liver Volumetry and vascular assessment****SS 12.01****Preoperative liver-volumetry: how does the slice thickness influence the accuracy of MDCT- and MR-based liver volumetry?**

C.S. Reiner, C. Karlo, H. Petrowsky, B. Marincek,
T. Frauenfelder, D. Weishaupt; Zurich/CH

Purpose: To investigate the influence of slice thickness (ST) on the accuracy of MR- and MDCT-based liver volumetry (LV).

Material and methods: 20 patients who underwent liver surgery were preoperatively imaged with either a 64-slice MDCT- (n=10) or a 1.5 T MR-scanner (n=10). MDCT- and 3D-GRE MR-images were reconstructed with different ST (2, 4, 6 and 8 mm). The total liver volumes (TLV) were measured by two independent readers based on different ST using semiautomatic software. Results were compared to the TLVs obtained at 2 mm ST which served as standard of reference (SOR). The time needed for each volumetry was recorded.

Results: When using MDCT, a statistical difference was seen only between the volumes based on 2 vs 8 mm ST for both readers (p=.012/.002). When MR-imaging was used for volumetry, there was no statistical difference between the volume of the SOR and the volumes based on thicker slices (4, 6 and 8 mm). Regarding the time to perform volumetry, there was a significant gain of time for both readers when volumetry was performed on 6 and 8 mm MDCT- and on 4, 6 and 8 mm MR-slices (p<.0167) compared to the SOR.

Conclusion: Accuracy of LV based on either MDCT- or MR-images is dependent on ST. With respect to accuracy of the calculated volume and the significant gain of time, 6 mm ST is preferable for CT-imaging and 8 mm ST for MR-imaging.

SS 12.02**Anatomic variations of the hepatic arteries in 250 patients studied with 64-row MDCT angiography**

C.N. de Cecco¹, R. Ferrari², P. Paolantonio², M. Rengo¹,
F. Vecchiotti², A. Laghi²; ¹Rome/IT, ²Latina/IT

Purpose: To present the findings of 250 consecutive CT angiographies of the hepatic arteries and to compare them with data from literature obtained in other large 4-16 row CT series.

Material and methods: A total of 250 consecutive 64-row CT angiographies (CTA) obtained using a high resolution protocol were retrospectively evaluated. Arterial phase images were analyzed by two radiologists in consensus using different reconstruction algorithms and the anatomic findings were grouped according to Michels classification. Arterial variants not included in Michels classification were separately recorded.

Results: A normal arterial pattern was observed in 64.8% of the cases. The most common anomaly was Michels type III (9.6%), followed by types V and II (6.0 and 4.8%), type VI (3.6%), type VII (2.0%), types IV and IX (1.6%), and type VIII (1.2%). No cases of Michels type X were detected. Additional, previously unclassified variations were observed in 4.8% of the cases.

Conclusion: 64-row CTA compared to previous work with 4-16 detectors permits to depict an higher number of accessory hepatic arteries, thanks to isotropic voxel, high resolution protocols and optimization of contrast administration. The visualization of these abnormalities may be a crucial point in programming operative procedures like liver transplantation, hepatic resections and chemo-embolizations. This approach could probably permit a reduction in iatrogenic lesion.

SS 12.03**Contrast enhancement with iomeprol-400 and iodixanol-320 in patients undergoing contrast-enhanced MDCT of the liver**

L. Grazioli¹, C. Catalano², L. Bonomo², J. Xu³, K. Chen³,
L. Romano⁴; ¹Brescia/IT, ²Rome/IT, ³Shanghai/CN, ⁴Naples/IT

Purpose: To compare contrast enhancement with iomeprol (400 mgI/mL) vs iodixanol (320 mgI/mL) in patients undergoing contrast-enhanced liver multidetector CT (MDCT).

Material and methods: 183 patients received equi-iodine doses (40 gI) of iomeprol-400 or iodixanol-320 IV at 4 mL/sec. Liver MDCT was performed using scanners with at least 4 detector rows. Two off-site, independent, blinded readers assessed images at the abdominal aorta, inferior vena cava (IVC), portal vein, and liver parenchyma. Descriptive statistics were used to summarize the contrast density (HU) measurements for the two study groups. The mean contrast densities achieved in each of the four regions of interest were compared and 95% confidence intervals estimated.

Results: 91 patients received iomeprol-400 while 92 received iodixanol-320. The two study groups were comparable with regard to sex, age, weight, and race. Iomeprol-400 resulted in significantly greater arterial phase enhancement of the abdominal aorta compared to iodixanol-320 (Reader 1: 339.7 vs 292.6 HU, 95% CI [19.4, 65.5], p=0.0004; Reader 2: 327.9 vs 293.0 HU, 95% CI [6.6, 54.3], p=0.01). Iomeprol-400 also led to greater enhancement of liver parenchyma during the portal-venous phase (significantly greater for Reader 1 [p=0.04] and of borderline significance for Reader 2 [p=0.05]). No significant difference was noted between the two study groups regarding enhancement of the IVC or portal vein.

Conclusion: Iomeprol-400 provides significantly greater enhancement in the arterial phase and improved enhancement of hepatic parenchyma in the portal-venous phase compared to iodixanol-320 at the same iodine dose in patients undergoing MDCT of the liver.

SS 12.04**Hepatic perfusion changes in experimental acute pancreatitis: demonstration by perfusion CT**

S. Tutcu, S. Sertler, Y. Kaya, E. Kara, N. Nese, G. Pekindil,
T. Coskun; Manisa/TR

Purpose: In different experimental studies, hepatic damages were shown histopathologically in acute pancreatitis but there are a few studies about perfusion disorders that accompany these histopathologic changes. Perfusion CT (pCT) provides the ability to detect regional and global alterations in organ blood flow. The purpose of the study was to describe hepatic perfusion changes in experimental acute pancreatitis model with pCT.

Material and methods: Forty Sprague-Dawley rats of both genders with average weight of 250 grams were used. Rats were randomized into two groups. pCT was performed. Perfusion maps were formed by processing the obtained images with perfusion CT software. Blood flow (BF) and blood volume (BV) values were obtained from these maps. All pancreatic and liver tissues were taken off with laparotomy and histopathologic investigation was performed. Student T test was used for statistical analyses.

Results: Our study showed the development of histopathologically changes like hepatic portal inflammation, sinusoidal dilatation and hepatocytes degeneration. In pCT, we found statistically significant increase in blood volume in both lobes of liver and in blood flow in right lobe of the liver ($p < 0.01$). Although blood flow in left lobe of the liver increased, it did not reach statistical significance.

Conclusion: The quantitative analysis of liver parenchyma with pCT showed that acute pancreatitis causes a significant perfusion changes in the hepatic tissue.

SS 12.05

Vascular enhancement in Gd-EOB-DTPA and Gd-DTPA enhanced dynamic liver MRI in an animal model: comparison of different injection regimens

C.J. Zech¹, B. Vos², M. Ulrich², M.F. Reiser¹, J. Breuer², H. Weinmann²; ¹Munich/DE, ²Berlin/DE

Purpose: To compare the peak enhancement of the liver vasculature in an animal model for the standard-dose of Gd-EOB-DTPA and Gd-DTPA with two different injection regimens.

Material and methods: Five pigs were examined on a 1.5 T MR-system (Avanto, Siemens Medical Solution, Germany) with a T1w-3D-GRE-sequence (12 slices a 3 mm; FOV 250 mm; matrix 128). This sequence was repeated over a period of 75 sec with an acquisition-time of 5 sec starting together with contrast-agent injection of 25 μmol Gd-EOB-DTPA (Primovist®)/kg body-weight or 100 μmol Gd-DTPA (Magnevist®)/kg, both Bayer Schering Pharma AG, Germany at a flow-rate of each 1 cc/sec and 2 cc/sec, flushed with 10 cc saline. Signal-intensities (SI) were measured in the liver-vasculature and the SI increase from baseline was calculated.

Results: Mean peak SI for 1 cc/sec respective 2 cc/sec in the aorta was 787.7 respective 701.4 ($p=0.04$) for Gd-EOB-DTPA and 849.7 respective 747.8 ($p=0.11$) for Gd-DTPA. Mean peak SI in the portal-vein was 382.6 respective 344.5 ($p=0.36$) for Gd-EOB-DTPA and 534.6 respective 542.6 ($p=0.89$) for Gd-DTPA. The shape of the enhancement curves in each individual pig for aorta and portal-vein were similar.

Conclusion: A decreased injection speed of 1 cc/sec significantly increases arterial peak-enhancement in EOB-enhanced dynamic liver MRI, whereas peak-enhancement in the portal-vein is not changed significantly. With regard to arterial enhancement, this injection regimen compensates for the lower dosage of 25 μmol Gd-EOB-DTPA/kg compared to a standard Gd-DTPA-protocol.

SS 12.06

Sinusoidal obstructive syndrome diagnosed with superparamagnetic iron oxide-enhanced MRI in patients with colorectal metastases treated with chemotherapy

J. Ward, J.A. Guthrie, M. Sheridan, S. Boyes, J.T. Smith, D. Wilson, J. Wyatt, D. Treanor, P.J. Robinson; Leeds/UK

Purpose: Oxaliplatin therapy for the treatment of colorectal metastases may induce sinusoidal obstructive syndrome (SOS). SOS causes the liver to become friable and haemorrhagic and so pre-operative diagnosis is important. This study investigated the diagnosis of SOS using superparamagnetic iron oxide (SPIO)-enhanced T2w GRE imaging.

Material and methods: 126 patients with treated colorectal metastases underwent unenhanced MRI followed by T2w GRE sequences after SPIO. The images were reviewed by two experienced observers in consensus who determined the presence and severity of linear and reticular hyperintensities, indicating SOS-type liver injury. In 60 patients with histological verification of the MR findings, sensitivity, specificity, PPV and NPV, for the detection of moderate to severe SOS, were calculated.

Results: 28/64 surgical and 21/62 non-surgical patients had moderate to severe SOS on post-SPIO MR; unenhanced images were unhelpful for diagnosis. 26/28 and 20/21 were treated with an oxaliplatin based chemotherapy regime. MR achieved a sensitivity of 87% (95% CI's: 66–97%), a specificity of 89% (95% CI's: 75–97%), PPV of 83% (95% CI's: 63–95%), and NPV of 92% (95% CI's: 77–98%). SOS was never found at surgery or histology in patients whose background liver parenchyma was normal on SPIO-enhanced MR.

Conclusion: SOS is present in a significant proportion of patients with treated colorectal metastases and is effectively detected on SPIO-enhanced T2-w GRE images.

SS 12.07

MRI of hepatic changes in patients with Rendu-Osler-Weber syndrome (hereditary hemorrhagic telangiectasia)

G.K. Schneider¹, A. Buecker¹, P.M. Fries¹, C. Sommavilla¹, A. Massmann¹, U.W. Geisthoff²; ¹Homburg/DE, ²Köln/DE

Purpose: To demonstrate liver imaging findings in patients with hereditary hemorrhagic telangiectasia (HHT).

Material and methods: 203 patients (87 men: 47.4±17.6 years; 116 women: 46.1±15 years) with diagnosed HHT or first degree relatives underwent screening MRI to ascertain cerebral, abdominal and pulmonary involvement. Of these patients, 38 presented with arteriovenous malformations (AVMs) of the liver and were further investigated before and after Gd-BOPTA administration at 0.05 mmol/kg bodyweight. Both dynamic and hepatobiliary phase imaging was performed.

Results: Patients with liver AVMs fell into two broad groups. In 19 patients, a prominent celiac trunk/hepatic artery and multiple regenerative hepatic lesions were present and the overall liver size was increased. The remaining 19 patients had hepatic AVMs, a prominent celiac trunk/hepatic artery and tortuous intrahepatic vessels but no regenerative nodules. In this group, the liver size was normal or decreased and 9 patients presented with RV-insufficiency.

Conclusion: Two distinct pathophysiologic mechanisms seem to occur: 1) if regenerative nodules are present, these seem to result from arterio-portal shunts with local overgrowth of hepatic tissue reflecting increased arterial supply. Lesions on MRI after Gd-BOPTA demonstrate similar enhancement to FNH suggesting a similar developmental mechanism; 2) in HHT patients without regenerative nodules, the blood-flow bypasses the liver through direct arterio-venous shunts. Thus, the liver size remains unchanged although an increased RV-volume load results in RV-insufficiency.

SS 12.08

Focal liver lesions in patients with cavernous transformation of the portal vein: diagnosis and MR features

A. Galluzzo¹, O. Bruno², G. Brancatelli¹, A. Plessier², B. Condat², M. de Maria¹, V. Vilgrain²; ¹Palermo/IT, ²Clichy/FR

Purpose: To retrospectively evaluate magnetic resonance (MR) imaging findings of focal liver lesions in patients with cavernous transformation of the portal vein.

Material and methods: Clinical, pathologic, and imaging findings were retrospectively reviewed in 29 patients with cavernous transformation of the portal vein. Two radiologists evaluated the presence of focal lesions. In patients with hepatic nodules, size, number and MR features (signal and enhancement of each lesion), and biopsy were assessed. Diagnosis of the liver lesions was based on typical imaging or liver biopsy.

Results: Thirteen patients had focal liver lesions (44.8% of all patients). Eight patients had a solitary lesion: 5 with FNH-like lesions and 3 with hemangiomas. Five patients had multiple lesions: 3 with FNH-like lesions, one with hemangiomas and one with the association between FNH-like lesions and a liver adenoma. The diagnosis of FNH-like lesion and liver adenoma were confirmed at pathology in three patients. The mean size of FNH-like lesions was 16 mm (range: 5–40 mm). The mean delay time between diagnosis of the portal vein thrombosis and the detection of FNH-like lesions was 4.5 years (range: 0–13 years).

Conclusion: Focal liver lesions are often observed in patients with cavernous transformation of portal vein. All lesions are benign. Most of them are FNH-like lesions.

SS 12.09

Withdrawn by authors

SS 12.10

Solitary necrotic nodules of the liver: radiological-histopathological correlation

E. Bozzi, L. Crocetti, M.C. Della Pina, E. Mauro, R. Lencioni, C. Bartolozzi; Pisa/IT

Purpose: Solitary necrotic nodule (SNN) of the liver is a rare benign lesion, typically incidentally found at imaging. The aim of our study is to correlate imaging findings with histopathological examination.

Material and methods: Twelve hepatic SNN have been observed in 9 non-

cirrhotic patients (50–63 years old). All patients underwent imaging examinations, including contrast enhanced ultrasound (CEUS), multidetector computed tomography (MDCT) and magnetic resonance (MR), followed by core biopsy.

Results: All lesions were located in the right hepatic lobe and were homogeneously hypoechoic at baseline US. At CEUS, the lesions appeared hypoechoic, without bubbles perfusion. At dynamic triple-phase MDCT, all lesions appeared hypodense both in pre-contrast and after contrast injections, without any significant contrast uptake. RM showed hypointensity in T1-w images in all lesions; in T2-w images, 10 lesions were iso-hypointense and 2 were hyperintense at the periphery, with hypointense central area. After Gadolinium-BOPTA administration, lesions were hypointense both in dynamic and hepatobiliary acquisitions. All patients underwent percutaneous US-guided core biopsy. At histopathology, all lesions consisted of a fibrotic capsule with inflammatory chronic cells and a central core of amorphous necrotic material. All specimens, analyzed with Ziehl-Neelsen, Gram and periodic acid schiff, were negative for bacteria, fungi or parasitic infection.

Conclusion: SNN shows typical imaging pattern that correlates with pathological findings. When typical pattern is demonstrated, the diagnosis of SNN can be confidently made by imaging.

11:00 - 12:30

Topkapi A

Scientific Session 13

Colon and rectum: multimodality approach

SS 13.01

MR-colonography to study colorectal diverticula: comparison of different MR sequences

G. Della Longa, I. Sansoni, R. del Vescovo, E. Piccione, F. Occhicone, B. Beomonte Zobel; Rome/IT

Purpose: To study diverticular disease with different MR sequences and define the more suitable study protocol.

Material and methods: A total of 29 consecutive patients with proven colon diverticula (CD) underwent MRC. Examinations were performed on a 1.5 T scanner equipped with high-performing gradients (amplitude 30 mT/m). On axial and coronal planes, we acquired T2-weighted sequences (HASTE and TSE with fat-saturation) e T1-weighted sequences (true-FISP and FLASH-2D with Fat-Suppression) sequences. FLASH images were also acquired 75 seconds after intravenous administration of paramagnetic contrast agent. Gold standard was considered the integration of all sequences and/or other imaging modalities (CT and conventional colonography).

Results: true-FISP showed to be the most accurate in diverticula identification and morphologic definition (100 vs 61% of FS-TSE, 14% of HASTE and 44% of FLASH) by standing out the colon profile; contrasted-FLASH demonstrated to be the more sensitive for diverticulitis diagnosis and identification of diverticula complication (90 vs 10% of FS-TSE) because it better demonstrates the flogistic reaction of colonic wall and pericolic tissues. FS-TSE showed the lowest sensitivity in identifying diverticula (61%), and low diagnostic capability in morphologic assessment (14 vs 100% of true-FISP). HASTE provided the worst performance.

Conclusion: MRC showed a high diagnostic accuracy and the integration of true-FISP and contrasted-FLASH sequences is sufficient to provide a satisfying evaluation of CD.

SS 13.02

The comparison between MRI and MSCT-enteroclysis in the diagnosis of bowel endometriosis

E. Biscaldi, A. Fasciani, S. Ferrero, V. Remorgida, G.A. Rollandi; Genoa/IT

Purpose: To compare the effectiveness of MRI and MSCT-enteroclysis (MSCTe) in determining the presence of bowel endometriosis (BEM) and the depth of bowel wall infiltration of the nodules.

Material and methods: We evaluated 26 women (aged 19–38) with signs and symptoms suggestive of colorectal endometriosis. Patients underwent MRI (1T magnet, phased array coil, multiplanar FSET1, T1 fat sat, T2, T1 post-Gado sequences) and MSCTe (16 rows). The exams were reviewed independently by two radiologists. All women underwent laparoscopy within 2 weeks; radiological

findings were compared with surgical and histological data. Statistical analysis was performed with SPSS 13.0.

Results: The presence of BEM was detected by MRI in 11 (42.3%) women and by MSCTe in 12 (46.2%). Surgery confirmed BEM in 12 patients identified by MSCTe. In the diagnosis, sensibility, specificity, PPV, NPV were 91.7, 100, 100, 93.3% for MRI and 100, 100, 97, 100% for MSCTe. 21 nodules were identified by MRI and 22 by MSCTe; surgery identified 25 nodules: 13 located on the rectum, 11 at sigmoid colon, and 1 at caecum. One false positive nodule was observed at MSCTe. Among correctly identified nodules, MRI estimated the depth of infiltration to the serosa in 8 cases and to the muscularis in 13. At MSCTe, 4 nodules were judged to infiltrate the serosa, 16 to reach the muscularis propria, and 1 the mucosa. MSCTe correctly estimated the depth of nodules infiltration, significantly more frequently than MRI ($p=0.048$; Fisher's exact test).

Conclusion: Both MRI and MSCTe reliably detect the BEM nodules; however, MSCTe is more accurate in estimating the depth of infiltration in the bowel wall.

SS 13.03

Intensive imaging surveillance following curative resection for colorectal cancer

J.K. Bell, S.H. Lee, D.K. Biyani, A.J.M. Watson; Manchester/UK

Purpose: Guidelines on follow-up imaging after curative surgery for colorectal cancer (CRC) are unclear. In the absence of definitive evidence, The Association of Surgeons of Great Britain recommends a single CT scan of the abdomen and thorax during the first two years. The aim of this study was to determine the benefit from more intensive imaging surveillance in identifying resectable liver metastases and the effect on survival outcome.

Material and methods: A prospective analysis of 125 patients, who underwent curative resection of CRC, was entered into an intensive imaging surveillance programme. Patients underwent a CT abdomen and thorax at 3–6 monthly intervals for two years and then annually for a further three years.

Results: Duke's stage was recorded at presentation (Duke's A 19%; B 43%; C1 34%; C2 4%). CT identified metastases in 18 patients (A 1; B 3; C1 12; C2 2). Twelve were diagnosed on the first CT, four on the second, two on the third and none on subsequent follow-up (liver: 16; liver and lung: 2). Five patients underwent hepatic resection and three are alive at two years. All resectable liver metastases were reported in the first year.

Conclusion: Patients with advanced stage CRC are at greatest risk of liver metastases and most present in the first post-operative year. Early intensive imaging surveillance increases the detection of resectable liver metastases and improves survival.

SS 13.04

CT perfusion of rectal carcinoma monitoring response to neoadjuvant treatment: initial results

P. Paolantonio¹, R. Ferrari², P. Lucchesi², F. Vecchietti², M. Rengo², A. Laghi²; ¹Rome/IT, ²Latina/IT

Purpose: To prospectively monitor changes in rectal cancer perfusion after combined neoadjuvant chemotherapy and radiation therapy with perfusion computed tomography (CT).

Material and methods: Eleven patients with rectal adenocarcinoma (7 men, 4 women) underwent perfusion CT on a 64-MDCT scanner; all of them underwent neoadjuvant chemotherapy and radiation therapy. In all patients, perfusion CT was repeated neoadjuvant therapy. Dynamic perfusion CT was performed for 50 seconds after intravenous injection of contrast medium. Blood flow (BF), blood volume (BV), mean transit time, and permeability–surface area product (PS) were calculated in the tumor and in normal rectal wall. Wilcoxon signed-rank was used for data comparison.

Results: BF, BV, and PS were significantly higher in rectal cancer than in normal rectal wall ($P<0.001$). BF, BV, and PS significantly decreased after combined chemotherapy and radiation therapy ($P<0.01$).

Conclusion: Perfusion CT has potential for monitoring the effects of combined neoadjuvant chemotherapy and radiation therapy.

SS 13.05

Whole-body MRI versus whole-body PET/CT in staging of colon cancer: initial clinical results

E. Squillaci, C. Ciccio, S. Mancino, R. Danieli, O. Schillaci, G. Simonetti; Rome/IT

Purpose: To assess the accuracy of whole-body MRI (WBMRI) in comparison with whole-body [18F]-2-Fluoro-2-deoxy-D-glucose (FDG) PET/CT (WBPET) for staging newly diagnosed colon cancer.

Material and methods: 20 consecutive patients with previously diagnosed colon cancer underwent WBMR at 3T (Philips Achieva, Best, The Netherlands) (unenhanced coronal T2w and T1w and T2w STIR sequence from head to toe, followed by successive ce-T1 w 3D sequences) and whole-body [18F]-2-Fluoro-2-deoxy-D-glucose (FDG) PET/CT (GE Discovery ST 16) for staging of lymph node (N) and distant metastases (M) after resection of the primary tumor. Evaluation was done according to the American Joint Committee on Cancer Staging classification. The MR images were evaluated by two radiologists while the PET/CT images were read by one radiologist and one nuclear physician. Histology and a mean clinical-radiological follow-up of 6–9 months served as the standards of reference.

Results: The mean follow-up time was 186 days. Regional lymph node involvement was correctly determined in 15/20 cases as N-positive for WB-MRI (75%, p<0.05) and in 18/20 (90% p<0.05) for PET/CT exam while overall M stage was diagnosed correctly in 17/20 (85%) patients for WBMR in comparison with 18/20 (90%) in PET/CT (p<0.05). N-stage was overstaged with WBMR in 2 patients (10%) and with PET/CT in no patients and understaged in 3 patients with WBMR and in no patients with PET-CT. Distant metastases were overstaged with PET/CT in 1 and understaged in 1 patients with WBMR in 1 and 4 patients, respectively.

Conclusion: WBMR is an effective and fast method for examining colon cancer patients but cannot reach the accuracy of PET-TC.

SS 13.06

Accuracy of USPIO-enhanced MRI for local staging of rectal cancer: a multicenter study in expert and 3 regional centers

M. Lahaye¹, G.L. Beets¹, S.M.E. Engelen¹, P. Post², J. Dohmen³, L. Opdenakker⁴, J.M.A. van Engelshoven¹, C.J.H. van de Velde⁵, R.G.H. Beets-Tan¹; ¹Maastricht/NL, ²Venlo/NL, ³Weert/NL, ⁴Roermond/NL, ⁵Leiden/NL

Purpose: To determine diagnostic performance of MRI for predicting T-stage and N-stage with and without lymph node specific contrast in primary non-locally advanced rectal cancer in three regional centers and one expert center.

Material and methods: From February 2003 till October 2007, 327 rectal cancer patients were enrolled and received an USPIO MRI (Sinerem®). The local radiologists (non-experts) and an expert MR radiologist prospectively predicted the T-stage and the N-status first on T2WTSE images (USPIO-), then on the combined T2WTSE and 3DT2*(USPIO+), blinded for each other's results. The expert prospectively double read each MR of the regional patients. Reference standard was histology.

Results: 130/327 were non-locally advanced patients and used for analysis (42/130 were regional inclusions). 42 out of these 130 had pN+.

Table 1

| pT0-2 | Non-expert | Expert |
|-------|------------|--------|
| AUC | 0.76 | 0.84 |
| Sens | 0.59 | 0.72 |
| Spec | 0.90 | 0.94 |
| PPV | 0.87 | 0.95 |
| NPV | 0.67 | 0.69 |

Table 2 Nonenhanced N-status

| | Non-expert | Expert |
|------|------------|--------|
| AUC | 0.76 | 0.84 |
| Sens | 0.59 | 0.72 |
| Spec | 0.90 | 0.94 |
| PPV | 0.87 | 0.95 |
| NPV | 0.67 | 0.69 |

Table 3 USPIO N-status

| | Non-expert | Expert |
|------|------------|--------|
| AUC | 0.87 | 0.92 |
| Sens | 0.92 | 0.95 |
| Spec | 0.69 | 0.81 |
| PPV | 0.57 | 0.70 |
| NPV | 0.95 | 0.97 |

Conclusion: 1. MRI has a high PPV both for experienced and nonexperienced readers for predicting tumors limited to the bowel wall (T0-2). Non-experts tend to overstage T0-2 tumors more often due to a learning curve and difficult interpretation of borderline cases. 2. MRI without lymph node specific contrast is not accurate for the detection of nodal metastases in rectal cancer, unless read by an expert. 3. Non-experts significantly improve their MR selection of N0 from non-reliable to reliable prediction with lymph node specific contrast.

SS 13.07

MRI evaluation and classification of anal and perianal fistulas in patients with Crohn's disease

M. Martinelli, F. Maccioni, G. Bella, M. de Vargas Macciucca, N. Al-Ansari, M. Marini; Rome/IT

Purpose: To determine the diagnostic accuracy of MRI in preoperative classification of Crohn's disease perianal fistulas, by evaluating the agreement between MRI and surgical-clinical findings.

Material and methods: 31 patients with Crohn's disease and clinical objectivity of anal fistulas underwent MRI examination (1.5 Tesla) with phased-array coil in supine position. Images were acquired on axial and coronal planes with TSE-HIRE best (Turbo Spin Echo - High Intensity Reduction) T2-weighted sequences, with and without fat-suppression, and FLASH (Fast Low Angle Shot) or TSE T1-weighted sequences, with fat suppression, after endovenous injection of gadolinium. Surgery and clinical exploration in sedation were considered as standard examination. MRI and surgical features were classified according to the Parks (5 classes) and St. James Hospital's classifications (degree 1–5).

Results: 15/31 patients underwent surgical intervention, 16/31 clinical evaluation, pharmacological treatment and follow-up. MRI findings were: 2 patients with sub mucosal fistulas; 7 patients with intersphincteric fistula (degree 1 and 2), 13 patients with transphincteric fistula (degrees 3 and 4), 5 patients with transelevator fistula (degree 5) and 2 patients with complicated ano-rectal fistulas. Agreement with surgical and clinical findings was obtained in 92%; 2 false negatives were observed (simple intersphincteric fistulas).

Conclusion: MRI is an accurate technique to evaluate and classify anal and perianal fistulas, especially for more complicated fistulas.

SS 13.08

Assessment of the MRI appearances and pattern of distribution of pelvic lymph nodes in anal cancer

J.V. Liaw, A. Nikapota, R. Glynne-Jones, V. Goh; Northwood/UK

Purpose: Whole pelvic nodal irradiation has a key role in management of pelvic malignancy. The purpose was to describe the MRI appearances and pattern of distribution of pelvic lymph nodes in squamous cell anal cancer to aid delineation for external beam radiotherapy.

Material and methods: 71 patients (32 male, 39 female; mean age 65 years) with proven squamous cell anal cancer underwent 1.5 T MRI before chemoradiation.

T1 and T2W images were reviewed by two radiologists in consensus. Pelvic nodal size (<5 mm; 5.1–10 mm, 10.1–15 mm, 15.1–20 mm, >20 mm), signal intensity (hypo-, iso- or hyper-intensity), appearances and distribution (inguinal, external iliac (anterior, medial, lateral groups), internal iliac, common iliac, obturator, presacral) were recorded for each patient. Follow up imaging (MRI or CT) allowed assessment of outcome; mean patient follow up was 14 months.

Results: 521 nodes were identified in the following distributions: inguinal (388 (74%)), external iliac (51(10%)), internal iliac (14 (3%)), common iliac (15 (3%)), obturator (16 (3%)), and presacral (37 (7%)). 103/521 (20%) nodes were greater than 1 cm in size; the majority were inguinal (79/103 (77%)) or external iliac (16/103 (16%)), of homogenous high signal intensity on T2W. No nodal relapse following chemoradiation was identified where nodes were <1 cm.

Conclusion: Nodal disease in squamous anal cancer most commonly involves inguinal, external iliac and obturator groups; these areas must be encompassed in radiotherapy.

SS 13.09

Intra and inter observer agreement for remote 3D anal endosonography reporting

P. Wyllie, R. Ahmad, S. Ghosh, M. Marshall, D. Burling; Harrow/UK

Purpose: To assess inter and intra-observer variability for anal endosonography (AES) using remote 3D volume review.

Material and methods: 50 consecutive AES examinations from patients with symptoms of anal incontinence (excluding fistula-in-ano) referred to our centre were accrued by a study coordinator and reviewed independently on remote workstations using commercially available 3D review software by two experienced radiologists (observers A and B; >1000 cases each), blinded to clinical history (no time constraint). The dataset was read twice to assess intra-observer agreement (temporal separation 4 weeks to reduce recall bias). Classification of internal and external sphincter disruption/degeneration was recorded by each observer and, following statistical advice, the resulting data (inter/intra-observer) was compared using weighted Kappa statistic.

Results: Dataset comprised 13 normal/37 abnormal examinations from 42 females/8 males (Median 57 yrs). For internal sphincter classification, observers A and B agreed with their initial read on 49 (98%) Kappa 0.95 (very good: standard error 0.14); and 41 (82%) Kappa 0.63 (good; SE 0.14) occasions, respectively. Corresponding data for external sphincter were 47 (94%) Kappa 0.79 (good; SE 0.14); and 37 (74%) Kappa 0.37 (fair; SE 0.13) for observers A/B. Inter-observer agreement was very good to moderate for both reads for internal sphincter classification (Kappa 0.91/0.50; SE 0.14/0.13) but varied between good/fair for external sphincter classification (Kappa 0.65/0.31; SE 0.14/0.12).

Conclusion: Intra and inter-observer agreement for remote AES reporting by highly experienced radiologists is variable but can be very good.

SS 13.10

Spectrum of MR-defecography findings in patients with anismus

C.S. Reiner, A. Solopova, R. Tutuiian, B. Marincek, D. Weishaupt; Zurich/CH

Purpose: To determine the frequency of MRI findings in patients with anismus and to compare these findings to a control group with constipation.

Material and methods: Forty eight patients (34 females, 14 males; mean age, 48 years) with clinically suspected anismus referred for anorectal manometry and MR-defecography were included. According to the final diagnosis, based on the Rome II criteria, patients were divided into two groups: patients with anismus (n=18) and constipated patients without anismus (control group, n=30). MR-images were retrospectively reviewed by two independent radiologists with regard to the time of evacuation, number of attempts to evacuate, changes in the anorectal angle on straining, paradoxical sphincter contraction, and the presence of additional pelvic floor abnormalities. Interobserver variability was analyzed by calculating kappa statistics.

Results: In patients with anismus, MR-defecography revealed evacuation inability in 9 patients (50%), increased time of evacuation compared to the patients with constipation (191 vs 113 sec, p<0.001), increased number of attempts to evacuate (mean 6.1 vs 3.5, p<0.05), higher frequency of abnormal anorectal angle changes on straining (9 (50%) vs 1 (3.3%)). Paradoxical sphincter contraction was observed solely in 15 (83.3%) patients with anismus. Interobserver agreement was good to excellent.

Conclusion: Using MR-defecography the detection of impaired evacuation (including the evacuation inability), increased number of attempts to evacuate and the presence of paradoxical sphincter contraction are highly suggestive for anismus.

11:00 - 12:30

Topkapi B

Scientific Session 14

Bile ducts: diagnosis and intervention

SS 14.01

Hepatobiliary kinetics of a liver-specific contrast agent (Gd-EOB-DTPA) in patients with diffuse liver disease at 1.5 T and 3 T

A. Bethke¹, K. Engelland¹, G. Gaffke², M. Laniado¹, C. Stroszczynski¹; ¹Dresden/DE, ²Magdeburg/DE

Purpose: Primary or metastatic liver tumors often arise in patients with preexisting diffuse liver disease; therefore, it is imperative to evaluate contrast agent performance under these conditions. The aim of the study was to investigate the hepatobiliary kinetics of a liver-specific contrast agent in patients with diffuse liver disease.

Material and methods: Eighty patients were divided in 4 groups: 1. no diffuse liver disease/control group (n=28), 2. cirrhosis (n=16), 3. chemotherapy-induced steatosis (n=20), and 4. cholestasis (n=16). Standard MRI-protocol was used in various scanners at 1.5–3.0 T. Manually defined regions of interest were used to measure signal intensity of the liver and the bile duct before and after contrast material administration (20 seconds, 60 seconds, 10 minutes and 20 minutes). Percentage increase of enhancement was evaluated.

Results: Percentage increase of enhancement (control group 114%) was significantly reduced in patients with liver cirrhosis (84%) or cholestasis (55%) but not in steatosis. Biliary excretion was significantly reduced in patients with cholestasis (145%) compared to groups 1–3 (1793%, 1409%, 1393%).

Conclusion: Hepatic enhancement with Gd-EOB-DTPA can be impaired by the presence of cholestasis and liver cirrhosis. However, enhancement was sufficient for diagnostic purposes. While T1-w imaging of the bile duct in patients with cholestasis is hampered by reduced enhancement, biliary excretion may be characterized.

SS 14.02

Safety and efficacy of CT cholangiography

K.P. Lim¹, N. Grunshaw²; ¹Yarm/UK, ²Darlington/UK

Purpose: CT cholangiography (CTC) is an alternative technique for biliary investigation in patients unable to undergo MRCP. Concerns regarding adverse reactions and image quality in the presence of impaired hepatic function have resulted in its relative underutilisation. The purpose of this study is to assess the diagnostic efficacy and safety profile of CTC with iotroxate infusion and to assess its success rate in the presence of abnormal liver function tests (LFTs).

Material and methods: A retrospective review of all patients undergoing CTC from 2002 to 2006 was performed. Medical notes were reviewed and data collected via proforma. All patients were admitted for 100 ml Meglumine Iotroxate (105 mg), diluted to 1L in normal saline and infused over 1 hour intravenously. All patients were monitored for adverse reactions.

Results: 102 patients were identified. 70 had abnormal LFTs, but optimal scans were obtained in 92.9% (n=65), 40% (n=26) of which demonstrated obstructive stone disease. There were 7 failures overall (6.9%) of which 5 occurred with abnormal LFTs, though there was no predictive pattern. There was one minor adverse reaction (0.9%).

Conclusion: Whilst MRCP remains the primary non invasive biliary investigation, we believe that CTC is a viable and safe alternative investigation in patients unable to undergo MRCP and may be successful even in the presence of abnormal LFTs.

SS 14.03**Accuracy of 3D CT cholangiography in the detection of choledocholithiasis**

S. Roy-Choudhury, D. Harji, S. Gan, B. Miller, A. Pallan, M. Richardson, H. Kumar, T. Ngatchu; Birmingham/UK

Purpose: To assess the accuracy of CT Cholangiography (CTC) in the detection of choledocholithiasis.

Material and methods: CTC post 100 ml biliscopin was performed on 96 patients. Images were obtained on 4 or 16 slice CT (Toshiba Medical Systems, Europe) and read with MPR and MIP reconstructions. Images were compared with ERCP, intraoperative findings or a clinical follow up of at least 6 months.

Results: 94/95 studies were adequate and 3 studies were repeated. 30/94 (31%) filling defects were noted of which 3 were artefacts. Of the 27 perceived stones, 14 were seen on ERCP, 1 on intraoperative cholangiography (IOC), 2 were treated conservatively being less than 3 mm, 3 were lost to follow up and 7 had no stones on ERCP or IOC. In 64/94 (68%) of patients, no CBD filling defects were visualised. 2/64 did and 62/64 did not have stones demonstrated either at ERCP, IOC, other non invasive biliary imaging or on clinical follow up. One stricture was shown on ERCP. There were no hospital readmissions related to biliary colic in the 2 year follow up in this group. Anatomical biliary abnormalities were noted in 10/38 cases (where reported). Sensitivity and specificity of CTC for choledocholithiasis were 97 and 61%, although the latter is likely to be due to stone passage between CTC and clinical studies.

Conclusion: CTC is a sensitive modality of in the detection of choledocholithiasis.

SS 14.04**Diagnostic performance of high-resolution isotropic 3D MRCP for suspected biliary pathology**

K. Nandalur¹, H.K. Hussain², W.J. Weadock², E.J. Wamsteker², A.S. Khan², T.D. Johnson², T.L. Chenevert²;
¹Charlottesville, VA/US, ²Ann Arbor, MI/US

Purpose: To retrospectively assess the diagnostic performance of magnetic resonance cholangiopancreatography (MRCP), using a high resolution isotropic three-dimensional fast-recovery fast spin-echo (3-D FRFSE) sequence with parallel imaging, for the evaluation of suspected biliary pathology.

Material and methods: One-hundred and nine patients (mean age 52 years, range 15–91 years; 65 female, 44 male) underwent MRCP using the respiratory triggered isotropic 3-D FRFSE sequence and direct visualization (98 endoscopic retrograde cholangiopancreatography (ERCP), 11 percutaneous transhepatic cholangiography (PTC)) between March 2003 and June 2007. Two independent readers evaluated the MRCP images for strictures, dilatation, sclerosing cholangitis (multiple intrahepatic and extrahepatic strictures), and intraductal filling defects. Sensitivity and specificity of each reader were determined.

Results: Prevalence of disease by ERCP/PTC was 39% (42/109) for strictures, 54% (59/109) for dilatation, 21% (23/109) for sclerosing cholangitis, and 23% (25/109) for choledocholithiasis. For reader 1, sensitivity and specificity for strictures were 93 and 94%, respectively, dilatation 98 and 98%, sclerosing cholangitis 87 and 92%, and choledocholithiasis: 76 and 98% (44% sensitivity (4/9) for ≤ 3 mm stones). For reader 2, sensitivity and specificity for strictures were: 93 and 91%, respectively, dilatation 97 and 98%, sclerosing cholangitis 87 and 95%, and choledocholithiasis 84% and 99% (56% sensitivity (5/9) for stones ≤ 3 mm).

Conclusion: MRCP using the respiratory triggered isotropic 3-D FRFSE sequence with parallel imaging demonstrates excellent diagnostic capabilities for suspected biliary pathology, although is limited for choledocholithiasis ≤ 3 mm.

SS 14.05**Diagnostic performance of MRI for the assessment of tumor involvement of biliary and vascular structures in patients with hilar cholangiocarcinoma**

C.S. Reiner, S. Breitenstein, M.L. de Oliveira, P. Clavien, B. Marincek, D. Weishaupt; Zurich/CH

Purpose: To assess the diagnostic performance of MR-imaging (MRI) for determining the extent of biliary and vascular involvement in hilar cholangiocarcinomas (HCAC).

Material and methods: Unenhanced and contrast-enhanced MRI, (including

MR-cholangiography (MRC)) was performed in 25 patients with pathologically proven HCAC using a 1.5 T-scanner. Images were analyzed by two readers independently with regard to visibility of bile ducts and vessels as well as to location and extent of biliary and vascular tumor involvement. MRI findings were correlated with a standard of reference consisting of intraoperative or imaging findings of other modalities.

Results: The readers rated the visibility of bile ducts and vessels as good or excellent in 83–92% of all structures. Overall sensitivity and specificity for tumor involvement of biliary and vascular structures for reader 1 (R1) and reader 2 (R2) were as follows: bile ducts, 85/88% (R1), 93/85% (R2); hepatic arteries, 79/93%, 79/95%; portal veins, 92/100%, 92/97%, and hepatic veins, 100/100%, 100/99%. In 83/67% (R1/R2) of patients with discrepancy of biliary tumor extension according the Bismuth-Corlette classification, incorrect assessment was due to artifacts caused by biliary stents or drains. In 43/50% (R1/R2) of incorrect arterial tumor involvement, incorrect results occurred for the same reason.

Conclusion: Dynamic MRI including MRC is useful as a sole preoperative (“all-in-one”) imaging modality for local staging of HCAC. The assessment is limited when biliary stents or drains are present.

SS 14.06**Bilio-enteric anastomoses: evaluation with Mn-DPDP-enhanced MR cholangiography**

F. Donati, P. Boraschi, R. Gigoni, S. Salemi, L. Faggioni, F. Falaschi, C. Bartolozzi; Pisa/IT

Purpose: To assess the usefulness of mangafodipir trisodium-enhanced MR cholangiography (MRC) for evaluating patients with bilio-enteric anastomosis.

Material and methods: Twenty-six patients with bilio-enteric anastomosis underwent MRC at 1.5 T-device. After acquisition of axial T1w/T2w images, conventional MRC was performed through respiratory-triggered thin-slab FRFSE T2w and breath-hold thick-slab SSFSE T2w sequences. In each patient, 3D fat-suppressed breath-hold gradient-echo T1w imaging was also obtained 30–40 minutes after the intravenous administration of mangafodipir trisodium (Mn-DPDP, Teslascan®; GE Healthcare). Two experienced observers evaluated the images for the following signs: depiction of intra- and extra-hepatic bile ducts and bilio-enteric anastomosis, dilation of biliary system, presence of biliary stricture, stone and leakage. Depiction of morphologic signs was graded on images using a 3-point scale: 0, absent; 1, visible; 2, excellent. Imaging results were correlated with direct cholangiography, surgery and/or follow-up.

Results: The grading of visualization and depiction of dilation of the intra-hepatic bile ducts was significantly superior on T2w MRC compared with Mn-DPDP-enhanced T1w MRC ($p < 0.0001$). On T2w MRC, the extra-hepatic biliary system and the anastomotic region could be visualized in 21/26 (81%) patients, whereas on Mn-DPDP-enhanced T1w MRC visualization of bilio-enteric anastomoses and excretion of Mn-DPDP into the jejunum loop were identified in 25 out of 26 cases. Stones and biliary strictures were correctly identified with both techniques.

Conclusion: Contrast-enhanced MRC using mangafodipir trisodium may provide both anatomical and functional information of bilio-enteric anastomoses.

SS 14.07**Differentiation of non-calculous ampullary obstruction on MR cholangiography**

H.M. Kim, M.J. Kim, M. Park, J.Y. Choi, J.S. Lim, J.H. Kim, H.S. Yoo, K.W. Kim; Seoul/KR

Purpose: To define the criteria for differentiation of non-calculous obstruction at the ampullary level by MR cholangiography (MRC).

Material and methods: MRC of 41 patients (19 with ampullary cancer and 22 with benign causes) with suspected non-calculous biliary obstruction at ampullary level were retrospectively reviewed. Two radiologists, who were blinded to the clinical records, determined the cause of obstruction and evaluated the presence of papillary mass and its size if present, the presence of papillary bulging, the pattern of CBD dilatation, the maximum diameters of biliary and pancreatic ducts, and the shape of the distal ends of CBD. A consensus of opinion was arrived at on all items.

Results: Differentiation of benign and malignant obstruction by consensus of two observers showed sensitivity (Se) of 84% and specificity (Sp) of 86%. A papillary mass was found 89% in malignancy and 27% in benign obstructions (Se 89%, Sp 77%). Mass sizes were not different between the two groups. Presence of papillary bulging showed Se of 95% and Sp of 86% and proportional

dilatation of bile duct, Se 68% and Sp 95%. Dilatation of biliary duct showed Se 68% and Sp 86% and pancreatic duct, Se 47% and Sp 90%.

Conclusion: The presence of ampullary mass and papillary bulging associated with proportional and severe dilatation of biliary and pancreatic ducts are suggestive findings for the diagnosis of malignant ampullary obstruction.

SS 14.08

ePTFE/FEP-covered metallic stents versus uncovered mesh stents for palliation of malignant jaundice due to cholangiocarcinoma: clinical results in 50 patients

M. Krokidis¹, F. Fanelli², A. Hatzidakis¹, G. Orgera², N. Gourtsoyiannis¹, R. Passariello²; ¹Heraklion/GR, ²Rome/IT

Purpose: To compare clinical effectiveness of ePTFE/FEP-covered-metallic stents with uncovered mesh-stents for palliative treatment of malignant jaundice due to cholangiocarcinoma.

Material and methods: 50 patients with Bismuth type I-II malignant stricture due to inoperable cholangiocarcinoma without hepatic metastasis were admitted for palliation. Stricture was located in the upper CHD (without infiltrating the duct confluence) in 4 patients, in the lower CHD in 13, in the upper CBD in 22 and in the lower CBD in 11. In none of the cases there was infiltration of the cystic duct. We used 36 Wallstents (Boston Scientific), 6–9 cm long and 10 mm wide in 30 patients (Group A) and 21 Viabil (W. L. Gore) covered stents with and without side holes in 20 patients (Group B). All patients were followed-up until death.

Results: Technical success was 100% in both groups. Early stent occlusion was noted in 1 patient of Group B, due to sludge, and was dilated. Complication rate was 13.3% in Group A and 10% in Group B. Mean survival was 155.8 days for Group A and 170.3 days for Group B patients. One year primary patency was 54% for Group A and 77.2% for Group B.

Conclusion: Viabil stents offer a significantly better 12-month primary patency rate than uncovered in the palliation of malignant strictures due to cholangiocarcinoma without hepatic metastasis.

SS 14.09

US-guided left subxiphoid approach to the left hepatic duct for percutaneous transhepatic biliary drainage: a safety and efficacy study

M. Midia¹, J. Kirby¹, P. Vora¹, J. Rawlinson¹, K. Cho²; ¹Hamilton, ON/CA, ²Ann Arbor, MI/US

Purpose: To evaluate the safety and efficacy of the left subxiphoid approach to the liver for percutaneous transhepatic biliary drainage (PTBD).

Material and methods: 121 patients, 72 men and 49 women, with a median age of 65.8 years (range 33–99) underwent PTBD for biliary obstruction. PTBD was performed from the right intercostal approach in 50 patients and from the left subxiphoid approach in 71 patients. The left subxiphoid approach was performed under real-time US guidance. Clinical outcome to be assessed included technical success rate, pleural complications, hemorrhage, bile leakage, protection of left hepatic lobe, management of the biliary tubes, and bile leakage.

Results: The left subxiphoid approach to the left hepatic duct was successful in 68/71 (96%) and the right intercostal approach to the right hepatic duct was successful in 48/50 (96%). The causes for biliary obstruction included hilar duct carcinoma (40), pancreatic and periampullary carcinoma (33), metastases, pancreatitis, and postsurgical recurrence and stricture (49). Eight patients had bilateral PTBD. Complications related to the left hepatic PTBD were hemobilia (1), bile leak (0) and sepsis (2).

Conclusion: The US-guided left subxiphoid approach to the left hepatic bile duct is safe and effective in treating both hilar and distal biliary ducts obstruction without significant complication.

SS 14.10

Fluoroscopically guided metallic stent placement in malignant gastroduodenal obstruction

E. Bulut, T. Ciftci, F. Ozkan, F. Islim, D. Akinci, M. Ozmen, O. Akhan; Ankara/TR

Purpose: To evaluate the clinical effectiveness of fluoroscopically guided placement of metallic stents in the palliation of malignant gastroduodenal obstruction (MGO).

Material and methods: Twenty-one patients (mean age: 59 years) underwent stent placement for symptoms of gastroduodenal obstruction. Underlying causes

of obstruction were gastric carcinoma in 8 patients, pancreas carcinoma in 7 patients, duodenal carcinoma in 2 patients, colon carcinoma with duodenal metastasis in 2 patients, periampullary tumor and cholangiocellular carcinoma in 1 patient. Self expandable noncovered metallic stents (Wallstent, Wallflex, Niti-S) were placed under fluoroscopic guidance (20 patients) or under combination of fluoroscopic and endoscopic guidance (1 patient). Stents were placed transorally in 15 patients and percutaneous gastrostomy tract was used in 5 patients. In one patient, duodenal stent was placed by transhepatic approach. Eleven patients also underwent biliary stent placement for biliary obstruction.

Results: Neither mortality nor major complication was encountered. A broken stent was replaced by a new one during the procedure in one patient. Mean follow-up time was 82 days. Seventeen patients (85%) could get solid foods, 2 patients (10%) could get fluids after stent placement. Oral intake of one patient did not improve. In one patient with afferent loop obstruction, afferent loop decompression was achieved with stenting.

Conclusion: Fluoroscopically guided metallic stent placement is an effective and safe method in the palliation of MGO.

11:00 - 12:30

Dolmabahçe A

Scientific Session 15 Abdominal interventions

SS 15.01

Multisampling needle core biopsy of hepatic nodules

S. Strasser, C.D. Becker, L. Rubbia-Brandt, L. Spahr, S. Terraz; Geneva/CH

Purpose: Multisampling needle core biopsy (NCB) has been evaluated in breast and lung lesions, but to date few data are available on hepatic nodules. The purpose of this study was to evaluate the safety and the efficacy of this technique for undetermined liver nodules.

Material and methods: Between January 2004 and December 2006, 104 consecutive NCB were performed in 101 patients with suspected hepatic malignancy. The mean diameter of the nodules was 3.5±2.7 cm (range, 0.8–16.0 cm). After local anaesthesia, a 17G outer canula was placed at the periphery of the nodule under US (n=87), CT (n=12) or MRI (n=5) guidance. An 18G biopsy needle was used for biopsy sample. Sample notch size was selected from 9 to 24 mm. One to 15 samples (median, 5 samples) were obtained per nodule and fixed. In 16 cases with elevated risk of haemorrhage, biopsy tract was embolised. Post-procedural imaging was performed to search for immediate complication. The medical charts, pathology reports and radiology files were retrospectively reviewed.

Results: Multisampling NCB was successfully completed in 102 of 104 procedures (98%), while two biopsies were discontinued due to vasovagal syncope. Tissue specimens were satisfactory for histologic diagnosis in 97 of 102 biopsies (95%). In five cases, samples were considered inadequate for specific diagnosis. There were 23 primary and 57 secondary malignant tumours, 17 benign tumours and 6 inflammatory lesions. According to SIR classification, no procedure-related complication was observed. Four minimal asymptomatic perihaptic collections were observed but not treated.

Conclusion: Multisampling NCB of hepatic nodules is safe and effective for specific histologic diagnosis. However, careful embolisation of biopsy tract is mandatory in patients with increased risk of bleeding.

SS 15.02

Percutaneous CT-guided catheter drainage of infected acute necrotizing pancreatitis

G. Baudin, S. Novellas, F. Berthier, E. Gelsi, G. Bernardin, X. Hébuterne, P. Chevaller; Nice/FR

Purpose: To assess the safety and efficacy of percutaneous catheter drainage (PCD) of infected acute necrotizing pancreatitis (ANP).

Material and methods: An eight-year period retrospective study including forty-eight consecutive patients (34 men, mean age: 58 y) with (ANP) treated for sepsis with one to four percutaneous catheters ranging in size from 14- to 30-French (24-French in mean). Ranson's score was equal in mean to 3.48 (range: 1–6) and CT-scans were classified Balthazar D or E, respectively, for 10.2 and 89.4% of patients. Univariate analysis using the Wilcoxon matched pairs test was

performed to assess factors influencing the clinical success and the 30-days mortality rate.

Results: The average catheter drainage time was 47.3 days (range: 11–96), each catheter being changed in mean 7.5 times per patient. Thirty-two patients (66.6%) were cured with only percutaneous drainage and this clinical success was influenced by the Ranson's score ($p: 0.01$), a multiorgan failure ($p: 0.009$), and the delay to start the drainage ($p: 0.003$). The 30-days mortality rate was equal to 29.2% (fourteen patients) and was influenced by the Ranson's score ($p: 0.01$), a multiorgan failure ($p: 0.02$), the delay to start the drainage ($p: 0.04$), and the C reactive protein value ($p: 0.03$). Two patients experienced catheter-related hemorrhages which spontaneously resolved.

Conclusion: PCD is a safe and effective technique for treating infected ANP.

SS 15.03

Intra-arterial chemotherapy for resectable periampullary cancer to prevent hepatic metastases (ESPAC-II trial): the Erasmus MC experience

N. Krak, J. Hermans, M. Morak, C. van Eijck; Rotterdam/NL

Purpose: To study the effect of celiac artery infusion (CAI) on the occurrence of hepatic metastases in patients with resectable UICC stage I-III periampullary cancer.

Material and methods: 120 patients were included in a prospective clinical trial and randomized to surgery, adjuvant CAI and radiotherapy (Arm A, 59 patients) or surgery alone (Arm B, 61 patients). CAI consisted of mitoxantrone, folinic acid, 5-FU and Cis-platinum at 4-weekly intervals. Six cycles were given unless toxicity or disease progression occurred. Development of liver metastases in Arm A and Arm B were compared. Technical aspects and complications of celiac axis catheter placement were recorded.

Results: In Arm B, 52 % of patients developed liver metastases, vs. 30% in Arm A. The percentage of liver metastases decreased from 78 to 11% with 2 vs. 6 CAI cycles. A total of 620 celiac axis catheterizations were performed in 43 patients who received at least 2 cycles of CAI. Catheters used were a celiac (90%), Sidewinder (7%) or SOS omni catheter (3%). Catheter luxations occurred in 12% of placements. Four patients experienced major complications, i.e. subtotal celiac trunk stenosis ($n=2$) and femoral or external iliac artery dissection ($n=2$).

Conclusion: Prolonged CAI decreases the occurrence of liver metastases. Catheter luxations occurred in 12% of catheter placements and major catheterization-related complications in 9% of patients, respectively.

SS 15.04

Radio-iodine therapy and helicobacter pylori infection: the first in vivo evidence on radiosensitivity of the bacteria

A. Gholamrezanezhad, S. Mirpour; Tehran/IR

Purpose: Helicobacter pylori (H.pylori) is the most important cause of gastritis and related morbidities. Following consumption, radioactive iodine accumulates considerably in stomach. Hence, we decided to find whether the high radiation induced by radio-iodine on stomach is effective in the eradication of H.pylori.

Material and methods: All consecutive patients with differentiated thyroid carcinoma, who were referred for radio-iodine therapy (Dose: 117.1 ± 24.4 mCi, Range: 100–200 mCi), were enrolled. To detect H.Pylori infection, Urease Breath Test (UBT) was performed 1–2 hours before radio-iodine consumption and was repeated two-months later.

Results: Out of 88 patients, 71 patients had pre-treatment positive UBT. Of these, 23 patients had negative post-treatment result, which means a significant reduction (26.1%, 95% CI: 16.8–35.5%) in the number of positive UBT results of our population with treatment (32.4% of UBT positive cases became UBT negative).

Conclusion: Considering the high prevalence of reinfection in developing countries, the therapeutic benefit would be more considerable if the second UBT was done with a lag time of <2 months. Although it is not a logical method for treatment of patients suffering from H.pylori, it is indirect evidence about radiosensitivity of bacteria, future clinical applications of which need to be further evaluated. Also, this finding can be useful for food industry where radiation is used in a wide scale to sterilize food. Regarding the possibility of H.pylori suppression, we recommend not using UBT for screening the infection within two months following radio-iodine.

SS 15.05

Radiologically inserted gastrostomies in head and neck cancer chemoradiotherapy

J.C. Jobling, P.D. Thurley; Nottingham/UK

Purpose: Head and neck cancer patients often develop severe mucositis from oncological therapy, requiring gastrostomies to maintain nutrition. We wished to assess success, complication and utilization rates of radiologically inserted gastrostomies (RIGs).

Material and methods: All oncology referrals for RIGs were identified retrospectively. Radiology reports and patient records were used to identify tube type, procedural success, complications and usage of the gastrostomy.

Results: 104 patients (75 males, 29 females; aged 25–85 years, mean 56.3, median 57.8) were referred for RIGs between 2004 and to date prior to chemoradiotherapy. 95 had head and neck cancers, 9 had other malignancies. 94 pull-down flanged and 10 self retaining loop catheters were inserted. Successful placement occurred in 103. One patient had an intrathoracic stomach (previous oesophagectomy); therefore, placement was not possible. 14% developed infections; in one patient, this delayed chemotherapy. 25% developed delayed stoma infections. One tube detached in the stomach during placement, requiring endoscopic retrieval. One patient developed small bowel obstruction. 1 patient died 29 days after insertion of unrelated causes. 10 (12%) had other minor complications. 73% patients used their RIGs (66% were dependent). 11% did not use their RIGs (2 did not receive any treatment). No information was available in 16%.

Conclusion: RIG insertion had a high success rate and low rate of serious complication other than infection in this group. Our unit now uses prophylactic antibiotics for RIG insertion.

SS 15.06

Management of chronic mesenteric ischemia with percutaneous transluminal angioplasty: short- and long-term outcomes

R. Loffroy, V. Molin, B. Kretz, B. Guiu, J.P. Cercueil, O. Bouchot, R. Brenot, M. David, D. Krausé, E. Steinmetz; Dijon/FR

Purpose: To assess the efficacy and long-term outcome of endovascular therapy for obstructive disease of the mesenteric arteries in patients with chronic mesenteric ischemia (CMI).

Material and methods: Retrospective review of 33 consecutive patients (20 females; 13 males; mean age, 67.3 years; range, 31–92 years) who underwent endovascular treatment for symptomatic CMI between 1989 and 2006. Indication for revascularization included postprandial abdominal pain (26), weight loss (21) with a mean weight loss of 12 kg (range, 2–30 kg), and gastroparesis (3). All patients had visceral occlusive disease with significant stenoses in one (11), two (20) or three (2) mesenteric vessels. Follow-up parameters included maintained patency on Doppler sonography and sustained clinical benefit.

Results: Balloon angioplasty alone was performed in only one of the arteries in 29 patients (superior mesenteric artery or SMA, 20; celiac artery or CA, 9) and in two arteries in 3 patients (SMA and CA). Stenting was required in 17 patients (SMA, 14; CA, 3). All procedures but one were technically successful (97%). Three major puncture-site complications required surgery (2 hematomas, 1 pseudoaneurysm). Immediate clinical success was achieved in 27 patients (93%). At a mean follow-up of 35 months (range, 3–108 months), 20 patients were symptom free, 7 had recurrent pain with angiographic restenosis successfully revascularized percutaneously (4) or surgically (3), 4 died of unrelated causes and 2 were lost to follow-up.

Conclusion: Endovascular treatment as first choice for chronic mesenteric arterial obstructive disease is effective in patients with symptoms of CMI, with a high technical success rate and acceptable long-term results.

SS 15.07

Endovascular treatment of visceral artery aneurysms: new techniques with stent-graft and amplatzer vascular plug

M. Rossi, M. Citone, A. Rebonato, L. Greco, P. Fina, C.N. de Cecco, V. David; Rome/IT

Purpose: To describe a 4-year experience of percutaneous treatment of Visceral Artery Aneurysms (VAAs) with stent-graft and Amplatzer-Vascular-Plug (AVP) to evaluate the efficacy of these techniques referred to immediate and long-term follow-up (FU).

Material and methods: Between 2004 and 2007, 15 patients underwent elective endovascular procedures for 10 splenic, 2 hepatic, and 3 renal artery aneurysms. Eight balloon expandable and 2 self-expandable stent-grafts were used in ten patients affected by 3–6 cm aneurysms. AVP was used to occlude the necks whereas cut up Teflon guidewire sheaths were employed to fill up the aneurysm sac in three patients with 9–13 cm Giant Splenic Aneurysms (GSA). CT-angiography was performed before patient discharge, at 6 and 12 months thereafter.

Results: Successful angiographic exclusion was obtained in all cases. Segmental splenic infarction occurred in all patients treated with embolization and in one treated with stent-graft. Post procedure CT showed complete aneurysms thrombosis and patency of the stent-grafts in all cases. At mean FU of 24 months, occlusion of the graft occurred in one case.

Conclusion: The endovascular treatment of VAAs with stent-graft and AVP represents a valid therapeutic option. The former are fully respective of the vascular anatomy while the latter reduce the risk distal migration during embolization of GSA with short and large proximal necks. Late FU confirms the durability of the aneurysm exclusion and the low clinical relevance of late stent graft occlusion.

SS 15.08

Initial experience with reconstruction of aortic pathologies based on 3D prototyping models generated from MDCT data

H.H. Karaman, P.B. Berman, J. Sosna; Jerusalem/IL

Purpose: Aortic and visceral artery pathologies can cause sudden death if left untreated. Conventional 2D and 3D reconstructions are generally adequate for vascular surgeons and angiographers but their ability to show complex 3D anatomical relationships can be limited. A promising new technique enables the creation of 3D models of vascular structures using computer-aided fabrication and polymer deposition to build plastic models based on MDCT 3D image data. Our purpose was to evaluate the usefulness of this technique for the treatment of vascular diseases.

Material and methods: From April 2005 to April 2007, we fashioned models for 4 male and 4 female patients aged 38–70 with abdominal, thoracoabdominal and hepatic aneurysms. CT imaging was performed on a 64-slice MDCT scanner (Brilliance 64, Philips Medical). Volumetric data was acquired. DICOM data was converted to stereolithography (STL) format. A photopolymer jetting device (Eden 500, Objet, Rehovot, Israel) “printed” alternate super-thin layers (down to 16 microns/0.0006 inches) of hard curable plastic and a gel-like photopolymer support material at 600 x 300 dpi to create the model. Final surgical results were gathered and the planning was assessed on a semi-quantitative scale.

Results: Rapid prototyping models accurately depicted the anatomic details of the vascular structure. Final surgical and endovascular results were considered excellent by the vascular surgeons and enabled real time use in the OR. Planning score improved from 1.8 to 2.3 on a 0–3 scale.

Conclusion: Reconstruction of vascular structures with rapid prototyping models generated is feasible, easing planning of surgery and endovascular treatment. Larger-scale studies for complex reconstructive surgery are underway.

SS 15.09

Treatment of plicature-induced transplant renal artery stenosis by primary stenting: technical results and clinical outcome

P. Goffette¹, M. Mourad¹, J.P. Squifflet², E. Danse¹, J.P. Lerut¹; ¹Brussels/BE, ²Liege/BE

Purpose: To evaluate the technical feasibility and clinical results of stenting of plicature-induced transplant renal artery (TRA) stenosis.

Material and methods: Over an eight-year period, stent placement was considered in 12 patients to manage plicature-induced TRA stenosis. All cadaveric arteries were anastomosed in an end-to-side fashion to the common iliac artery via an aortic patch. Patients suffered from severe hypertension (n=2), impaired renal function (n=2), or both (n=8). In all patients, stent implantation was performed immediately after complete recoil of post-anastomotic arterial plicature after percutaneous transluminal angioplasty. Palmaz (n=4), Hercules (n=6), or Tsunami (n=2) stents were placed to straighten the artery and keep the stenotic area open.

Results: Stent placement was 100% successful. The renal artery peak blood flow velocity fell from 324±65 to 154±18 cm/s. The mean systolic blood pressure

fell from 175±32 to 135±18 mm Hg. Allograft function improved in eight patients (serum creatinine from 3.2±1.1 to 1.5±0.4 mg/dl) and stabilized in two. During the follow-up period (3 month- 9.5 years, median 5 years), asymptomatic <50%-intra-stent stenosis were left untreated in three patients. Redo-transplantation was performed in two patients because of irreversible renal failure due to refractory intra-stent stenosis (n=1) and recurrent glomerulonephritis (n=1).

Conclusion: Stents placement revealed very useful in managing plicature-induced TRA stenosis. Medium-term stent patency and clinical outcome are promising. Redo-surgery or re-transplantation is avoided in most patients.

SS 15.10

Pelvic abscesses: results of percutaneous drainage

O. Ergun, T. Ciftci, O. Temizoz, D. Akinci, M. Ozmen, O. Akhan; Ankara/TR

Purpose: To evaluate the efficacy and safety of percutaneous drainage (PD) of pelvic abscesses (PA) with follow-up results.

Material and methods: A retrospective evaluation of PD of 98 PA in 83 patients (58 female, 25 male) was performed. Mean age of the patients was 49 (9–80 years). Transabdominal route was used in 72 abscesses and the remaining 26 abscesses were drained by transvaginal, transgluteal and transrectal routes. CT guidance was used in 12 abscesses, whereas 86 abscesses were drained under US and fluoroscopy guidance. Catheter drainage was used in 93 abscesses with 8-14F locking pigtail catheters; remaining 5 abscesses were drained by simple aspiration.

Results: There were no periprocedural complications. Initial cure and failure rates were 35.7% (35/98) and 8.2% (8/98), respectively. Fifty-five abscesses were either palliated or temporized. Recurrence rate was 5.1% (5/98), and 4 of them were treated by recatheterization. Overall success and failure rates with temporized, palliated and recatheterized abscesses were 96 (94/98) and 4% (4/98), respectively. Thirty-day mortality rate was 7.2% (6/83). Mean catheterization time was 13 days (2–52 days) and mean follow-up time was 16 months (1–53 months).

Conclusion: PD of PA under imaging guidance is a safe and effective procedure.



DIAGNOSTIC

Diagnostic / Bile Ducts

P-001

MRCP findings of biliary tree involvement in autoimmune pancreatitis: a pictorial essay

C. Besa Correa, A. Huete Garin; Santiago/CL

Learning objectives: To present a spectrum of findings of biliary duct alterations associated with AIP illustrated by MRCP and MRI.

Background: Autoimmune pancreatitis (AIP) is a form of chronic pancreatitis with a background of fibrosis and a lymphoplasmacytic infiltration. The most common extrapancreatic organ involved is the biliary tree, with narrowing of the distal common bile duct (CBD) and sclerosing cholangitis (SC) being the major associated findings described.

Imaging findings OR Procedure details: We retrospectively reviewed the MR and MRCP imaging findings of 16 patients with AIP diagnosed or treated in our institution between 2001 and 2007. MR were analyzed for the following features: presence and location of biliary strictures and wall thickening, presence of a SC pattern defined as multifocal intrahepatic disease with one or more strictures with or without extrahepatic bile duct involvement, presence of a peribiliary mass and gallbladder involvement. We identified four major patterns of compromise: distal CBD stricture (31%), extrahepatic bile duct disease (suprapancreatic) (31%), SC (31%) and a central peribiliary mass (25%). In two patients (12.5%), a diffuse gallbladder involvement was noted.

Conclusion: Bile ducts alterations in AIP are well known features of this multisystemic disease, where distal biliary involvement mimics pancreatic cancer-related stricture and suprapancreatic and intrahepatic involvement may simulate a cholangiocarcinoma or primary SC. Thus, adequate diagnosis is crucial, since steroid therapy can lead to recovery.

P-002

Cholangiocarcinoma: MR findings

J.M.G. Lourenço, C. Lam, R. Santos, A. Marques, I. Oliveira, M.E. Silva, Z. Seabra; Lisbon/PT

Learning objectives: To review the imaging characteristics of CC in MR. To discuss the different patterns of presentation, the differential diagnosis and resectability evaluation.

Background: Cholangiocarcinoma (CC) is an uncommon malignancy. It is an adenocarcinoma that may arise from any part of the bile duct epithelium, being classified in intrahepatic peripheral, intrahepatic hilar (Klatskin tumour) and extrahepatic. Three growth patterns are known: exophytic, infiltrative and polypoid. The extrahepatic and hilar forms usually present as obstructive jaundice. The intrahepatic form as to be differentiated from other liver masses. With the proximity of several vascular structures and the infiltrative nature of the tumour, resectability evaluation is a major issue, where MR has clear advantages over other techniques.

Imaging findings OR Procedure details: By reviewing the clinical and MR findings of patients with CC in our archive, we present a clear illustration of the different growth patterns, localizations and resectability criteria, including the infiltration extent of the biliary tree, lobar atrophy, vascular invasion (venous and arterial) and metastization. We used a combination of MR cholangiography and cross sectional pre and post gadolinium enhanced acquisitions.

Conclusion: CC can present in different locations and forms that may overlap other conditions. Familiarity with the spectrum of radiologic presentation and an understanding of the staging criteria may lead to improved diagnostic and therapeutic accuracy.

P-003

Normal MR and Pathologic Conditions of the Ampullary Area: a Pictorial EssayX. Merino-Casabiel¹, Y. Martinez-Alvarez², R. Dominguez-Oronoz¹, V. Pineda-Sanchez¹, S. Gispert-Herrero¹, T. de la Espriella¹; ¹Barcelona/ES, ²Madrid/ES

Learning objectives: To illustrate the range of appearances of the normal papilla with MR as well as some frequent pathologic conditions. To emphasize the

difficulty of evaluating this area and the importance of its correct assessment in routine hepatobiliary MR and MRCP studies. To differentiate normal variants and benign conditions such as spasm or papillitis from malignancy.

Background: Hepatobiliary MR and MR cholangiography have become routine examinations in most MR departments as useful tools to depict the biliary tree and the pancreatic ducts. However, assessment of the Ampulla of Vater area remains a challenge for the radiologist, due to a variety of normal appearances and benign conditions that may mimic malignancy.

Imaging findings OR Procedure details: In this exhibit, we will first describe the technical details of the MR exploration, then illustrate and describe the spectrum of normal (open papilla, spastic papilla) and postoperative appearances of the papilla (common bile duct stump) as well as its pathologic conditions (papillitis, periampullary diverticulum, cholangitis, pancreatitis or groove pancreatitis, choledochocoele and tumors such as intraductal papillary mucinous tumor, ampullary adenoma and carcinoma).

Conclusion: MR has proved effective in depicting the biliary tree and demonstrating many of its pathologic conditions such as dilatation, choledocholithiasis or tumors. It is essential to be familiar with the normal and postoperative appearances of the papilla in order to be able to rule out pathology of this anatomic region.

P-004

MRI of cholangiocarcinoma: experience from a tertiary hepatobiliary centre

H.A. Ansari, F.M. Grieve, C. Liew, B. Rajashanker; Manchester/UK

Learning objectives: Describe the MRI technique for CAC evaluation. Review MRI characteristics of various types of CACs. Describe various hepatobiliary diseases that mimic CAC. Describe criteria for tumour resectability and palliative treatment.

Background: Cholangiocarcinoma (CAC) is the most common primary malignancy of the biliary tree and is classified as either intra or extra hepatic, and their typical growth pattern can be classified as mass-forming, periductal-infiltrating, or intraductal-growing type. CAC is further classified according to its anatomic location and longitudinal extension along the bile ducts into four types which has therapeutic and prognostic implications.

Imaging findings OR Procedure details: CAC demonstrates a wide spectrum of radiological appearances and is characterised using US, CT and MRI. MRI and MRCP due to their intrinsic high tissue contrast and multiplanar capability are more effective in detecting, preoperatively assessing, and predicting involvement of bile ducts, vessels and hepatic parenchyma. CAC appear hypointense on T1W and hyperintense on T2W images. On dynamic imaging, CACs show moderate peripheral enhancement followed by progressive and concentric contrast enhancement. Using gadolinium contrast with biliary excretory properties can accurately locate the exact site of biliary obstruction.

Conclusion: Good quality gadolinium-enhanced MR is the optimal, non-invasive imaging examination for staging and determining resectability of suspected CAC.

P-005

Atypical MRCP appearances of the operated biliary system: a pictorial review

X. Merino-Casabiel, R. Dominguez-Oronoz, S. Gispert-Herrero, V. Pineda-Sanchez, I. Miranda; Barcelona/ES

Learning objectives: To describe the common and non-common features and principal complications of the operated biliary system by means of MRCP.

Background: MRCP is a fast, non-invasive, effective technique for imaging the biliary-pancreatic duct. The increasing use of laparoscopic biliary surgery, creation of biliary-enteral anastomoses, and progressive increase in liver transplantations requires a technique that allows early accurate diagnosis of postoperative complications and provides information for their management.

Imaging findings OR Procedure details: We reviewed MRCP examinations performed in our center since August 1996, selecting postoperative studies of the biliary duct. Several types of atypical MRCP appearances of the operated biliary system are shown: (1) complications related to biliary anatomic malformations (e.g., low insertion of the cystic duct, aberrant right hepatic duct, etc.); (2) complications related to the surgical techniques – cholecystectomy, biliary-enteral anastomoses, etc. (e.g. common and non-frequent causes of stenosis, bile leak, cystic duct dilatation, distal bile duct stump disease, etc.); and (3) biliary complications associated with liver transplantation.

Conclusion: MRCP allows early detection of biliary surgery complications but it is essential to be familiar with all the range of postoperative appearances of the biliary system, in order to be able to rule out pathology.

P-006

MDCT imaging findings of xanthogranulomatous cholecystitis: correlation with pathologic findings

C. Başaran, F. Yildirim Donmez, E.M. Kayahan Ulu, A. Ozturk, M. Coskun; Ankara/TR

Purpose: The purpose of our study was to evaluate the MDCT features of xanthogranulomatous cholecystitis (XGC), correlating the pathologic findings.

Material and methods: Retrospective analysis was performed in 13 patients with pathologically diagnosed XGC from January 2002 to December 2007. The patients were 7 women and 6 men with a mean age of 63 years. All patients had preoperative CT examination. CT scans of the abdomen were performed with 16-row MDCT (Sensation, Siemens, Erlangen, Germany). The following MDCT features were evaluated: maximum wall thickness, intramural hypodense nodules, mucosal line, patterns of wall thickening and enhancement, surrounding fat, surrounding liver and the presence of stones.

Results: The mean thickness of the gallbladder wall was 1.1 cm (diffuse in eleven patients and focal in two patients). Intramural hypodense nodules were seen in all patients. The mucosal line was observed in all patients (continuous in four and focally disrupted in nine). On CT, intramural hypodense nodules in the wall of XGC correlated with foam and inflammatory cells or necrosis and/or abscess in XGC. Continuous mucosal line of gallbladder wall represented preservation of the epithelial layer. The early-enhanced areas of the liver bed on dynamic CT images corresponded to accumulation of inflammatory cells and fibrosis.

Conclusion: Although the preoperative imaging diagnosis of XGC is difficult, our results indicate that MDCT findings correlate well with the histopathologic findings of XGC.

P-007

Gallbladder carcinoma: pre- and post-treatment imaging evaluation

A. Furlan¹, J.V. Ferris², K. Hosseinzadeh², A.A. Borhani², T.C. Gamblin³, D.A. Geller²; ¹Udine/IT, ²Pittsburgh, PA/US

Learning objectives: To describe the appearance of gallbladder carcinoma (GBC) at US, CT, PET-CT, MRI, MRCP, and ERCP and to review the ability of each modality to diagnose and stage tumor extent. To discuss triage to available treatments according to tumor stage. To illustrate sequelae of different therapies.

Background: GBC is the most common biliary tract malignancy, yet often eludes early diagnosis because symptoms tend to manifest at later stages when prognosis is grim. Surgery may be curative for early stages or palliative for later stages with a modest improvement in 5-year survival curves. As only one-third of patients are surgical candidates, chemo- and radiotherapy have been used with varying results.

Imaging findings OR Procedure details: US, CT and MR are the imaging modalities most used in cases of suspected GBC. Usual appearances include diffuse asymmetric or focal gallbladder wall thickening, intraluminal polypoid mass, or a mass replacing the gallbladder lumen, with variable enhancement patterns after intravenous contrast administration. CT, MR and increasingly PET-CT are used to assess direct extension to the liver and adjacent organs, as well as spread to lymph nodes and distant sites.

Conclusion: Accurate diagnosis and staging is critical toward triaging patients with GBC to the most appropriate treatment. Although GBC is often detected first by US, CT and MR are more reliable for evaluation of tumor resectability and for monitoring therapy.

P-008

Roles of radiologists in the management of hilar cholangiocarcinoma patients

H.J. Kim, D.H. Lee, J.W. Lim, Y.T. Ko; Seoul/KR

Learning objectives: After completing the material in this exhibition, the learner should be able to: 1. understand the general concept in the management of patients with HCAC; 2. make a proper preoperative evaluation plan for patients with HCAC using various imaging modalities; 3. provide the surgeon with essential information about curative resection.

Background: Currently, more patients with hilar cholangiocarcinoma (HCAC)

may be potential candidates for curative resection because of advances in imaging modality and surgical technique. The role of radiologist is essential in the management of hilar cholangiocarcinoma because of complex anatomy in hepatic hilum and necessity of interventional procedures.

Imaging findings OR Procedure details: 1. Algorithm in the evaluation of HCAC (US, CT, MRCP, conventional direct cholangiography, and 3D direct MDCT cholangiography). 2. Factors that should be considered in candidates for curative resection. 3. Surgeons are curious about: road map of biliary invasion and anatomic variations. 4. Clinical significance of the caudate lobe in surgery of HCAC. 5. Interventional procedures in HCAC. 6. Roles of radiologist in the management of inoperable HCAC patients.

Conclusion: Radiologists are playing important roles in the management of HCAC. Understanding various radiologic modalities is necessary for radiologists in the management of HCAC.

P-009

MRCP: technical improvements with parallel imaging technique

A. Furlan, R. Girometti, L. Cereser, G. Como, C. Zuiani, M. Bazzocchi; Udine/IT

Learning objectives: To review the current state-of-the-art MRCP sequences. To describe the distinct parallel imaging (PI) algorithms that can be applied to MRCP sequences. To understand the technical advances and improvements with PI with respect to the image acquisition and image quality of MRCP in diagnosing pancreatico-biliary pathologies.

Background: PI techniques use the spatial sensitivity information inherent in an array of multiple receiver surface coils to partially replace time-consuming spatial encoding usually performed by switching magnetic field gradients. The reduction of the number of phase-encoding steps allows decreasing the acquisition time and, in single-shot sequences, the length of the echo train (ETL) and thus the duration of the readout period.

Imaging findings OR Procedure details: Standard MRCP sequences described will include the following T2-weighted sequences: 1) projection technique, 2D thick slab half-Fourier-acquired single-shot turbo-spin echo (HASTE); 2) 2D multi-slice HASTE; and 3) 3D turbo-spin-echo (TSE). The distinct effects of PI on standard MRCP sequences will be described in detail: When applied to HASTE sequences, PI technique shortens the ETL and thus reduces the blurring of the image. When applied to 3D TSE sequence, PI reduces the acquisition time and allows obtaining of high resolution imaging with isotropic voxel size.

Conclusion: PI increases quality and performance of MRCP sequences. Ultimately, these improvements in image quality may manifest better diagnostic accuracy.

P-010

Value of contrast-enhanced MR-cholangiography in patients with iatrogenic bile duct leaks after cholecystectomy

B. Cusati¹, F. Palmieri², G. Di Costanzo², A. Ragozzino²; ¹Naples/IT, ²Pozzuoli (NA)/IT

Purpose: We assessed the role of mangafodipir (Teslascan)-enhanced magnetic resonance (MR) cholangiography in the detection and location of bile duct leaks after laparoscopic cholecystectomy.

Material and methods: Between June 2006 and December 2007, 13 patients with clinical suspicion of bile duct leak after cholecystectomy underwent MRI. MR studies were performed on a 1.5-T scanner. The study included axial heavily T2-weighted images, 3D MR cholangiography and three-dimensional T1-weighted MR prior to and 30 minutes in average after IV administration of mangafodipir trisodium.

Results: On the non contrast-enhanced, the bile collection was visualized in 13 patients, the bile duct discontinuity in 3 patients and residual calculosis in 2 patients. On CE, MR images the fistula between bile duct and collection was visualized in 9 patients; in 4 patients the fistula not was visible. The results were correlated to surgery (n=7), endoscopic retrograde cholangiography (n=2), and clinical follow-up (n=4).

Conclusion: Mangafodipir trisodium-enhanced MR cholangiography is a non invasive technique that can successfully detect the presence of bile duct leaks. The combination of T2 weighted MR cholangiography and mangafodipir trisodium-enhanced T1 weighted MR cholangiography increases the sensitivity in detection and localization of the site of bile leak compared with the non CE MR cholangiography alone.

P-011**The double duct sign on CT: referral practice in a tertiary referral centre**

E.M. Godfrey, D. Humphries, A. Roseman, N. Carroll; Cambridge/UK

Purpose: The double duct sign describes simultaneous dilatation of the common bile duct (CBD) and pancreatic duct (PD). We examined whether patients with this finding on CT, but without an obstructing mass, were appropriately referred for endoscopic ultrasound (EUS).

Material and methods: A radiology database was interrogated for CT examinations with the double duct sign for 18 months following 1.1.06. Patients were followed up using electronic histology and clinical record databases.

Results: 66 patients with the double duct sign were identified. 36 had no obstructing mass visible on CT. Of these 36 patients, 12 were not referred for further imaging on the basis of radiological findings (metastatic disease at presentation or longstanding CBD/PD dilatation). Of the remaining 24 patients, 3 were deemed unfit for surgery and conservatively managed. 3 died soon after the initial CT. 18 patients were therefore retrospectively considered to have been suitable candidates for EUS. 8/18 patients not referred for EUS but were followed up with ERCP, CT or US. 10/18 patients were referred for EUS. The findings were benign in 7/10. 2/10 were palliated for unresectable malignancy. 1/10 underwent a Whipple's procedure for a resectable ampullary tumour.

Conclusion: There is variation in referral for imaging following the CT double duct sign. We propose that in patients with double duct dilatation and no obstructing mass, the reporting radiologist should explicitly recommend referral for EUS to improve the chances of diagnosing resectable disease.

P-012**The value of MR cholangiography in early and late postcholecystectomy biliary disorders**

F. Palmieri¹, B. Cusati², G. Di Costanzo¹, A. Ragozzino¹; ¹Pozzuoli (NA)/IT, ²Naples/IT

Purpose: To assess the role of magnetic resonance (MR) cholangiography in early and late postcholecystectomy syndrome.

Material and methods: One hundred and two patients had a clinical suspicion of post-cholecystectomy syndrome, 42 with an early and 60 with a late syndrome. All patients underwent single slab 2D Haste and 3D multislice T2 weighted and post-contrast 3D gradient-echo sequences, with Maximal Intensity Projection reconstructions. Two readers, unaware of surgical, histopathologic, or other imaging findings, independently reviewed the MR cholangiographic images. Final diagnoses were established with surgery, imaging other than MR or follow-up.

Results: Forty two patients with early postcholecystectomy syndrome showed iatrogenic bile duct lesions (n=20); iatrogenic vascular lesions (n=3), biliary leaks (n=9), functional syndrome (n=10). Sixty patients with late post-cholecystectomy syndrome showed bile duct stones (n=38), bilomas (n=3); bile duct stones (n=6); mucocele of cystic duct (n=5), cholangitis (n=4) and functional syndrome (n=4). The two readers had an excellent interobserver agreement (kappa=0.82).

Conclusion: MR cholangiography is an accurate, noninvasive modality for the assessment of postcholecystectomy biliary disorders, able to distinguish functional from organic syndrome and identify the causes.

P-013**Multimodality imaging of biliary dilatation**

L. Goncalves, S.C.C. Dias, H. Torrão, S. Kurochka, A.C. Costa, V. Mendes, C. Pina Vaz; Braga/PT

Learning objectives: We review multimodality imaging of benign and malignant BD, valuing its diagnostic and therapeutic contributes.

Background: Biliary dilation (BD) is a common problem, most frequently caused by benign acquired strictures, but that can also be originated by malignancy. So early diagnosis is mandatory, in order to plan appropriate and timely management. Ultrasonography (US) is frequently the first technique performed, providing fundamental diagnostic information. Computed tomography (CT) and magnetic resonance (MR) allow extensive extrabiliary imaging and aid in determining the severity of dilation and the precise level and extent of obstruction, strongly contributing to the final etiology and staging of malignancy, thus enabling helpful diagnostic and therapeutic data.

Imaging findings OR Procedure details: We illustrate US, CT and cross-

sectional and cholangiography MR (CMR) distinguishing features of various benign and malignant forms of BD. Among the benign, we consider congenital and inflammatory causes, strictures, lithiasis, parasites and extrinsic compression by liver cyst. CMR was especially useful in characterizing intraluminal disease, frequently avoiding diagnostic retrograde cholangiography. Special emphasis is given to distinction between benign and malignant obstruction, with extrabiliary as well as ductal and dilation related key features being pointed out. The management impact of the dilation degree, level and extent of obstruction, and of staging are also exemplified.

Conclusion: Multimodality imaging techniques of BD are complementary, providing crucial diagnostic and therapeutic features, which often avoid diagnostic invasive procedures.

P-014**Anatomic variations of the bile duct bifurcation: diagnosis with MRCP**

F. Obuz, A. Ucar, F. Uysal, M. Secil, E. Igci, O. Dicle; Izmir/TR

Purpose: Anatomic variations of the bile ducts may complicate surgeries such as laparoscopic cholecystectomy and living donor liver transplantation. The aim of this study is to evaluate the frequency of anatomic variations of the bile duct bifurcation (BDB) using MRCP.

Material and methods: Between May 2002 and December 2007, 1160 consecutive patients suspected with pancreatobiliary disease and referred to our department to be performed MRCP were reviewed retrospectively. MRCP examination was performed on a 1.5 Tesla MR unit using phased-array coil. In all patients, single slice and multi-slice TSE T2 weighted and high resolution 3D-TSE T2 weighted paracoronar images were obtained. Two reviewers evaluated the presence of anatomic variants.

Results: One hundred forty-nine patients were excluded from analysis because the MR examination did not image the biliary bifurcation clearly. The BDB was demonstrated in 803 patients (79.4%). Trifurcation was found in 8% patients, an aberrant right hepatic duct emptying into the common hepatic duct was demonstrated in 7.2% patients, and right dorsocaudal branch draining into the left hepatic duct was shown in 4.1% patients.

Conclusion: MRCP is helpful and a non-invasive technique in the diagnosis of bile duct variations. Preoperative description of these variations may prevent some surgical complications.

Diagnostic / GI Tract / Colon**P-015****The utility of diagnostic imaging in irritable bowel syndrome patients**

S.E. Mc Sweeney, K. O'Regan, M. Ryan, E. Quigley, M. Maher; Cork/IE

Learning objectives: To review the literature and discuss the appropriateness of diagnostic imaging in the evaluation of patients with IBS. To discuss the diagnostic yields, limitations and disadvantages (such as radiation dose) of these imaging modalities. To discuss the perspective of the gastroenterologist in choosing appropriate imaging for IBS. To propose an appropriate evidence-based imaging algorithm for the evaluation of patients with IBS.

Background: Irritable Bowel Syndrome (IBS) affects 14–24% of women and 5–19% of men and is characterised by abdominal pain, bloating and disturbed defecation.

Imaging findings OR Procedure details: Imaging is frequently utilised in these patients to exclude more sinister pathology including bowel carcinoma, inflammatory bowel disease and ovarian lesions. This educational exhibit will review the literature using evidence-based techniques and draw on local experience to discuss the appropriateness of imaging modalities employed in IBS including plain radiography, ultrasonography, computed tomography, barium studies and MRI. The diagnostic yields, limitations and disadvantages (such as radiation dose) of these imaging modalities will be discussed. The perspectives of gastroenterologists will also be included in these discussions.

Conclusion: Imaging is frequently employed in the evaluation of patients with IBS. Appropriate imaging algorithm will be proposed based on the review of local experience and a thorough review of the literature.

P-016**Imaging strategies in the management of diverticulitis: how can radiologists do it better?**

F.M. Gómez¹, J.M. Mayol², J.V. Rambla¹, J.G. Pamies¹, M.L. Lloret¹, O.L.T. Ramírez¹, M.M. Ballesta¹, N. Madroñal¹; ¹Valencia/ES, ²Madrid/ES

Learning objectives: Optimizing imaging strategies in diverticulitis. Knowing therapeutic implications of radiological findings in diverticulitis.

Background: The management of left colon diverticulitis remains controversial. Adequate patient selection for surgery is the key to reduce morbidity and mortality. Surgeons rely on radiologists to diagnose and stage patients according to the modified Hinchey classification. Although CT scanning is the most frequently used technique to image these patients, ultrasonography may be an important tool in this setting.

Imaging findings OR Procedure details: Stages 0, 1a and 1b with abscess smaller than 5 cm can be managed with diet and antibiotic therapy. Stages 1b and 2 with percutaneous approachable abscess larger than 5 cm are treated on NPO with antibiotic and drainage. Non approachable abscess and stages 3 and 4 require urgent surgery. Radiologists play a central role in classifying each patient and giving the surgeon the precise information they need for an adequate patient management. CT should be considered in case of pneumoperitoneum on X-rays or ultrasonographic evidence of: peritoneal stripe enhancement sign, free abdominal fluid, bad delimited collection, non percutaneous approachable collection larger than 5 cm or open communication with bowel lumen.

Conclusion: Imaging strategies combining US and CT are critical in selecting the most adequate treatment for patients with acute diverticulitis. Ultrasonography may be useful in identifying patients at early stages (0 and 1a) avoiding unnecessary ionizing radiation.

P-017**Key learning objective: to illustrate the radiological presentation of Crohn's disease in the elderly**

S. Ghosh, N. Power; London/UK

Learning objectives: To illustrate the radiological appearance of Crohn's disease in the elderly.

Background: Crohn's disease typically presents at 2 peaks, commonly in the younger age group and less so in the older age group. However, with the use of cross sectional imaging, Crohn's disease has become increasingly recognized in the older age group where the radiological presentation may be difficult to distinguish from other common disorders. Imaging appearances can easily be confused with diverticulitis, ischaemia and carcinoma.

Imaging findings OR Procedure details: This poster illustrates the difficulty and dilemmas of diagnosing Crohn's disease on imaging.

Conclusion: This pictorial review will illustrate the radiological manifestations of Crohn's disease as a mimic of other potential differential diagnosis.

P-018**Is preoperative whole-body CT screening mandatory for endoscopically cT1 colorectal cancer?**

H. Furukawa, K. Asakura, A. Sawada, M. Moriguchi; Shizuoka/JP

Purpose: The usefulness of preoperative CT scans for colorectal cancer was reported in many studies. However, the patient populations in previous studies were biased in favor of advanced-stage tumors. The aim of this study is to describe the clinical utility of routine preoperative CT scanning for patients with endoscopically diagnosed cT1 colorectal cancer.

Material and methods: Between October 2002 and November 2006, 165 consecutive patients proved to have a cT1 colorectal cancer endoscopically. In 85 of 165 cases, endoscopic resections were preceded, and additional resection was recommended under histopathological evaluation of the resected specimen. All patients underwent preoperative MDCT with 16 detectors. Scan data were acquired from the neck to the upper femur within one breath hold. CT images were prospectively evaluated, and these findings were compared with surgical and histopathological results.

Results: Of all patients with endoscopically cT1 lesions, pT2 and pT3 lesions were demonstrated pathologically in 17% (28/165). MDCT correctly indicated an advanced cancer in 32% (9/28). MDCT overstaged as cT2 or cT3 in 12% (17/137). Overall accuracy of T factor was 78% (129/165) on MDCT. The pathological

node-positive rate was 13% (21/165). Sensitivity, specificity, positive predictive value, negative predictive value, and overall accuracy of lymph node metastases on MDCT were 19% (4/21), 100% (144/144), 100% (4/4), 87% (144/161), and 90% (148/165), respectively. One patient had liver metastases and MDCT correctly showed the lesions. There were no synchronous findings other than colorectal cancer that influenced therapeutic decision makings.

Conclusion: Whole-body CT screening of endoscopically cT1 colorectal cancer is not mandatory for preoperative treatment planning.

P-019**CT and MR manifestations of local and distant colorectal cancer recurrence**

S.Y. Liang, D. Awad, W.J. Blackshaw, D. Kasir, S. Sukumar; Manchester/UK

Learning objectives: 1. To review the anatomy of the colon and rectum relevant to the radiologist. 2. To describe typical and atypical patterns of local and distant spread of colorectal cancer recurrence. 3. To illustrate subtle early local and distant recurrences.

Background: Colorectal cancer is the second most common malignancy in Western societies. Recurrence has been reported to occur in up to 50% of patients following surgery with curative intent. Early detection of recurrence through intensive follow-up has been shown to significantly improve long-term survival. Imaging has an important role in follow-up, with CT imaging often being performed for the detection of recurrences and MR imaging performed in selected cases for problem solving or restaging.

Imaging findings OR Procedure details: We have reviewed images of colorectal cancer patients followed up at our centre between January 2004 and January 2008. Relevant colorectal anatomy including vascular supply and lymphatic drainage will be reviewed. We will present CT and MR images of local and distant recurrences. Some examples include recurrences involving the vaginal vault, seminal vesicles, pelvic wall and retroperitoneum. We will also describe and illustrate subtle, early recurrences and progression over time.

Conclusion: Early detection of recurrence following curative colorectal cancer surgery is important as it can enable more effective treatment and improve patient survival. An appreciation of patterns of spread and appearances of early recurrence is important for the radiologist.

P-020**CT examination for diagnosing appendicitis: clinical, pathological and CT correlations**

Y. Kobashi¹, H. Okamoto², R. Kodama², Y. Nakajima², K. Shimoyama¹; ¹Fujisawa/JP, ²Kawasaki/JP

Purpose: To categorize acute appendicitis using CT examination and correlate with clinical and pathological findings.

Material and methods: We investigated 32 patients (male 17, female 15, mean age 31.1 years and ranging from age 13 to 80) who were diagnosed with acute appendicitis on both of CT and operation. The acute appendicitis was classified into following three CT findings considering pathological findings before operation; 1) Appendiceal wall thickening and enhancement without periappendiceal enhancement which were suspected with catarrhal appendicitis by pathology, 2) Appendiceal wall thickening and enhancement with periappendiceal enhancement which were suspected with phlegmonous appendicitis by pathology and 3) Periappendiceal enhancement with/without abscess formation, cecal edema without appendiceal enhancement which were suspected with gangrenous appendicitis by pathology. We correlated these findings with operative findings and pathological diagnosis.

Results: Ten patients were categorized with catarrhal appendicitis, fourteen patients with phlegmonous appendicitis and three patients with gangrenous appendicitis. We misdiagnosed four patients of appendicitis. Three patients had no obvious findings for acute appendicitis on CT but were operated and diagnosed catarrhal appendicitis. One patient was diagnosed with enterocolitis on CT but operated. He was diagnosed with gangrenous appendicitis with perforation by pathology.

Conclusion: We should know that acute catarrhal appendicitis is not shown on any CT findings and severe gangrenous appendicitis is suspected for other abnormal diseases. Then, relationship between clinical and CT findings is more important.

P-021**MRI versus double contrast barium enema for the assessment of rectal or colonic localization of endometriosis**

G. Restaino, M. Missere, M. Ciuffreda, E. Cucci, M.V. Occhionero, A. Pierro, G. Sallustio; Campobasso/IT

Purpose: To assess the accuracy of magnetic resonance imaging (MRI) for the identification of rectal or colonic localization of pelvic endometriosis in comparison with double contrast barium enema (DCBE) and laparoscopic or surgical findings.

Material and methods: 15 patients with clinical and US suspicion of rectal or colonic localization of pelvic endometriosis were prospectively evaluated with MRI and DCBE. MRI was performed with 1.5 T magnet and phased-array surface coil; high resolution T2-weighted and T1-weighted fat-suppressed images were acquired after administration of a spasmolytic agent. DCBE was performed according to the classical technique with air and barium. MRI and DCBE were independently evaluated by two radiologists: quality of examination, visibility of colonic wall, presence, number, location and extent of rectal/colonic endometriosis localization were recorded. The results of the two procedures were compared with laparoscopic or surgical findings.

Results: MRI and DCBE correctly identified colonic and/or rectal localizations of endometriosis in 6/15 patients with 100% sensitivity. In 2 patients with false positive results at DCBE, MRI correctly excluded endometriosis infiltration, showing better specificity than DCBE (100 vs 81%). Moreover, MRI identified multiple localization of deep pelvic endometriosis that was missed by DCBE.

Conclusion: MRI is more accurate than DCBE for the diagnosis of rectal/colonic localization of endometriosis, can identify foci of deep endometriosis and has no radiation burden, which is crucial in childbearing age endometriosis patients.

P-022**The sigmoid colon revisited**

D. Kasir, L.R. Williams, R.J. Johnson, S.Y. Liong, S. Sukumar, V. Rudralingam; Manchester/UK

Learning objectives: 1. To demonstrate the anatomy and review the disease processes affecting the sigmoid colon and its mesentery. 2. To illustrate the features of benign, inflammatory and neoplastic processes of the sigmoid colon.

Background: The sigmoid colon and its mesentery are commonly involved by inflammation and neoplastic processes. Differentiating between these two entities is a frequent challenge to the radiologist and often requires endoscopic correlation. The location of the sigmoid colon adjacent to the pelvic organs creates a recognizable pattern of local spread of disease and fistula formation. The attachment of the sigmoid mesocolon predisposes to volvulus and creates a potential space for internal hernias.

Imaging findings OR Procedure details: A range of disease involving the sigmoid colon and mesentery will be illustrated using US, CT and MRI with pathological correlation. The examples include diverticular disease, infective colitis, neoplastic strictures, endometriosis, fistulas and sigmoid mesenteric cyst.

Conclusion: The awareness of the cross sectional imaging appearances of the different disease processes affecting the sigmoid colon and diagnostic limitations is important to reach the correct diagnosis.

P-023**Contrast-enhanced PET/CT in recurrent colorectal cancer: a pictorial review**

N.M.G. Caserta, S. Dragosavac, M.L. Cunha, D.M. Morita, N.M. Hanaoka; Campinas/BR

Learning objectives: 1. To pictorially demonstrate the different aspects of recurrent CRC that can be evaluated with PET/CT. 2. To review the imaging patterns of these lesions. 3. To recognize the role of PET/CT in the management of patients with CRC.

Background: A widely accepted application of PET/CT is in the detection of recurrence and restaging of colorectal cancer (CRC). This exhibit presents a pictorial review of how the disease manifests in a variety of aspects. We demonstrate recurrent lesions such as distant metastasis, peritoneal implants, lymph node enlargement, urinary obstruction, periumbilical tumor, local recurrence at anastomotic site, differentiation from fibrosis, and other situations.

Imaging findings OR Procedure details: Through an integrated 16MDCT

scanner and using oral and intravenous iodinated contrast, we performed PET/CT in patients being considered for recurrent CRC. Many of these cases showed findings such as hepatic, osseous, pulmonary and nodal metastasis, peritoneal implants, infiltration of abdominal wall, scar and fibrosis difficult to differentiate from local recurrence, and other manifestations.

Conclusion: Imaging patterns of recurrent CRC can be accurately evaluated with PET/CT. It is important to be familiar with these findings that can contribute to changes in treatment strategy.

P-024**CT patterns of bowel wall thickening as a diagnostic tool in patients with acute abdomen**

E.M. Dieguez Costa, S.M. Novo, M. Barxias, B. Gonzalez, P. Borrego; Madrid/ES

Purpose: CT has been proven a useful method to evaluate those patients with acute abdomen because of its ability to display both mural and extraluminal abnormalities. The purpose of this study was to assess the capability of CT to categorize the major differential diagnosis in those cases of acute abdomen that course with bowel wall thickening (BWT).

Material and methods: The CT scans of 320 patients who were admitted to the emergency room in our institution over a period of two years were retrospectively reviewed.

Results: We found 220 cases with BWT. Among them, the following diagnoses were obtained: Neoplastic disease 40, ischemic colitis 11, infectious colitis 14, bowel inflammatory disease 30, diverticulitis 80, appendicitis 39, intramural hemorrhage 2, hypoalbuminemia related conditions and miscellaneous 4.

Conclusion: BWT is a valuable CT sign in patients with acute abdominal pain. By analyzing symmetry and degree of wall thickness, wall attenuation, distribution and length of extent, contrast enhancing pattern, and perienteric change it was possible to substantially narrow the broad spectrum of differential diagnosis.

P-025**Unusual submucosal tumors of the colon: imaging findings with colonoscopic and pathologic correlation**

J.Y. Oh, K. Nam, J. Cho, H. Choi; Busan/KR

Learning objectives: To describe the imaging features of various submucosal tumors of the colon and correlate with colonoscopic and pathologic findings.

Background: Colonic submucosal tumors are not encountered as often as carcinomas of the colon are. Furthermore, they sometimes have similar radiologic findings that make differentiation difficult. However, some tumors have unique radiologic features that may suggest a specific diagnosis. We will demonstrate various radiologic findings of unusual submucosal tumors of the colon with colonoscopic and pathologic correlation.

Imaging findings OR Procedure details: Benign submucosal tumors of the colon consist of hemangioma, lymphangioma, lipoma, schwannoma, leiomyoma and inflammatory fibroid polyps. Malignant submucosal tumors of the colon are GIST, leiomyosarcoma, malignant schwannoma, primary lymphoma and carcinoid tumor. Hemangiomas of colon manifest vascular engorgement and phlebolith within thickened colonic wall and pericolic fat area. Lipomas are usually showed as well-circumscribed submucosal masses with fat attenuation. Lymphangiomas manifest as non-enhancing submucosal masses with homogeneous low attenuation on CT. Lymphomas of colon may have more pronounced and homogeneous mural thickening comparing with adenocarcinoma of the colon. Colonic carcinoids mostly occur in rectum and usually appear as small broad-based submucosal masses.

Conclusion: Despite overlap of radiologic findings in submucosal tumors of the colon, some tumors have characteristic radiologic features that may suggest a specific diagnosis. Familiarity with the radiologic features of these unusual tumors can help ensure correct diagnosis.

P-026

Withdrawn by authors

P-027**Diagnosis of colonic volvulus: the crucial role of MDCT**

C. Vandendries, M. Zins, M.C. Jullès, I. Boulay-Coletta; Paris/FR

Learning objectives: 1- To explain the physiopathology of colonic volvulus through the knowledge of embryology. 2- To explain why and how one should perform a MDCT scan in patients presenting with suspicion of colonic volvulus. 3- To emphasize all useful key findings to make precise topographic diagnosis in frequent (sigmoid or caecal volvulus) but also in rare forms (transverse or right-colon volvulus, ileo-sigmoid knot). 4- To emphasize all useful CT features allowing establishing the diagnosis of severe form of sigmoid volvulus indicating for prompt surgical management.

Background: CT is the standard of reference technique for assessment of many acute abdominal conditions. Colonic volvulus is a life threatening condition in which MDCT technique and features have to be known.

Imaging findings OR Procedure details: 1- Epidemiology of colonic volvulus – what the radiologist should know to improve patient management. 2- Physiopathology: from gastro-intestinal embryology to colonic volvulus. 3- How to perform an emergency MDCT scan in case of a supposed colonic volvulus: usefulness of MPR associated with colonic enema. 4- Precise topographic diagnosis. 5- Assessment of severe forms: analyzing volvulus mechanism, whirl sign, and ischemic changes.

Conclusion: Radiologists can help in the efficient management of patients with colonic volvulus by demonstrating strong evidences of the necessity for emergency surgery. MDCT depicts all useful findings to achieve topographic diagnosis and precise assessment of severe forms.

P-028**Correlation of TNM staging of colorectal cancer on multislice CT with histopathology single vs 16 vs 64 slice**

S. Ryan, A. Haj, P.A. Kane, J. Karani, S. Papagrigroriadis; London/UK

Purpose: The purpose of the study is to correlate the TNM staging of colorectal cancer, based on multislice CT (MSCT), with the final histopathological outcome. The performance of single slice vs 16 slice vs 64 slice, in terms of overall accuracy within our institution, will be evaluated.

Material and methods: The CT scans of 160 patients, with surgically proven colorectal cancer, who have all had staging with either a single, a 16 slice or 64 slice CT scanner, over an 18 month period, will be evaluated by two experienced radiologists, blinded to the eventual outcome of the histology. Correlation with the final histopathological staging will be made.

Results: The results will be presented. The performance of the different scanners, as measured by accuracy of staging, will be evaluated.

Conclusion: MSCT is a reasonable method of staging the degree of mural invasion with colorectal cancer. It is insensitive in determining the malignant potential of lymph nodes. MSCT scanning increases the degree of confidence in diagnosing transmural invasion compared with single slice CT.

P-029**Preoperative evaluation of mesenteric vascular variations using a 64-channel MDCT before laparoscopic colorectal surgery**

S. Kumano, M. Okada, M. Kuwabara, Y. Yagyu, I. Imaoka, T. Shimono, R. Ashikaga, T. Murakami; Osakasayama/JP

Learning objectives: 1. Explain the current status and indications for laparoscopic colorectal surgery. 2. Understand the vascular anatomy and variations around colon. 3. Review the 64-channel MDCT technique to demonstrate the mesenteric arteries and veins. 4. Illustrate the value of 3D-CTA for preoperative visualization of laparoscopic colorectal surgery.

Background: Laparoscopic surgery in colorectal cancer has been generally accepted because the technique is less invasive than open surgery. However, in this procedure, it is difficult to obtain images of the entire operative field under laparoscopy. Therefore, it takes a long time to identify the proper vessels where there might be major variations in each patient. Moreover, vessels and organs could be injured during lymph nodes dissection and vessel ligation under laparoscopic guidance. Therefore, it is quite important to perform a preoperative assessment of the vascular anatomy using a 3D-CTA before surgery.

Imaging findings OR Procedure details: We performed multiphase contrast-

enhanced examinations using a 64-channel MDCT. A total of 100 ml of nonionic contrast material was injected intravenously at a rate of 4 ml/s. Timing for arterial phase scanning was determined using bolus tracking technique. Portal phase imaging was performed 70 s after the start of bolus injection. 3D-CTA was reconstructed from CT images of 0.625-mm thickness on computer workstations by using volume rendering and maximum intensity projection techniques.

Conclusion: A 3D-CTA is useful for the preoperative visualization of laparoscopic colorectal surgery.

P-030**Interposition of the left colon**

S. Uysal Ramadan, D. Gokharman, M. Kacar, I. Tuncbilek, P. Kosar, U. Kosar; Ankara/TR

Learning objectives: To investigate the prevalence of ILC by CT and to discuss the significance of ILC.

Background: The interposition of left colon (ILC) has been documented recently and reported more rarely than right colon variations. ILC was classified as retrogastric and retrosplenic types.

Imaging findings OR Procedure details: The abdomen or chest CT examinations were performed by 64 slices CT scanner in 200 patients who suffered from different clinical symptoms. Among them, the ILC was identified in 3 (1.5%) patients. The upper part of the descending colon was located between the spleen and the left kidney, and extended up to the hemidiaphragm (retrogastric type) in two patients. In the third patient, the splenic flexure was seen in front of the left kidney, between the hemidiaphragm and spleen. The last ILC was a variant of the retrosplenic interposition because his spleen was located more caudally than normal position. For this reason, to the best of our knowledge, this type of ILC has been described for the first time in our study.

Conclusion: ILC is a benign anatomical variation and can be easily diagnosed on CT images. Radiological recognition of ILC is important to prevent misdiagnosis of the colon such as abscess and to avoid unnecessary colon perforation during percutaneous nephrostomy or biopsy.

P-031**Pictorial review of complications of colonic diverticulosis**

T. Ichikawa, S. Kawada, J. Koizumi, Y. Iwata, Y. Imai; Isehara/JP

Learning objectives: To review the radiological findings of complications of colonic diverticulosis on CT and others. To understand the clinical features of the various colonic complicated diverticulosis for surgical management.

Background: The most common complication of diverticulosis is diverticulitis. Colonic diverticulosis is the most frequent cause of severe rectal bleeding. Complications of colonic diverticulitis include hemorrhage, perforation, fistulization, panperitonitis, abscess formation, and others. The latter occurs in more than 8% of patients with acute diverticulitis.

Imaging findings OR Procedure details: We reviewed abdominal CT of patients of acute abdomen with colonic diverticulosis. Colonic perforation with intraperitoneal free air, fistulization and spread of inflammation well depicted axial and optimal multiplanar reformatted images using MDCT with 0.6-1 mm of collimation. A rare perforation of sigmoid colon was caused by the impact of ingested foreign body in diverticulum. The hemorrhage from diverticula was diagnosed by pre- and post contrast-enhanced CT, and interventional treatment was done. Serious complications of colonic diverticulitis were thrombosis and gas formation of portal venous system, and perforation with venous intravasation of barium. One case was seen with splenic infarction due to thrombosis of portal and splenic vein secondary cholecystitis because of ascending colonic diverticulitis.

Conclusion: CT is a valuable imaging tool for determining the degree of diverticulitis and complications by means of which patients can be stratified according to the severity of the disease; furthermore, this tool is of assistance in surgical of interventional planning of colonic diverticulosis.

P-032**CT evaluation of intussusception in two children due to unusual lead points: mucinous adenocarcinoma and lymphoma along with a foreign body**

H.O. Akay, S. Senturk, K. Cigdem, A.H. Bayrak, C.A. Ozmen, I. Kilinc, H. Nazaroglu; Diyarbakir/TR

Purpose: Intussusception (IS), an emergent condition, is usually idiopathic in infants five to nine months of age. However neonates, older children and adults commonly have lead points. The purpose of this report is to describe CT findings of two cases with IS due to unusual pathologic lead points.

Material and methods: Abdominal CT scan of two patients was performed with a preliminary diagnosis of chronic intestinal obstruction.

Results: Case 1: A four-year-old boy had asymmetrical prominent wall thickening in the terminal ileum and right-sided colonic segments, and a metallic foreign body in cecum. Besides, there was an intracolonic soft tissue mass representing ileocolic IS in the right hemicolon. Laparotomy revealed ileocolic IS due to ileocecal mass along with a coin. Burkitt lymphoma was determined at histological examination. Case 2: A twelve-year-old girl had small bowel dilatation on CT. There was wall thickening at the ileocecal region, and a small soft tissue mass that was suspicious of IS was observed in cecum. At endoscopic evaluation of the colon, cecal ulcerated mass and ileocolic IS were determined. Histological examination of the biopsy material revealed mucinous adenocarcinoma of cecum.

Conclusion: CT can help predict pathological lead points of IS in older children with atypical presentation of intestinal obstruction. Although it is extremely rare in childhood, colon carcinoma and lymphoma along with a foreign body can act as lead points.

P-033**Prediction of locally advanced colon cancer using high resolution T2-weighted MRI**

E. Rollvén, L. Blomqvist, T. Holm, J. Lindholm; Stockholm/SE

Purpose: To investigate the potential of high-resolution magnetic resonance imaging (MRI) for local tumour staging of colon cancer.

Material and methods: Twenty-four patients with colonic tumours were included and examined on a 1.5 T unit using a five-element phased-array coil. T2-weighted turbo spin-echo sequences (voxel size 3 x 0.5 x 0.5 mm) in the coronal and transverse as well as perpendicular to the long axis of the intestine at the tumour level were performed. The tumours were assessed with respect to localisation, relation to the peritoneum, retroperitoneal structures and adjacent organs. Surgical specimen were examined by a GI pathologist being the reference standard together with surgical findings.

Results: Five patients were excluded due to not satisfactory MRI quality (n=3), not verified cancer diagnosis after surgery (n=1), no surgery (n=1). Of the remaining 19 patients, according to histopathology, one patient had a T1-tumour, six T2, seven T3 and five T4 tumours, respectively. T-stage agreement between histopathology and MRI was achieved in 15 of 19 patients with MRI overstaging in three and understaging in one. In 80%, locally advanced disease was predicted by MRI.

Conclusion: Selection of patients with locally advanced colon cancer for neoadjuvant treatment is needed, but there is yet no established imaging technique. In our study, 80% was correctly classified with preoperative high-resolution MRI. These data are promising for MRI to be the technique of choice.

P-034

Withdrawn by authors

P-035**Evaluation of routine use of chest CT in the workup and follow-up of patients with resectable liver metastases from colorectal carcinoma**H. Dekker¹, T. Ruers², Y. Hoogeveen¹, J. Barentsz¹; ¹Nijmegen/NL, ²Amsterdam/NL

Purpose: The purpose of this study is to evaluate the routine use of chest CT as part of the extent-of-disease work-up in selecting patients for resection of colorectal liver metastases (LM), and to assess its post operative value during patient follow-up.

Material and methods: Patients with potentially resectable LM from colorectal cancer were evaluated using liver CT in combination with chest CT. Postoperatively, all patients were monitored for the development of pulmonary metastases. Chest CT was performed with a slice thickness of 3 mm. Patients with highly suspicious pulmonary lesions on the chest CT and limited to ≤ 3 in number underwent a metastasectomy.

Results: Forty-eight colorectal cancer patients with LM were evaluated. All patients underwent a liver resection and/or radiofrequency ablation. Of these, preoperative chest CT showed no lesions in 16 patients, while chest CT was positive in 32 patients (67%): 25 patients with lesions 1–5 mm and 7 patients with lesions 6–10 mm. Twelve patients (25%) developed pulmonary metastases during follow-up: one patient in the initial group without lesions (6%), 5 patients in the group with 1–5 mm lesions (20%) and 6 patients in the group of 6–10 mm lesions (86%). Three patients underwent a metastasectomy of pulmonary metastases.

Conclusion: Chest CT appears valuable in determining the extent of pulmonary lesions and importantly in discriminating lesions > 5 mm suspicious for pulmonary metastases.

Diagnostic / GI Tract / CT Colonography / Results**P-036****Evaluation of preoperative staging and resectability of colon cancer using CTC: correlation with surgical results**A. Stagnitti¹, F. Iafrate¹, A. Perrone¹, R. Ferrari², M. Marini¹, A. Laghi²; ¹Rome/IT, ²Latina/IT

Purpose: To evaluate the diagnostic performance of CTC in the evaluation of preoperative staging and resectability of colon cancer (CC).

Material and methods: Fifty-eight patients with CC who underwent surgical treatment and had available preoperative CTC with i.v contrast were included in the study. All the images of preoperative CTC were independently analyzed by two radiologists with different experience and the differences in their assessment were analyzed by consensus using MPR reconstructions and 3D images. The radiologists were asked to determinate the depth of invasion of the colon wall (T stage) classifying into $\leq T2$, T3 and T4; involvement of loco-regional nodes (N stage) and distant metastasis (M stage). TNM staging with CTC were correlated with surgical results.

Results: The overall accuracy values for T staging of reviewer 1, reviewer 2 and consensus reading were 91.6, 86.2 and 92.8%, respectively; 92.2, 79.8 and 92.5% for $\leq T2$; 88.1, 85.5, and 89.7% for T3; and 94.5, 93.5 and 96.2% for T4. Two out of 14 T4 lesions were understaged due to inadequate distension (n=1) and misinterpretation of adjacent organ involvement as partial volume averaging (n=2). The accuracy values for N staging and M staging were 81.8, 94.0% for reviewer 1; 78.2 and 88.1% for reviewer 2; and 81.8 and 94.0% for consensus reading, respectively.

Conclusion: Contrast enhanced CTC shows good performance in the preoperative evaluation of staging and resectability of CC.

P-037**Evaluation of the ratio between length and thickness of the involved segment of the colon in distinguishing neoplastic and inflammatory processes: an MDCT colonography study**

J.M. Pienkowska, E. Szurowska, J. Wierzbowski, M. Studniarek; Gdansk/PL

Purpose: The aim of the study was the assessment of the ratio between length and thickness of the involved segment of the colon that may help in distinguishing neoplastic and inflammatory processes.

Material and methods: A total of 74 selected patients (33 females, 41 males, age range 30–81), with strong clinical suspicion of colorectal cancer (positive fecal occult-blood test, altered bowel habits, anemia of unknown cause, weight loss, abdominal pain), underwent MDCT-colonography. The length, thickness and the ratio between the length and thickness were estimated. All results were correlated with histopathological findings.

Results: MDCT colonography correctly detected 44 cases of colorectal cancer

and 18 inflammations. The lengths of the involved segment were 27–140 mm (mean 65.89) for colon cancer and 30–250 mm (mean 127.94 mm) for inflammations. The wall thickening was 9–63 mm (mean 26.05) for neoplastic and 3–15 (mean 6.88) for inflammatory processes. Statistical analysis of the data showed that the ratio between the length and the thickness had the highest specificity for differentiation colon cancer from inflammatory bowel disease ($p < 0.05$). The ratio ≤ 5.4 is characteristic for colon cancer (sensitivity 97.7%, accuracy 93.3%). The ratio > 5.4 is the most specific for inflammatory processes.

Conclusion: Evaluation of the ratio between length and thickness of the involved colon segment can be used as a precise indicator to differentiate between neoplastic and inflammatory processes.

P-038

CTC in the diagnosis of large colonic lipomas

I.G. Crespo, D. Cano, I. Vivas, M. Arraiza; Pamplona/ES

Learning objectives: CTC has a role in the evaluation of the colon, especially when due to the lesion a complete colonoscopic examination may not be possible. Using 3D endoluminal images with different endoluminal rendering presets and 2D images, we can navigate through the entire colon to look for the lesion and we can not only see the fatty texture of the lesion but also localize the lesion more precisely. Surgical resection seems to be the ideal treatment. If the preoperative diagnosis and location can be made correctly, extent of surgery may be appropriately limited.

Background: Colonic lipomas are the third most common benign colonic tumor, after hyperplastic polyps and adenomatous polyps. They are relatively rare with incidence reported between 0.03 and 4.4%. Most of them are small and asymptomatic and are found incidentally. About 20–25% of patients with a large lipoma more than 2 cm have related symptoms. The differential diagnosis is sometimes difficult, often misinterpreted with malignant tumors.

Imaging findings OR Procedure details: We describe two cases of symptomatic giant lipoma of the colon, diagnosed by virtual colonoscopy following incomplete colonoscopy.

Conclusion: Virtual colonoscopy is an excellent method not only to diagnose the colonic lipomas and to examine the rest of the colon in case of incomplete colonoscopy but also to provide surgeons a more precisely anatomic location of the lesion.

P-039

CTC in acromegaly

L. Bacigalupo, A. Tagliafico, E. Melani, G. Giordano, E. Resmini, G.A. Rollandi; Genoa/IT

Purpose: Acromegalic patients have an increased risk for the development of colon cancer. Since 1996, screening colonoscopy has been recommended to all patients with acromegaly. The aim of our study is to evaluate the feasibility and the results of CTC in acromegalic patients.

Material and methods: Between January 2006 and August 2007, we examined 24 acromegalic patients with no history of colonic cancer (11 female and 12 male; age range 18–79 years; mean 54.9 ± 3.20 ; body mass index 25.2 ± 0.90 ; disease duration range 1–15 years, 5.1 ± 0.85 years) with CTC. Twenty of them underwent traditional colonoscopy following CTC. The local ethics committee approved the study and written informed consent was obtained from all subjects involved in the study.

Results: CTC examinations resulted adequate in 17 (71%) of cases. We found 12 polyps in 8 patients (33%), 95% of them confirmed by colonoscopy, and 1 cancer confirmed by surgery. There were no polyps found by traditional colonoscopy that CTC was not able to identify. The lesions were located in right colon (2), transversum (3), left colon (5) and sigma (2). Patient acceptance of the technique was good in 65%, medium in 20%, and poor in 15%.

Conclusion: From our preliminary data, CTC has the potential to replace traditional colonoscopy in acromegalic patients.

P-040

Withdrawn by authors

Diagnostic / GI Tract / CT Colonography / Technique

P-041

Bowel preparation for multidetector row CTC: comparison of three different cleansing preparations

M. Slattery, E. Thornton, M. Morrin; Dublin/IE

Purpose: Sodium phosphate has been the main colonic cleansing agent utilised prior to CT colonography (CTC). However, concerns regarding safety have led to restriction in its use. This study prospectively compares three bowel cleansing preparations.

Material and methods: Group 1 (n=20) received single dose Sodium phosphate; Group 2 (n=20) received sodium picosulphate (Picolax) and senna; and Group 3 (n=20) received a combination of Picolax and 1L 2% oral diatrizoate meglumine (gastrograffin). Overall preparation quality and diagnostic confidence between groups was analysed using the Kruskal-Wallis test and Dunn's post hoc analysis. Colonic distension scored similarly in all 3 groups ($p > 0.05$). There was significantly less retained fluid ($p < 0.05$) and significantly more residual faeces ($p < 0.05$) in subjects prepared using sodium phosphate. No significant difference in terms of residual fluid or faeces was observed between Groups 2 and 3 ($p > 0.05$) and overall study quality was superior in subjects prepared with Picolax and senna (Groups 2 and 3) ($p < 0.05$). Overall confidence in diagnosis was significantly higher where oral labelling with gastrograffin was performed (Group 3) ($p < 0.05$).

Results: Picolax preparations are superior to sodium phosphate preparation prior to CTC. The increased overall confidence in diagnosis observed in subjects who received a combination of Picolax and oral gastrograffin is attributable to the quality of labelling of residual fluid and faeces.

Conclusion: Picolax preparations are superior to sodium phosphate preparation prior to CTC.

P-042

CTC: which are the right scanner parameters to use?

P. Paolantonio¹, R. Ferrari², P. Lucchesi², F. Vecchiotti², C.N. de Cecco¹, A. Laghi²; ¹Rome/IT, ²Latina/IT

Learning objectives: To describe acquisition parameters of CTC protocols using different scanners generations moving to single slice spiral CT to the 64-MDCT.

Background: Nowadays, the "panorama" of technical approaches for CTC is expanding offering a wide spectrum of different possibilities. As technology continues to advance, there will be a continuing need to reassess the relative tradeoffs among scan width, image noise, patient dose, image artefacts, breath-hold times, and the number of reconstructed images to be viewed and archived.

Imaging findings OR Procedure details: We will discuss the relationship among collimation, tube current settings, patient dose exposure and accuracy in polyp detection of various CTC protocols valid for different scanner generation. We will offer some practical guidelines for CTC technique based on evidences of literature and our personal experience of more than 800 CTC examinations performed on different scanners generation including a 64-MDCT (VCT; GE).

Conclusion: A single scanning protocol with identical parameters for all scanners and patients cannot be recommended due to technological differences as well as different clinical indications to CTC. What is possible to do is to offer general guidelines according to the consensus statement on CTC. Collimation should not be larger than 5 mm for SSCT and no larger than 3 mm for MDCT. With the advent of 64-slice MDCT, sub-millimeter collimation will be mandatory, although clinical benefits are still unclear.

P-043

Ileocecal valve at CTC: normal findings, anatomic variants and pathology

M. Rengo¹, F. Iafra², F. Vecchiotti¹, R. Ferrari¹, P. Paolantonio¹, A. Laghi¹; ¹Latina/IT, ²Rome/IT

Learning objectives: We will illustrate the normal anatomy of ICV and the anatomic variants, the most frequent pathologic conditions as well as some pitfalls encountered during the analysis of CTC images. We will present the multidetector CTC findings with endoscopic correlation and the possible pathologies and the practical implications.

Background: Ileocecal Valve (ICV) is a normal structure, with several anatomical variants, possibly involved by different pathologic conditions, either neoplastic or

inflammatory. Radiologists should be aware of possible anatomical variants as well of different pathologic processes, benign and malignant, which might affect the ICV, in order to avoid image misinterpretation.

Imaging findings OR Procedure details: We will illustrate appearance and typical findings of normal and pathologic ICV at 64 MDCT. We will illustrate different examples on 2D axial and MPR and 3D endoluminal views with endoscopic correlation.

Conclusion: Knowledge of the potential variants of ICV, the most frequent pathologic conditions as well as some pitfalls encountered during the analysis of CTC images are thus indispensable for radiologists who perform and interpret such examinations and for general practitioners who are approaching this technique.

P-044

Primary 3D review of CTC using radial ray-casting mode: diagnostic performance and time efficiency in comparison with conventional endoluminal fly-through

S.S. Lee, S.H. Park, J.K. Kim, A.Y. Kim, H.K. Ha; Seoul/KR

Purpose: To evaluate the diagnostic performance and time efficiency of primary three-dimensional (3D) review of CT colonography (CTC) using radial ray-casting in comparison with conventional endoluminal fly-through.

Material and methods: The study data set consisted of 52 patients who underwent the same day virtual and optical colonoscopy from a larger multi-institutional database of CTC data published previously (accessed at <http://nova.nlm.nih.gov/WRAMC/>). Two experienced radiologists performed primary 3D interpretation of the data sets independently with radial ray-casting mode and conventional endoluminal fly-through. Radial ray-casting mode reconstructs whole circumference of colonic surface without anatomic distortion using an array of centrifugal rays that are emitting from centerline to the wall and are perpendicular to the centerline. The diagnostic performance and interpretation time were compared between two review modes.

Results: Sensitivity of radial ray-casting mode and conventional endoluminal fly-through in detecting polyps ≥ 6 mm was not significantly different in both readers: 82.1 vs 74.4% for reader 1 ($p=0.250$) and 82.1 vs 84.6% for reader 2 ($p>0.999$). Per-patient specificity was 96.2 vs 100% for both readers ($p>0.999$). Mean reading time was significantly shorter with radial ray-casting method that with endoluminal fly-through: 9.25 min vs 11.05 min, respectively, for reader 1 ($p<0.0001$) and 9.23 min vs 13.65 min, for reader 2 ($p<0.0001$).

Conclusion: Compared with conventional endoluminal fly-through, radial ray-casting mode is more time efficient and has a comparable accuracy in detecting colorectal polyps.

P-045

Optimization of oral labelling in CTC: two hours versus twenty-four hours of oral labelling prior to CTC

E. Thornton, M. Slattery, J. Bracken, M. Morrin; Dublin/IE

Purpose: Despite bowel cleansing for CT colonography (CTC), residual fluid/stool may be problematic. Oral labelling of fluid/stool helps distinguish true polyps from fluid/stool. We compared CTCs of those who consumed oral diatrizoate meglumine (Gastrograffin) for 2 hours before CTC with those who consumed Gastrograffin for 24 hours before CTC.

Material and methods: This was a prospective study of 40 patients, who received full bowel preparation with sodium picosulphate and oral labelling with 1000 cc 2% Gastrograffin. Group 1 ($n=20$) consumed 1000 cc Gastrograffin over 2 hours before CTC. Group 2 ($n=20$) consumed 1000 cc Gastrograffin over 24 hours before CTC. Using axial images, the colon was evaluated by segment and analysed regarding colonic distension, residual fluid/stool, and quality of labelling of fluid/stool using 5-point scales. Overall examination quality and overall diagnostic confidence for each group was also analysed. Statistical analysis included Mann Whitney U test. $p<0.05$ was taken as statistically significant.

Results: 100% cases had good/excellent colonic distension. Residual fluid/stool was similar in both groups ($p<0.05$). Labelling of fluid and stool was significantly better in Group 2 ($p<0.01$ and $p<0.05$, respectively). Overall quality and overall confidence in diagnosis was significantly better in Group 2 ($p<0.05$ and $p<0.01$, respectively).

Conclusion: This study demonstrated that oral labelling over 24 hours before CTC results is significantly better in overall quality and overall confidence in diagnosis, when compared with oral labelling over 2 hours before CTC.

P-046

Non-laxative CTC: incremental benefit of simultaneous PET acquisition on diagnostic performance and reporting confidence

S.A. Taylor, R. Greenhalgh, J. Bomanji, G. Cattani, A. Groves, J. Dickson, S. Halligan, P. Ell; London/UK

Purpose: To investigate the incremental benefit of supplementing non-laxative CT colonography (CTC) with simultaneous PET acquisition.

Material and methods: Non-laxative PET-CTC [24 hour low residue diet, 3 oral doses of 40%w/v barium-sulphate] was performed in 22 symptomatic patients (12 female, mean age 65) post injection of 130 MBq FDG in the supine and prone position using CO₂-insufflation. Patients underwent conventional colonoscopy within 2 weeks. An experienced radiologist reported the CTC data, also recording confidence a large polyp or cancer could be excluded from each of 6 colonic segments (from 1 to 4 (high)). Combined PET-CTC data was then reviewed in consensus with a nuclear-medicine physician and the incremental benefit of PET on sensitivity/specificity (in comparison to a full colonoscopic reference) and diagnostic confidence (Fisher exact test) calculated on statistical advice.

Results: 6/22 patients harboured 7 polyps. CTC sensitivity for polyps 1–5 mm, and >10 mm was 1/5 (20%, 95% CI 0 to 55) and 2/2 (100%), respectively with no incremental benefit with PET. Polyps >1 cm were PET avid. However, three PET non-avid CTC false positives (9, 12, 6 mm) were correctly dismissed after combined review improving specificity from 0.82 (95% CI 0.62 to 1.0) to 1.0. Diagnostic confidence was ≤ 2 in 9/132 colonic segments on CTC, improving to a score of 4 in all 9 after combined PET-CTC review ($p=0.002$).

Conclusion: Simultaneous PET acquisition with non-laxative CTC helps improve specificity and diagnostic confidence, but not sensitivity. Recruitment continues and full data will be presented.

Diagnostic / GI Tract / MR of Bowel

P-047

MR is a reliable technique for assessment of disease activity and severity in colonic Crohn's disease

S. Rodriguez Gomez, J. Rimola, O. Garcia Bosch, E. Ricart, J. Panes, C. Ayuso Colella; Barcelona/ES

Purpose: The objective of the current study was to determine the value of Magnetic Resonance Colonography (MRC) for the assessment of colonic Crohn's Disease (CD).

Material and methods: 36 patients with CD underwent colonoscopy and MRC using a 3.0 T unit. T2-weighted and pre- and post-contrast-enhanced T1-weighted sequences were acquired. Endoscopic lesions were graded as inactive, mild/moderate and severe. The MRC parameters evaluated in each colonic segment were: wall thickness, pre- and post-contrast wall signal intensity, relative contrast enhancement, edema, ulcers, pseudopolyps, and adenopathies.

Results: A total of 121 colonic segments were available for evaluation (inactive $n=71$, mild/moderate $n=29$, severe $n=21$). Significant differences were found between inactive and mild/moderate disease, and between the latter and severe disease for wall thickness, post-contrast wall enhancement, relative enhancement, edema and ulcers. Linear logistic regression analysis demonstrated that the variables with independent predictive value for determining disease activity and severity were wall thickness, signal intensity after contrast, % enhancement and presence of ulcers. Applying the corresponding coefficients, the sensitivity and specificity for detecting disease activity were 0.83 and 0.84, and for detection of severe lesions 0.96 and 0.93, respectively.

Conclusion: The high sensitivity and specificity of MRC for detection of disease activity and for assessment of lesion severity bring about the possibility of using MRC as an alternative to endoscopy for the evaluation of colonic CD.

P-048

Imaging of GI and hepatic diseases during pregnancy

P.A. Hodnett, S.E. Mc Sweeney, K. O'Regan, M. Ryan, M. Maher; Cork/IE

Learning objectives: To discuss differential diagnosis of abdominal pain (AP) in pregnancy. To discuss role and appropriate choice of imaging in diagnosis of AP

in pregnancy. To illustrate typical imaging findings of range of conditions which result in AP in pregnancy on various modalities and potential pitfalls that can lead to mis-diagnosis. To discuss limitations and specific safety issues in imaging of abdomen in pregnancy.

Background: Imaging of abdomen for suspected GI and hepatic disease during pregnancy is assuming greater importance. Like clinical evaluation, imaging of the abdomen and pelvis is challenging but is vitally important to prevent delayed diagnosis or unnecessary interventions. Choice of imaging modality is impacted by factors which impact fetal safety such as ionizing radiation and MRI.

Imaging findings OR Procedure details: The most common indication, excluding fetal assessment, for abdominal imaging during pregnancy, is abdominal pain. There is a broad differential diagnosis for abdominal pain (AP) including conditions which are not related to pregnancy and pregnancy-related conditions. This educational exhibit will discuss issues in abdominal imaging in pregnancy, including safety issues and difficulties in interpretation in three trimesters.

Conclusion: Imaging of the acute abdomen for AP in pregnancy is increasingly requested by clinicians. Appropriate utilisation and interpretation of imaging is vital to allow accurate diagnosis, expeditious management and avoid potential risks to mother and fetus.

P-049

MR-enterography in paediatric patients: an overview of technical features and clinical results

P. Paolantonio¹, R. Ferrari², P. Lucchesi², F. Vecchiatti², M. Maceroni², A. Laghi²; ¹Rome/IT, ²Latina/IT

Learning objectives: To illustrate the major clinical indications for MRE in paediatric patients. To outline the advantages and limitations of the technique and to illustrate clinical results based on a series of 215 paediatric patients.

Background: In this exhibit, we will describe the MR-enterography (MRE) performed with a biphasic oral contrast agent with the most suitable indications, results, advantages and limits of this technique in a paediatric population. 215 paediatric patients with clinical suspicion of small bowel disorders underwent MRE. The major clinical indication is represented from the work-up of children with suspected IBD. Other clinical indications are mainly represented by the work-up of patients with celiac disease or other intestinal malabsorption. MR findings of several small bowel disorders with emphasis on Crohn's disease and celiac disease will be presented.

Imaging findings OR Procedure details: Small bowel distension was obtained by means of oral administration of 15 ml/kg/BW of barium sulphate and sorbitol mixture (Volumen; E-Zem) immediately before the examination. MR examinations were performed using T2W HASTE, True-FISP and T1W FLASH sequences acquired after iv injection of Gd-DTPA on both axial and coronal planes.

Conclusion: MRE represents a feasible and valid diagnostic tool for the small intestine evaluation also on a paediatric population.

P-050

The role of MR enterography for detection of enteral fistulas in Crohn's disease: correlation with radiological and surgical findings

K. Katulska, M. Stajgis, W. Paprzycki, A. Dobrowolska-Zachwieja, D. Mañkowska-Wierzbicka, K. Linke, M. Drews; Poznań/PL

Purpose: Crohn's disease (CD) is a chronic inflammatory disease. CD is accompanied by fistulas in 40–50% of the patients during the course of illness. The aims of this study are to evaluate the diagnostic value of MR enterography (MREG) in the detection of enteral fistulas.

Material and methods: 23 patients with known CD were enrolled in the study. All of them were suspected of fistulating CD, 12 patients underwent previous operation. The MREG was performed at 1.5 T after the oral administration of 6% mannitol solution. The MREG protocol included TrueFISP, HASTE sequences before intravenous contrast administration and Gd-enhanced T1-weighted fat-suppressed Flash 2D + 3D and Vibe sequences. The results of clinical examination and fluoroscopy after administration of barium were used as references. In 7 cases, results were compared with following surgical findings.

Results: 29 fistulas were found in twenty two patients in MREG. Overall sensitivity, specificity and accuracy for fistula detection were 76.5, 71.2 and 75.2%, respectively. Sensitivity and specificity for correct localisation were 74.1

and 75.6%, respectively, with visualization of the fistulous tract in all cases. Interobserver agreement for detection, localization and etiology for each fistula was calculated ($p < 0.05$).

Conclusion: MREG is an accurate tool for the detection of enteral fistulas in CD. Gadolinium-enhanced T1-weighted (Flash 2D + 3D) fat-suppressed imaging provides the greatest conspicuity for delineation of the fistulous tract.

P-051

MRI findings of carcinoma in perianal Crohn's disease

M.A. Haider¹, S.V. Lad¹, C.J. Brown², R.S. McLeod¹;

¹Toronto, ON/CA, ²Vancouver, BC/CA

Learning objectives: To recognize the MRI patterns of carcinoma developing in perianal fistula of Crohn's disease. To appreciate the value of contrast enhancement in the distinction of carcinoma from inflammatory changes in Crohn's disease.

Background: Patients with Crohn's disease have an increased risk of colorectal carcinoma. The incidence of carcinoma in perianal Crohn's disease is 0.7%. Although MRI is often performed in cases of complex anal fistulae, cancer can be difficult to prospectively diagnose because of concomitant changes related to inflammation. Biopsy at examination under anesthesia is usually performed for diagnosis. Knowledge of MRI features that distinguish fistulae and abscess from carcinoma with MRI are essential to avoid delayed diagnosis.

Imaging findings OR Procedure details: MRI characteristics of carcinoma in fistulae are irregular inner wall contours and delayed mild enhancement of internal tissue while the granulation tissue of the fistulae walls often displays smooth intense enhancement. A double layer of outer smooth enhancement and internal irregular hypoenhancing tumor is seen most often in squamous carcinomas. Mucinous adenocarcinomas display a pattern of lobulated fluid filled cavities with delayed internal tissue enhancement. This is not seen in most benign abscess which have smooth outer walls and no internal enhancing components.

Conclusion: Knowledge of the patterns of contrast enhancement and morphology is valuable in the MRI diagnosis of carcinoma in perianal Crohn's disease.

P-052

Does the second MRI scan post neo-adjuvant long-course treatment for rectal cancer alter management?

A.J. Sambrook, A. Lowe, A. Thrower, C. Kay, Bradford/UK

Purpose: In our institution, in accordance with Regional Cancer Network Guidelines, patients who receive neo-adjuvant long-course chemoradiotherapy for rectal cancer undergo a post-treatment scan to determine tumour response before surgery. This study examines whether this scan alters patient management.

Material and methods: A retrospective audit was performed of 65 patients who had undergone long-course chemoradiotherapy (2004–2007). The surgery planned following the initial multidisciplinary meeting was recorded. A copy of the operative notes was then reviewed, and the actual surgery performed recorded.

Results: 65 patients underwent chemoradiotherapy. Five did not proceed to surgery (patient choice/unsuitability for anaesthesia). Of the remaining 60 patients, 56 underwent a standard abdomino-pelvic resection. The other four patients had pelvic clearance surgery, which was predicted as necessary on the initial scan. The post treatment MRI did not change the surgical approach in any of the 60 cases.

Conclusion: The post treatment scan did not affect the surgery in any of the patients. At a cost of £75 per scan (in our institution), the potential cost saving of not performing the second scan in these patients is £5,500 per annum. Furthermore, the results of this study indicate, at the very least, the need for a more extensive review of the requirement for this costly and potentially unnecessary examination.

P-053**Extra-intestinal fistula: MR colonography evaluation with water-gadolinium enema**

M. Aduna, J.A. Larena, I. Aguirre, J.A. Arevalo, S. Lazaro; Galdakao/ES

Purpose: To determine the diagnostic value of MR-colonography (MRC) with water-gadolinium enema evaluating the presence, localization and activity of acquired extra-intestinal fistulas.

Material and methods: 40 patients with clinical suspicion of extra-intestinal fistula were studied. MRC included TrueFisp on coronal, sagittal and axial planes as well as coronal and axial/sagittal FS GRE 3D T1 (VIBE) using a 1/200 gadolinium/water enema. 13 patients were also examined after Valsalva maneuvers. Image analysis was performed by two radiologists not blind to clinical data and focused on the presence, localization and activity of the extra-intestinal fistulae.

Results: 31 fistulas (21 active and 10 inactive) in 20 patients were surgically (12) or colonoscopy/cystoscopy (8) proved: 3 rectovaginal, 17 entero /colovesical, 1 rectovagino-vesical, 11 non-visceral (cutaneous (5), muscular (1), others (5)). MRC was able to define the presence and localization of all fistulas (100% sensitivity). 19 patients showed no fistula that was verified by surgery (5) or clinically/with other diagnostic tools (14). MR correctly ruled out fistulas in these patients and had a false positive rectovaginal fistula (95% specificity) due to anal extravasation of contrast that was distributed along the external genital organs. MR correctly assessed activity in all cases. In 4/11 patients, activity of fistula was proved only after Valsalva maneuvers.

Conclusion: MRC with water-gadolinium enema can contribute to the diagnostic assessment of acquired extra-intestinal fistulas.

P-054**MR enterography in patients with Crohn's disease: accurate tool in detection of inflammations activity**

K. Katulska, M. Stajgis, W. Paprzycki, A. Dobrowolska-Zachwieja, D. Mañowska-Wierzbicka, K. Linke, M. Drews; Poznań/PL

Purpose: The aim of this study is to assess the diagnostic accuracy of MR-enterography (MREG) in detection of inflammation in small bowel and to compare with endoscopy, surgical interventions and histology findings.

Material and methods: 75 patients underwent an MREG: 42 of patients with known Crohn's disease (CD) – group 1, and 33 with clinical suspicion of CD – group 2. The MREG was performed at 1.5 T after the oral administration of 6% mannitol solution. The protocol included TrueFISP, HASTE sequences before intravenous contrast administration and Gd-enhanced T1-weighted fat-suppressed Flash 2D and 3D and Vibe sequences. Small bowel inflammation was documented on bowel wall thickness, contrast enhancement, presence of perienteric vessels, fatty infiltration and focal lymph nodes. All patients were scored using CD activity index (CDAI).

Results: Our data diagnosed 45 patients with active disease (31 in group 1 and 14 in group 2), and 30 patients with inactive disease (11 in group 1 and 19 in group 2). The MREG technique showed an accuracy of 87.3%, sensitivity of 90.2% and specificity of 83.6% for active disease. The pathological signs of the disease showed strong correlation with the CDAI score in MREG ($r=0.69$).

Conclusion: It is seen that the MREG technique with oral contrast administration is an accurate tool in the detection of inflammation's activity.

P-055**MR colonography with fecal tagging technique in patients with inflammatory bowel disease**

P. Boraschi, F. Donati, R. Gigoni, V. Battaglia, S. Salemi, A. Costa, F. Falaschi, C. Bartolozzi; Pisa/IT

Purpose: To assess the usefulness of MR colonography (MRC) with fecal tagging technique in patients with inflammatory bowel disease (IBD).

Material and methods: Twenty-two patients with suspected or known IBD underwent MRC at 1.5 T-device (Siemens). Fecal tagging was performed by oral administration of dense barium-sulfate (200 ml) at major meals starting two days before MRI. Patients were instructed not to eat fiber-rich and high manganese containing food. After water enema (1500–2000 ml), MR protocol first included HASTE and true-FISP sequences. Coronal T1w 3D VIBE (2.0 mm thick) was obtained before and 60 seconds after intravenous administration of Gd-chelate.

MR images were evaluated in conference by two observers by seeking for bowel abnormalities and were correlated with conventional colonoscopy (CC) in all cases and with surgery in 8/22 patients.

Results: MRC could be successfully performed in all cases, whereas CC was incomplete in 6/22 patients. MRC correctly defined bowel wall thickening, stenosis and extension of the inflamed colon in 5/6 patients with ulcerative colitis. In 11/15 patients with Crohn disease, involvement of both large and small bowels was demonstrated; perianal abscesses (n=2) and fistulas (n=3) were also identified. In one remaining case, no abnormality was found at MRC and final histological diagnosis was not surely diagnostic for IBD.

Conclusion: MRC with fecal tagging technique is a promising, minimally invasive technique for evaluation of the bowel in patients with suspected IBD.

P-056**Improving sensitivity of screening MR colonography for detecting colonic pathologies**

B.S. Narin Anil¹, G. Kilicoglu¹, D. Arslan¹, S. Goehde², T.C. Lauenstein², D.F. Joerg², M.M. Simsek¹; ¹Istanbul/TR, ²Essen/DE

Purpose: The aim of this study is to compare the magnetic resonance colonography (MRC) with conventional colonoscopy for the detection of the colorectal pathologies.

Material and methods: 368 patients were included in this study undergoing MRC followed by conventional colonoscopy. After rectal filling with rectal enema, 3D T1w gradient echo sequence in coronal plane was acquired with the patient in prone position. Gadopentate dimeglumine (Multihance, Bracco) was injected intravenously in a dose of 0.2 mmol/kg at a flow rate of 3.0 ml/s. The analysis of the images was based on multiplanar reconstruction (MPR), targeted MIP projections and virtual endoscopic endoluminal views. The signal intensity (SI) of the normal bowel wall, polyps and other colon masses are measured on unenhanced and enhanced 3D GRE images. Results of the MRC were compared to the conventional colonoscopy.

Results: MRC revealed a total of 61 pathologies in 368 patients, with 18 polyps, 30 diverticulosis, 2 ileitis, 6 colitis, 2 pathologic wall thickness of caecum, 1 mass in the caecum, 1 stenosis of the sigmoid colon and 1 mass in the rectum. In addition to the morphologic appearance of polyps and other colonic masses, the criterion for the differentiation was increased uptake of lesions (191.14±44.17%) compared to the normal bowel wall (58.7±19.1%).

Conclusion: MRC is an efficient and well tolerated modality in detecting colon pathologies.

P-057**Crohn's disease and dark-lumen-MR: whole intestinal distension with oral administration of polietilenglicole in "2 steps"**

I. Sansoni, R. del Vescovo, G. Della Longa, E. Piccione, B. Beomonte Zobel; Rome/IT

Purpose: Crohn's Disease (CD) contemporary affects small and large bowels. We propose an alternative method to distend and evaluate the whole unprepared bowel: dark-lumen-MR technique with oral administration of polietilenglicole (PEG) in 2 stages.

Material and methods: 45 patients with suspected CD have been examined, with no previous intestinal cleansing. They were asked to drink twice 1.5 liters of a polietilenglicole solution: 2–4 hours and 45 minutes before MR examination. A dark-lumen-MR protocol has been acquired on a 1.5 Tesla magnet: T2-weighted and True-FISP sequences on axial and coronal planes and T1-weighted sequences, in basal condition and after paramagnetic contrast e.v. administration on axial plane. Grading of bowel distension, cleansing and parietal inflammation (active, inactive, negative) was defined for each segment using conventional colonoscopy, post-biopsy histopathology results and serological tests findings as gold standard.

Results: Only 9% of bowel segments were not correctly distended (mainly the jejunum), and 7% of colonic segments were hindered by feces (especially distal colon). In 26 pathologic segments, a complete correlation of presence and location of flogosis has been evidenced, but in 6 segments (all in the same patient) the grading of flogosis was not correct.

Conclusion: Whole bowel assessment with "2 steps" distension is feasible, satisfying, does not need for particular colonic preparation and does not present the discomfort of direct retrograde colonic water distension, especially when perianal complications are present.

P-058**Colorectal diverticula: evaluation with dark-lumen MR colonography by means of oral distension**

G. Della Longa, I. Sansoni, E. Piccione, R. del Vescovo, F. Occhicone, B. Beomonte Zobel; Rome/IT

Purpose: The aim of our study is to assess the capability of dark-lumen MR-Colonography (MRC) in detecting the number, localization and complication of colorectal diverticula (CD) obviating colonic cleansing and manual colon retrograde distension.

Material and methods: A total of 29 symptomatic patients, referred for conventional colonography and/or CTC underwent MRC without any previous bowel cleansing and manual distension. MRC protocol was acquired on a 1.5 T scanner with high-performing gradients on axial and coronal planes using T2-weighted (TSE and HASTE), unspoiled (true-FISP) and spoiled (FLASH) GRE T1-weighted sequences. Spoiled GRE was acquired before and 75 seconds after intravenous administration of paramagnetic contrast agent. MR examinations were analysed on per-patient basis and on a per-segment basis (ascending, transverse and descending colon and rectum) that were stratified per number of diverticula (0, 1, 2, 3, 4, 5–10, >10).

Results: The “per-patient” analysis demonstrated a good diagnostic accuracy subordinated to patient compliance (93%), whereas the “per-segment” defines a higher representation of diverticula in sigmoid tract (65% of patients) than in cecum and rectum (0% of patients).

Conclusion: Dark-lumen MRC is a promising modality with high accuracy for detecting CD. This technique, moreover, overcomes the risk of diverticulum perforation, inherent in retrograde bowel distension and that of ionising radiation.

P-059*Withdrawn by authors***Diagnostic / GI Tract / Oesophagus****P-060****EUS in Barrett's oesophagitis with dysplasia**A.R. Wray¹, M.H.S. Love¹, P.F. Rice²;
¹Belfast/UK, ²Craigavon/UK

Purpose: With the advent of ‘conservative’ therapies including photodynamic therapy and endoscopic mucosal resection for Barrett's oesophagitis and high grade dysplasia, accurate staging has become increasingly important. We report our experience in these patients with EUS.

Material and methods: Retrospective review of 25 consecutive patients referred for EUS for assessment of Barrett's with high grade dysplasia and/or stricture or polyp. The findings were compared with subsequent oesophagectomy histology or endoscopy and biopsy follow up.

Results: 9 patients were found to have invasive tumour on EUS and this was confirmed in all 9 either by oesophagectomy, OGD and oncology follow up, or by endoscopic mucosal resection. 8 patients underwent oesophagectomy, 6 for invasive tumour and 2 for dysplasia only, with pathological agreement with EUS findings in 7/8. The one discrepancy was a EUS case of thickening only with no invasion, but pathology showed a T1 lesion. 13 patients with no evidence of invasion were followed up with OGD and biopsy, with or without photodynamic therapy, for an average of 15.8 months, with no cases of ‘missed’ invasion occurring. Therefore, in our experience, the sensitivity, specificity and positive predictive value of EUS in complex Barrett's was 90, 100 and 100%, respectively.

Conclusion: EUS is valuable in the assessment of Barrett's oesophagitis and high grade dysplasia where conservative therapy is increasingly being used.

P-061**The utility of MDCT perfusion examination in detection of metastatic lymph nodes of esophageal cancer**

G. Tóth, L. Tóth, E.C. Turupoli, V. Bérczi; Budapest/HU

Purpose: Assessment of the role of computed tomography perfusion (CTP) study for differentiation between malignant and benign mediastinal and

retroperitoneal lymph nodes in oesophageal cancer.

Material and methods: A prospective study was conducted on 14 consecutive patients (9 M, 5 F aged 37–62) with histologically proven esophageal cancer. Perfusion study was done after contrast-enhanced conventional chest and abdominal MDCT study. Perfusion values were calculated by using a modified deconvolution-based analysis, with the application of CT perfusion software. Region of interest placed over the biggest lymph node was found in a previous CT study. Postprocessing-generated maps showed perfusion (P), peak enhancement intensity, time to peak (TTP), blood flow (BF), blood volume ml/100ml (BV). Data were statistically analyzed with Wilcoxon sign test, and results were compared with histopathological findings.

Results: Histologically proven malignant lymph nodes perfusion values were significantly different from those in benign lymph nodes. The mean values of BF were 11.7 (± 3.1), BV was 2.7 (± 0.26) and TTP was 22 sec (± 3.9 sec). Compared to non-malignant nodes, the malignant ones showed significantly lower BF and BV values (p<0.009). The accuracy of detecting malignant nodes was 87%, sensitivity 92%, specificity 84%, positive predictive value 91.5%, and negative predictive value 75.9%.

Conclusion: CTP can be a good tool in distinguishing benign and malignant lymph nodes in esophageal cancer and can increase the diagnostic accuracy.

P-062**Oesophageal resection: postoperative anatomy and complications on CT**

O. Bashir, K. Latief; Nottingham/UK

Learning objectives: To illustrate postoperative anatomy and complications of oesophageal resection surgery as demonstrated by CT. Correlation with conventional imaging findings is also described to improve the understanding of common complications of oesophageal resection.

Background: Oesophageal resection is performed for both benign and malignant oesophageal conditions. This procedure is associated with significant morbidity and CT is frequently undertaken to diagnose complications and disease recurrence.

Imaging findings OR Procedure details: Routine assessment with water soluble contrast swallow is carried out seven days after oesophageal resection surgery at our institution. This allows for the early detection of anastomotic leaks. Additionally, certain complications of major thoracic surgery such as atelactasis and pneumonia can be seen on plain chest radiographs. However, several complications of oesophageal resection including ARDS, empyema, diaphragmatic hernia and disease recurrence are best demonstrated on cross-sectional imaging. CT is a frequently performed investigation for the diagnosis of complications of oesophageal resection.

Conclusion: Oesophagectomy is associated with a significant morbidity. CT is frequently carried out to evaluate post oesophagectomy patients. CT findings of various post oesophagectomy complications are described. An understanding of postoperative anatomy and pathology is crucial for the accurate diagnosis of complications and helpful in guiding patient management.

P-063**Radiology of eponymous and non-eponymous esophageal and gastric surgeries**B. Thomas¹, A. James¹, K. Subramanian²; ¹Manchester/UK, ²Blackburn/UK

Learning objectives: The major teaching points of this exhibit are 1. Understanding of various eponymous and non-eponymous surgeries of esophagus and stomach 2. Recognizing the normal post-operative appearances. 3 Identifying complications related to these surgeries.

Background: Major advances have taken place in curative and palliative surgical techniques of the upper GIT. These include transthoracic esophagectomy, Ivor Lewis procedure, McKeown procedure, transhiatal esophagectomy, various forms of bypass surgeries, Nissen's fundoplication, Billroth I and II, Roux en Y procedures etc. A clear idea of the normal post operative appearances and complications is essential to avoid pitfalls in radiological interpretation.

Imaging findings OR Procedure details: This exhibit will aim to: 1. Review the indications of various esophageal and gastric surgeries. 2. Present an overview of the common upper GI surgical procedures. 3. Familiarize the postoperative imaging features on CT and upper GI studies. 4 Review the complications of these procedures.

Conclusion: Interpretation of post-operative abdomen is made considerably

easier by knowledge of the underlying surgical techniques and familiarization with the imaging appearances. Knowledge of various surgical procedures of esophagus and stomach, choosing appropriate post operative investigations and interpretation of normal and abnormal findings are invaluable and paramount in patient care after these complex surgical procedures.

P-064

Upper gastrointestinal tract due to foreign bodies perforations: diagnostic pathway

P. Giusti, S. Giusti, V. Morigoni, C. Bartolozzi; Pisa/IT

Learning objectives: To show the pathognomonic oesophagogastric digital fluoroscopic findings detected in case of oesophageal perforations in order to early diagnose them and to plan the proper and resolute therapy.

Background: We reviewed the radiological findings from 14 patients who have accidentally ingested foreign bodies causing oesophageal perforation. Different agents may be responsible for these rare but severe conditions. In our experience, we studied very singular ingestions as chickenbone, fishbone, small toys and perforations due to iatrogenic injuries.

Imaging findings OR Procedure details: All cases have been approached with a conventional radiography of the chest, followed by an oesophagogastric digital fluoroscopic study performed in emergency with high frame velocity (3/sec), during oral administration of iodinated contrast medium. When necessary, we completed our conventional examination with MDCT scans useful for identifying more exactly contrast medium spreadings. Radiological findings identified with conventional technique were: irregularity of oesophageal wall, fat stranding, contrast spreadings, pneumomediastinum, and broncho-oesophageal fistulas.

Conclusion: Digital fluoroscopic study represents the gold standard technique to make a prompt diagnosis of upper gastrointestinal tract perforations.

P-065

The radiological diagnosis and management of oesophageal perforation

A.J. Phillips¹, R.J. Krysztopik¹, N.K. Thayur²;

¹Bath/UK, ²Bristol/UK

Learning objectives: To discuss the advantages and limitations of various diagnostic imaging modalities in the diagnosis and management of OP. To highlight the radiological features of OP. To discuss the surgical and radiological options for the treatment of OP.

Background: Oesophageal perforation (OP) is a life-threatening condition that poses both diagnostic and management challenges. The clinical features of OP are often non-specific and radiological imaging is essential to achieve early diagnosis and reduce mortality. Knowledge of the usefulness of various imaging modalities, the radiological features of OP, and of management options is crucial to achieve accurate diagnosis, interpret follow-up studies, and guide management.

Imaging findings OR Procedure details: Recognition of the features of OP on an initial chest X-ray guides the use of specific imaging techniques, including luminal contrast studies, computed tomography (CT), and CT esophagography in the initial diagnosis and follow-up of this condition. We discuss the advantages and limitations of these imaging modalities and the radiological features of OP and its complications. We discuss the surgical and interventional radiology management options and illustrate their appearances on follow-up imaging studies.

Conclusion: OP is a life-threatening condition. Knowledge of the radiological features of OP and its complications, the advantages and limitations of various imaging modalities, and the treatment options is crucial to achieve accurate diagnosis, interpret follow-up studies and guide management.

Diagnostic / GI Tract / Other

P-066

Pathways of nodal metastasis from upper GI tumours: the role of MDCT

D. Kasir, L.R. Williams, V. Rudralingam, S.W. Gallaway, S. Sukumar; Manchester/UK

Learning objectives: 1 To illustrate the anatomy of thoracic and abdominal lymph node stations relevant to upper GI malignancy. 2 To demonstrate the pathway of disease spread in upper GI malignancy. 3. To highlight the importance of using the correct nomenclature for disease staging and treatment planning.

Background: The combination of PET-CT and MDCT has revolutionised the staging and management of upper GI tumours. These tumours commonly spread to lymph nodes. The precise location of the involved lymph node is essential for the correct stage. For example, in lower oesophageal cancer, a gastrohepatic ligament node is considered a local N1 node. However, a coeliac axis lymph node is upstaged as M1a disease.

Imaging findings OR Procedure details: The lymph node stations will be demonstrated using illustrations and cross sectional images. The potential pitfalls that can incorrectly stage the patient will be highlighted.

Conclusion: A common understanding of the precise anatomic position and terminology used by the radiologist and the surgeon is important for correct staging and surgical treatment planning.

P-067

Static and dynamic pelvic floor MRI: correlation with symptoms and function

S.A. Taylor, K. Thiruppathy, D. Chatoor, S. Halligan, A. Emmanuel; London/UK

Purpose: The role of puborectalis in the aetiology of faecal incontinence (FI) remains uncertain. The purpose was to correlate measurements of pelvic muscle bulk on MRI with objective measurements of function and patient symptoms.

Material and methods: 26 female patients (mean age 43, [27–56]) with FI underwent static (T2 TSE) and dynamic MRI (sagittal TrueFISP) of the pelvic floor and then perineal dynamometry to assess peak puborectalis strength. All completed a Wexner incontinence score. From the static MRI, the right and left external sphincter (superficial and deep) and puborectalis muscles were measured by an experienced radiologist using electronic callipers. The anorectal angle (mid anal canal to posterior rectal wall) was measured on the dynamic scan during maximum staining. Data were correlated using Kendalls rank correlation on statistical advice.

Results: Mean superficial external sphincter thickness (0.24cm±0.1), deep external sphincter thickness (0.34cm±0.1) and puborectalis thickness (0.49cm±0.2) all significantly correlated with pelvic floor strength (maximum contraction during dynamometry ($r=0.56$, $p<0.0056$, $r=0.49$, $p<0.02$, and $r=0.78$, $p<0.0001$, respectively). Mean Wexner score (11 + 6.2) negatively correlated with external sphincter thickness ($r=-0.42$, $p<0.025$) only. The anorectal angle on straining correlated with FI scores ($r=0.43$ $p<0.03$) and was negatively correlated with pelvic floor strength ($r=-0.51$ $p<0.01$).

Conclusion: Static and dynamic MRI measurements correlate with patient symptoms and objective measurements of pelvic floor strength. There is no clear relationship between puborectalis bulk and FI.

P-068

Evaluation of traumatic mesenteric and bowel injury with MDCT

L. Jimenez Juan, C. Mc Gregor, S. Whitley, D. Cheng, J. Sarrazin, P. Hamilton; Toronto, ON/CA

Learning objectives: Review the mechanisms of traumatic mesenteric and BI. Recognize the key imaging features of mesenteric and BI with special attention to the bowel wall. Understand the clinical implications of prompt diagnosis of the different types of traumatic mesenteric and BIs.

Background: Although bowel injury (BI) occurs in a small percentage of abdominal trauma, delay in diagnosis can increase mortality and morbidity. In haemodynamically stable patients, MDCT is useful to determine the location and the extent of BI as well as to help triage the patient to conservative or operative management.

Imaging findings OR Procedure details: We illustrate a spectrum of direct and indirect signs of mesenteric and bowel wall injury and associated findings in the trauma setting. The direct signs include bowel wall defect, extraluminal air and extravasation of oral contrast material. The indirect signs are non-specific but their presence is suspicious for BI and include diffuse or isolated wall thickening, intramural air, abnormal bowel wall enhancement, free fluid and adjacent mesenteric hematoma. MDCT imaging patterns were correlated with surgical findings on a patient-by-patient basis.

Conclusion: Knowledge and recognition of trauma-related mesenteric and BIs on CT is essential for the correct management of haemodynamically stable patients to avoid mortality and morbidity of delayed diagnosis.

P-069

PET/CT imaging features of peritoneal carcinomatosis: a pictorial review

N.M.G. Caserta, S. Dragosavac, M.L. Cunha, D.M. Morita, N.M. Hanaoka; Campinas/BR

Learning objectives: 1. To recognize the role of PET/CT as a new imaging modality in the evaluation of peritoneal metastasis. 2. To illustrate features of PC. 3. To demonstrate how PET/CT can accurately evaluate malignant tumoral seeding at different sites of the peritoneum.

Background: Detection of peritoneal metastasis is often difficult. PET/CT is increasingly used in management of patients with cancer and can improve diagnostic accuracy of peritoneal carcinomatosis (PC). This exhibit presents a pictorial review of how this disease can be detected by this hybrid imaging modality.

Imaging findings OR Procedure details: We performed PET/CT on numerous patients with a variety of primary malignancies and have identified a wide spectrum of findings of peritoneal disease. These cases showed findings such as metastasis involving the bowel, infiltration and thickening of the peritoneum, mesentery or omentum, associated ascites, clustered nodules of peritoneal implants, scalloping on the liver surface, metastatic deposits on the periumbelical area and a variety of abnormal metabolic pattern in the peritoneum.

Conclusion: PET/CT is a powerful imaging modality that can contribute to the diagnosis of PC in the appropriate clinical setting.

P-070

Neuroendocrine tumors of the GI tract: spectrum of CT and pathologic findings

H.J. Kim, D.H. Lee, J.W. Lim, Y.T. Ko; Seoul/KR

Learning objectives: After completing the material in this exhibition, the learner should be able to: 1. describe the new WHO classification for NEN of the GI tract and 2. explain the wide spectrum of CT image findings of NEN of the GI tract.

Background: Most radiologists are not familiar with the new WHO classification of neuroendocrine neoplasms (NEN) involving the GI tract because previous radiologic reports are based on old terminology, such as carcinoid, malignant carcinoid, and small cell carcinoma. Therefore, correlation between CT image findings of NEN and pathologic findings according to the new WHO classification is important.

Imaging findings OR Procedure details: A small nodule with prominent enhancement is a common CT finding of well-differentiated endocrine tumor. Marked wall thickening, infiltration into adjacent organ, and metastases are common findings of poorly differentiated endocrine carcinoma. Well-differentiated endocrine carcinoma shows intermediate CT findings, i.e. between CT findings of well-differentiated endocrine tumor and poorly differentiated endocrine carcinoma. It is hard to differentiate well-differentiated endocrine carcinoma from adenocarcinoma involving the GI tract.

Conclusion: Well-differentiated endocrine tumor involving the GI tract may show specific CT findings. Well-differentiated endocrine carcinoma shows non-specific CT findings, similar to those of the adenocarcinoma of the GI tract. Poorly differentiated endocrine carcinoma may show aggressive CT image findings.

P-071

MDCT and MR of mesenteric pathology: explaining a misty subject

L.R. Williams, D. Kasir, S.Y. Liong, S. Sukumar, V. Rudralingam; Manchester/UK

Learning objectives: 1. To explain the normal anatomy of the mesenteries of the stomach, small bowel and colon with reference to diagrams and cross-sectional imaging. 2. To gain understanding of the various mesenteric pathologies and their appearances on abdominal MDCT and MR. 3. To illustrate the importance of various patterns of mesenteric disease and their role in forming a differential diagnosis.

Background: Many disease processes can involve the mesenteries of the stomach, small bowel and colon. Pathologies can be both primary and secondary. These include infective, inflammatory, ischemic, traumatic and neoplastic processes. Knowledge of the various pathological appearances can guide the abdominal radiologist to the final diagnosis.

Imaging findings OR Procedure details: The role of MR and MDCT in defining mesenteric disease will be discussed. Explanations of normal anatomy will be given with the aid of diagrams and cross-sectional imaging. Pathologies illustrated include inflammatory processes such as sclerosing mesenteritis, primary neoplasms (e.g. desmoid tumours and mesothelioma), secondary tumours, infective processes and ischemia. Pathologies can also be subdivided according to their imaging appearances, which include ill defined/infiltrative processes, cystic masses and solid lesions.

Conclusion: It is important for abdominal radiologists to have a thorough understanding of mesenteric anatomy and pathology. The imaging appearances on cross-sectional imaging aid in forming a diagnosis, especially when knowledge of the various patterns of disease are applied.

P-072

Dual energy CT: preliminary observations and potential clinical applications in the abdomen

A. Graser¹, T.R.C. Johnson¹, H. Chandarana², M. Macari²; ¹Munich/DE, ²New York, NY/US

Learning objectives: To understand the technical principles, applications, and dose considerations of DECT in the abdomen.

Background: Various abdominal CT applications like imaging of renal, adrenal, or pancreatic masses, abdominal aortic aneurysms and renal stones benefit from dual energy CT using two different tube currents in one single CT scan, thereby allowing for assessment of iodine distribution, calculation of virtual non contrast images, and characterization of materials in the scan field.

Imaging findings OR Procedure details: Dual energy CT (DECT) is a new technique that allows differentiation of materials and tissues based on CT density values derived from two synchronous CT acquisitions at different tube potentials. With the introduction of a new dual source CT scanner, this technique can now be used routinely in abdominal imaging. Potential clinical applications include evaluation of renal masses, liver lesions, urinary calculi, small bowel, pancreas and adrenal glands. In CT angiography of abdominal aortic aneurysms, dual energy scanning can be used to remove bones from the datasets, and virtual non contrast images allow differentiation of contrast agent from calcifying thrombus in patients with endovascular stents. This review describes potential applications, practical guidelines, and limitations of DECT in the abdomen.

Conclusion: DECT has various promising applications in abdominal imaging which are making a faster and more accurate diagnosis at less possible radiation exposure.

P-073

Radiologic spectrum of GI stromal tumors: emphasis on unusual findings and pathologic correlation

J.Y. Oh, K. Nam, J. Cho, H. Kwon; Busan/KR

Learning objectives: To demonstrate various and unusual imaging findings of GISTs and correlate them with pathologic findings.

Background: Gastrointestinal stromal tumors (GISTs) are the most common mesenchymal neoplasms of the GI tract and are defined by their expression of KIT (CD117). Radiologic findings of GISTs are various depending on tumor size and organ of origin. Although the imaging features of GISTs are often distinct from those of epithelial tumors, it is difficult to differentiate GISTs from other mesenchymal tumors on the basis of imaging alone, especially when they reveal

unusual manifestation. We describe the imaging findings of a wide spectrum of GISTs with an emphasis on unusual findings and pathologic correlation.

Imaging findings OR Procedure details: CT imaging of small GISTs typically show round and homogeneous low-density intramural mass with intact overlying mucosa, but necrosis, cavity formation and exophytic growing pattern are commonly noted in large GISTs. Calcification, cystic necrosis in small GIST, circumferential mural thickening pattern mimic lymphoma, extra-gastrointestinal GISTs, and atypical findings of hepatic metastasis are unusual radiologic findings of GISTs.

Conclusion: Radiologic findings of GISTs are various, so it is important that radiologists are familiar with these findings. An awareness of the various radiologic manifestations in GISTs can help ensure a correct diagnosis and proper management.

P-074

Upper GI injuries of caustic ingestion: a pictorial review

A. Maroto Genover, M. Febrer Febrer, M. Osorio Fernández, J. Soriano Viladomiu, J. Gironès Vilà, L. Valls Masot; Girona/ES

Learning objectives: To illustrate the spectrum of different radiological findings of upper GI lesions due to caustic ingestion. To discuss the role of imaging (upper GI series and CT) in the management of these lesions.

Background: The ingestion of caustic substances either accidentally or for suicidal purposes produces severe injury in the upper GI tract. Extension and seriousness of the lesions are related to chemical composition, concentration and volume of the caustic agent and time of contact between upper GI mucosa and caustic. Radiological examinations are used to define the extension of acute-subacute digestive lesions and also to detect the development of late complications. Classically upper GI series were the method of choice, but CT has an increasing role in the evaluation of these cases.

Imaging findings OR Procedure details: In acute setting, chest and abdominal radiographs are performed looking for signs of perforation. Acute-subacute lesions can be seen as atony, dilatation, sloughing and irregular contours, thickened and irregular folds and ulceration in upper GI series. CT can depict more accurately the extension of mural lesions and extraluminal findings. These radiographic findings reflect mucosal destruction and intramural edema and/or hemorrhage. Chronic lesions are mainly single or multiple stenosis associated with various degrees of obstruction. Rigidity and lack of mucosal relief are other signs which correlate with fibrotic changes and cicatrization of the lesions.

Conclusion: Radiological studies may provide valuable information during both the acute and the chronic stages of caustic GI injuries.

P-075

Withdrawn by authors

P-076

A pictorial review of the manifestations of cystic fibrosis in the abdomen

A.C. Gomez, O.J. Arthurs, F.A. Hampson, P.A. Set, A.H. Freeman; Cambridge/UK

Learning objectives: To discuss the abdominal manifestations of CF. To present a pictorial review of the range of imaging findings.

Background: Cystic fibrosis (CF) is the most common inherited fatal disease in Caucasians, with an incidence of approximately 1 in 2000 live births. Although pulmonary involvement occurs in 90% of patients, surviving the neonatal period and end-stage lung disease is the principal cause of death. Abdominal manifestations are common in both the paediatric and adult populations.

Imaging findings OR Procedure details: Abdominal manifestations affect multiple organ systems. Nearly the entire digestive tract is affected in patients with CF and GI complications include gastroesophageal reflux and peptic ulceration, meconium ileus with associated complications during the neonatal period, distal intestinal obstruction syndrome, intussusception, appendicitis, fibrosing colonopathy, pneumatosis intestinalis, rectal mucosal prolapse, pseudomembranous colitis and malignancy. Hepatobiliary complications include gallbladder disease, fatty infiltration of the liver, bile duct abnormalities, focal biliary fibrosis and multinodular cirrhosis and associated portal hypertension. Pancreas involvement may result in acute pancreatitis, fatty replacement, calcification, cysts, duct abnormalities and carcinoma. We provide a pictorial review of the imaging findings.

Conclusion: As life expectancy of individuals with CF continues to increase with advances in disease management (currently, the median age of survival is 36.8 years), knowledge of the wide spectrum of abdominal manifestations and imaging findings in both the paediatric and adult populations is important for patient management.

P-077

Mesenteric panniculitis

A. Lefkopoulos¹, A. Harsoula¹, C. Manika¹, M. Potsi¹, B. Demirler Simsir², A. Haritanti¹, A.S. Dimitriadis¹; ¹Thessaloniki/GR, ²Ankara/TR

Learning objectives: MP is a chronic, tumor-like, aseptic inflammatory process of the adipose tissue of the mesentery. Although MP is a rather rare condition, the use of abdominal CT as well as the awareness of modern radiologists about this pathology and its specific signs has made the diagnosis more frequent. The objective of our study was to describe the specific signs of MP with CT.

Background: We retrospectively evaluated 1500 abdominal CTs of adult patients (between ages 51 and 85) that were performed over a period of 5 years in our department. Patients with ascites, abdominal trauma, malignant tumors of the pancreas and pathology of the lymphatic system were excluded.

Imaging findings OR Procedure details: In our study, 45 of the abdominal CTs showed signs of mesenteric panniculitis (MP) (3%). The characteristic CT signs of MP are: hyperattenuation of the mesenteric adipose tissue was observed in 100%, "fat-halo" sign in 60%, nodules (diameter <10 mm) in 84.4%, and pseudocapsule in 18%. The exact etiology of the disease is not known. Yet studies have suggested that MP consists of a paraneoplastic response.

Conclusion: Abdominal CT is the radiologic method of choice for the diagnosis of MP. Although MP is usually asymptomatic and does not require therapy, its early diagnosis is necessary because according to recent literature it is regarded as a paraneoplastic condition.

P-078

CT of lymphoma: spectrum of abdominal disease

A. Canelas, B. Graça, M.F.S. Seco, P.A. Belo-Soares, L. Teixeira, F. Caseiro-Alves; Coimbra/PT

Learning objectives: Review the common and uncommon CT appearances of lymphoma in the abdomen. Describe the implications of imaging findings for disease management.

Background: Abdominal lymphoma has a wide variety of imaging appearances and definitive diagnosis relies on histopathologic analysis. CT has been shown to be useful to define the extent of disease, assist in treatment planning, evaluate the response to therapy and monitor patient progress and possible relapse.

Imaging findings OR Procedure details: In this exhibit, we describe and illustrate: 1. The CT technique, appearance and implications of imaging findings for disease management in patients with lymphomatous involvement of the: 1.1 Liver; 1.2 Spleen; 1.3 Kidney; 1.4 Adrenal glands; 1.5 Pancreas; 1.6 Stomach; 1.7 Small bowel and mesentery; and 1.8 Colon.

Conclusion: CT continues to remain the imaging study of choice for the staging and follow-up of cases of lymphoma. Because some findings are nonspecific and because lymphomatous disease may mimic a broad spectrum of diseases and treatment-related complications, familiarity with the features specific to lymphomas may help improve the accuracy of diagnosis and staging and thus allow better disease management.

P-079

CT of extraluminal abdominal gas: the outside gas imaging insight

L. Goncalves, S.C.C. Dias, S. Kurochka, H. Torrão, C. Leite, C. Pina Vaz, V. Mendes; Braga/PT

Learning objectives: We review imaging of various conditions associated with extraluminal abdominal gas and highlight its diagnostic and clinical significance.

Background: Although extraluminal gas most commonly manifests benign conditions, namely iatrogenic manipulations and fistulous connections, it also relates to a wide range of traumatic, infectious, ischemic and tissue necrosis mediated diseases. It is an important finding with diagnostic value, especially in patients with vague symptoms presenting at the emergency department, possibly heralding potentially life-threatening conditions. While abdominal radiographs and US are often the first radiological examination performed, computed

tomography (CT) is the most sensitive and specific technique for detection of gas. It also provides adequate evaluation of intra-abdominal organs, frequently leading to a specific diagnosis. Additionally, it establishes gas extension and precise anatomic location, aiding in therapeutic decision making.

Imaging findings OR Procedure details: We describe CT imaging spectrum of extraluminal gas on the abdomen, often with correlative abdominal radiographs or CT topograms. The radiological diagnoses were confirmed by reviewing clinical, pathological and surgical records. We illustrate spurious, iatrogenic, traumatic, infectious, ischemic and neoplastic conditions that are depicted by pneumoperitoneum, emphysema, pneumatosis, portomesenteric venous gas, pneumobilia and abscesses, valuing its pathologic and clinical correlation. Helpful hints for differential diagnosis and features with therapeutic relevance are also stressed out.

Conclusion: CT is the most accurate technique for imaging extraluminal abdominal gas and has diagnostic and therapeutic impact.

P-080

GI tract diverticula: beyond the left lower quadrant

S. Thipphavong, R.E. Seppala, M.A. Fraser-Hill, N. Fasih;
Ottawa, ON/CA

Learning objectives: To present a series of well documented cases of GI tract diverticular disease, including: pharyngeal Zenker's diverticulum, Killian-Jamieson diverticulum, mid-esophageal tuberculosis-related traction diverticulum, epiphrenic diverticulum, congenital gastric diverticulum, duodenal diverticulum and diverticulitis, small bowel diverticulosis and diverticulitis, Meckel's diverticulum with intussusception, appendiceal diverticulum, right-sided diverticulitis, complicated sigmoid diverticulitis, colonic diverticulitis containing carcinoma and giant colonic diverticulum. To demonstrate and discuss the role of multimodality imaging in the diagnosis of these various GI tract diverticula.

Background: A wide variety of GI tract diverticular disease extends beyond the left lower quadrant. Diverticula can occur anywhere along the GI tract and have the potential to be symptomatic, thereby warranting imaging. Imaging studies, including barium examinations and cross-sectional imaging (CT), are essential in diagnosing symptomatic diverticular disease and identifying complications.

Imaging findings OR Procedure details: Imaging features of GI tract diverticular disease listed in the Learning objectives: will be discussed. The role of conventional GI studies and CT for the diagnosis of symptomatic diverticular disease will be highlighted. Acute and chronic complications associated with various common and uncommon diverticula will be outlined.

Conclusion: Apart from colon, diverticula may arise from any segment of the GI tract. Symptomatic diverticular disease warrants imaging with contrast GI studies or CT. Imaging allows for definitive diagnosis of symptomatic diverticular disease and can further characterize complications, thereby directing management.

P-081

Pictorial review of diaphragmatic rupture/hernia after trauma

Y. Sheikh, S.E. Mc Sweeney, P.A. Hodnett, E. Fitzgerald,
M. Ryan, M. Maher; Cork/IE

Learning objectives: a) To discuss the use of diagnostic imaging in the diagnosis of acute and chronic diaphragmatic injuries. b) To discuss some more subtle signs of diaphragmatic injuries which require careful analysis of CT images and examination with MRI in specific situations.

Background: Traumatic rupture of the diaphragm may result from blunt or penetrating injuries. Unilateral hemi diaphragm injury is more common with injuries to the left hemi diaphragm occurring three times more frequently than the right. Various imaging modalities including chest radiography, CT and abdominal US may be used for diagnosis of diaphragmatic injury.

Imaging findings OR Procedure details: This poster will utilise a number of interesting examples which illustrate imaging findings of traumatic diaphragm rupture/herniation in the acute and chronic settings. We will focus on the role of CT and advantages of multiplanar reconstruction. We will also illustrate common and unusual complications of acute and chronic diaphragm rupture.

Conclusion: Various radiological modalities are necessary to make an accurate diagnosis of diaphragmatic injury and CT currently is the modality of choice. A high index of suspicion within the appropriate clinical setting should be maintained to allow correct diagnosis. Early diagnosis and repair prevent potentially devastating complications that result from visceral herniation through the post-traumatic diaphragm defect.

P-082

MDCT in the acute abdomen from small bowel obstruction: criteria for diagnosis of ischemia with correlative surgical findings

S. Romano, P. Lombardo, T. Cinque, G. Bartone, L. Romano;
Naples/IT

Learning objectives: To attest the essential role of MDCT in small bowel obstruction imaging, regarding the evaluation of the site of obstruction versus the various stages of disease, especially concerning the irreversible ischemic complications.

Background: Small bowel complicated obstruction with ischemia is an important event reporting high mortality rate if the diagnosis is too late, that is when infarction of the intestine is confirmed. The usefulness of MDCT in diagnosis of site and cause of an intestinal obstruction is already known in the scientific literature; however, less has been described regarding criteria for specific diagnosis of an ischemia caused by advanced degree of intestinal obstruction.

Imaging findings OR Procedure details: Our work is based on a retrospective evaluation of the emergency MDCT imaging findings of a large adult patient population with proven small bowel obstruction. All examinations were performed after i.v. contrast material administration, without endoluminal opacification. Correlation between the surgical results and the imaging findings (small bowel dilatation, transition point evidence, suggestive or evident cause of obstruction, presence and extension of alterations in bowel wall enhancement) was made in all cases.

Conclusion: Various degrees of wall thickening and mural enhancement were listed and correlated with the definitive diagnosis of complicated small bowel obstruction by intestinal ischemia. Advanced ischemia and infarction have been mostly observed in patients with volvulus.

P-083

Multi-detector-row CT of mesenteric ischemia: a meta-analysis of the literature

L. Saba, G. Mallarini; Cagliari/IT

Purpose: The aim of this work was to evaluate the diagnostic efficacy of multi-detector-row CT (MDCT) in the study of mesenteric ischemia and to identify the radiological signs that allow for making diagnosis. We performed a meta-analysis of the literature by evaluating sensitivity, specificity and diagnostic efficacy of MDCT. We evaluated also the impact produced by the newest CT scanner in the bowel ischemia diagnosis.

Material and methods: A comprehensive analysis of the literature was performed by using the medical literature database of PubMed and Cochrane as data sources. We searched for articles published in English language from January 1998 to October 2007.

Results: Our search results detected 24 studies that met the inclusion criteria of the 112 overall analyzed. We observed that MDCT sensitivity increased by using post-processing procedures such as MPR and MIP. The most frequent pathological signs described were intramural pneumatosis, bowel wall thickening, mesenteric arterial or venous thromboembolism, halo sign and mesenteric or portal venous gas.

Conclusion: Results of our study suggests that MDCT is an optimal technique to study patients with suspected mesenteric ischemia because it offers high sensitivity in detecting radiological signs of mesenteric ischemia. In particular, the use of MDCT angiography is very effective in the evaluation of abdominal vessels, giving the opportunity of a better definition of vascular map and its complications.

P-084

Abdominal CT findings in adult cystic fibrosis patients presenting with abdominal pain

S.Y. Liong, D. Awad, S. Mulrennan, S. Sukumar;
Manchester/UK

Purpose: Abdominal manifestations of cystic fibrosis (CF) are becoming more commonplace as the life expectancy of CF patients continues to increase. Imaging is often used in the evaluation of adult CF patients presenting with abdominal pain because a cause is not often discernable clinically. We sought to describe abdominal CT findings in these symptomatic adult CF patients.

Material and methods: Imaging histories of 323 adult CF patients on our database were analysed. CT images of adult CF patients who presented with abdominal pain between January 2001 and January 2008 were reviewed by consultant gastrointestinal radiologists.

Results: Seventeen abdominal CT scans were performed in adult CF patients presenting with abdominal pain. No cause for pain was identified in three cases. Four scans revealed dilated small bowel loops containing faeces in keeping with distal intestinal obstruction syndrome. Thickening of small and large bowel wall was observed in four cases. In two of these, there were associated peri-enteric fibro-fatty proliferation and lymphadenopathy, a pattern mimicking Crohn's disease, but not histologically proven in either case. Of the remaining, there were four cases of intussusception and one case of chronic pancreatitis with peripancreatic collection.

Conclusion: A spectrum of CF related gastrointestinal causes requiring different management strategies was observed on CT. An appreciation of these causes is important for the radiologic assessment and management of adult CF patients presenting with abdominal pain.

P-085

High density enteral contrast for CT demonstration of site of post-operative leaks

G. Alluvada, A. Razack; Hull/UK

Learning objectives: HDC is better for demonstration of post-operative leaks and should be used in the first instance to avoid repeat examinations.

Background: Oral contrast at dilutions of 2 to 5% is traditionally used to outline bowel in abdominal CT scans. This, however, is not dense enough to confidently identify the site of enteral leaks. Presence of free air is used to assess for leaks; however, this is fraught with difficulties of interpretation in post-operative patients.

Imaging findings OR Procedure details: We used high density contrast (HDC) at concentrations of 20–25% to identify the presence and site of post-operative leaks. We present imaging findings of six cases of post-operative enteral leaks. We performed CT scans for suspected enteral leaks with HDC (Iopamidol 300 mg/ml, 100 ml diluted in 400 ml of water) as opposed to 3% (Urografin 150 mg/ml, 30 ml in 800 ml of water) contrast used in our hospital. Four patients had previously undergone CT with 3% urografin and the presence and site of leak could not be demonstrated which was essential for their management. CT with HDC demonstrated the presence and site of leaks which was confirmed at surgery.

Conclusion: HDC is very useful in demonstrating the actual site of the post-operative leaks. This does not cause streak artefacts in MDCT scanners and in our experience has no disadvantages. We recommend the use of HDC for patients with suspicion of post operative leaks.

P-086

Abdominal X-rays and outcomes

N. Jagirdar¹, M.H. Thoufeeq², A. Haroon¹, R. Jones³;
¹Leicester/UK, ²Hull/UK, ³Boston/UK

Purpose: We wanted to assess if Royal College of Radiologists (RCR) UK guidelines on requesting abdominal X-rays were followed at our hospital.

Material and methods: A retrospective study looking at patients who had abdominal X-rays done in late 2006 looking at their clinical notes, X-ray requests, final outcomes and reports.

Results: 96 patients had abdominal X-rays done during this period. The patients' ages were between 18 and 94, median being 58. Their presenting complaints were abdominal pain in 74%, vomiting 9%, loin pain 5%, and collapse 4%. Haematemesis, rectal bleeding, constipation, chest pain, urinary retention, confusion and drowsiness formed 1% each. On looking at the clinical notes, we found constipation in 10%, ureteric colic 10%, possible abdominal aortic aneurysm rupture in 10%, biliary colic 4%, appendicitis 4%, haematemesis 3%, and possible perforation 3%. 9% had non-perforation type abdominal pain, urinary retention 2%, retroperitoneal abscess and strangulated hernia 1% each. 35% had other medical conditions. 76% were admitted, 22% discharged and 2% patients died. 85% were reported normal, 5% as faecal loading, ureteric stones and phleboliths as 3% each, 2% as calcified abdominal aortic aneurysm and 1% as subacute intestinal obstruction.

Conclusion: We noted that RCR guidelines were not followed. Abdominal X-rays did not change patient management in majority (95%) of our cases and expose patients to unnecessary radiation.

P-087

Very rare cases of variable foreign bodies in the GI tract or abdomino-pelvic cavity

J. Chung, J. Yu, J.H. Kim; Seoul/KR

Learning objectives: 1. To know the plain radiological findings of the very rare foreign bodies introduced into the gastrointestinal tract or abdomino-pelvic cavity. 2. To understand the plain radiographic and CT findings according to the materials of foreign bodies, such as glass bottle, plastic bottle, and metal.

Background: On daily practice, we have met the very rare cases of variable foreign bodies in the gastrointestinal tract (GIT) or abdomino-pelvic cavity. However, if it was the first time to meet the very rare foreign bodies, it was not easy to interpret those cases. Those foreign bodies can be introduced by accident, surgery, iatrogenic procedure or prank.

Imaging findings OR Procedure details: There are 12 patients with variable foreign bodies in GIT or abdomino-pelvic cavity. Some of foreign bodies were removed by surgery, endoscopic procedure or natural defecation. Twelve cases with foreign bodies were composed as follows: 1) rectum: a plastic bottle for hair spray, a glass bottle for juice, a masturbator unit, a broken metallic stent; 2) stomach: a tooth brush, a gold tooth; 3) small bowel: a gold tooth; 4) appendix: a metallic material; 5) abdomen: an acupuncture needle traversing the abdomen, a few acupuncture needles in the peritoneal cavity, a cloth pin and 6) pelvic cavity: a thumbtack in right pelvic wall for hemostasis during operation for rectal cancer.

Conclusion: This exhibition shows 12 cases of very rare, variable foreign bodies in the GI tract or abdomino-pelvic cavity.

P-088

Cisterna chyli (abdominal confluence of lymph trunks): imaging demonstration with MDCT

M. Kiyonaga¹, H. Mori², M. Sai², Y. Yamada², S. Matsumoto², K. Kosen¹; ¹Yufu-shi/JP, ²Oita/JP

Learning objectives: 1. To understand the normal CT anatomy of the cisterna chyli obtained by imaging reconstruction (1 mm-slice) with multiplanar reformation using MDCT. 2. To review the pathological conditions of the cisterna chyli from various diseases.

Background: The abdominal confluence of lymph trunks, the so called cisterna chyli, is a dilated lymphatic sac in the retrocrural space and is located at the origin of the thoracic duct. It receives the lymph mainly from bilateral lumbar trunks and the intestinal trunks. The cisterna chyli can be involved in various diseases, such as heart failure, liver cirrhosis, and gastrointestinal tumors. Knowledge of the CT imaging of normal and pathological conditions is clinically important. Recently, thin-slice images using multi-detector row CT (MDCT) allow the CT anatomy of the cisterna chyli, but there are no reports evaluating the cisterna chyli using MDCT.

Imaging findings OR Procedure details: In this education exhibit, we will demonstrate the normal CT anatomy of the cisterna chyli obtained by imaging reconstruction every 1 mm with multiplanar reformation using MDCT. Furthermore, we will review the CT imaging of the cisterna chyli in pathological conditions.

Conclusion: Thin-slice images using MDCT can clearly depict the cisterna chyli in normal and pathological conditions.

P-089

Study of evacuation disorders with defecography

N. Faccioli¹, A. Comai¹, P. Mainardi², M. D'Onofrio¹, R. Pozzi Mucelli¹; ¹Verona/IT, ²Negrar/IT

Learning objectives: To describe the principal morphofunctional imaging features, physiologic and pathologic, of the recto-anal region and pelvic floor as depicted with conventional video defecography.

Background: Defecography dramatically improved our knowledge of the evacuation dysfunctions. Most frequent indications and related disorders are presented from a database of more than 1500 examinations conducted in two radiology departments over a 7 year period.

Imaging findings OR Procedure details: Imaging features of the most involved recto-anal and pelvic floor disorders are described: rectal prolapse, rectocele, intussusception, descending pelvic floor syndrome, puborectalis muscle syndrome, enterocele and sigmoidocele.

Conclusion: Conventional video defecography still represents the gold standard examination for the identification and staging of morphological and functional anomalies of the recto-anal region and pelvic floor implied in evacuation dysfunctions.

P-090**Contrast-enhanced US in assessment of activity of Crohn's disease: comparison with Crohn's disease activity index**

K.T. Szopinski, A. Cybulska, M. Jedrzejczyk, R.Z. Slapa, W. Jakubowski; Warszawa/PL

Purpose: To evaluate the usefulness of contrast-enhanced ultrasound (CEUS) in the assessment of activity of Crohn's disease (CD).

Material and methods: Sixty-three CEUS examinations of the bowels were performed in 42 patients (19 male, 23 female, mean age 32 years) with confirmed CD. The Crohn's disease activity index (CDAI) was calculated in all patients. In 19 patients, a follow-up examination was performed, and in 2 patients 2 follow-up examinations were performed. The bowels were imaged on a Voluson 730 Expert (General Electric) machine using a 2-5 MHz convex probe. Before contrast administration, the small and large bowels were examined in gray-scale. Contrast-enhanced images were obtained after intravenous administration of 1.2 ml of SonoVue (Bracco).

Results: The CDAI score was >150 in 19 cases, and ≤150 in 44 cases. In 34 examinations, intense enhancement of the bowel was observed, and in 7 examinations assessment of the enhancement was not possible due to motion artifacts. In patients with CDAI>150, intense enhancement of the bowel wall was observed in 15/18 examinations (83%), and in patients with CDAI ≤150 intense enhancement was observed in 18/38 examinations (47%).

Conclusion: Intense contrast enhancement of the bowel in CD is seen in majority of patients with high CDAI. In patients with low CDAI, contrast enhancement may be an indicator of disease activity despite clinical remission.

P-091**MDCT imaging findings in peritoneal carcinomatosis**

L. Saba, G. Mallarini; Cagliari/IT

Learning objectives: The purpose of this work is to understand the pathogenesis of peritoneal carcinomatosis according to the primitive causes and to review clinical, pathologic and radiological manifestations of peritoneal carcinomatosis.

Background: Peritoneal carcinomatosis refers to a wide variety of tumors that present with extensive peritoneal involvement with or without parenchymal involvement of solid organs such as the liver, spleen and lymph nodes. It is a common evolution of cancers of the digestive tract such as stomach, small bowel, colon rectum, appendix and pancreas. Other tumors that may lead to these conditions include ovarian, mesothelioma, sarcoma and pseudomyxoma peritonei. In the last decade, CT has significantly altered the diagnostic approach to peritoneal carcinomatosis influencing also the therapeutic approach in the current practice.

Imaging findings OR Procedure details: In this work, we describe and show several MDCT imaging findings of peritoneal carcinomatosis including parietal peritoneal thickening, tumor involvement of the omentum (soft tissue permeation of the fat, enhancing nodules, and omental cake) and ascites. We include several examples by using MDCT source axial images and post-processing techniques as Multi-planar Reconstruction (MPR), Maximum Intensity Projection (MIP) and Volume Rendering (VR).

Conclusion: Peritoneal carcinomatosis shows a broad spectrum of radiological manifestations and sometimes may simulate other neoplastic and inflammatory conditions and so it is mandatory for a tight integration between radiological, anamnestic and clinical signs.

P-092**Imaging dilemma in carcinoid tumours: what are the options?**

M.G. Mulla, J. Birchall, S. Puri, R. Singh; Derby/UK

Learning objectives: 1. To learn the common imaging findings of carcinoid tumours on CT, MRI, EUS, Barium studies and on Indium-111 octreotide scan. 2. To demonstrate the complementary nature of the above imaging modalities.

Background: FLL can be benign or malignant. Commonly seen benign lesions are cysts, haemangiomas, focal nodal hyperplasia, hepatic adenomas and biliary cyst adenomas. Malignant lesions can be primary or secondary. It is important to differentiate between the two to optimize treatment and to avoid unnecessary interventions. Various radiological imaging modalities are employed for the diagnosis and characterization of FLL. The enhancement pattern of a lesion constitutes the mainstay of its characterization with contrast-enhanced CT or MRI.

Imaging findings OR Procedure details: Anatomical imaging, dual phase contrast CT and MRI including post gadolinium determines site and size, whereas functional imaging with In111-Octreoscan enables receptor density of somatostatin receptor type 2 and 5 to be determined. We present illustrative cases with characteristic images from different imaging modalities to reveal the advantages and necessity of multidisciplinary approach for diagnosis and management of carcinoids.

Conclusion: MDT approach improves results in appropriate management of patients with carcinoid tumours. The combination of anatomical imaging with functional imaging is recommended in making crucial management decisions.

P-093**Variation of abdominal fat content after gastrointestinal surgery: a comparison between stomach surgery and colon surgery**

C.H. Lee, K.A. Kim, J.M. Lee, J.W. Choi, C.M. Park; Seoul/KR

Purpose: To evaluate the change of body fat after gastrointestinal surgery.

Material and methods: A study was made of 159 persons whose abdominal CT was taken before surgery (90 stomach cancers, 69 colon cancers). Body fat volume was automatically extracted using a Philips EBW2. Body fat was classified into total abdominal fat (TAF) and visceral fat (VF). The average ratio of fat change between the two cancer groups was compared using a t-test. The stomach cancer group was divided into subtotal gastrectomy (SG) and total gastrectomy (TG), and the average ratio of fat between SG and TG were also compared.

Results: The TAF and VF ratios of post-surgeries against pre-surgeries regarding stomach cancer were 0.94 ± 0.48 and 0.77 ± 0.37 , respectively, and those for the colon cancer group were 1.32 ± 0.6 and 1.29 ± 0.76 , respectively. There was a noticeable statistical difference between stomach and colon cancers ($p=0.000$). 60 of stomach cancer patients had SG, and 30 had TG. The TAF and VF ratios for SG were 1.03 ± 0.48 and 0.85 ± 0.38 , respectively, and those of TG were 0.77 ± 0.43 and 0.62 ± 0.31 , respectively. There was a noticeable difference between SG and TG ($p<0.01$).

Conclusion: The stomach cancer surgery group showed a significant reduction of body fat when compared with colon cancer. The TG in particular showed a significant reduction of body fat. Therefore, great caution should be taken when making node evaluations on CT after stomach cancer surgery due to reduced visceral fat.

P-094**MDCT assessment of the therapeutic response of a tumor: comparison of the use of unidimensional, bidimensional, and area measurements for gastrointestinal cancer**

C.H. Lee, S.H. Kim, K.A. Kim, J.M. Lee, J.W. Choi, C.M. Park; Seoul/KR

Purpose: The purpose of this study is to compare unidimensional (WHO), bidimensional (RECIST), and area measurements with use of free-line ROI (FLR) to assess therapeutic response in patients with gastrointestinal cancer.

Material and methods: By analyzing 47 lesions of 41 digestive cancer patients who had hepatic and lymph node metastases, changes in lesions were retrospectively measured at the initiation of treatment and at 6 months after treatment. Following WHO and RECIST criteria, patients were categorized into 4 treatment response classifications—complete response, partial response, disease progression, and stable disease. The cross section area of the lesions was determined by using FLR. The extent of concordance between each pair of measurements was analyzed by kappa statistics.

Results: Response to treatment was in agreement for 41 cases (87.2%) between WHO and RECIST, for 42 cases (89.4%) between RECIST and FLR, and for 46 cases (97.9%) between WHO and FLR. There were five disagreements as determined by the use of RECIST and WHO. The same number of disagreements was seen for the use of RECIST and FLR. The former and latter disagreements in measurements applied to the same lesion; the shape of the lesion changed to an oval appearance after treatment.

Conclusion: There was disagreement for the use of RECIST and the other two measurements when the shape of a lesion changed to oval after cancer treatment. There was no meaningful difference between WHO and FLR.

P-095**Small and large bowel intussusception in adults**

H. Anderson¹, T. Latham², M.D. Tam¹, W. Howard², S. Jain²;
¹Norwich/UK, ²Southend/UK

Learning objectives: To demonstrate illustrative cases of small and large bowel intussusception primarily on multislice CT. These cases are supported by further imaging with MRI and also surgical and pathological correlations.

Background: Adult intussusception is rare. It is responsible for 1% of bowel obstruction. One third are colonic, two thirds are small bowel. 80–90% have intra-luminal pathology and the majority of cases are malignant in etiology.

Imaging findings OR Procedure details: We show illustrative cases which demonstrate the classic target sign, the intussusceptum and intussusciptens. Our case with a Dukes' C1 pT3 N1 adenocarcinoma in the distal transverse colon developed between a mobile and fixed section of the colon. In the small bowel, our case demonstrates a well-differentiated adenocarcinoma in the mid-jejunum presenting acutely with pain. These findings are supported with MRI and intra-operative pictures.

Conclusion: Multislice CT can demonstrate intussuscepting lesions in adults, which are an important, though rare, cause of obstruction.

P-096**Pneumatosis intestinalis, pneumoperitoneum and portomesenteric venous gas on MDCT and its clinical significance**

Y. Ku¹, S.L. Lee², S.N. Oh², J.Y. Byun²; ¹Uijeongbu/KR,
²Seoul/KR

Learning objectives: List the various conditions of intra-abdominal air collections of pneumatosis intestinalis, pneumoperitoneum, and portomesenteric venous gas. Review the pathophysiology and clinical significance.

Background: The frequency of detection of pneumatosis intestinalis, pneumoperitoneum, and portomesenteric venous gas appears to be increasing according to increased usage of CT at the practical fields.

Imaging findings OR Procedure details: A retrospective review was conducted on 81 patients (F: 44, M: 37, Mean age: 66.2 (41–91) between September 2006 and September 2007) with the diagnosis of pneumatosis intestinalis, pneumoperitoneum, and portomesenteric venous gas at the Department of Radiology, Uijeongbu St. Mary's Hospital, South Korea. After reviewing the analysis of radiographic findings, a chart review of the 81 patients was conducted. Specific factors included in our analysis were age, gender, presenting signs and symptoms, surgical and pathologic diagnosis, additional radiological findings, clinical course, and surgical versus nonsurgical management.

Conclusion: Familiarity with the imaging features and differential diagnoses of various conditions of pneumatosis intestinalis, pneumoperitoneum, and portomesenteric venous gas will facilitate prompt, accurate diagnosis and selection of adequate treatment option.

P-097

Withdrawn by authors

P-098**CT findings of lymphoma with peritoneal, omental and mesenteric involvement: peritoneal lymphomatosis**

D. Karaosmanoglu, M. Karcaaltincaba, D. Akata, M.N. Ozmen, O. Akhan; Ankara/TR

Purpose: We investigated CT findings in patients with peritoneal, omental and mesenteric lymphoma involvement.

Material and methods: We searched our archive retrospectively to find out patients with peritoneal, omental and mesenteric lymphoma involvement. We found 16 patients with non-Hodgkin lymphoma meeting these criteria. CT studies of these patients were reevaluated for presence of peritoneal involvement, ascites, omental mass, organomegaly, retroperitoneal lymphadenopathy, bowel wall thickening and other associated findings.

Results: There were 14 males and 2 females with peritoneal and/or mesenteric and omental lymphoma involvement. Mean age was 39 (range 4–76). Subgroups of non-Hodgkin lymphoma were diffuse large B-cell lymphoma (n=11), small cell lymphocytic lymphoma (n=2), small cleaved cell lymphoma (n=1), T-cell lymphoma (n=1) and Burkitt's lymphoma (n=1). Peritoneal involvement was seen

in 15 (94%) patients in the form of linear (n=12) and nodular (n=3) thickening. Ascites was seen in 12 (75%) patients. Omental and mesenteric masses were present in 10 (66.6%) and 10 (66.6%) patients, respectively. Bowel wall thickening, retroperitoneal lymphadenopathy and hepatosplenomegaly were also common and observed in 10, 10 and 11 patients, respectively. Solid organ involvement in form of liver and splenic lesions was seen in 9 (56%) patients.

Conclusion: Peritoneal involvement can be seen in many subtypes of lymphoma and most frequently in diffuse large B-cell lymphoma. Peritoneal lymphomatosis can mimic peritoneal carcinomatosis and should be included in differential diagnosis list in patients with ascites, hepatosplenic lesions and unidentified cause of peritoneal thickening on CT in a male patient.

P-099

Withdrawn by authors

P-100**Perfusion imaging of neuro-endocrine carcinoma in the mesentery with 320-slice dynamic volume CT**

C. Kloeters, S. Kandel, V.C. Romano, H. Meyer, F.J.F. Engelken, P. Rogalla; Berlin/DE

Purpose: Surgical resection of mesenteric neuro-endocrine carcinoma (NEC) may depend on the extent of bowel and vascular infiltration. Dynamic imaging of the mesentery is desirable for preoperative cancer staging with focus on perfusion information and motion analysis.

Material and methods: A 65 year-old patient with suspected NEC in the mesentery was referred for CT evaluation. A 320-slice dynamic volume CT was performed using a dynamic scanning protocol involving 17 low-dose acquisitions spread over a total of 40 seconds. Images were registered centered on the tumour for motion correction, and perfusion maps were generated based on the multiple acquisitions. Bowel motion was visualized by means of a movie generation.

Results: The tumour in the mesentery showed a clearly different perfusion pattern compared to the surrounding tissue. The extent of bowel infiltration was diagnosed by means direct morphologic visualization and through demonstration of motion restriction of the infiltrated small bowel loops. Based on the perfusion findings, surgical resection was performed confirming the extent of infiltration.

Conclusion: Perfusion imaging of the mesentery may provide valuable information and carries the potential to direct patients to tumour surgery. Image registration appears mandatory for calculation of perfusion maps.

P-101**Multidetector-row CT: how to avoid the misdiagnosis of appendicitis?**

A. Filippone, R. Cianci, S. Valeriano, M.L. Storto; Chieti/IT

Purpose: To establish potential causes of misdiagnosis in patients with surgically proven appendicitis not detected on multidetector-row CT (MDCT).

Material and methods: CT scans of 21 patients with surgically proven acute appendicitis incorrectly diagnosed on the preoperative MDCT were reviewed in consensus by two experienced abdominal radiologists who had knowledge only of a possible diagnosis of acute appendicitis. Readers were asked to record the following: visualization of the entire appendix, the maximal appendiceal diameter greater than 7 mm, thickening of the appendiceal walls, periappendiceal inflammatory changes, presence and location of fluid collection and/or gas bubbles. Any other abnormal CT finding was recorded including small bowel obstruction and diverticulosis. The degree of intraabdominal fat content according to a subjective scale (1-minimal; 2-moderate; 3-marked) as well as technical factors potentially responsible of misdiagnosis were also considered.

Results: Only 7/21 patients presented marked amount of intraperitoneal fat. Intravenous contrast material was administered in 9/21 patients. In 3/21 patients, most of the appendix appeared normal since only a small portion of the distal appendix was involved. Appendiceal inflammation resulted in small bowel obstruction in 5/21 patients and was confused with gynaecological disease or complicated diverticulitis, especially when perforation was present.

Conclusion: Suboptimal CT studies, tip appendicitis, atypical presentation of appendiceal inflammation may lead to misdiagnosis of appendicitis at MDCT. Knowledge of these pitfalls enables us to improve our diagnostic accuracy.

P-102

Withdrawn by authors

Diagnostic / GI Tract / Rectum

P-103

Rectal carcinoid: imaging features based on various imaging modalities with pathologic correlation

B.J. Park, M.G. Song, S.S. Lee, D.J. Sung, Y.H. Kim, K.B. Chung; Seoul/KR

Purpose: To provide the spectrum of radiological and pathologic finding in rectal carcinoid (RC) as rare neuroendocrine neoplasm.

Material and methods: From August 2001 to May 2007, 125 patients with RC were registered at our pathologic registry. Twenty-two patients (14 men; 8 women; age range 23–67 years) performed by variable imaging modalities involving MDCT, CTC, MRI, barium enema, octreotide scintigraphy, and EUS were enrolled. Two radiologists retrospectively evaluated gross morphology; the value of enhancement; size; perirectal lymph node or infiltration; and metastasis by means of consensus.

Results: There were mainly two types of diffuse and polypoid in RC. Eccentric or circumferential wall thickening with perirectal infiltration and lymphadenopathies, termed diffuse type, were 6 of 22 patients (27.3%). Polypoid type (size range 0.4–6 cm) was identified in 16 of 22 patients (72.7%). They showed various enhancements ranging from 53 to 192 HU, irrespective of type; isointense and slightly hyperintense on T1/T2WI on MRI; smoothly marginated polypoid lesion on CTC and barium enema; variable echoic submucosal tumor on EUS. In one case, multifocal uptakes were shown by rare bony metastasis of carcinoid on ¹¹¹Indium-octreotide scintigraphy.

Conclusion: RC had frequently diffuse type mimicking rectal cancer which has not been defaulted in the available literatures, although variable image findings of RCs were often indistinguishable from adenomatous polyp or other submucosal tumor on multiple imaging modalities.

P-104

Double reporting improves accuracy of staging in rectal cancer

A. Rajesh, R. Verma, A. De, A. Deshpande, P. Rodgers, S. Campbell; Leicester/UK

Purpose: To determine if double reporting improves accuracy of MRI staging in rectal cancer.

Material and methods: Forty six consecutive patients who had rectal cancer staging with MRI and who underwent surgery were included in the study. Histopathologic staging was considered as gold standard. All the initial T staging mentioned in the radiology reports were recorded and accuracy was calculated. All the MRI scans were then restaged by two gastrointestinal radiologists who were blinded to the initial staging and final histopathologic staging. Accuracy was calculated for double reporting.

Results: Of the 46 patients who had MRI surgery, the initial staging accuracy for T staging was 54%. Ten patients were overstaged and 8 were understaged. The staging was equivocal in three patients. Twenty five patients were correctly staged. Double reporting in consensus improved the staging accuracy to 92%.

Conclusion: Double reporting of MRI scans for staging of rectal cancer significantly improves the accuracy of staging.

P-105

USPIO MRI after neoadjuvant chemoradiation: criteria for predicting involved nodes in rectal cancer patients

M. Lahaye¹, G.L. Beets¹, S.M.E. Engelen¹, A.H.F. Kessels¹, A.P. de Bruïne¹, A.P. Willig², J.M.A. van Engelshoven¹, R.G.H. Beets-Tan¹; ¹Maastricht/NL, ²Roermond/NL

Purpose: To determine the USPIO MRI criteria for prediction of nodal involvement after chemoradiation of locally advanced rectal cancer patients.

Material and methods: 39 Locally advanced rectal cancer patients received preoperative chemoradiation and underwent a postchemoradiation MRI with 2DT2WFSE, 3DT1WGRE and 3DT2*-weighted sequences. Each visible node was prospectively evaluated for: border irregularity, short/long axis and estimated percentage of white region within the node, categorized as: <30, 30–50 or >50% by two radiologists independently and blinded to each other's result. Furthermore, RatioA (area of white region within the node/area of the total node) was calculated. Each MR characteristic was validated using lesion-by-lesion histology as

reference standard. Receiver operating characteristic (ROC) curves were constructed.

Results: A lesion-by-lesion was feasible in 201 lymph nodes. 40/201 nodes were pN+. The area under the ROC-curve (AUC) of border, short and long axis, estimated percentage of white region within the node and measured RatioA for observers 1 and 2 are given in table 1. The interobserver agreement for each criterion is shown in tables 2 and 3.

Table 1: AUC of all used criteria

| Criterion | Observer1 | Observer2 |
|-------------------|-----------|-----------|
| Short axis | 0.89 | 0.87 |
| Long axis | 0.87 | 0.88 |
| Border | 0.70 | 0.85 |
| Est. white region | 0.97 | 0.98 |
| RatioA | 0.98 | 0.99 |

Table 2: Intra Class Correlation (ICC)

| | |
|------------|------|
| Short axis | 0.94 |
| Long axis | 0.97 |
| RatioA | 0.83 |

Table 3: Interobserver agreement (Kappa)

| | |
|-------------------|------|
| Long axis | 0.36 |
| Est. white region | 0.79 |

Conclusion: 1. Size criteria such as short and long axis diameters - previously shown to be inaccurate for rectal cancer nodes - seem to be accurate predictive criteria for node prediction in irradiated rectal cancer patients. 2. However, the estimated percentage of white region and measured RatioA are the most accurate criteria.

P-106

Severe constipation and pelvic floor disorders: evaluation with colon transit time and dynamic digital colpo-cysto-defecography

P. Giusti, S. Giusti, F. Cerri, V. Morigoni, G. Naldini, C. Bartolozzi; Pisa/IT

Learning objectives: To show the accuracy of CTT and ddCCD in pts with severe constipation and clinically suspected pelvic floor dysfunction.

Background: We reviewed the findings from dynamic digital colpo-cysto-defecography (ddCCD) and colon transit time (CCT) in 134 women examined within a 4-years time period. Each patient was given 400 mL of 60% density barium to opacify the small bowel; the bladder was filled with 200 mL of an iodinated contrast medium; the vagina was opacified with a tampon soaked in an iodinated contrast agent; and the rectum was filled with 200 mL of a high density barium suspension. CTT was documented with an abdominal plain, since patients have ingested 24 markers up to 5 days.

Imaging findings OR Procedure details: Abnormal findings revealed by CTT (CTT+) were present in 92 pts (68.6%), while in 42 pts (31%) all markers were evacuated within 5 days (CTT-). Comparing these different groups with ddCCD, we detected: anterior rectoceles (34 pts with CTT-; 68 pts with CTT+), intussusception (36 pts with CTT-; 88 pts with CTT+), pubo-rectal muscle hypertone (6 pts with CTT-; 6 pts with CTT+); reduction of ano-rectal angle (11 pts with CTT-; 15 pts with CTT+). In 45/134 pts ddCCD revealed an enterocele, in 23/134 a cystocele.

Conclusion: Constipation is often associated with compartment defects in pelvic floor and moreover this chronic syndrome is due to anomalies of ano-rectal region rather than an impairment of colonic motility.

P-107**Role of dynamic digital colpo-cysto-defecography in preoperative planning of patients with pelvic floor and anorectal dysfunction**

P. Giusti, S. Giusti, F. Cerri, V. Morigoni, G. Naldini, C. Bartolozzi; Pisa/IT

Learning objectives: To enhance the role of preoperative ddCCD examination in pts with pelvic floor and anorectal dysfunction.**Background:** Between January 2005 and March 2007, 55 consecutive females (mean age: 61.4 yrs) with urinary and genital disorders and obstructed defecation were studied prospectively. To opacify the small bowel patients (pts) were ingested 400 mL of 60% density barium suspension; the bladder was then opacified by the administration of 300 mL of an iodinate contrast medium, and the rectum was filled with 200 mL of a high density barium suspension.**Imaging findings OR Procedure details:** The dynamic digital colpo-cysto-defecography (ddCCD) examination revealed the presence of an anterior rectoceles associated with a severe intussusception in 52/55 pts, enterocele in 22/55 pts, sigmoidocele in 8/55 pts, rectal prolapse in 19/55 pts, and cystocele in 4/55 pts. All pts underwent surgery to resolve the above mentioned pelvic floor dysfunctions. The presence of enterocele, sigmoidocele and/or cystocele required a different surgical approach respect to those pts who presented only with anorectal disorders.**Conclusion:** The ddCCD examination allows determining the presence of associated urinary, genital and anorectal abnormalities in women with pelvic floor dysfunctions in order to preoperatively plan and optimize the proper surgical repair.**P-108****Phased-array MRI rectal cancer staging**

S. Giusti, P. Giusti, E. Fruzzetti, P. Buccianti, M. Castagna, C. Bartolozzi; Pisa/IT

Learning objectives: Describe the MRI TNM staging of rectal cancer. Describe the MRI TNM staging of rectal cancer and its morphological changes after neoadjuvant therapy. Show the corresponding histopathological slices.**Background:** Rectal carcinoma is a common cause of cancer death in Europe and the United States. Its prognosis is related to the extent of extramural spread into the mesorectum at the time of diagnosis, and to the ability to achieve surgical clearance at the circumferential resection margins. We describe the phased-array MR TNM features of rectal cancer, before and after neoadjuvant chemoradiation therapy showing the corresponding histopathological slices.**Imaging findings OR Procedure details:** All patients underwent MR staging at time of diagnosis and again prior to surgery for restaging of disease. We acquired axial and sagittal T2w. Sagittal images were used to plan large FOV axial sections useful to evaluate the whole pelvis, from the iliac crest to the symphysis pubis, and again to plan high-resolution 3-mm-section axial images, acquired perpendicularly to the long-axis of the rectal tumour and performed by using a smaller FOV.**Conclusion:** Phased array MRI is an excellent technique to preoperative local stage rectal carcinoma allowing to: evaluate mesorectum and pelvis; plan surgery, optimizing a complete excision; decide about the use of neoadjuvant therapy in order to downstage lesions and to perform a sphincter-preserving surgery in those pts who otherwise would require colostomy.**P-109****Diffusion MRI in rectal carcinoma**

G. Engin, R. Sharifov, Z. Almac, E. Kaytan Saglam, E. Balik, S. Yamaner; Istanbul/TR

Learning objectives: Describe fundamental features of diffusion-MRI. List the applications of this technique in rectal tumors. Discuss articles related to diffusion-MRI in rectal tumors.**Background:** The intent of this review is to acquaint the reader with the fundamental features of diffusion-weighted (DW) MRI as applied to rectal tumor assessment and to introduce the reader to new applications of this technique for the evaluation of therapeutic response.**Imaging findings OR Procedure details:** DW-MRI enables noninvasive characterization of biologic tissues on the basis of their water diffusion properties; it provides information about cell organization and density, microstructure, and microcirculation of tissue. In the intracellular area, diffusion is relatively slow,

whereas diffusion is relatively fast in the extracellular area. Tissue diffusion variations can be assessed by the construction of diffusion maps and quantitative estimations that reflect by the apparent diffusion coefficients (ADCs). Diffusion maps provide images with improved signal-to-noise ratios; reversal of the contrast of these images resulted in black-and-white images. Diffusion maps have substantial implications for diagnosis, targeting of focal treatments and measuring treatment responses. Low ADC values may indicate malignancies or hypercellularity. Therefore, quantitative DW-MRI may allow the cellularity of tumors to be graded noninvasively and assessment of early tumour's therapy response.

Conclusion: DW-MRI appears to have great promise for increasing our understanding of rectal tumors and the effects of therapy.**P-110****The utility of MDCT perfusion examination in detection of metastatic lymph nodes of rectal cancer**

L. Tóth, G. Tóth, E.C. Turupoli, Z. Vígáry; Budapest/HU

Purpose: Assessment of the role of computed tomography perfusion (CTP) study for the differentiation between malignant and benign enlarged perirectal, pelvic, and retroperitoneal lymph nodes.**Material and methods:** A prospective study was conducted on a 21 consecutive patients (12 M, 9 F aged 45–72) with a histologically proven rectal cancer. The perfusion study was done after contrast-enhanced conventional abdominal MDCT study. A dynamic acquisition (8x3 mm slices) was performed and the perfusion values were calculated using a modified deconvolution-based analysis, with the application of CT perfusion software. Region of interest placed over the biggest lymph node was found in a previous CT study. Postprocessing-generated maps showed perfusion (P), peak enhancement intensity (PEI), time to peak (TTP), blood flow (BF), blood volume ml/100ml (BV). Data were statistically analyzed with Wilcoxon sign test and results compared with histopathological findings.**Results:** On the perfusion maps, metastatic nodes showed hypoperfusion compared to benign ones. The mean value of BV was 2.9 (±0.29) and TTP was 25 sec (±4.2 sec). Compared to non-malignant nodes, the malignant ones showed significantly lower BF and BV values (p<0.008). The accuracy of detecting malignant nodes was 89%, sensitivity 91%, specificity 83%, positive predictive value 90.5%, and negative predictive value 76.7%.**Conclusion:** CTP can be a good tool in distinguishing benign and malignant lymph nodes in rectal cancer and might be useful in re-staging.**P-111****T1 rectal cancer on preoperative transrectal ultrasonography: long-term follow-up results after surgical resection**

M.J. Kim, S.J. Lee, H.K. Chun, D. Choi, H.K. Lim, S.Y. Song; Seoul/KR

Purpose: To evaluate the long-term follow-up results of T1 rectal cancer on preoperative TRUS treated with surgical resection.**Material and methods:** During a recent 7 years, 44 patients were diagnosed with T1 rectal cancer on preoperative TRUS. Forty patients underwent transanal endoscopic microsurgery (TEM) and four patients were performed low anterior resection. All patients were followed up every 6 months to 1 year with contrast enhanced CT (mean, 40.5 months). We correlated preoperative TRUS staging with postoperative pathologic staging. The rates of local and distant recurrence, disease-free and cumulative survival rates were analyzed.**Results:** In T1 rectal cancer, the positive predictive value of preoperative TRUS was 93%. Four patients (9%) of 44 patients were underestimated to T1 on preoperative TRUS. The mean size of the tumor was 2.1 cm. The salvage operation after TEM was performed in five patients (two of T2 and three of deep invasion of submucosal layer of T1). There was no local recurrence and two patients (5%) showed distant metastasis. Only one patient died of distant metastasis at 7 months after operation. The 1-, 3-, and 5-year disease-free survival rates were 98, 98, and 92% and the overall 5-year survival rates were 98%.**Conclusion:** TRUS is an accurate technique for preoperative staging of T1 rectal cancer and the surgical treatment result in adequate local control of those T1 rectal cancers.

P-112**Ultra small paramagnetic iron oxide MRI for prediction of malignant lymph nodes in rectal cancer: a lesion by lesion analysis in 577 nodes**

M. Lahaye¹, S.M.E. Engelen¹, G.L. Beets¹, A.P. de Bruïne¹, M.F. van Meyenfeldt¹, J.M.A. van Engelshoven¹, C.J.H. van de Velde², R.G.H. Beets-Tan¹; ¹Maastricht/NL, ²Leiden/NL

Purpose: To determine the accuracy of USPIO MRI for the prediction of malignant nodes in patients with primary rectal cancer.

Material and methods: From February 2003 till present, 59 patients with primary non-locally advanced rectal cancer enrolled in this ongoing study and underwent 1.5-T high-resolution MRI 24 hr. after administration of USPIO (Ultra Small Paramagnetic Iron Oxide - Sinerem®) contrast agent. Sequences used were axial 2D T2W FSE, 3D T1W GRE and 3D T2*. A MR radiologist prospectively predicted each visible mesorectal node for benign or malignant. All patients were treated with 5x5 Gy radiotherapy, followed by TME. Lesion by lesion analysis was performed with histology as the gold standard.

Results: 577 lymph nodes in 59 patients were predicted on MRI and matched with histology. 60 lymph nodes in 21 patients were malignant at histology. Sensitivity, specificity, PPV and NPV on a lesion by lesion basis are 97 (58/58+2), 93 (482/482+35), 62 (58/58+35) and 99% (482/482+2), respectively. The patient-based sensitivity, specificity, PPV and NPV were, respectively, 100 (21/21+0), 58 (22/22+16), 57 (21/21+16) and 100% (22/22+0).

Conclusion: USPIO MRI has a high sensitivity, specificity and NPV, indicating that N0 patients can be accurately identified, however, at the expense of a low PPV.

P-113**CT features of uncommon rectal tumors with pathologic correlation**

J. Cho, K. Shin, H.Y. Han, J.K. Sung, H.Y. Jeong, K.S. Song, J. Kim; Daejeon/KR

Learning objectives: To pictorial review the CT features with pathologic correlation of various uncommon or rare tumors of the rectum.

Background: The most common tumor of the rectum is adenocarcinoma and other tumors are uncommon or rare. Uncommon or rare tumors of the rectum include neuroendocrine tumor, gastrointestinal stromal tumor (GIST), lymphoma, metastasis, and so on. CT features of these uncommon tumors of the rectum may overlap with rectal carcinoma. However, with recent advances of helical CT or MDCT, the CT features with pathologic correlation of various uncommon or rare tumors of the rectum may help narrow differential diagnosis.

Imaging findings OR Procedure details: We retrospectively reviewed the CT features with pathologic correlation in 20 patients with surgically or pathologically proven uncommon tumors of the rectum. Helical CT or 16-MDCT imaging was obtained during the arterial and portal venous phases. Uncommon or rare tumors of the rectum were GIST (n=5), neuroendocrine tumors (n=4), metastasis of linitis plastica pattern from gastric cancers (n=3), lymphomas (n=2), melanomas (n=2), cloacogenic cancers (n=2), papillary cystadenocarcinoma of the mesorectum (n=1), and malignant fibrous histiocytoma (n=1).

Conclusion: Familiarity with the CT features and pathologic correlation of various uncommon or rare rectal tumors can help ensure differential diagnosis and proper management.

P-114**Defecography nowadays: why, when and how?**

R. Santos, E. Alves, J. Lourenço, P. Gil; Lisbon/PT

Learning objectives: To stress the role of conventional defecography in clinical practice nowadays. To review symptoms, risk factors, physiologic grounds and pathologic defecographic patterns.

Background: Disorders of defecation represent a common health problem with increasing trend and substantial impairment in quality of life, carrying inherent cost to patients, families and society. Greater availability of therapeutic options for defecation disorders is creating considerable clinical demand for defecography. Conventional defecography is the current imaging gold standard in assessing anorectal and pelvic floor dysfunction, with high interobserver accuracy and yield of positive diagnosis.

Imaging findings OR Procedure details: The procedure and interpretation methodology are described. Graphics and tables show results from 52

examinations performed at our department between July/2006 and December/2007. 88% patients were women; mean age 62 years. 25% had previous perianal surgery. 44.2% had impaired defecation; 9.6% showed incontinence; the remaining had normal defecation duration and efficacy but with associated dynamic and morphologic changes. Results are discussed, including prevalence of defecation disorders: significant perineum descent (76.9%); rectocele (67.3%); rectal intussusception (61.5%); non-relaxing pubo-rectalis (50%); anal dysfunction (34.6%); and rectal prolapse (7.7%). Challenging examinations are also exhibited.

Conclusion: Defecography is a well-tolerated, easily feasible, valuable method with great cost-benefit ratio in the evaluation of defecation disorders. It is important that radiologists and clinicians understand this dynamic procedure, which is becoming increasingly requested and is central in the management of defecation disorders.

P-115**Gastrointestinal stromal tumors of the anorectum: CT, MRI and endorectal US findings**

C. Campos, J. Venâncio; Lisbon/PT

Purpose: To describe and illustrate CT, MRI and endorectal US findings of gastrointestinal stromal tumors (GISTs) of the anorectum.

Material and methods: We reviewed clinical files and radiological exams of five patients (two men and three women, mean age 55±9.5 years, age range 45–69 years) with histological and immunohistochemical diagnosis of anorectal GISTs. CT, MRI and endorectal US findings were assessed for tumor location, approximate size, morphologic appearance, perirectal extension, presence of lymph node and metastatic disease.

Results: All the tumors were located in the distal rectum and anal canal. The mean diameter was 6.7±2.8 cm (range 2.7–10 cm). Tumors were typically well-circumscribed, heterogeneous mural masses on CT scans, with uniform low-signal intensity on T1WI and intermediate-signal intensity on T2WI. On US, GISTs appeared as solid hypoechoic lesions, located in the muscularis propria, expanding the rectal wall, with exophytic growth. Perirectal spread occurred with extension into the rectovaginal septum. There was no evidence of infiltration of ischioanal fossa, prostate or seminal vesicles. Lymph node and metastatic disease were not detected.

Conclusion: Anorectal GISTs are large, well-circumscribed mural masses on CT scans with low-signal intensity on T1WI and intermediate-signal intensity on T2WI. There was no evidence of lymph node or metastatic disease. On US, GISTs appeared as solid hypoechoic wall lesions with exophytic growth, extending into the rectovaginal septum.

P-116**Comparison of preoperative MDCT and MRI for the assessment of circumferential margin infiltration in rectal cancer: preliminary data**

J.R. Ayuso, C. Ayuso, M. Pagés Llinás, C. De Juan, S. Rodríguez, F. Balaguer, S. Delgado; Barcelona/ES

Purpose: To compare the results and to evaluate the preoperative accuracy (A) of MDCT and MRI with multiplanar reformations in the prediction of circumferential margin involvement in rectal cancer (RC).

Material and methods: Thirty patients with RC were prospectively evaluated with high resolution MDCT and MRI. Circumferential margin infiltration was considered when solid tumoral tissue or tumoral lymph nodes were present in the mesorectal fat and was located 2 mm or less from the mesorectal fascia. K statistic was used to compare both techniques. Twelve patients were initially treated with total mesorectal excision and were used to calculate sensitivity (S), specificity (SP) and A of both techniques.

Results: MDCT and MRI showed agreement for the assessment of the circumferential margin in 28/30 patients. (K=0.856). For the 12 surgical patients, S, SP and A for MDCT were 50, 87.5 and 75% and for MRI were 50, 100 and 83%, respectively.

Conclusion: MDCT with high resolution multiplanar reformations is similar to MRI for the assessment of a free circumferential resection margin in initial staging of rectal cancer.

P-117**Gadolinium based blood pool MR contrast agent for detection of lymph nodes in rectal cancer: the results of a pilot study**

M. Lahaye¹, G.L. Beets¹, M. Voth², D. Lambregts¹, T. Leiner¹, A.P. de Bruïne¹, C.J.H. van de Velde³, S.M.E. Engelen¹, R.G.H. Beets-Tan¹; ¹Maastricht/NL, ²Berlin/DE, ³Leiden/NL

Purpose: To determine whether MS325 MRI is feasible for prediction of the N-status in patients with primary rectal cancer. MS325 is a gadolinium-based blood pool MR contrast agent and has shown its potential in distinction between malignant from benign nodes in a rabbit model (Herborn et al AJR 2002;179(6):1567-1572)

Material and methods: From June 2006 till present, seventeen patients with primary rectal cancer selected for 5x5 Gy +TME were enrolled in this study and underwent 1.5T high-resolution MRI. Sequences were axial 2DT2WFSE, 3DT1WGRE & 4DTHRIVE before and 15 minutes after intravenous administration of MS325 at 0.12 ml/kg. An expert MR radiologist prospectively predicted each visible mesorectal node for benign or malignant with a confidence level score from 0 (definitely benign) to 4 (definitely malignant) for ROC-analysis. Lesion-by-lesion analysis was performed with histology as reference standard.

Results: 122 lymph nodes in 17 patients were predicted on MRI. 8 lymph nodes in 5 patients were malignant at histology. The area under the ROC-curve(AUC) was 0.89 for the prediction of malignant nodes, with a best cut off at sensitivity, specificity, PPV and NPV of 83%,89%,28% and 99%, resp.

Conclusion: MS325 MRI has a high sensitivity,specificity and very high NPV(99%) however at the expense of a low PPV.Because of the promising results further studies in multicenter setting are undertaken to evaluate whether a MS3325 could be reliable in general setting for selecting N0-patients.

Diagnostic / GI Tract / Small Bowel**P-118****Obscure GI bleeding: gastroenterological and radiological approaches**

B. Graça, P. Freire, J. Brito, J. Ilharco, V. Carvalho, E. Caseiro-Alves; Coimbra/PT

Learning objectives: To provide an overview of the diagnostic imaging modalities of OGIB including double balloon enteroscopy, wireless capsule endoscopy, MDCT, angiography, and bleeding scanning with labeled red blood cells.

Background: Obscure gastrointestinal bleeding (OGIB) is defined as an intermittent or continuous loss of blood in which the source has not been identified after upper endoscopy and colonoscopy. Whether an obscure site of bleeding is clinically evident by obvious symptoms or signs, or silent and manifest only as refractory iron deficiency anemia, it constitutes a diagnostic and therapeutic challenge for the clinician. Gastroenterology and radiology provide the essential diagnostic imaging modalities in OGIB, each one with its strengths and weaknesses.

Imaging findings OR Procedure details: Through case illustration, the authors will discuss the role, indications, advantages and limitations of double balloon enteroscopy, wireless capsule endoscopy, MDCT, angiography and bleeding scanning with technetium 99m-labeled RBC in the evaluation of the patient with OGIB.

Conclusion: Recognition of the cause and site of GI bleeding is instrumental to guide treatment planning. Gastroenterological and radiological imaging approaches should be tailored according to the clinical scenario.

P-119**Comparison of perfusion MDCT results with Crohn's disease activity index**

G. Tóth, L. Tóth, E.C. Turupoli, V. Bérczi; Budapest/HU

Purpose: The purpose of this study was to evaluate the utility of perfusion MDCT in predicting the activity of Crohn's disease.

Material and methods: We examined 48 patients with known Crohn's disease. These patients had thickened wall small or large bowel segment. 32 patients had clinically suspected exacerbation of Crohn's disease. Methylcellulose solution was administered for small bowel distension. Region of interest were placed over the most thickened segment of small or large bowel. In this level, we measured the perfusion of the wall and adjacent mesentery. We administered 1.5 ml/kg i.v. contrast material. The flow was 3.5 ml/s. Acquisition started after 20 sec of administration of the contrast material and lasted for 45 sec at a rate of one image per 1.5 sec. Collimation was 8x3 mm. The slope of enhancement, perfusion (P) ml/100ml/min, peak enhancement intensity (PEI), time to peak enhancement (TTP), and blood volume (BV) ml/100g were determined. These results were compared with CDAI. Statistical analysis was performed using the Wilcoxon rank sum test.

Results: The signal intensities of the perfusion scans were measured and displayed in a graph. The graphs showed a typical enhancement pattern in patients with CDAI higher than 350. A good correlation was found between CDAI and P, TTE and BV (0.902, 0.932, 0.954), p<0.008.

Conclusion: Perfusion CT can be valuable tool in assessing Crohn's disease activity.

P-120**Setting up a CT enteroclysis service: a practical guide**

A.J. Phillips, G. Whitmarsh; Bath/UK

Learning objectives: To highlight the practical issues involved in setting up and maintaining a successful and efficient CTE service.

Background: In recent years, CT Enteroclysis (CTE) has emerged as a promising technique for the investigation of small bowel disease. However, the widespread use of CTE has been limited by concerns over the acceptability of the technique to patients, radiologists and radiographic staff. The main issues are the invasiveness of the technique, ease of achieving consistent technical success, time constraints of pressurized CT lists and demand on radiologist's time. A number of simple practical steps can improve the acceptability and efficiency of this valuable means of imaging the small bowel.

Imaging findings OR Procedure details: We discuss the practical issues involved in setting up and maintaining a successful and efficient CTE service. These include: 1) Careful patient selection, patient information and preparation, choice of enteroclysis catheter and use of conscious sedation to improve patient acceptability; 2) Choice of enteral contrast media, infusion techniques and CT parameters to achieve optimal small bowel visualization and 3) Organization of examinations to maximize workflow efficiency.

Conclusion: CTE is a valuable tool for the investigation of small bowel disease. Attention to a number of simple practical steps may improve the acceptability and efficiency of this technique, and result in a successful CTE service.

P-121**MDCT findings and correlation with endoscopy in patients with previous intestinal surgical resection for Crohn's disease**

L.M. Minordi, G. Poloni, L. Guidi, G. Fedeli, A. Vecchioli, L. Bonomo; Rome/IT

Purpose: To evaluate the ability of the MDCT in the identification of the relapse in patients with previous intestinal resection for Crohn's disease.

Material and methods: 21 patients were studied by 16 MDCT after oral administration of polyethylene glycol solution (PEG) (n=11) or after administration of methylcellulose by naso-jejunal tube (n=10). Unenhanced and contrast-enhanced CT was performed. The following parameters have been evaluated: bowel wall thickening, enhancement, presence of target sign, comb sign, fibrofatty proliferation and complications. Endoscopy was performed in all patients.

Results: We found bowel wall thickening (range 2-12 mm) of ileo-colic anastomosis in 15 patients. Other sites were pathological in the remaining patients (distal ileum in 3 patients, proximal ileum in one, and distal jejunum in 2). The target sign was present in 11 patients, perienteric stranding in 12, comb sign in 6, fibrofatty

proliferation in 4, stenosis in 5, and fistulas in 3. Concordance with endoscopy was present in 19/21 patients. 1 patient was negative in the endoscopy but CT showed the presence of disease in the distal jejunum; 1 patient was a positive false case of the CT.

Conclusion: MDCT with neutral intestinal contrast and i.v. contrast seems to be a reliable method in the diagnosis of the relapse in patients with intestinal resection.

P-122

A perivascular epithelioid cell tumour of the duodenum: a rare tumour of the duodenum presenting as an acute GI bleed

M.A. Puckett¹, D. Buckley¹, S. Narayanaswamy²;
¹Torbay/UK, ²London/UK

Learning objectives: With improved immunohistochemistry, more PEComas will become evident and therefore should be included in the differential diagnoses of tumours arising within the GI tract.

Background: Perivascular Epithelioid Cell tumours (PEComas) are rare mesenchymal tumours. PEComas belong to a group of tumours which include angiomyolipoma and lymphangiomyolipoma. PEComas rarely occur in the GI tract. There is only one published case occurring in the duodenum.

Imaging findings OR Procedure details: An adult patient presented with haematemesis and melaena. A CT showed a 3 cm enhancing submucosal mass at the junction of the second and third parts of the duodenum. There was no evidence of metastases or lymphadenopathy. A diagnosis of a GI stromal tumour was made. Upper GI endoscopy showed a 3 cm, sub-mucosal tumour with an ulcerated central dimple. There was no evidence of active bleeding. Biopsies were non diagnostic. The patient underwent localised resection.

Conclusion: PEComas tend to have a benign course, although malignant lesions have been described. The precise biological and clinical behaviour of this tumour is yet to be established as very few tumours have been reported in the literature. These tumours need to be distinguished from other tumours of GI tract, the most common being GISTs. It is difficult to differentiate between GISTs and PEComas based on their radiological appearance. Both tumours shows avid peripheral contrast enhancement with a central zone of diminished contrast enhancement.

P-123

Revisiting the role of small bowel barium series for diagnosis of GI tuberculosis: an indian perspective

S. Hazarika, K. Chetri, H. Goswami, R. Baruah; Guwahati/IN

Learning objectives: Various forms of tubercular pathology have distinct but still nonspecific appearance in barium meal X-rays. Combined with clinical background, the radiological findings may be sufficiently conclusive for treatment. Recognition of radiological features of GI tuberculosis in barium series helps in case selection for biopsy or trial of antitubercular drugs.

Background: In India, 3–20% of intestinal obstruction and 5–7% of perforation is attributed to intestinal tuberculosis (IT). Incidence of IT is about 5.1% in autopsy series. About 0.8% hospitalisation is for IT in Delhi hospitals.

Imaging findings OR Procedure details: Commonly, GI tuberculosis involves distal small bowel and proximal colon centering the ileo-caecal region. Ulcerative, hypertrophic and mixed forms are described. Early lesions are predominantly ulcerative. hypertrophic form of ileocaecal TB cause narrowing of preterminal ileum, gapping of the valve with caecal wall retraction. Standard barium examination with adequate screening under image intensifier has acceptable pick up rate for various pathological changes in the intestine. Four categories of findings of barium examination will be discussed with numerous pictorial illustrations: a) findings highly suggestive of tuberculosis, b) findings moderately suggestive, c) non-specific and d) normal. Illustration of extra-intestinal manifestations like adenopathy, ascites, omental thickenings and few associated visceral lesions will be shown in USG and CT images.

Conclusion: Experience of interpreting barium series is still a valuable tool for diagnosis of IT.

P-124

CT and US imaging of intestinal obstruction

Y.H. Lee, Y.J. Shon, K.H. Yoon, S.E. Yoon; Iksan/KR

Learning objectives: The purpose of this exhibit is to illustrate CT and US findings of various causes and complications of intestinal obstruction.

Background: Intestinal obstruction can be diagnosed by physical examination

and plain radiography. CT and US imaging studies are performed in order to know not only the site and etiology of obstruction but also the presence of complications. Thanks to advanced CT technology providing high image quality, MDCT has become modality of choice in evaluation of intestinal obstruction. Ultrasonographic imaging is not routinely performed in evaluation of intestinal obstruction; however, in some equivocal cases, it can provide more useful information.

Imaging findings OR Procedure details: In this exhibit, a comprehensive review of US and CT findings of variable causes and complications associated intestinal obstruction is presented. The common causes of bowel obstruction are adhesive bands, bezoar, inflammatory bowel disease, hernia, primary and secondary malignant tumor, intussusception, volvulus, adhesion due to localized peritonitis and acute infectious diseases such as bacterial or parasite infection. CT findings of complications such as ischemia, strangulation or perforation and severity of obstruction are well correlated with clinical and pathologic findings. 3D MPR images provide additional useful clues that cannot be detected on axial images only. In some equivocal cases on CT images, US imaging is often useful for detection of obstruction site, causes and associated inflammatory process in peritoneal cavity. However, abundant bowel gas is the major obstacle of US imaging.

Conclusion: MDCT with 3D MPR images is useful in the evaluation of site, level, cause and possible complications of intestinal obstruction. Additional ultrasonographic imaging is complementary useful in cases of equivocal findings on MDCT.

P-125

Transabdominal ultrasonography and multi-slice computed tomography in the diagnosis of the pathologies in the ileocecal area

E. Onur, E. Igci, M. Secil, F. Obuz, O. Dicle; Izmir/TR

Learning objectives: The aim of this study is to present the contributions of the TUS and MS-CT on the diagnosis and differential diagnosis of the ileocecal area pathologies based on clinical cases.

Background: Ileocecal area includes the cecum, terminal ileum, ileocecal valve, and appendix. The diagnosis of the diseases in the ileocecal area is still difficult despite technological advances. The assessment of the whole segments of the GI system cannot be carried out correctly sometimes. Hence, the radiological imaging modalities gain importance in the diagnosis of the diseases in the ileocecal area. In this study, the transabdominal ultrasonography (TUS) and multi-slice CT (MS-CT) findings of the pathologies in the ileocecal area are compared and discussed with their clinical findings.

Imaging findings OR Procedure details: Inflammatory and infectious diseases that are involved in the ileocecal area, benign-malign neoplasias, ischemic pathologies, various radiological findings such as postoperative and/or the secondary changes in the radiotherapy, important characteristic properties in the diagnosis and differential diagnosis are discussed along with clinical, histopathological information and related literature.

Conclusion: Being a non-invasive technique, TUS can easily and rapidly be used in the ileocecal pathologies. It also enables the assessment of the outer-colon pathologies and their complications.

P-126

Retrospective comparison between video capsule endoscopy and MSCT enterography in the assessment of bowel pathologies

A. Garlaschi, L. Bacigalupo, E. Biscaldi, D. Schettini, M. Oppezzi, G.A. Rollandi; Genoa/IT

Purpose: This retrospective study compares the results of video capsule endoscopy (VCE) and MSCT enterography in the assessment of bowel pathology.

Material and methods: Thirty-four patients examined first with VCE and then with MSCT enterography were extracted from our 2007 patient database including 186 MSCT exams and 101 VCE exams. MSCT examinations of these 34 patients were mainly requested for anemia (n=11), diarrhea (n=8), positive fecal occult blood test (n=3), and abdominal pain (n=3). Contrast enhanced MSCT exams were performed after distension of the bowel with water or polyethylen glycol at the portal phase. The PillCam (Given Imaging) was used for the VCE exams.

Results: In 26/34 cases, there was agreement between VCE and MSCT. In 6/34

cases, VCE identified pathology not detected at MDCT: mucosal erosions (n=2), angiodysplasia (n=2) and Crohn's disease (n=2). In 2/34 cases MSCT, identified findings not detected at VCE: jejunal adenocarcinoma (n=1) and colic adenocarcinoma of the hepatic flexure (n=1). Significant non bowel pathologies were identified by MSCT in 7 cases.

Conclusion: Our data appear in accord with the current literature that report better results of VCE compared to MSCT for the assessment of pathology of the bowel mucosa. Still, MSCT appears able to identify lesions missed by VCE and depict non bowel pathology.

P-127

Utility of MDCT enterography with neutral enteral and IV contrast enhancement in detection of A-V malformation

E.C. Turupolij, G. Tóth, L. Tóth, V. Bérczi; Budapest/HU

Learning objectives: To show the usefulness of MDCT enteroclysis in the diagnosis of A-V malformation causing GI bleeding. To show the typical CT signs of A-V malformation.

Background: MDCT enteroclysis has proven to be useful for evaluating minimal bowel wall thickening and pathological dilatations of arteries and veins in bowel wall and mesentery. Our goal was to localise the focus of GI bleeding if gastroscopy and colonoscopy were negative. We present the typical imaging findings of our experience of MDCT enteroclysis. We demonstrate some of our cases.

Imaging findings OR Procedure details: From December 2005 to January 2007, 220 CT enteroclysis were performed to investigate unexplained anaemia or GI bleeding. Positive findings were demonstrated in 35 of 220 patients. We found 6 A-V malformations, confirmed by surgery or interventional procedure. CT enteroclysis were performed using the following parameters: slice 1mm, with overlap scans, reconstruction interval 1mm, after administration of methylcellulose by nasojejunal tube, before and after infusion of 120 ml iv. contrast agent, at a rate of 4 ml/s with a scan delay of 35 seconds. In all cases, multiplanar and curved planer reformatted images were performed. Collimation was 16x0.75 mm. We studied normal appearances and pathological changes (wall thickening, pathological vessels, enhancement, extravasation, and mesenteric changes).

Conclusion: MDCT enteroclysis with neutral enteral and IV contrast can be a good tool in detecting A-V malformation in small bowel.

P-128

Small bowel obstruction on multidetector-row CT: a to z

J.K. Lee, S.Y. Baek; Seoul/KR

Learning objectives: 1. To understand the definition of SBO differentiating from adynamic ileus. 2. To explain degrees of SBO on MDCT. 3. To detail various causes of SBO on MDCT. 4. To illustrate complications of SBO on MDCT. 5. To discuss the advantage of MDCT for deciding proper management of patients with SBO.

Background: Imaging has played an important role in the evaluation of small bowel obstruction (SBO). Recent advances in the technology enable CT to be the most accurate modality for diagnosing SBO. Multidetector-row CT (MDCT) has been reported to have an accuracy of 78–100% for the detection of complete and incomplete high-grade small bowel obstruction and to have accuracy of 63–100% for detection of strangulation. Therefore, radiologists should be familiar with various findings of SBO on MDCT. Information from MDCT is essential for deciding proper management and subsequent operation as well as diagnosing SBO.

Imaging findings OR Procedure details: For the definition, SBO is differentiated from adynamic ileus on MDCT. Degrees of SBO are defined by MDCT. This exhibition covers various causes of SBO visualized on MDCT such as adhesion, hernias, tumors, inflammation, bezoar, intussusception, etc. Complications of SBO including strangulation and perforation are demonstrated on MDCT.

Conclusion: MDCT is the most accurate imaging modality for diagnosing SBO. MDCT provides essential information for deciding proper management of patients with SBO.

P-129

Usefulness of the multidetector PEG-CT and enteroclysis CT in the evaluation of the small bowel neoplasms

L.M. Minordi, A. Vecchioli, P. Mirk, G. Poloni, L. Bonomo; Rome/IT

Purpose: To evaluate the reliability of multidetector CT (MDCT) in evaluation of small bowel neoplasms (SBN).

Material and methods: 120 patients with suspected small bowel disease were studied by 16 MDCT after administration of oral polyethylene glycol solution (n=56) or after administration of methylcellulose by nasojejunal tube (n=64). Unenhanced and contrast-enhanced CT were performed. Contrast-enhanced CT images were acquired 40 seconds after i.v. injection of 130 mL contrast agent at a rate of 3 mL/sec. Post-processing and multiplanar reformatting and interpretation were performed at the end of the exams.

Results: 15 SBN were found (6 patients with non-Hodgkin lymphoma, 3 with carcinoid tumour, 2 with Peutz Jeghers syndrome, 2 with adenocarcinoma, 2 with metastasis from melanoma, and 1 with lipoma); in the remaining cases, 58 cases of Crohn's disease and 7 other abnormalities were detected. All findings were confirmed by barium studies, surgery or endoscopy.

Conclusion: MDCT with neutral intestinal contrast and IV contrast seems to be a reliable method in the diagnosis of SBNs.

P-130

New imaging modalities in Crohn's disease

E. Frampas, F. Leaute, G. Meurette, A. Bourreille, B. Dupas; Nantes/FR

Learning objectives: To know the different new imaging modalities in CD. To recognize the different forms of disease. To understand the impact of imaging description for therapeutics. To write an optimal report to answer clinicians' questions.

Background: Crohn's disease is a chronic inflammatory disease involving young people. Indications and monitoring of new treatments require a more precise evaluation of disease extent, severity and activity. We propose an educational study including all imaging modalities in CD (US, MDCT, MRI, videocapsule) involving bowel, liver, and pelvic floor.

Imaging findings OR Procedure details: Early detection relies on endoscopy and videocapsule if not contraindicated by stenosis. MDCT and MRI help in defining disease extent. MRI has a marked advantage in pelvic floor evaluation, searching for abscesses and fistulas. Whatever the imaging modality is, description has to be optimal, assessing inflammatory activity, combining morphologic abnormalities and enhancement patterns, localization and length of disease including stenosis and complications. Optimal protocols and reports will be presented in order to answer clinicians' questions for therapy and illustrated.

Conclusion: The role of imaging has changed dramatically over the recent years due to technical improvement and new therapies. Acute complications seem to be best evaluated with MDCT, while MRI is a major tool for activity evaluation and pelvic examination. Disease characteristics, treatment challenges, imaging modalities advantages and limits have to be known by radiologists.

P-131

Differentiation of inflammatory and fibrostenotic strictures in Crohn's disease using CT enteroclysis

K. Sandrasegaran, D. Maglante, M.V. Chiorean; Indianapolis, IN/US

Purpose: To determine the accuracy of CT enteroclysis (CTE) in differentiating inflammatory and fibrostenotic strictures in patients with Crohn's disease.

Material and methods: Retrospective review of CTE database was performed to identify patients with CD who had preoperative CTE. CTE findings were reviewed, blinded to pathology findings, for mucosal and mural enhancement, wall thickness, mesenteric vascularity and the presence of adenopathy and strictures. The presence of inflammation and fibrostenosis were scored on 4- and 3-point scales, respectively. Patients were excluded if they had non-resective surgeries or a diagnosis of malignancy.

Results: Of the 54 patients enrolled, 10 were excluded. The remaining patients (61% female, 84% white) underwent 44 surgical interventions generating 47 bowel segments that were pathologically analyzed. The accuracy of CTE for inflammatory and fibrostenotic lesions was 76.6 and 78.7%. There was good correlation of pathological findings with CTE inflammatory (Spearman's $r=0.7$,

$p < 0.0001$) and fibrostenosis ($r = 0.6$, $p < 0.0001$) scores. The pathological presence of inflammation was significantly associated with CTE findings of mucosal hyperenhancement and mesenteric hypervascularity (Mantel-Haenszel Chi-square $p = 0.04$, and < 0.0001 , respectively). The pathological presence of fibrostenosis was significantly associated with the presence mural thickening and absence of mesenteric hypervascularity ($p = 0.001$ and 0.007 , respectively).

Conclusion: CTE may reliably differentiate between inflammatory and fibrostenotic lesions and may have an important role in the management of Crohn's disease.

Diagnostic / GI Tract / Stomach

P-132

The radiographic appearance of band erosion with intragastric penetration as a late complication of laparoscopic gastric banding

M. Dvoyris¹, M. Vasserman², P. Gottlieb²;

¹Petah Tikva/IL, ²Zerifin/IL

Purpose: Laparoscopic adjustable gastric banding (GB) is a popular bariatric operation. Gastric band erosion, as a late complication of ALBG, is not always diagnosed properly in outpatient clinics. Its variable clinical presentation complicates the diagnosis. The purpose of our study is to establish the proper radiographic signs for this complication.

Material and methods: GB was performed on 310 patients between 1998 and 2006. Band erosion developed in 5 patients (1.6%) and was diagnosed in the period of 12–60 months post-surgery. Plain abdominal film, GI-series, CT scans and endoscopy were used during the diagnostic process.

Results: Clinical findings included epigastric abdominal pain, an increase in body mass, vomiting, access port infection and gastrocutaneous fistula. However, some patients were asymptomatic and their diagnosis was established through GI-series. The pathognomonic sign of band erosion in GI-series is a flow of contrast outside the band. This sign is commonly associated with an unlikely position of the band, which appeared partially or completely inside the gastric lumen. Extraluminal air near the band is a sign of gastric wall perforation, and a fistula may be present.

Conclusion: Following the initial tear, the band will slowly grow through the gastric wall and may penetrate into the lumen of stomach. The radiographic appearance of this condition is pathognomonic, and the condition will usually require a prompt surgical intervention.

P-133

MDCT of the gastric submucosal tumors: spectrum of diseases

J.H. Lee, J.K. Kim, T.H. Kim; Suwon/KR

Learning objectives: 1. To demonstrate the spectrum of imaging findings of gastric submucosal tumors. 2. To understand the radiologic findings of these lesions on the basis of endoscopic and pathologic findings. 3. To describe key imaging features for the differential diagnosis of various lesions.

Background: Multidetector computed tomography (MDCT) offers near-isotropic imaging of the stomach and allows more detailed evaluation of gastric morphology by high-quality multiplanar reformation and three-dimensional reconstruction of gastric images.

Imaging findings OR Procedure details: We retrospectively reviewed the imaging findings of the various gastric non-epithelial tumors and various lesions that may mimic gastric submucosal tumors. Diagnostic pitfalls, diagnostic difficulties, and differential diagnoses are emphasized. Other imaging modalities such as EUS and endoscopic or gross pathologic findings were compared. Gastric non-epithelial tumors include leiomyoma, schwannoma, granular cell tumor, inflammatory fibroid tumor, glomus tumor, leiomyosarcoma, GIST (gastrointestinal stromal tumor), Kaposi sarcoma, malignant lymphoma, and lipoma. Other lesions that may mimic gastric submucosal tumors include carcinoid, gastric varix, ectopic pancreas, and duplication cyst.

Conclusion: With this exhibit, the radiologist will have an enhanced understanding of various gastric submucosal tumors including histopathology and radiologic features. Familiarity with radiologic findings of these various lesions will make correct diagnosis possible and help the endoscopist and surgeon.

P-134

There is more to it than what meets the eye: subtle but important CT findings in Bouveret's syndrome

S. Gan, S. Roy-Choudhury, S. Agrawal, A. Pallan; Birmingham/UK

Learning objectives: We aim to alert the physician to some previously undescribed signs that can help in the diagnosis of an uncommon condition.

Background: Gallstones are a rare cause of duodenal or gastric outlet obstruction. It is usually diagnosed radiologically, while investigating insidious and non-specific symptoms. Rigler's triad of pneumobilia, bowel distension and an ectopic gallstone, however, is seen in very few cases of such high obstructions. Even with CT scans, 25% of cases are still misdiagnosed – often because the size of the offending gallstone is underestimated. If the size of the stone is more accurately assessed, then it is likely that fewer cases would be missed.

Imaging findings OR Procedure details: We describe some subtle but nonetheless important CT findings that will help to better assess the size of an intra-duodenal gallstone. These include compressed air in dependant areas within the duodenal lumen, an area of soft tissue density surrounding the calcified rim of the stone, a faint lucency within or beyond this soft tissue area which could represent laminations of fat or air within the stone, and a focal distension of the duodenum proximal to the point of obstruction, indicative of an intra-luminal mass.

Conclusion: It is highly unlikely that any one sign will be seen in all patients with Bouveret's syndrome, but a combination of findings should increase the likelihood of making the correct diagnosis.

P-135

The evidence base for staging gastric cancer

B.G. Rock¹, D. Buckley², M. Puckett²;

¹Plymouth/UK, ²Torquay/UK

Purpose: Accurate staging of gastric adenocarcinoma is essential to identify patients who will benefit from radical curative surgery, spare those without prospect of cure from invasive procedures, and plan appropriate oncological/palliative approaches. Following technological advances in diagnostic staging modalities over the past ten years, ongoing appraisal of evidence for the most appropriate staging technique is required in light of the ever-growing literature body.

Material and methods: A systematic PubMed literature search was performed using evidence-based methodology. Articles published between 1997 and 2007 were identified using appropriate Medical Sub-Heading (MeSH) search terms. Critical appraisal of literature was performed.

Results: Much of current practice is based on relatively small single centre comparative studies. Whilst evidence exists to guide use of CT, EUS and laparoscopy in staging, the evidence base for use of modalities such as PET and MRI remains limited. A brief overview of the literature is presented, and systematic flaws in current evidence are discussed.

Conclusion: The roles of diagnostic modalities used in staging gastric cancer are evolving; whilst evidence supports the established roles of CT, EUS and laparoscopy, evidence for other modalities currently remains in its infancy.

P-136

Bariatric procedures: digital fluoroscopic role in complications evaluation

P. Giusti, S. Giusti, V. Morigoni, A. Bardine, M. Anselmino, C. Bartolozzi; Pisa/IT

Purpose: To show the digital fluoroscopic examination usefulness and accuracy in the follow up of patients who underwent bariatric procedures (BA).

Material and methods: From 2001 to 2006, we radiologically reviewed 408 patients submitted to adjustable gastric band, 299 gastric bypass, 16 sleeve gastrectomy and 107 intragastric balloons. The early examinations were performed 2–5 days after the surgery using water-soluble iodinated contrast agent, to highlight gastroenteric canalization, fistulas or contrast media leakages. The late examinations were performed one year after, using barium sulphate.

Results: We observed the following early complications: 18 leakages and one communication between the pouch and the gastric remnant, depicted after gastric bypass. The late complications were: 40 migrations of gastric band, 10 migrations of intragastric balloon and one dehiscence of sleeve-gastrectomy.

Conclusion: The rise in BA is exponential because of their greater acceptance

due to the high incidence of patients affected by pathologic obesity. Although post surgery complications rate is relatively low, they can result in severe disability. Digital radiology, in all cases, enables the detection of early and late postoperative complications, showing the right treatment and so gaining a fundamental role in follow up of patients who underwent BA.

P-137

Postoperative stomach: a pictorial review

C. Leal, J. Raposo, A. Vasconcelos, P. Alves, N. Costa, R.M. Marques; Lisbon/PT

Learning objectives: To illustrate the principal gastric surgery protocols, recognizing the important role of radiology in the follow-up of these patients.

Background: Gastric surgery may have a place in the therapeutic approach of tumors and peptic disease, but also for morbidly obese patients. Knowledge of the surgical protocols and postoperative anatomy is essential for radiologists to be proficient in the specific evaluation of this frequent clinical condition.

Imaging findings OR Procedure details: Bilroth I and II, gastric bypass, sleeve gastrectomy, adjustable gastric banding and biliopancreatic diversion (duodenal switch) are some of the surgical protocols presented and illustrated. Upper GI series still remain the primary radiological tool, because of a better anatomic depiction.

Conclusion: Radiology plays a crucial role in the postoperative evaluation of gastric surgical procedures, both in the immediate as well as late follow-up periods. For that, the radiologist must be aware of the various technical approaches in gastric surgery.

P-138

Giant paraesophageal hernia with intrathoracic chronic gastric volvulus

B. Baysal, C. Cimsit, H. Baysal, A. Hayirlioglu, I. Kuru, R. Yigitbasi; Istanbul/TR

Purpose: We report a giant hiatal hernia with intrathoracic organoaxial chronic gastric volvulus, which is an uncommon entity and describe the imaging findings through chest X-ray, upper gastrointestinal barium studies, and multidetector computerized tomography (MDCT).

Material and methods: A 70-year-old female was admitted to the hospital with a two month history of retrosternal pain and epigastric distention. Chest radiograms and plain abdominal radiograms were followed by upper gastrointestinal barium studies, MDCT, and endoscopy.

Results: The chest X-ray revealed a retrocardiac lesion with air-fluid interface. On MDCT scans, the entire stomach was displaced into the thoracic cavity and was rotated 180° along the longitudinal axis. The large diaphragmatic defect was seen on the multiplanar reconstruction CT images. The patient underwent laparoscopic repair.

Conclusion: The most common cause of gastric volvulus is hiatal hernias, but the principal predisposing factor is ligamentous laxity. Gastric volvulus can be classified according to its location with reference to the diaphragm and on the basis of the axis of rotation as organoaxial and mesenteroaxial volvulus. The diagnosis is radiologically suspected if air-fluid interface is seen in the chest X-ray. CT provides a comprehensive intrathoracic lesion description with respect to the anatomic landmarks by means of the multiplanar imaging features. Intrathoracic organoaxial gastric volvulus may end up with complications leading to surgical emergency or may get elective treatment because of non-specific chronic symptoms.

P-139

Comparison of blinded and partially blinded evaluation for detection of gastric cancer using MDCT

H.J. Kim, D.H. Lee, J.W. Lim, Y.T. Ko; Seoul/KR

Purpose: To evaluate the accuracy of blinded versus partially blinded evaluation for detection of gastric cancer using MDCT.

Material and methods: Forty-four patients with gastric cancer underwent MDCT. Surgery was performed in 38 patients and endoscopic mucosal resection in six patients. For blinded evaluation, 38 MDCT examinations which had no focal gastric lesion on endoscopy were added. Two radiologists, blinded to the presence, number, and location of tumor, evaluated transverse CT and MPR images of 82 MDCT examinations. For partially blinded evaluation, the same radiologists evaluated transverse CT and MPR images of 44 MDCT examinations

in patients with gastric cancer.

Results: Forty-five gastric cancers were found in surgical and EMR specimens. Detection rates of gastric cancer on blinded and partially blinded transverse CT and MPR images were 62% (28/45), 64% (29/45), 64% (29/45), and 71% (32/45), respectively. False detection rates on blinded and partially blinded transverse CT and MPR images were 7% (3/45), 7% (3/45), 13% (6/45), and 11% (5/45), respectively. Non-detection rates on blinded and partially blinded transverse CT and MPR images were 31% (14/45), 29% (13/45), 22% (10/45), and 18% (8/45), respectively. There is no statistical significance in comparison between blinded and partially blinded evaluation in detection rate, false detection rate, and non-detection rate of gastric cancer.

Conclusion: The detection rates of gastric cancer using MDCT show no specific difference between blinded and partially blinded evaluation.

P-140

Follow up CT findings of various types of recurrence after endoscopic resection of early gastric cancer

S.S. Hong, J.H. Kim; Seoul/KR

Learning objectives: To review the cases of recurrence after endoscopic treatment of EGC. To analyze the missing cause on routine follow up CT.

Background: When performed in carefully selected cases, the endoscopic treatment of early gastric cancer (EGC) yields results which are comparable to the conventional surgical treatment, but with lower morbidity and mortality and better quality of life. In spite of early detection and curative treatment, local or systemic recurrence can develop in various locations of the abdomen and pelvic through the several routes. In this exhibit, we will present the recurrence pattern and site, which demonstrated on follow up CT after endoscopic treatment of EGC. Emphasis lay on analysis of missed lesion which was not identified on routine preoperative CT or follow up CT, especially lymph node metastasis.

Imaging findings OR Procedure details: The main pattern of tumor recurrence after endoscopic treatment of EGC which was presented on follow up CT was as follows: local recurrence of stomach, lymph nodes, peritoneal seeding, hematogenous metastasis including the liver, lung, or bone, and rare unusual metastasis.

Conclusion: Follow up CT plays an important role in identification of tumor recurrence after endoscopic treatment of EGC. Because early identification may allow patients to respond better to chemotherapy or radiation therapy, familiarity with the CT findings of tumor recurrence after endoscopic treatment of EGC is important.

P-141

Intra gastric hematoma mimicking a gastric neoplasm: clinical and imaging findings

D. Emlik, D. Aydogdu Kiresi, S. Gumus, K. Odev; Konya/TR

Purpose: To present the radiological findings of a large gastric hematoma secondary to duodenal peptic ulcer disease.

Material and methods: 68 years-old male with severely having epigastric pain accompanied by melena and hypotension found to have a focal mass in the epigastric region. There was no vomiting or hematemesis. The patient refused the barium study because of his clinical and hematological deterioration. Ultrasonography, spiral CT and T1 and T2 MRI were performed.

Results: Ultrasonography showed a large heterogeneous hypoechoic mass with having multiple acoustic posterior shadowing areas within the stomach. Spiral CT scan revealed a marked dilatation of the stomach and a huge, moveable hypodense mass inside the stomach and duodenum. Precontrast and postcontrast CT scan revealed that intra gastric mass had the same density in both studies. MRI confirmed the CT findings. At surgery, there was a duodenal ulcer and huge hematoma within the lumen of the stomach and duodenum that caused complete obstruction of the passage. During the operation, active bleeding was not controlled and unfortunately the patient died in a few hours.

Conclusion: Although endoscopy and barium studies are still very important for the diagnosis of upper GI bleeding, CT scan may also be a useful method in determining of complications that occur due to ulcer bleeding.

Diagnostic / GI Tract / Swallowing

P-142

The videofluoroscopic swallowing study: clinical and radiological correlation

C. Cousins, E.M. Armstrong, B. Fox; Plymouth/UK

Learning objectives: To provide a comprehensive overview of the videofluoroscopic swallowing study in modern radiological practice, focussing on the importance of clinico-radiological correlation in identifying abnormalities and their impact on patients' lives.

Background: Swallowing abnormalities are a diverse group of disorders affecting patients of every age. The videofluoroscopic swallowing study (VFSS) is a technique commonly used to investigate this problem. It requires an excellent understanding of the anatomy, physiology and pathology of swallowing. Most importantly, VFSS is a dynamic study requiring real-time correlation of clinical and radiological findings if it is to be used to full advantage.

Imaging findings OR Procedure details: We describe the comprehensive VFSS service provided in our centre. We outline the technique itself, highlighting tips for best practice and potential pitfalls. We then review the range of disorders encountered, stressing the importance of clinico-radiological correlation by presenting video clips of patients with various disorders performing the study alongside the imaging findings themselves.

Conclusion: VFSS is a dynamic technique demanding excellent clinical and radiological skills. We review the art and science of this important aspect of modern radiological practice.

Diagnostic / Liver / CT / MRI

P-143

Monitoring therapeutic response of liver metastases from colorectal cancer treated with percutaneous radiofrequency ablation by diffusion-weighted MRI

E. Szurowska, J.M. Pierkowska, D. Zadrozny, E. Izycka-Świeszewska, W. Adamonis, M. Studniarek; Gdansk/PL

Purpose: The purpose of our study was to evaluate the usefulness of quantitative diffusion-weighted MRI in monitoring therapeutic response of liver metastases from colorectal cancer treated with percutaneous radiofrequency ablation (RFA).

Material and methods: 40 patients (15 women and 25 men) with 72 hepatic metastases from colorectal cancer were prospectively evaluated with diffusion-weighted imaging (DWI) one day before and 6 weeks after RFA using 1.5 T MR system. Apparent diffusion coefficients (ADCs) were measured in all lesions before and after treatment for different b factors (b= 0-15; 0-30; 0-300; 0-500; 0-2000 s/mm²) and the relative posttreatment change in the ADC value for each tumor was calculated. All lesions were divided into two groups based on their treatment response using multislices CT scans performed 6- and 24-weeks after therapy: complete response (group A) was defined as avascular liver lesion in CT scans and incomplete response (group B) when residual tumor was observed in CT images. Changes in ADC value were compared between two groups.

Results: In 54 metastatic foci, complete responses for RFA therapy were observed (group A) and in the rest of lesions (18 metastases) active neoplastic processes were noted. Change in the ADC value and in relative post-treatment ADC value was statistically greater in group A. The mean post-treatment ADCs and relative post-treatment ADCs of completely responding metastases increased significantly 6 weeks after RFA compared to mean pretreatment and relative pretreatment ADCs (Wilcoxon-test, p=0.006 and 0.001).

Conclusion: The ADC value on DWI is a promising tool for monitoring the therapeutic response of liver metastases treated with percutaneous RFA.

P-144

Pictorial review of combined hepatocellular and cholangiocarcinoma focused on the MRI features

J.H. Lee¹, J.K. Kim¹, T.H. Kim¹, J.Y. Choi², M. Park², K.W. Kim²; ¹Suwon/KR, ²Seoul/KR

Learning objectives: To review the MRI features of combined HCC-CC and to correlate the radiologic and pathologic findings.

Background: Combined hepatocellular and cholangiocarcinoma (HCC-CC) is a rare tumor showing histological evidence of both hepatocellular and biliary epithelial differentiation. Because of its rarity, there have been few reports about the imaging findings of this tumor.

Imaging findings OR Procedure details: We retrospectively reviewed MR findings of pathologically confirmed combined HCC-CC in 11 patients (all men; mean age, 50.9 years). The tumors were divided into three groups by gross pathologic examination: HCC type (n=2), CC type (n=8), and collision type (n=1). The images and pathologic findings were retrospectively compared. All patients showed high signal on T2 weighted images. Three tumors revealed focal high signal intensity on T1 weighted image due to necrosis. The CC types demonstrated peripheral rim-like enhancement (n=8) and irregular margin (n=7) with cirrhotic feature (n=8). The HCC types were well enhanced in the arterial phase and low signal intensity in the delayed phase. Lymph node enlargement and bile duct invasion were observed in two and one patients, respectively.

Conclusion: The diagnosis of combined HCC-CC should be considered if the tumors have similar findings to cholangiocarcinoma on cirrhotic liver. Although the combined HCC-CC is a rare hepatic tumor, MR image can predict the dominant component of HCC-CC.

P-145

Hepatic capsular enhancement mimicking Fitz-Hugh-Curtis syndrome in various diseases: its characteristics and diagnostic role

S.J. Park, J.S. Park, B.H. Yi, H.K. Lee, H. Lim; Bucheon-si/KR

Learning objectives: 1. To learn disease spectra showing HCE, similar to FHCS. 2. To discuss the incidence and pathophysiology of HCE. 3. To illustrate various CT features of HCE and discuss its diagnostic role.

Background: Fitz-Hugh-Curtis syndrome (FHCS) is characterized by focal perihepatitis accompanying pelvic-inflammatory-disease (PID). Hepatic capsular enhancement (HCE) on arterial phase of CT is a well recognized finding of FHCS. But we can see HCE in patients without evidence of PID. Therefore, the authors retrospectively reviewed 797 arterial and portal phases of abdominal CT to evaluate incidence of HCE to classify HCE pattern and evaluate causative diseases of HCE.

Imaging findings OR Procedure details: HCE are presented in 47 patients (5.9%) of arterial phase abdominal CT scan. HCE was persistently shown on portal phase scan in 32 of 47 patients (68.1%). Six patients (12.8%) were diagnosed as FHCS. The other causes of HCE include 20 inflammatory conditions (panperitonitis (n=7), choledocholithiasis (n=4), pancreatitis (n=2), diverticulitis (n=1), cholecystitis (n=1), hepatitis (n=1), inflammatory bowel disease (n=1), APN (n=1), phlebitis (n=1), postoperative state (n=1)), 13 malignancy (gastrointestinal (n=9), hepatobiliary (n=2), and gynecological (n=2)), and 8 other diseases. HCE pattern of focal or diffuse was not significantly different between inflammation and malignancy (p=0.246).

Conclusion: HCE is not a unique finding in FHCS, and it could be presented in broad disease spectra of inflammation, malignancy, and the other diseases in the abdomen and pelvis. HCE may be one of the important findings that represent any kinds of inflammation or malignancy in the abdomen and pelvis.

P-146

Morphologic changes of the liver: how to recognize and analyze at CT and MRI

O. Bruno¹, G. Brancatelli², A. Galluzzo², M. Giraud¹, M.P. Vullierme¹, V. Vilgrain¹; ¹Clichy/FR, ²Palermo/IT

Learning objectives: To review the CT and MRI findings of liver morphology changes occurring in different conditions.

Background: Knowledge of anatomic landmarks is crucial to recognize morphologic changes of the liver.

Imaging findings OR Procedure details: Morphologic changes of the liver may be lobar or segmental and are mostly related to biliary strictures or vascular obstruction. We will review the most helpful hepatic anatomic landmarks in order to recognize liver morphology changes at imaging. We will review the morphologic changes occurring in liver cirrhosis and in those diffuse liver diseases that could be mistaken for cirrhosis, such as chronic Budd-Chiari syndrome, congenital hepatic fibrosis, pseudocirrhosis secondary to metastatic breast adenocarcinoma, and atrophy-hypertrophy complex secondary to cavernomatous transformation of the portal vein among others.

Conclusion: The goals of this exhibit are to increase the radiologists' ability to: differentiate cirrhosis from diffuse liver disease mimicking cirrhosis; generate a differential diagnosis among those conditions causing liver morphology changes; and understand what type of vascular and biliary changes are more often associated with focal and diffuse morphological changes of the liver.

P-147

Diffusion-weighted MRI in the evaluation of liver hydatid cysts

S. Bayramoglu, O. Kilickesmez, F. Palabiyik, E. Ozbalci, A. Kayhan, T. Cimilli; Istanbul/TR

Purpose: The purpose of our study was to evaluate the signal intensities of hydatid cysts on diffusion-weighted MRI (DWI-MRI) and the value of DWI in the differential diagnosis of simple and hydatid cysts of the liver.

Material and methods: Thirty-four simple and 73 hydatid cysts were included in this study. All hydatid cysts were examined by sonography and classified according to the World Health Organization. The diagnosis of hydatid cysts was confirmed by biopsy or positive serology. DWI were acquired using the following b values: 0,500 and 1000 s/mm². ADC maps were reconstructed from these images. On DW trace images, signal intensity of cysts were visually compared with the signal intensity of the liver using a 5 point scale. The signal intensity of the cysts, cyst to liver signal intensity ratios, ADC of the cysts and cyst walls, cyst to liver and wall to liver ADC ratios were compared between the groups quantitatively.

Results: All ADC values and ratios were shown to gradually decrease parallel to the maturation of cysts. In visual scoring with a b factor of 1000, the signal intensities were different between simple cysts and complete liquid type hydatid cysts (p=0.032).

Conclusion: Hydatid cysts show restricted diffusion parallel to the increase of their maturation. DWI may be helpful in differentiation of complete liquid type hydatid and simple cysts of the liver.

P-148

The hypointense liver lesion on T2-weighted images

L. Curvo-Semedo, J. Brito, B.J.A.M. Gonçalves, J.F. Costa, C. Marques, F. Caseiro-Alves; Coimbra/PT

Learning objectives: To discuss the causes and mechanisms of hypointensity of liver lesions on T2-weighted images. To illustrate the various types of focal liver lesions presenting this imaging finding.

Background: Contrarily to the most frequently seen MRI pattern, liver nodules may show total or partial hypointensity on T2-w images. T2-w hypointensity can be absolute or relative depending on the native signal intensity of the normal parenchyma and/or sequence used. Causes for absolute hypointensity include haemorrhage, iron (native or exogenous from contrast agents), calcium, copper or melanin deposition, and also abundant fibrous or smooth muscle stroma. Relative hypointensity is seen in lesions with a fatty component.

Imaging findings OR Procedure details: Despite rare, low signal intensity regarding the surrounding liver on T2-w images may be found in a wide spectrum of lesions. Examples shown include focal nodular hyperplasia, hepatocellular adenoma (HCA), hepatocellular carcinoma (HCC), metastases (including metastatic melanoma), leiomyoma, nodular regenerative hyperplasia/regenerative nodules, dysplastic nodules, siderotic nodules, nodules in Wilson's disease, granulomas and inactive hydatid cysts. Lipoma, angiomyolipoma, HCA and HCC may also display T2-w hypointensity depending on the technique used to achieve fat-suppression.

Conclusion: T2-w hypointensity, although a less common presentation of focal liver lesions, has a variety of causes. Their knowledge is helpful to derive the correct diagnosis, integrated in the clinical context. In some cases, however, radiological-pathological correlation is necessary to understand the full-blown picture for the hypointense appearance.

P-149

Imaging findings of portal venous pathology

D. Karaosmanoglu, M. Karcaaltincaba, D. Akata, M.N. Ozmen, O. Akhan; Ankara/TR

Learning objectives: To demonstrate congenital and acquired portal venous pathology. To demonstrate CT and MR portography findings.

Background: Portal venous pathology is relatively common and can be well

demonstrated by CT, US and MRI.

Imaging findings OR Procedure details: We searched our archive for portal vein (PV) pathology. A wide array of several acquired and congenital disorders of the PV and its branches are presented in this educational exhibit with CT and MRI findings. Among these are acute and chronic thrombosis of the PV and cavernomatous transformation, agenesis of the PV, gas in the PV due to mesenteric ischemia, bland and tumor thrombus of the PV in the setting of HCC, invasion of the PV secondary to extrahepatic malignancies and a very rare case of agenesis of the PV in a pediatric patient with biliary agenesis. Also, imaging findings of patent ductus venosus and anomalous pulmonary venous return to PV are included.

Conclusion: Prompt and precise diagnosis of PV pathology may dramatically affect the treatment work-up of the patients. Therefore, we think that the in-depth knowledge of these processes is the sine qua non of a successful practice in both abdominal and general radiology.

P-150

MRI after percutaneous liver tumor ablation

S. Tatli, M. Acar, K. Tuncali, S.G. Silverman; Boston, MA/US

Learning objectives: Surveillance of MRI protocol after percutaneous liver tumor ablation. Typical MRI appearances of uncomplicated liver tumor ablation site, residual recurrent tumors, and post procedure complications.

Background: Percutaneous tumor ablation techniques have attained an important role in the management of primary and metastatic liver tumors. Magnetic resonance imaging (MRI) has been used in the surveillance of these patients due to exquisite soft tissue contrast capability without ionizing radiation. As more patients undergo liver tumor ablation procedures, it will become increasingly important that radiologists be able to recognize typical postablation MRI findings. In our department, more than 200 liver tumors (130 cryoablations, 99 RF ablations, and 16 alcohol injections) have been ablated, a majority of which has been followed up with MR imaging. In this presentation, we reviewed post ablation MR imaging features of liver tumors with illustrated examples.

Imaging findings OR Procedure details: After successful ablation, liver tumors typically show no enhancement. Although a thin peripheral rim of enhancement may be seen in completely ablated tumors and may last several months, areas of nodular enhancement at the site or vicinity of an ablation zone is suggestive of residual/recurrence tumor.

Conclusion: MRI is a useful modality in surveillance of liver tumor following percutaneous ablation. Subtraction is helpful to demonstrate unenhanced ablation zone and detect abnormal enhancement.

P-151

The value of the multi-detector-row CT angiography in the study of hepatic arterial variants

L. Saba, R. Sanfilippo, R. Montisci, G. Mallarini, Cagliari/IT

Learning objectives: 1) To review hepatic arterial vascular anatomy. 2) To learn, according to Michels' classification, the types of hepatic arteries anomalies and its frequencies. 3) To analyze the MDCT technical parameters to be used: volume and concentration of contrast material, mAs and kVs, and the correct delay time. 4) To understand the indications for performing hepatic CT angiography underlining radiation exposure, cost and diagnostic efficacy. 5) To show which post-processing techniques can be used including multi-planar reconstruction (MPR), maximum intensity projection (MIP) and volume rendering (VR).

Background: The study of hepatic arteries results is extremely important in several pathological conditions, in particular in pre-surgical planning for patients undergoing hepatic surgery or in patients undergoing selective chemotherapeutic infusion. Multi-detector-row CT angiography (MDCTA) can produce excellent image quality and detail of hepatic arteries by correctly identifying anatomical variants.

Imaging findings OR Procedure details: In this educational exhibition, we describe MDCTA technical parameters for the study of hepatic arteries. We present also examples both of normal hepatic arteries and hepatic variants by using axial images and reconstruction methods (MIP, MPR and VR). We present and discuss some relevant cases in order to underline benefits and pitfalls of MDCTA.

Conclusion: MDCTA allows an optimal visualization of hepatic arteries. The use of MIP and VR post-processing techniques allows an excellent arterial visualization, extremely useful to the surgeons prior to hepatic surgery.

P-152**Hepatic arterial anatomy: modern concepts and clinical implications of 64-row CT angiography**C.N. de Cecco¹, R. Ferrari², P. Paolantonio², M. Rengo¹, F. Vecchietti², A. Laghi²; ¹Rome/IT, ²Latina/IT

Learning objectives: - To know the main hepatic vessel anomalies. - To know the 64-row CT angiography protocols and clinical implications.

Background: - To review the hepatic arteries anomalies and their clinical relevance. - To analyze Michels' classification according to recent literature. - To evaluate the clinical implications of state-of-the-art vascular imaging with 64-row CTA on the depiction of these anomalies.

Imaging findings OR Procedure details: 1) Hepatic arterial supply: Normal anatomy. 2) Hepatic arterial supply: Anatomic variations. 3) Michels' classification and literature review. 4) Surgical and radiological implication of vascular anomalies. 5) State-of-the-art vascular imaging and its clinical relevance. 6) Future directions.

Conclusion: - Aberrant hepatic arteries can be of major surgical significance. Preoperative knowledge of these anomalies is of greater importance in the planning and performance of surgical and interventional radiological procedures in the upper abdomen. - The new generation of 64-row MDCT scanners allows an optimal visualization of splanchnic vascular anomalies, which is extended also to those vessels presenting a small calibre and slow flow resulting in a difficult recognition by other imaging techniques.

P-153**Current staging of primary hepatic tumor: imaging implications**

F. Cavalheiro, B. Graça, L. Curvo-Semedo, M.F.S. Seco, B. J.A.M. Gonçalves, C. Marques, F. Caseiro-Alves; Coimbra/PT

Learning objectives: Providing an educational and pictorial review of radiologic staging of primary hepatic tumors. Discussing the potential extent of resection required in operable candidates.

Background: The resectability of primary hepatic tumors depends largely on the distribution of lesions in the liver and their relationships to vascular structures. Accurate delineation of the tumor extent poses a great challenge to modern imaging methods and MDCT as a single modality has the potential to comprehensively evaluate each patient for all the criteria of unresectability. It also has the potential of obviating the need for preoperative angiography in most cases. Magnetic resonance imaging (MRI) along with magnetic resonance cholangiopancreatography (MRCP) is ideally suited to evaluate the bile ducts and also identifies intrahepatic mass lesions.

Imaging findings OR Procedure details: We will review HCC and intrahepatic colangiocarcinoma separately. Current staging system will be presented and illustrated in a multimodality approach, focusing of the criteria of resectability. MDCT 3D reconstructions and corresponding evaluation of the potential extent of resection required in operable candidates is discussed.

Conclusion: The role of imaging, particularly volumetric MDCT, is crucial in preoperative staging and determining resectability of primary hepatic cancer. Adequate preoperative staging affects the therapeutic management and outcome of patients.

P-154**Hepatic enhancement in multiphase MDCT: analysis of the different concentration and same iodine total dose with the same iodine flux administration in the same chronic liver disease patients**N. Takeyama¹, Y. Ohgiya², T. Hayashi¹, Y. Kinebuchi¹, H. Shinjyo³, T. Kitahara¹, T. Gokan²; ¹Yokohama/JP, ²Tokyo/JP, ³Fukushima/JP

Purpose: To evaluate the hepatic enhancement and image quality in patients who underwent contrast-enhanced dynamic imaging on MDCT twice using 80 ml of 370 mg I/ml contrast material (CM) and 100 ml of 300 mg I/ml CM with the same iodine flux administration during follow-up periods.

Material and methods: Twenty-four patients weighing 50–65 kg with cirrhosis or chronic hepatitis were the subjects of the study. MDCT examinations using 100 ml of 300 mg I/ml at a flow rate of 4.0 ml/sec (1.2 g/sec) in protocol A, and 80 ml of 370 mg I/ml at a flow rate of 3.2 ml/sec (1.184 g/sec) in protocol B were performed in the same patients. After unenhanced scans, multiphase scanning

at 25, 40, 70, 180 sec was started after CM injection. Bolus tracking and saline flushing were not used. The CT values of hepatic parenchyma, abdominal aorta, and portal vein were measured. Their mean enhancement value was quantitatively analyzed. Hepatic enhancement and vascular enhancement were assessed qualitatively using a 4-point scale.

Results: There were no significant differences between the two groups in the mean enhancement of hepatic parenchyma, abdominal aorta, and portal vein. Quantitative assessment for the segmental branch of hepatic artery, intrahepatic portal vein, and hepatic parenchyma show no significant difference between two groups.

Conclusion: We conclude that MDCT using 80 ml of 370 mg I/ml CM can decrease flow rate, while maintaining the same qualitative and quantitative performance.

P-155**Segmental high intensity on T1-weighted hepatic MR images**

M. Hashimoto, J. Heianna, K. Yasuda, J. Watarai; Akita/JP

Purpose: We evaluated the diagnostic importance of segmental high-intensity (SHI) areas not corresponding to mass lesions on T1-weighted MR images.

Material and methods: We conducted a retrospective investigation of hepatic MR images obtained from patients during a 4-year period at our institution. There were 16 patients (2.5%) with SHI areas not corresponding to a mass lesion. We compared MR images with plain computed tomographic (CT) scans (n=16), angiograms (n=12), and histologic findings (n=10).

Results: The segments with intrahepatic bile duct dilatation showed hyperintensity on T1-weighted images. In six of 16 patients, the biliary duct was more dilated in the area of hyperintensity than in areas without hyperintensity. The SHI areas appeared as areas of low attenuation (n=13), high attenuation (n=1), or isoattenuation (n=2) on plain CT scans. Histologically, these areas showed ductular proliferation and deposition of bile pigment within the hepatocytes.

Conclusion: Segmental areas of increased hyperintensity on T1-weighted images were probably due to intrahepatic cholestasis.

P-156**Incidence of new foci of HCC in patients who underwent radiofrequency ablation of HCC: role of MDCT**

T.V. Bartolotta, M. Maniaci, L. Putignano, A. Taibbi, M. Galia, M. Midiri, R. Lagalla; Palermo/IT

Purpose: To assess the incidence of new foci of hepatocellular carcinoma (HCC) by means of multidetector CT (MDCT) in patients undergone radiofrequency ablation (RFA) of HCC.

Material and methods: MDCT studies of 129 patients (mean age: 72 years), with RFA-treated HCC and followed-up for 1–68 months (mean: 22 months), were retrospectively reviewed to detect the presence of new foci of HCC, defined as hypervascular focus in the arterial phase with wash-out in the portal-venous or equilibrium phases, arising at least at 2.1 cm from the treated nodule either in the same or in a different liver segment. All new nodules were definitively proven through biopsy and/or MRI and contrast-enhanced US findings.

Results: 189 new HCCs (mean size: 1.7 cm) were detected in the same (n=38; 20%) or in a different (n=151; 80%) liver segment (p<0.001) in 70/129 (54.3%) patients, followed-up for 1–59 months (mean: 26 months). 25/70 patients had a single new HCC, whereas 45/70 patients had two (17 patients), three (10), four (6), five (4), six (3), seven (2) or eight (3) new HCCs. The remaining 59 patients without new HCC were followed-up for 1–68 months (mean: 15 months) (p<0.001).

Conclusion: MDCT follow-up in patients with RFA-treated HCC reveals, especially when follow-up is longer than one year, a high incidence of new HCCs mainly detected in a liver segment different from that of treated HCC.

P-157**Potentialities of multi-detector-row CT angiography in the study of hepatic vein variants**

L. Saba, G. Mallarini; Cagliari/IT

Learning objectives: The objectives of this work are: To understand the normal anatomy of hepatic veins and their variations. To study the CT technical parameters to be used and which techniques can be used including the visualization difference between maximum intensity projection (MIP), multi-planar reconstruc-

tion (MPR) and volume rendering (VR). To review the current indications for performing a study of hepatic veins by using multi-detector-row CT, underlining radiation exposure and diagnostic efficacy.

Background: A correct assessment of the hepatic vasculature and, in particular, precise delineation of hepatic venous architecture, is important in several conditions: in particular pre-surgical planning for patients undergoing hepatic surgery (tumor resection, transplants). Multi-Detector-Row CT Angiography (MDCTA), by using fast patient scanning and thin collimation, can obtain near-isotropic voxels, producing excellent image quality and detail.

Imaging findings OR Procedure details: In this work, we will present several imaging findings examples of normal anatomy of hepatic veins and their variants by using source axial images and post-processed methods. We present also relevant case studies.

Conclusion: MDCTA allows to obtain optimal image quality in the study of hepatic veins in order to correctly plan a liver resection.

P-158

MDCT of hepatic artery

M. Karcaaltincaba, B. Erol, D. Karaosmanoglu, D. Akata, M.N. Ozmen, O. Akhan; Ankara/TR

Learning objectives: To demonstrate normal MDCT findings of HA anatomy and its variations. To demonstrate MDCT findings of HA pathologies.

Background: MDCT enabled evaluation of hepatic artery (HA) anatomy and pathologies comparable to digital subtraction angiography. HA has many variations which is important in liver transplant donor evaluation. HA pathologies are rare but diagnosis by MDCT is possible.

Imaging findings OR Procedure details: We searched our archive for HA variations and pathologies. MDCT examinations were performed by 4-, 16- or 64-MDCT. MIP and volume rendered images were used for display. HA pathologies included are aneurysms, arterioportal fistula, vasculitis, stenosis and occlusion. HA aneurysms can be fusiform, giant, segmental and multiple. HA dilatation can be seen in Osler-Weber-Rendu disease and portal hypertension.

Conclusion: Various pathologies and anatomic variations of HA can be confidently diagnosed by MDCT.

P-159

Feasibility of CT perfusion in liver metastases of endocrine tumor

A. Guibal, N. Mennesson, A. Guyennon, J. Chayvialle, C. Lombard-Boahs, F. Pilleul; Lyon/FR

Purpose: To prospectively describe parameters of CT perfusion for evaluation of tumor vascularity in different aspects of liver metastases from endocrine tumor.

Material and methods: Prospective analysis of CT perfusion was performed in 16 patients with 30 liver metastases which were classified in 3 groups: hyperdense, hypodense on arterial phase and necrotic. Sequential acquisition of the liver was performed before and during 2 min after intravenous injection at 4cc/sec, 0.5 mg/kg of contrast medium. Data were analyzed using deconvolution analysis to calculate blood flow (BF), blood volume (BV), mean transit time (MTT), Arterial hepatic index (AHI) and bi-compartmental analysis to obtain vascular surface permeability (SP). Post treatment was performed by a radiologist and ROI were plotted on metastases, normal liver, aorta and portal vein.

Results: In case of necrotic metastases, none of the CT perfusion parameters was changed. Compared to normal liver, significant difference was found for all CT perfusion parameters in case of hyperdense metastases and only for AHI and MTT in case of hypodense metastases. No significant difference was found for MTT and AHI between hypo and hyperdense metastases; otherwise, we describe significant decrease of SP in hyperdense lesion and significant decrease of BV and BF in hypodense lesions.

Conclusion: Results suggest that CT perfusion allows differentiating tumor vascularity in case of liver metastases from endocrine tumor.

P-160

Usefulness of multiplanar reconstruction with multislice CT to assess HCC response after transcatheter arterial chemoembolization

T.V. Bartolotta, V. Macchiarella, V. Bova, A. Taibbi, F. Cannizzaro, M. Midiri, M. de Maria; Palermo/IT

Purpose: To evaluate the role of multiplanar reconstructions with multislice computed tomography (MSCT) in the assessment of transcatheter arterial chemoembolization (TACE) therapeutic response of hepatocellular carcinoma (HCC).

Material and methods: Fifty-seven patients (mean age: 68.3 years) with unresectable HCC (mean size: 3.4 cm) treated with TACE underwent multiphase MSCT one month after treatment. To evaluate the necrosis rate on MSCT, the following formula: (unenhancing area)+(iodized oil retaining areas)/(total tumoral area) x 100 was calculated on three planes (axial, coronal, and sagittal), choosing the slice in which the tumor showed the largest diameter and the mean value was obtained. As complete necrosis was considered the absence of enhancing portion within or at the margin of the nodule during the arterial phase, with homogeneous deposition of Lipiodol within the lesion whereas as residual tumoral an irregular peripheral-enhancing focus in the arterial phase with irregular or incomplete Lipiodol retention. Responders were patients with a necrosis rate >50%, whereas non-responders were patients with a necrosis rate <50%.

Results: At MSCT, one month after treatment, 35/57 (61.4%) patients were considered as responders, whereas 22/57 (38.6%) as non-responders. On the basis of the one-month MSCT features, 19 patients underwent a second TACE. Survival rates were 73.1 and 53.6% at 12 and 20 months, respectively.

Conclusion: Multiplanar reconstructions with MSCT are suitable for the evaluation of the efficacy of TACE for HCC.

P-161

Esophagogastric veins: can their calibration changes be used as a diagnostic sign for portal hypertensive gastropathy?

A. Erden, R. Idilman, I. Erden, A. Özden; Ankara/TR

Purpose: We analyze whether esophagogastric venous caliber changes can be accepted as an indirect diagnostic evidence for the presence of portal hypertensive gastropathy (PHG).

Material and methods: The images of 57 patients with portal hypertension in whom MR portography has been performed were evaluated retrospectively. The diameters of the left gastric, esophageal mural and paraesophageal veins as well as azygos veins were measured. The mean diameters of the above-mentioned veins in patients with and without PHG were compared with Mann-Whitney U test. In addition, the diametral relationship between the left gastric and azygos veins (largeness or smallness of the left gastric vein compared to the azygos vein) were assessed with Fisher's Exact test with respect to the formation of PHG.

Results: PHG was detected in 15 (26.3%) patients at endoscopy. In patients with PHG, the mean diameters of the left gastric, esophageal mural, paraesophageal, and azygos veins were not statistically different from those in patients without PHG ($p>0.05$). There was no significant difference in diametral relationship between the left gastric and azygos veins in patients with and without PHG.

Conclusion: Interpretation about the presence of the PHG cannot be made by considering the esophagogastric venous calibrations. Largeness or smallness of the left gastric vein with respect to the azygos vein is not a factor that effects the formation of PHG.

P-162

Arterial analysis of the medial segment of the left hepatic lobe using MDCT

L. Saba, G. Caddeo, G. Mallarini; Cagliari/IT

Purpose: Evaluating the arterial map of the medial segment of the left hepatic lobe (segment IV) is extremely important in pre-hepatic surgical planning. The purpose of this study was to assess multi-detector-row CT angiography (MDCTA) potentiality in detecting segment IV arteries and to compare the diagnostic efficacy of Maximum Intensity Projection (MIP) post-processing method and source axial images.

Material and methods: Sixty-seven patients (43 male, 24 female, mean age 64 years, age range 39–78 years) were retrospectively analyzed. Each exam was performed with a multi-detector-row CT scanner using a 110–140 ml of non-ionic

(370 mg/ml) contrast material with a flow rate of 3–5 ml/sec. Two observers evaluated independently axial images and MIP images.

Results: By analyzing axial images, reader 1 detected 69 arteries in 60 patients (89.5% sensitivity) and reader 2 detected 69 arteries in 62 patients (92.5% sensitivity) with a kappa value of 0.782 (good agreement). By analyzing MIP images, reader 1 detected 75 arteries in 64 patients (95.5% sensitivity) and reader 2 detected 75 arteries in 65 patients (97% sensitivity) with a kappa value of 0.813 (very good agreement).

Conclusion: The results of this study suggest that MDCTA is an effective method to study segment IV arteries. The use of MIP produces excellent results with an optimal inter-observer agreement.

P-163

Abdominal lymphoma: special focus over liver

A.S. Preto, M. Pimenta, A. Carneiro, D.M. Rocha, I. Ramos; Porto/PT

Learning objectives: Discuss the spectrum of CT findings in Hodgkin and non-Hodgkin lymphoma involving the liver. Review key imaging findings helpful to the diagnosis. Comment on differential diagnosis and potential pitfalls.

Background: Lymphoma is a type of cancer that originates in lymphocytes or, more rarely, of histiocytes. Infiltration of the liver at time of presentation is frequent. CT has many roles in the evaluation of Hodgkin and non-Hodgkin lymphoma. It is used to define the full extent of the disease, allow accurate staging, assist in treatment planning, and monitor patient progress and possible relapse. Radiology is important in diagnosing and following-up this form of cancer.

Imaging findings OR Procedure details: Diffusely distributed, uniformly small nodules, larger masses, or a combination of the two, may be identified. Hepatomegaly is almost invariably present.

Conclusion: CT is the study of choice for the detection and staging of Hodgkin and non-Hodgkin lymphoma. CT enables accurate measurement of both tumor extent and volume and provides information that can be used to plan an appropriate therapeutic regimen as well as follow the patient response to therapy.

P-164

Withdrawn by authors

P-165

Comparing volumetry to RECIST in multi-slice CT follow-up of untreated liver metastases

S.M. Berggruen, A. Korutz, R. Salem, V. Yaghamai; Chicago, IL/US

Purpose: The purpose of our study was to evaluate volumetry versus RECIST measurements of hepatic metastases for the purpose of estimating change in tumor bulk.

Material and methods: Thirty-nine non treated solid hepatic metastases (27 left and 12 right lobe lesions) on baseline or follow up contrast-enhanced multislice CT in twelve patients undergoing selective transcatheter arterial radioembolization were evaluated. The average time interval between CT exams was 6.2 weeks (range 3–18 weeks). Two radiologists evaluated the metastases by using automated software (Siemens Medical Solutions, Forchheim, GER) to obtain RECIST, volume and density measurements for each lesion. Paired T test was used to evaluate mean percentage change of volume, RECIST and density measurements. $P < 0.05$ was considered significant.

Results: The mean RECIST measurement increased from 28.7 to 30.8 mm (11.03%, $P < 0.0018$) while the mean volume for the same lesions increased from 13.5 to 17.0 mL (55.0%, $P < 0.014$). The mean HU change was minus 4.51.

Conclusion: Our results suggest that RECIST criteria underestimate change in tumor bulk. Automated volumetry of solid liver masses may be a more accurate method of measuring tumors, allowing for better approximation of tumor progression.

P-166

A simple method for estimation of liver volume using multidetector CT and MR

T. Frauenfelder, M.A. Müller Zurich/CH

Purpose: To prospectively assess whether an approximative calculation of the liver volume is possible with a simple formula with the usage of three diameters.

Material and methods: In 50 MR and 50 CT examinations of 100 patients with no free fluid, no liver lesion > 1 cm in diameter and no respiratory or motion artifacts, two readers measured the largest ventrodorsal (a) and lateral (b) diameter in the axial plane and the largest craniocaudal (c) diameter in the coronal plane. The total liver volume was approximated using the formula $a \times b \times c \times 0.3$. As reference standard for comparison, the total liver volume was determined by volumetry by a third reader.

Results: There was no significant disagreement between readers 1 and 2 regarding the approximated liver volumes ($p = 0.87$). The correlation between the liver volume estimation of readers 1 and 2 and the volumetric data was significant for CT and MR data ($r = 0.9$, $p < 0.0001$). In 80% of the formula-based estimations of the liver volume, the error of the approximated volume was $< 10\%$. The maximal error that occurred was 22%.

Conclusion: An approximative calculation of the liver volume is possible with the formula $a \times b \times c \times 0.3$. The standard error with such a calculation is in most cases $< 10\%$ and about 160–170 ml.

P-167

MR and MDCT based liver volumetry: is there a need for a conversion factor?

C. Karlo, C.S. Reiner, S. Breitenstein, D. Weishaupt, B. Marincek, T. Frauenfelder; Zurich/CH

Purpose: To correlate the virtually measured volume of resected liver specimen based on MDCT- or MR-imaging to the intraoperatively measured weight and volume with and without the use of a conversion factor.

Material and methods: 20 patients underwent partial liver surgery and were examined by 64s-MDCT ($n = 10$) or 1.5T-MRI ($n = 10$) before and by 1.5T-MRI ($n = 20$) 8 days after surgery. The resected volume was measured on the preoperative scan by two readers with dedicated software using the postoperative MR images as visual aid. All volumes were multiplied by conversion factors known from literature. The converted virtually measured volumes were compared to the intraoperatively measured weight and volume. Wilcoxon signed-rank test, Pearson correlation coefficient and Bland-Altman plot were used for statistical analyses.

Results: There was a strong positive correlation between the virtually measured volumes and the intraoperative measured volumes. Using no conversion factor, significant differences were seen between the volumetry and the intraoperative assessed weight and volume of the liver specimen. With correction factors of 0.8 and 0.75, no significant differences were found (Wilcoxon signed-rank test). A Bland-Altman plot showed a slightly better result using a conversion factor of 0.8 for CT-group and 0.75 for the MR-group.

Conclusion: The use of a conversion factor (0.8 for CT and 0.75 for MR) is highly recommended if absolute weights and volumes of liver segments are demanded.

Diagnostic / Liver / Diffuse Liver Disease

P-168

Evaluation of fibrosis in liver cirrhosis by superparamagnetic iron oxide-enhanced MRI: does the radiological noninvasive fibrosis index correlate with the laboratory noninvasive fibrosis index?

S.K. Kim, C.H. Lee, K.A. Kim, J.M. Lee, J.W. Choi, C.M. Park; Seoul/KR

Purpose: To evaluate the correlation between the radiological noninvasive hepatic fibrosis index (RNHFI) as determined by superparamagnetic iron oxide (SPIO)-enhanced MRI, and the laboratory noninvasive hepatic fibrosis index (LNHFI).

Material and methods: 99 patients who underwent SPIO-enhanced MRI were

included in the study. These patients were subdivided into a liver cirrhosis group (LCG) and a non-liver cirrhosis group (non-LCG). We measured the RNHFI (mean standard deviation of hepatic signal intensity (SD), noise-corrected coefficient of variation (CV)) of three ROIs in the liver parenchyma on SPIO MRI. The LNHF (AST-platelet ratio index (APRI)) of all patients was also calculated. We compared the RNHFI and APRI of the LCG with those of the non-LCG using the Student's t-test. A bivariate correlation was performed to investigate the relationship between the RNHFI and APRI in the LCG.

Results: For the LCG, the mean values of SD and CV on SPIO-enhanced MRI were 10.3 ± 3.7 and 0.19 ± 0.08 , respectively. For the non-LCG, the mean values of SD and CV were 6.5 ± 1.6 and 0.08 ± 0.05 , respectively. The mean APRI of the LCG and the non-LCG were 2.04 ± 1.7 and 0.32 ± 0.32 , respectively. The SD, CV and APRI were significantly different between the LCG and non-LCG ($p < 0.05$). In all patients, there were significant correlations between CV and APRI ($r = 0.438$, $p < 0.001$), and between SD and APRI ($r = 0.633$, $p < 0.001$).

Conclusion: The RNHFI and APRI were significantly different between the LCG and non-LCG. The RNHFI was significantly correlated with APRI.

P-169

SPIO-gadolinium MRI in cirrhotic patients: radiologic findings

B. Guiu, R. Loffroy, S. Guiu, J. Jouve, A. Lambert, L. Mezzetta, P. Hillon, D. Krausé, J.P. Cercueil; Dijon/FR

Purpose: To describe the radiologic findings observed with double-contrast MRI (DC-MRI) with SPIO and gadolinium, and to determine the role of DC-MRI in screening for hepatocellular carcinoma (HCC) in cirrhotic patients.

Material and methods: We retrospectively included 160 DC-MRI scans done as second-line investigations in 119 patients with cirrhosis over a 25-month period. Two radiologists independently classified the MRI scans as strongly suggesting HCC (HCC Group), showing benign nodules (Benign nodules Group), showing no nodules (No-nodules Group) or indeterminate; they assigned a diagnostic confidence score (DCS) using a 0 to 10 scale. The reference standard was histology or results of follow-up investigations. Mean follow-up was 16.9 months (12–28 months).

Results: The radiologists disagreed for two scans ($\kappa = 0.98$). Of 112 scans (Benign nodules Group [$n = 32$] and No-nodules Group [$n = 80$]), 11 were excluded (3 patients lost to follow-up and 8 who died with no known cancer) while a HCC was detected during follow-up in 8 patients, yielding a NPV of 92% (93/101) (95% confidence interval, 85–97%). The DCS was in the 4–6 range (indicating uncertainty) for only 6 (3.75%) scans.

Conclusion: Liver fibrosis is clearly visible with DC-MRI. Regenerative nodules, flow-related abnormalities and nodules of confluent fibrosis as well as HCCs are also well depicted. DC-MRI is reliable and reproducible. Its high NPV suggests a role as a second-line investigation after ultrasonography, for HCC screening.

P-170

Pregnancy and hepatic dysfunction: a pictorial review of imaging and histological findings

D. Huang, D. Lewis, P. Peddu, S. Ryan, P.A. Kane, J. Karani; London/UK

Learning objectives: The aim of this exhibit is to review the imaging and histological findings of the pathological changes that can occur in liver during pregnancy. Three categories are considered: 1) Liver dysfunction specific to pregnancy, 2) Pre-existing disorders that may be aggravated by pregnancy and 3) Liver disease coincident with pregnancy.

Background: The liver is subject to changes in pregnancy, some physiological and others pathological. In some patients, this is life threatening and requires urgent management. Knowledge of these and of their imaging appearances is essential for the radiologist to ensure appropriate treatment.

Imaging findings OR Procedure details: 1) Physiological changes in the liver in pregnancy. 2) Imaging features with histological correlation of liver diseases specific to pregnancy: - Acute fatty liver of pregnancy - Intrahepatic cholestasis - Hypertension-associated liver disease - pre-eclampsia-hepatic infarction and rupture-HELLP syndrome. 3) Pregnancy and pre-existing liver disease: - Liver tumours - Portal hypertension - Congenital hyperbilirubinemia. 4) Liver disease coincident with pregnancy: - Biliary disease - Budd-Chiari syndrome.

Conclusion: This review has shown the physiological and pathological changes that may occur in the liver during pregnancy with the spectrum of hepatic diseases and their characteristic imaging findings.

P-171

Non-invasive assessment of hepatic fibrosis with MR elastography and spectroscopy: initial results

E.M. Godfrey, I. Joubert, A. Priest, N. Griffin, G.J. Alexander, A.E. Gimson, M. Allison, S. Davies, A. Shaw, D.J. Lomas; Cambridge/UK

Purpose: Early and moderate stages of hepatic fibrosis are difficult to diagnose accurately using most imaging techniques making invasive liver biopsy necessary and serial studies difficult to undertake. Several MR techniques have recently been shown to improve on standard imaging. This work describes our initial experience with: Liver stiffness measurement using MR elastography (MRE), ³¹P phosphorus hepatic spectroscopy and T2w morphological imaging.

Material and methods: 10 consecutive patients with clinically suspected hepatic fibrosis referred for liver biopsy were recruited. Each patient underwent MR examination including: Multishot T2w RARE, MRE and ³¹P spectroscopy. The patients underwent a liver biopsy the same day as the MR examination. Each sequence was independently evaluated for: liver stiffness (kPa), PME/PDE ratio and morphological evidence of fibrosis. The liver biopsy was graded independently by a pathologist using the Ishak Fibrosis Score.

Results: A broad range (1–6) of Ishak fibrosis scores were found at histology. These correlated well (0.86 Pearson rank) with MRE stiffness values which ranged from 2.7 to 12.7 kPa. The correlation was poor (-0.15) with PME/PDE ratio which ranged from 17.9 to 46.2%. All except one examination was graded as normal morphologically on T2w imaging.

Conclusion: Although involving a small group of patients, the initial results suggest that MRE measurements of liver stiffness correlate well with histological fibrosis score in suspected liver fibrosis and appear to perform better than either morphological imaging or ³¹P spectroscopy.

P-172

Apparent diffusion coefficient measurements with diffusion-weighted MRI for evaluation of hepatic cirrhosis

E. Szurowska, J.M. Pienkowska, E. Lzycka-Świeszewska, R. Rzepko, D. Zadrozny, W. Adamonis, M. Studniarek; Gdansk/PL

Purpose: The purpose of this study was the evaluation of the apparent diffusion coefficients' value (ADCs) of diffusion-weighted MRI for the assessment of liver cirrhosis.

Material and methods: A total of 75 patients were prospectively evaluated with diffusion-weighted MRI using 1.5 T system. T1 and T2-weighted SE, FSE sequences and echo-planar diffusion-weighted MR study with different b factor ($b = 0-15; 0-30; 0-300; 0-500; 0-2000$ s/mm²) were performed. Region of interests (ROIs) were set on ADC map in each hepatic segment and mean ADC for the liver of each patient was calculated. The patients were divided into two groups: group A - 33 patients with clinical signs of cirrhosis (Child-Pugh stage A) confirmed by liver biopsy and group B - 42 patients with normal liver function. The mean ADC for cirrhotic (group A) and non-cirrhotic liver for different b factor were compared.

Results: The ADCs value was lower in group A than in group B, but statistical differences were observed for low b factor: $b = 0-15$ and $0-30$ s/mm² (retrospectively $p = 0.001$ and $p = 0.002$).

Conclusion: ADCs measurements for low b factor are potentially useful for the evaluation of cirrhotic liver.

P-173

Non-invasive quantification of hepatic steatosis with 3.0 Tesla MR spectroscopy in an experimental rat model

J.R. van Werven, H.A. Marsman, A.J. Nederveen, F.J. ten Kate, T.M. van Gulik, J. Stoker; Amsterdam/NL

Purpose: Proton magnetic resonance spectroscopy (1H-MRS) could be a non-invasive alternative to needle biopsy in the assessment of hepatic steatosis (HS). The purpose of this study was to quantify HS with 1H-MRS in a rat model and correlate these 1H-MRS measurements with histopathological and biochemical assessments of hepatic fat.

Material and methods: HS was induced by feeding rats a methionine choline deficient diet (MCD) for 0, 1, 3 or 5 weeks ($n = 5$ per group). 1H-MRS was performed on a 3.0 Tesla scanner using an experimental micro-coil. A ratio representing hepatic fat was calculated from CH₂ fat peak versus the reference

H₂O peak. This ratio was correlated (Spearman) with histopathological macrovesicular steatosis and biochemical (triglycerides and total fatty acids) parameters in the liver.

Results: Median hepatic fat ratio measured by 1H-MRS increased from 0.01 at baseline to 1.37 after 5 weeks of MCD diet. This increasing ratio significantly differed per MCD diet group ($p < 0.001$). Furthermore, we found significant correlations between measurements of hepatic fat by 1H-MRS, and macrovesicular steatosis ($r = 0.93$, $p < 0.001$), triglycerides content ($r = 0.96$, $p < 0.001$) and total fatty acids in the liver ($r = 0.89$, $p < 0.001$).

Conclusion: 3.0 Tesla 1H-MRS is able to accurately measure hepatic fat content in this rat model and strongly correlates with histopathological and biochemical analysis of hepatic fat. These results encourage the application of 1H-MRS for non-invasive assessment of HS in clinical practice.

P-174

Reproducibility of 3.0 Tesla MR spectroscopy to measure hepatic fat content

J.R. van Werven¹, J.M. Hoogduin², A.J. Nederveen¹, A.A. van Vliet³, D. Kappers³, E. Wajs⁴, P. Vandenberg⁴, J. Stoker¹;
¹Amsterdam/NL, ²Groningen/NL, ³Zuidlaren/NL, ⁴Beerse/BE

Purpose: Proton magnetic resonance spectroscopy (1H-MRS) is a non-invasive alternative to liver biopsy in the assessment of hepatic steatosis. Despite the increasing use of 1H-MRS in determining hepatic fat content, there is little literature addressing the reproducibility of this technique. The purpose of this study was to investigate the reproducibility of 1H-MRS to measure hepatic fat content.

Material and methods: 1H-MRS was performed in twelve subjects on a 3.0 T Philips scanner. Each subject underwent four 1H-MRS scans: two in fasting condition on the same day, and two one week later, before and after a high fat breakfast. From the spectra, a ratio representing hepatic fat content (mg fat per gram liver tissue) was calculated and used to compare the 1H-MRS scans to assess reproducibility (Wilcoxon signed rank test and intra class correlation coefficient).

Results: Mean hepatic fat content in scan one and two was 37.1 and 37.0 mg/g, for scan three and four 40.1 and 42.4 mg/g. We found no significant difference in hepatic fat content between scan 1 and 2 ($p = 0.62$), scan 1 and 3 ($p = 0.20$) and scan 3 and 4 ($p = 0.11$). The intra class correlation coefficient between all four 1H-MRS scans was 0.98 ($p < 0.001$).

Conclusion: [1]H-MRS is highly reproducible in non-invasive measuring of hepatic fat content. There is excellent agreement between the different [1]H-MRS measurements. There is no significant effect of food ingestion on hepatic fat content measured by [1]H-MRS.

Diagnostic / Liver / Focal Liver Lesions / Detection

P-175

Fibrolamellar and HCC: a rare coexistence

B.S. Narin Anil, G. Kilicoglu, M.M. Simsek; Istanbul/TR

Purpose: Fibrolamellar carcinoma (FLC) is a rare variant of hepatocellular carcinoma (HCC) which occurs in noncirrhotic liver. 200 cases have been reported in the literature; among these cases the coexistence of HCC and FLC is quite rare.

Material and methods: A 64 year-old female patient was referred with progressive abdominal pain and distention. MRI revealed two heterogeneous masses of 11x10 cm and 7.5x7 cm in size and indistinguishable from each other and located in the 8th, 7th ve 6th segments of the liver. Dynamic contrast enhanced upper abdominal MRI exhibited hypointense lesions with distinctly hyperintense center. AFP levels were normal.

Results: An extended right hepatectomy was performed. Histopathology showed that the larger mass was a classical FLC while the smaller one was HCC.

Conclusion: FLC may be distinguished from HCC by its presentation at a younger age, occurrence in noncirrhotic livers and not demonstrating the fetoprotein inclusions. FLC is less aggressive than HCC. Vascular invasion is rare. MRI examination generally demonstrates FLC as isointense masses in both T1 and T2W images with well-defined lobulated contours, and prominent early

arterial enhancement. The lesion becomes isointense to liver parenchyma in the portal venous phase, while HCC appears hypointense to liver with enhancement of the capsule. Our case is not typical for FLC with its age at presentation and for HCC with the clinical and laboratory findings. Both cases can be atypically seen in elderly ages.

P-176

Liver metastases from hypervascular tumors: do we really need the arterial phase of spiral or multislice CT?

V. Maniatis¹, N. Gavalakis², A. Papadopoulos³, J. Tzovara³, E. Stamoulis³, H. Vardak³, K. Foufa³, A. Roussakis³;
¹Palini/GR, ²Patras/GR, ³Athens/GR

Purpose: To assess the usefulness of hepatic arterial phase (of a spiral or multislice CT) in depicting hepatic metastases in patients with a history of a hypervascular (not of hepatic origin) neoplasm.

Material and methods: 131 patients with hepatic metastases due to hypervascular neoplasm are included: breast cancer (52 patients), melanoma (25), renal cancer (17), sarcoma (14), carcinoid tumor (14), medullary thyroid cancer (5) and islet cell tumors (4). Triphasic (non contrast- NCP, hepatic arterial- HAP and portal venous phase- PVP) spiral or multislice CT was performed. Number of lesions seen at each phase and their enhancement patterns were encountered. The contribution of hepatic arterial phase (HAP) to the diagnostic results was specifically estimated.

Results: 706 metastatic lesions were found: 491 on NCP images, 570 on HAP images and 583 on PVP images. 10.5% of the hepatic metastases were found only on hepatic arterial phase (HAP). The diagnostic results' improvement due to HAP was statistically significant in patients with renal cancer, carcinoid tumor, islet cell tumors and medullary thyroid cancer but not in patients with breast cancer, melanoma and sarcoma.

Conclusion: HAP must be a part of the CT protocol in cases of renal cancer, carcinoid tumor, islet cell tumors and medullary thyroid cancer. HAP is not mandatory in cases of breast cancer, melanoma and sarcoma.

P-177

Atypical features of focal nodular hyperplasia on MRI

B. Rajashanker, T.C. Oh, C. Liew; Manchester/UK

Learning objectives: 1. To learn about atypical FNH 2. To understand the pattern of atypia seen in state-of-the-art MRI imaging 3. Understand some of the reasons behind these atypia. 4. Avoid diagnostic pitfalls.

Background: Focal nodular hyperplasia (FNH) is a non-neoplastic regenerative lesion of liver commonly encountered in clinical practice. Two types, the classical and non classical, are recognised. Imaging features of FNH are fairly typical, but atypical features are increasingly recognised and reported.

Imaging findings OR Procedure details: State-of-the-art MRI imaging with T1, T2 Weighting, gadolinium enhanced dynamic 3D sequences and use of liver specific contrast agents like super paramagnetic iron oxide (SPIO) is currently the modality of choice for imaging these lesions most accurately. However, several atypical features that are recognised include internal haemorrhage on T1W, abnormal signal intensity on T2W images, absence of central scar, abnormal signal of central scar (typically hyperintense on T2W), varying patterns of enhancements, lack of uptake of SPIO. These atypical features are demonstrated with examples, and pathological correlation provided where appropriate.

Conclusion: Atypical features of FNH are common, and are increasingly recognised with improvement in imaging techniques. Familiarity with these features help in avoiding diagnostic pitfalls.

Diagnostic / Liver / Focal Liver Lesions / Differential Diagnosis

P-178

Diffusion-weighted MRI: a reliable test for the differentiation of malignant from benign focal liver lesions?

R. Jain, S. Sawhney, D. Jaju; Muscat/OM

Purpose: To evaluate the utility of Diffusion-Weighted Imaging (DWI) in the differentiation of malignant from benign focal liver lesions (FLL).

Material and methods: 127 studies were performed in 108 consecutive patients with suspected FLL. Unidirectional echoplanar-(EP)-DWI of the liver was performed on 1.5 T MRI unit during free-breathing at three gradient strengths $b=0, 300, 600$. Trace images, Apparent Diffusion Coefficient (ADC) maps and MRI with iron-oxide/Gadolinium contrast enhancement were obtained. Two radiologists independently measured ADC values of $FLL > 1$ cm diameter. The final diagnosis of FLL was by histopathology, MRI characterization or clinico-radiological follow-up. Differences between mean ADC values of various FLL were compared using Student's t-test.

Results: 315 ADC measurements were made. The observed number of measurements/ADC values (mean \pm SD \times 10 $^{-5}$ mm 2 /sec) were as follows: normal liver parenchyma (74/0.09 \pm 0.59), cirrhosis (41/3.77 \pm 13.97), HCC (64/140.57 \pm 33.43), metastasis (92/154.02 \pm 2.12), other malignancy (6/228 \pm 60.44), adenoma (7/225.93 \pm 41.28), hemangioma (15/363.91 \pm 83.96), cyst (12/363.91 \pm 83.96) and abscess (4/105.75 \pm 53.4). Benign FLL (adenoma+heman gioma+cyst) had significantly higher ADC values compared with malignant FLL (HCC+metastases+other malignancy) (275.0 \pm 90.4 v/s 147.9 \pm 47.2, 95% CI 148.3, 105.9 and $p < 0.0001$). Using a threshold ADC value of 200 \times 10 $^{-5}$ mm 2 /sec, sensitivity 92% (95% CI 0.88, 0.96), specificity 89% (95% CI 0.81, 0.97), PPV 96%, NPV 79%, LR+ 8.6 and LR- 0.09 were observed for the differentiation of malignant from benign FLL.

Conclusion: EP-DWI is a reliable test for the positive differentiation of malignant from benign FLL, using a threshold ADC value of 200 \times 10 $^{-5}$ mm 2 /sec.

P-179

Withdrawn by authors

P-180

Size variation in focal nodular hyperplasia assessed by MRI

C. Ramírez Fuentes, P. Bartumeus, L. Marti-Bonmati, D. Frota Barroso, A. del Val Montañana; Valencia/ES

Purpose: To evaluate the variations in size in a series of focal nodular hyperplasia (FNH) lesions as assessed by MRI.

Material and methods: The medical records of patients with a final diagnosis of FNH with at least two MRI examinations were reviewed. All the patients were examined with a dynamic contrast-enhanced MR T1W sequence. Finally, 17 patients were included with a total of 28 FNH lesions. Lesions size in its greater diameter was measured in millimeters, at each contrast-enhanced MR examination. The percentage of variation was calculated (difference in maximal diameter normalized to the initial size). A significant variation was considered when there was a size changed greater than 15%.

Results: The mean time interval between the two imaging examinations for the whole group was 925 days (\pm 521). Six out of 28 lesions (21%) showed a significant variation at its largest diameter. Four of them decreased in size while two increased, changes being modified as much as 48%. The other 22 lesions remained stable during the follow-up period. Change in size could not be related to any predisposing factor.

Conclusion: FNH can vary significantly in its diameter during follow-up examination. As many as 21% of these lesions either enlarge or decrease in size. No relationship could be found between size variation and predisposing factors.

P-181

Quantitative diffusion-weighted MRI of focal hepatic lesions using parallel imaging techniques

O. Kilickesmez, S. Bayramoglu, E. Inci, S. Aksoy, G. Yirik, S. Aydin, E. Hocaoglu, S. Dogan, T. Cimilli; Istanbul/TR

Purpose: The purpose of this study was to investigate the value of diffusion-weighted magnetic resonance imaging (DW-MRI) in the discrimination of mass lesions of the liver using parallel imaging technique.

Material and methods: A total of 77 patients (mean age, 59), and 65 healthy controls (mean age, 37.6) were enrolled in the study. SS SE EPI DW-MRI was performed with b factors of 0, 500 and 1000 s/mm 2 . ADC values of the normal liver and the lesions were calculated.

Results: There was statistically significant difference among ADCs of four liver segments. The mean ADC value of the liver lesions was as follows: simple cysts (3.16 \pm 0.18 \times 10 $^{-3}$ mm 2 /s), hydatid cysts (2.58 \pm 0.53 \times 10 $^{-3}$ mm 2 /s), metastases (1.14 \pm 0.41 \times 10 $^{-3}$ mm 2 /s) and hepatocellular carcinomas (HCC) were (1.15 \pm 0.36 \times 10 $^{-3}$ mm 2 /s). The mean ADC values of all of the lesion groups were statistically significant when compared with mean ADC value of the normal liver (1.56 \pm 0.14 \times 10 $^{-3}$ mm 2 /s), ($p < 0.01$). There was also statistically significant difference among the ADC values of hemangiomas and HCCs-metastases, simple and hydatid cysts. However there was no statistically significant difference between HCCs and metastases.

Conclusion: The present study showed that ADC measurement has a potential ability to differentiate focal hepatic lesions. We propose to add the DW sequence in the abdominal MR protocol for the detection and discrimination of hepatic lesions and particularly in the differentiation of benign and malignant ones.

P-182

The role of diffusion weighted MRI to the differential diagnosis of hepatic masses

I. Guvenç, M. Kocaoglu, I. Karademir, N. Bulakbasi, C. Tayfun; Ankara/TR

Purpose: The purpose of this study was to evaluate the diagnostic role of diffusion weighted MRI using apparent diffusion coefficient (ADC) values and in the characterization of hepatic mass lesions.

Material and methods: 96 patients who had 129 lesions were examined and underwent abdominal MRI at 1.5 T, including T1- , T2- weighted, and dynamic gadolinium-enhanced imaging. Axial diffusion weighted images was performed before contrasts administration with a single-shot spin-echo echo-planar imaging sequence using b-values of 50,400, and 800 seconds/mm 2 . ADC maps were obtained automatically by the device and all ADC values of the lesions were measured. Statistical analyses were performed using the T test and Mann-Whitney U test in a computer software (SPSS Inc., Chicago, Illinois, USA). The differences were considered significant when p values were less than 0.05.

Results: The lowest ADC values among the malignant masses belonged to metastases. Hepatocellular carcinomas ADC values were slightly higher than metastases. All malignant liver lesions characterized by high signal intensity (SI) in b=800 images and low SI in ADC map images. The highest ADC value was for simple cysts. All benign lesions had high SI in ADC map images. The difference between the mean ADC values of benign and malignant lesions was statistically significant ($p < 0.01$).

Conclusion: Diffusion weighted images with ADC measurement can differentiate benign from malignant lesions.

P-183

Multiple hyperechoic liver lesions: an early indicator of haemochromatosis?

S.J. Amonkar¹, L. Tandon², C.K. Liew¹, S. Sukumar¹;
¹Manchester/UK, ²Blackpool/UK

Learning objectives: To consider HC in the differential diagnosis of multiple HLL in the adult patient with deranged liver function tests (LFTS).

Background: Haemochromatosis (HC) is characterised by a gradual increase in body iron, and can be hereditary or secondary. Both types cause abnormal iron deposition in multiple organs, most commonly the liver. If untreated, the subsequent cirrhosis significantly increases the risk of HCC. Current radiological evaluation is principally centred around MRI, and to a lesser degree, CT. Although often a first line investigation, limited literature exists relating to the role of US in the diagnosis of HC.

Imaging findings OR Procedure details: We consider 4 cases that initially presented with abnormal LFTS and were later proven to have HC. In these cases, the initial US showed multiple hyperechoic liver lesions (HLL) where the differential diagnosis included haemangiomas, focal fatty infiltration, metastases and hepatic adenomas. We will illustrate these findings with correlation to MRI and CT images where available. Histological correlation will also be illustrated with a review of the literature. Although these lesions had imaging characteristics of fat containing lesions, it is interesting that this particular pattern was noticed in the presence of underlying HC.

Conclusion: Early diagnosis of HC could prevent the development of fatal complications, and although non-specific, it should be considered in the differential diagnosis of multiple HLL.

P-184

Gamut of focal fatty liver masses: value of cross-sectional imaging in diagnosis with emphasis on MRI

N. Fasih, S. Thippavong; Ottawa, ON/CA

Learning objectives: To present a series of well documented cases of benign and malignant liver lesions that may typically or occasionally contain fat. Benign fat-containing liver lesions include: Focal nodular hepatic steatosis, Giant hepatic echinococcal cyst, Focal nodular hyperplasia (FNH), Hepatic angiomyolipoma, and Hepatic adenoma. Malignant fat-containing liver lesions include: Hepatocellular carcinoma (HCC) and metastatic liposarcoma. To demonstrate and discuss the role of multimodality imaging in the diagnosis of fat-containing liver lesions.

Background: When fat is seen within a liver mass, a spectrum of lesions needs to be considered. Although some lesions are benign and uncomplicated, others may be malignant. Cross-sectional imaging including CT, MRI and even US can diagnose intra-lesional fat with high accuracy. Characterization of these lesions on imaging can allow for a specific diagnosis or can help narrow the differential diagnosis. By combining the radiological findings and patient characteristics, the nature of the lesion can often be determined. Often, this may obviate the need for biopsy.

Imaging findings OR Procedure details: Clinical and imaging features of benign and malignant fat-containing lesions mentioned in the Learning objectives: will be discussed. Utilization of CT Hounsfield units for macroscopic fat determination, combined with additional imaging features and patient factors, to determine a diagnosis or generate a differential diagnosis. Emphasis on MRI fat-saturation and chemical shift sequences for the determination of macroscopic and intracellular lipid-containing lesions, respectively.

Conclusion: A variety of fat containing lesions may be encountered within the hepatic parenchyma. Cross-sectional imaging, especially MRI, can make a specific diagnosis or narrow the differential diagnosis, thereby facilitating correct management.

P-185

Withdrawn by authors

P-186

Pure bile ductular carcinoma: imaging pathologic correlation in comparison with ordinal type of cholangiocellular carcinoma

K. Kozaka, O. Matsui, S. Kobayashi, Y. Nakanuma, Y. Zen; Kanazawa/JP

Purpose: To assess CT findings of bile ductular carcinoma with correlation to pathologic findings in comparison with ordinary cholangiocarcinoma.

Material and methods: 21 surgically resected peripheral cholangiocarcinomas were divided into three types: adenocarcinomas resembling proliferating reactive bile ductules (bile ductular carcinoma, pure type), variably sized tubular, solid or micropapillary adenocarcinomas (ordinary type) and mixed type. Tumor growth patterns were classified pathologically as replacing growth pattern and compressive growth pattern. The tumor and peritumoral enhancement patterns of these three types were examined.

Results: All pure type showed replacing growth pattern. All pure type showed diffuse stain and 3 of 6 pure type showed peritumoral wedge shaped stain. None of 6 accompanied intrahepatic bile duct dilatation. 6 of 8 mixed type showed replacing growth and the remaining 2 showed compressive growth. 7 of 8 mixed type showed peripheral rimlike enhancement. 6 of 8 mixed type showed

peritumoral wedge shaped stain and 3 accompanied intrahepatic bile duct dilatation. 4 of 7 ordinary type showed replacing growth and the remaining 3 showed compressive growth. 4 of 7 ordinary type showed diffuse stain and the remaining 3 showed peripheral rimlike stain. 6 of 7 showed peritumoral wedge shaped stain and 4 accompanied intrahepatic bile duct dilatation.

Conclusion: The CT findings of pure type may be characterized by diffuse stained tumor without intrahepatic bile duct dilatation.

P-187

Imaging findings of hepatic tumors that can contain large amount of fat

J.Y. Woo, I. Yang, S.Y. Chung; Seoul/KR

Learning objectives: To illustrate characteristic appearance and discuss differentials of hepatic tumors that can contain a large amount of fat. To emphasize on early diagnosis of well-differentiated liposarcoma of the liver.

Background: Hepatic tumors that can contain large amount of fat are lipoma, angiomyolipoma, and well-differentiated liposarcoma. Hepatic lipomas are rarer than angiomyolipomas and can occur sporadically. Hepatic angiomyolipoma is a rare benign mesenchymal tumor. Well-differentiated liposarcoma is a rare malignant tumor. Because of their rarity and similar imaging findings, we often consider masses containing large amount of fat as benign lesions. So early diagnosis of well-differentiated liposarcoma is not easy. According to the clinical course, liposarcoma of the liver has a high rate of recurrence. Generally, the prognosis is poor without treatment. The well-differentiated type is considered to have low-grade malignancy. Other types are regarded as intermediate or highly malignant tumors. It is possible to differentiate the well-differentiated liposarcoma from an angiomyolipoma or lipoma on MDCT and MR imaging.

Imaging findings OR Procedure details: An angiomyolipoma presents with central vessels within the lesion as a characteristic feature and lipoma appears as a pure fat-containing lesion on CT and MR. Well-differentiated liposarcomas show an almost fatty, lobulated mass with a few, random distributed vascular structures and small areas of nodular enhancement.

Conclusion: Well-differentiated liposarcoma of the liver should be included in the differential diagnosis of hepatic masses containing large amount of fat when imaging findings show an almost fatty, lobulated mass with a few, random distributed vascular structures and small areas of nodular enhancement.

P-188

Contrast enhanced US in the characterization of small liver lesions (≤ 1 cm), indeterminate on MDCT in neoplastic patients: a preliminary study

E. Gatti, P. Cabassa, F. Pittiani, P. Narbone, E. Fogari, R. Maroldi; Brescia/IT

Purpose: To assess the efficacy of contrast enhanced US (CEUS) in the characterization of hepatic lesions (<1 cm), defined too small to be characterized at MDCT, in neoplastic patients.

Material and methods: 33 consecutive indeterminate lesions <1 cm in 16 neoplastic patients were depicted on 16 rows MDCT. All lesions underwent B mode baseline US and CEUS. CEUS was performed with the standard dose of 2,4 ml Sonovue using real time continuous scanning during arterial, portal and late phase with specific contrast setting (contrast coherent imaging: CCI) at low MI (0.1–0.2). The gold standard was clinical follow-up of at least 6 months with adequate imaging findings (MR, US, MDCT).

Results: Final diagnoses were: 13 cysts, 3 hemangiomas, 2 metastasis, 4 benign lesions, not characterized, but unmodified during follow up. 11 lesions were undetected both at baseline US and CEUS. Imaging follow-up shows no lesions within the liver in these patients. 9 lesions in 4 patients were cysts, detected with B-mode US without contrast administration. In 12 patients, CEUS correctly characterized 21/24 lesions (87.5%). Overall US (B-mode and CEUS) has correctly characterized 30/33 lesions (90.1%).

Conclusion: Although most lesions were benign, CEUS could play a relevant role in characterizing subcentrimetric lesions and therefore obviate the need of cost and time consuming alternative techniques.

P-189

Different imaging modalities and characteristic features of common focal liver lesions: a pictorial review

M.G. Mulla, R. Singh; Derby/UK

Learning objectives: 1. Overall view of different modalities of imaging used to diagnose and characterize FLL. 2. Define radiographic appearances of these lesions on different imaging modalities.

Background: Focal liver lesions (FLL) can be benign or malignant. Commonly seen benign lesions are cysts, haemangiomas, focal nodal hyperplasia, hepatic adenomas and biliary cyst adenomas. Malignant lesions can be primary or secondary. It is important to differentiate between the two to optimize treatment and to avoid unnecessary interventions. Various radiological imaging modalities are employed for the diagnosis and characterization of FLL. The enhancement pattern of a lesion constitutes the mainstay of its characterization with contrast-enhanced CT or MRI.

Imaging findings OR Procedure details: Based on our experience, we present a spectrum of appearances of FLL seen on USS, CT scan and MRI. CT images were obtained pre and post intravenous contrast. Liver specific contrast agents and gadolinium were used for MRI scan. The characteristic appearances of the mentioned lesions are described here in a pictorial review.

Conclusion: Different modalities contribute to the diagnostic assessment and have their own advantages and disadvantages. USS is highly sensitive in the diagnosis, but less specific in characterizing these lesions. However, MRI with newer liver specific contrast agents is more sensitive and specific in the diagnosis of FLL compared to multislice spiral CT.

P-190

Focal nodular hyperplasia or hepatic adenoma? How MRI can help us using liver-specific contrast agents

P. Paolantonio¹, R. Ferrari², P. Lucchesi², F. Vecchietti², M. Rengo², A. Laghi²; ¹Rome/IT, ²Latina/IT

Learning objectives: To illustrate pharmacodynamic and pharmacokinetic properties of Gd-BOPTA, Gd-EOB-DTPA and ferucarbutran. To show pathological features of FNH and HA with imaging correlation. To show typical and atypical features of FNH and hepatic adenoma at MRI using different classes of hepatospecific contrast agents.

Background: Differential diagnosis between Focal Nodular Hyperplasia (FNH) and Hepatic Adenoma (HA) is crucial for patient management. An accurate and non-invasive differential diagnosis using MRI is possible based on both dynamic imaging and functional information of liver-specific contrast-agents.

Imaging findings OR Procedure details: The identification and characterization of FNH and HA requires an accurate dynamic study of the liver for the assessment of lesion vascularity. Unfortunately, a definite differential diagnosis on the basis of morphology and lesion vascularity is not always possible. Functional information offered by liver specific contrast agent may help us in this diagnostic challenge.

Conclusion: The use of liver specific contrast agents offers functional information on lesion cellularity that is extremely useful in differentiating FNH by HA. Information on lesion bile ducts offered by hepatobiliary agents represents an accurate marker of FNH nodule respect to HA.

P-191

Withdrawn by authors

P-192

Inhomogeneity is frequently encountered in focal nodular hyperplasia on delayed with Gd-EOB

R.H.C. Bisschops, M.S. van Leeuwen; Utrecht/NL

Purpose: Dynamic MRI with Gd-EOB can be used to characterize focal nodular hyperplasia (FNH). However, the optimal time window for delayed enhancement is not yet defined and atypical enhancement patterns are reported. We prospectively evaluated 10 probably FNHs with dynamic MRI using Gd-EOB, using multiple time delays.

Material and methods: T1w, T2w and THRIVE unenhanced, arterial (20 sec), portal (50 sec), equilibrium (3 min) and delayed phase (10, 20 and 30 min after injection of Gd-EOB) were obtained. Lesion signal intensity and homogeneity were graded for each sequence and time window. Presence of a central scar and time of biliary excretion was noted.

Results: Nine FNHs showed typical homogeneous enhancement during arterial, portal and equilibrium phases, seven with a scar and two without a scar. One atypical FNH was iso-intense on portal phase and slightly hypo-intense in the equilibrium phase with no central scar. On delayed imaging, two FNHs were iso- and slightly hypointense. Five FNHs showed marked inhomogeneity, four only

during delayed enhancement, one during all time windows. No significant difference was observed between 10, 20 or 30 minutes images. Biliary excretion was seen from 10 minutes onward in nine patients.

Conclusion: Using Gd-EOB, inhomogeneity is frequently encountered in FNHs on delayed imaging. A delay of 10 minutes may be sufficient for the hepatobiliary phase.

Diagnostic / Liver / Other

P-193

Fat-containing lesions of the liver: a common diagnostic challenge

C.K. Liew, T.C. Oh, F.M. Grieve, J.K. Bell, B. Rajashanker; Manchester/UK

Learning objectives: To identify and describe a wide spectrum of fat-containing lesions in the liver and the imaging characteristics that distinguish them. To review current MRI techniques used in characterisation of these lesions.

Background: A fat-containing lesion within the liver is frequently encountered in clinical practice. The causes are diverse and can range from benign lesions to malignant neoplasm. The benign entities include hepatic steatosis, hepatic adenoma, focal nodular hyperplasia, angiomyolipoma, lipoma, teratoma, adrenal rest tumour and Langerhans cell histiocytosis. Malignant lesions include HCC, liposarcoma and metastatic liver lesions.

Imaging findings OR Procedure details: Both US and CT can be useful to demonstrate the presence of fat. However, MRI is the most sensitive modality in the characterisation of these liver lesions. Several MRI sequences including in- and opposed phase gradient echo T1W sequence, spin echo T2W sequence, dynamic post contrast images and the use of liver specific contrast agents help to differentiate these lesions and aid in achieving an accurate diagnosis. In this pictorial review, we illustrate the radiographic features of various entities of focal and diffuse fat-containing lesions of the liver, with focus on MRI. A detailed understanding of these lesions is essential for further appropriate management.

Conclusion: This presentation will help the readers to provide clinicians with the diagnosis or relevant differential diagnoses when confronted with a fat containing lesion of the liver.

P-194

A pictorial review of patterns of vascular involvement by HCC

D. Lewis, P. Peddu;, A. Quaglia, P.A. Kane, J. Karani; London/UK

Learning objectives: To demonstrate the breadth of liver vascular abnormalities associated with HCC.

Background: HCC is a common, potentially curable primary liver malignancy but the presence of macrovascular tumour invasion alters both clinical presentation and subsequent treatment. Recognition of the patterns of arterial and venous tumour infiltration in HCC is an essential radiological skill which forms the basis of diagnosis and management.

Imaging findings OR Procedure details: Multimodality techniques are used to demonstrate intrahepatic tumour stage, arterial venous and caval tumour/thrombus infiltration and arterio-venous shunting. This exhibit will present a pictorial essay of these vascular complications, including hepatocyte specific contrast enhanced MRI, MDCT and angiography.

Conclusion: Staging and determination of management of HCC requires accurate radiological depiction of macrovascular tumour invasion. This presentation uses case example to demonstrate the breadth of radiological appearances in this regard.

P-195

The relationship between hepatic MRI for fat quantification and hepatic vein waveform in patients with nonalcoholic steatohepatitis

S. Ulusan, T. Yakar, Z. Koc; Adana/TR

Purpose: To investigate the relationship between hepatic vein waveform (HVW) and hepatic fat fraction was evaluated in patients with nonalcoholic steatohepatitis (NASH) using spectral Doppler US recordings and phase contrast MRI.

Material and methods: A total of 52 patients, ages 26 to 70 years old with NASH underwent hepatic MRI for fat quantification. The degree of hepatic steatosis was assessed by MRI through chemical shift imaging using a modification of Dixon method. The Doppler US examination of middle hepatic vein was performed in all patients. The Doppler US pattern was classified in to two groups according to Doppler signal characteristics: abnormal (monophasic and biphasic) and normal (triphasic). The degree of correlation between the Doppler signal characteristics and hepatic fat fractions was assessed using a linear regression test.

Results: In 23 patients (44%) with NASH, the Doppler US spectrum of the middle HVW was monophasic-biphasic. Triphasic HVWs (normal waveform) were found in 29 (56%) patients. The results of Doppler US were correlated with the hepatic fat fraction ($p < 0.0001$).

Conclusion: On duplex Doppler sonography, the abnormal (monophasic and biphasic) flow pattern in the middle hepatic vein is mainly caused by the level of hepatic fat fraction in patients with NASH.

P-196

The role of imaging techniques in acute bleeding liver: a rational approach

J.C. Quintero, S. Mourelo, C. Roqué, J. Sampere, J.A. Jiménez, E. Barluenga; Badalona/ES

Learning objectives: 1) Recognize the imaging radiology manifestation of hemoperitoneum originate in the liver and identify key CT features that may help direct management. 2) Establish the differential diagnosis of hemorrhagic hepatic conditions, traumatic and no traumatic.

Background: Spontaneous hepatic bleeding is a rare condition. In the absence of trauma or anticoagulant therapy, hepatic hemorrhage may be due to underlying liver disease. The most common causes of no traumatic hepatic hemorrhage are HCC and hepatocellular adenoma. Such hemorrhage can also occur in patients with other liver tumors, and other conditions.

Imaging findings OR Procedure details: We reviewed retrospectively 29 patients with acute bleeding liver diagnosed in our institution. We present a comprehensive algorithmic approach to diagnose in acute bleeding liver. 1) Traumatic conditions (11); 2) HCC (6); 3) Hepatocellular adenoma (2); 4) Other liver neoplasms: focal nodular hyperplasia (1), hepatic hemangioma (1), hepatic metastasis (3) hepatic hamartoma (1) and primary hepatic lymphoma (1); and 5) Other conditions associated with spontaneous hepatic haemorrhage: HELLP syndrome (2), amyloidosis, peliosis, connective tissue diseases, infectious diseases, and parasitic diseases (1).

Conclusion: Hemoperitoneum may occur in various emergent conditions. In the trauma setting, evidence of intraperitoneal blood depicted at CT should lead the radiologist to conduct a careful search of images for the injured visceral organ. Imaging plays a significant role in the diagnosis and management of this potentially lethal entity.

P-197

Hepatic fascioliasis: imaging characteristics with a new finding

Z. Koc, S. Ulsan, N. Tokmak; Adana/TR

Purpose: To present the imaging characteristics of four patients with hepatic fascioliasis (HF) showing a new finding.

Material and methods: Imaging and clinical findings of four patients diagnosed with HF were evaluated retrospectively. All patients were examined by abdominal US and MDCT, and two of them additionally evaluated by abdominal MRI, MRCP and ERCP. Diagnosis was confirmed by serological and parasitological tests in all patients.

Results: Presenting complaints were abdominal pain and fever in all patients. All patients also had eosinophilia and abnormal liver function tests. In all patients, US examinations showed irregular marginated hypochoic areas, and MDCT examinations showed branching irregular linear and nodular nonenhancing hypodense areas in the liver. Apart from these findings, hyperdense materials identified in the dilated bile ducts in one patient were revealed as a new finding. MRI showed hypo (T1) and hyperintense (T2) areas of liver parenchyma in two patients, with peripheral enhancement in one of them. Filling defects and dilation of the intra-extrahepatic bile ducts were identified by US and MRCP in two patients. In these two patients, fasciola flukes were removed by ERCP. Medical treatment (triclabendazole) was successful in all patients.

Conclusion: HF is a rare disease that may have typical imaging findings in the liver and bile ducts. Imaging characteristics with clinical findings may have a diagnostic clue especially in endemic areas.

P-198

Frequency of asymptomatic intrahepatic spontaneous portosystemic venous shunts on abdominal MDCT

S. Senturk, A.T. Ilica, A. Bilici; Diyarbakir/TR

Purpose: The portosystemic venous shunts within the hepatic parenchyma are considered to be rare and their cause is controversial. With recent advances in diagnostic imaging techniques, the number of reports of intrahepatic portosystemic venous shunts identified incidentally in asymptomatic patients is increasing. The purpose of this study is to determine the frequency of asymptomatic intrahepatic portosystemic venous shunts on MDCT of the liver.

Material and methods: We retrospectively reviewed 196 dynamic CT examinations of the liver, which were performed using a 64-detector unit between April 2006 and December 2007. The study included 196 patients, aged 22–77 years (mean 52 years). All patients were administered 120 mL of intravenous contrast material at an injection rate of 4 mL/sec. The images acquired at arterial and portal venous phases were reviewed using multiplanar reconstructions and maximum-intensity-projection. The clinical data of patients with intrahepatic portosystemic venous shunts was obtained from hospital records.

Results: We determined 3 patients with intrahepatic spontaneous portosystemic venous shunts. Although portosystemic venous shunts could lead to hepatic encephalopathy, all of the patients we studied were asymptomatic. One of the patients had a small shunt related to portal hypertension. The other two patients had no additional abdominal pathologies.

Conclusion: MDCT can be used to identify asymptomatic small intrahepatic portosystemic venous shunts, which are probably more common than they are considered to be.

P-199

Portal venous gas: is sonography a better technique than CT?

P.A. Santos, R. Maia, M. Gomes, J. Pires, F. Reis, M. Ribeiro; Porto/PT

Learning objectives: To understand the major causes and mechanisms leading to the presence of gas in hepatic portal system and the role of US and CT studies in this setting based on imaging findings in 6 cases.

Background: Presence of gas in the portal vein is a rare entity. Once detected, it should be considered a life-threatening event until proven otherwise, depending, above all, on the underlying aetiology. Intestinal necrosis is the leading cause of portal venous gas (PVG) and is associated with higher mortality rates. First reports of PVG were based on plain film findings, which have a poor sensitivity. The advent of sonography and CT allowed the detection of smaller amounts of gas in the portal system.

Imaging findings OR Procedure details: PVG was considered present when sonography showed multiple high-amplitude echoes moving within the lumen of portal vein in the direction of blood flow. At CT, portal vein gas appears as tubular areas of decreased attenuation in the liver, predominantly in the left lobe. In the study group, US proved to be more sensitive than CT in the detection of PVG, which was reported and explained in some previous papers.

Conclusion: Recognition of PVG indicates, generally, a life-threatening acute abdominal process. However, this finding is no more than a radiological clue and not a diagnosis. In our experience, sonography proved to be the most sensitive method in the detection of PVG. However, the goal of radiologic techniques, besides PVG confirmation, is to establish the underlying pathological process, which is best carried out by CT.

P-200

The significance of the right hepatic artery originating from the superior mesenteric artery in patients with portal vein thrombosis

A. Erden, E. Düşünceli, E. Üstüner; Ankara/TR

Purpose: Dilatation of the hepatic artery in response to the decrease in portal vein flow is known as "hepatic arterial buffer response" (HABR). In this study, the effect of HABR on variant hepatic arterial anatomy is investigated by analyzing the frequency of right hepatic artery originating from superior mesenteric artery (variant artery) and by searching dimensional relationship exists between variant artery and common hepatic artery (CHA) in patients with portal vein thrombosis (PVT).

Material and methods: Ninety patients who were referred for contrast-enhanced abdominal MR angiography were evaluated under three groups as those with PVT

(group I, n=24), with recanalized PVT (group II, n=11), and without PVT (group III, n=55).

Results: The mean diameter of the CHA and variant artery in group 1 was significantly ($p<0.01$) larger than that of the control group. The mean diameter of the CHA in subjects with the variant artery was significantly smaller ($p<0.05$) than that of the subjects without variant artery when all groups were taken into account. The area under the ROC curve (0.906 ± 0.075) indicated that the variant artery was a significant parameter ($p<0.01$) at separating the patients with and without PVT.

Conclusion: In conclusion, HABR is effectual on variant artery in patients with PVT.

P-201

Evaluation of portal venous velocity with Doppler US in patients with nonalcoholic steatohepatitis

S. Ulasan, T. Yakar, Z. Koc; Adana/TR

Purpose: The aim of our study was to determine the relationship between portal venous velocity and hepatic-abdominal fat evaluated in patients with nonalcoholic steatohepatitis (NASH) using spectral Doppler US recordings and MRI.

Material and methods: In this prospective study, 35 patients with NASH and 29 normal healthy adults who served as control group underwent portal Doppler US. The severity of hepatic steatosis in patients with NASH was assessed by MRI through chemical shift imaging using a modification of Dixon Method. Abdominal (intra-abdominal and subcutaneous) fat was measured using MRI.

Results: The difference in the portal venous velocity between the patients with NASH and the control group was significant ($p<0.0001$). There was not any correlation between the degree of abdominal or hepatic fat and the portal venous velocity ($p>0.05$).

Conclusion: Patients with NASH have a lower portal venous velocity than normal subjects.

P-202

Contrast-induced nephropathy following the intravenous injection of iso-osmolar and low-osmolar contrast media: a pooled analysis

H.S. Thomsen¹, S.K. Morcos², C.M. Erley³, L. Romano⁴, D. Sahani⁵; ¹Herlev/DK, ²Sheffield/UK, ³Berlin/DE, ⁴Naples/IT, ⁵Boston, MA/US

Purpose: To compare the incidence of contrast-induced nephropathy (CIN) after administration of low-osmolar contrast media (iomeprol-400 or iopamidol-370) or iso-osmolar iodixanol-320 in patients with chronic kidney disease undergoing MDCT.

Material and methods: 301 patients with CrCl < 60 mL/min received LOCM (n=153), or IOCM (n=148) in two double-blind studies. A subset of patients (n=67; LOCM, n=52; IOCM) had CrCl <40 mL/min and SCr >2.0 mg/dL. All patients received a similar CM dose (40 gI) IV at 4 mL/s. Blood samples were collected pre-dose and at 2–3 days post-dose for SCr determinations in the same central laboratory. CIN endpoint was an increase in SCr >0.5 mg/dL from baseline. Baseline patient characteristics were compared using a chi-square test or the unpaired t-test, as appropriate. CIN rates were compared using a chi-square test.

Results: The two groups were comparable at baseline for all the variables tested. A significantly greater change in SCr from baseline was seen in patients receiving IOCM compared with patients receiving LOCM (0.05 ± 0.25 vs. -0.02 ± 0.18 mg/dL, $p=0.008$). The rate of post-dose SCr increases >0.5 mg/dL was 4.7% (7/148) after IOCM and 0/153 after LOCM ($p=0.007$). In patients with CrCl <40 mL/min and SCr >2.0 mg/dL, the rate of CIN was 11.5% (6/52) after IOCM, 0/67 after LOCM ($p=0.006$).

Conclusion: In high-risk patients receiving IV contrast, the rate of CIN may be higher following the IOCM than the LOCM.

P-203

Radiological characteristics of HCC in children: a 16 year experience in a tertiary paediatric hepatology centre

D. Lewis, P.A. Kane, B. Portmann, M. Sellars, M. Samyn, N. D. Heaton, J. Karani; London/UK

Purpose: Hepatocellular carcinoma [HCC] is an extremely rare and commonly fatal malignancy in childhood. Early recognition allows opportunity for surgical cure. We have reviewed our experience in order to define the radiological characteristics of HCC in this population in association with pathological subtype.

Material and methods: We undertook a retrospective review of clinical, radiological and pathological and surgical data of all children with HCC referred to our unit between 1991 and 2007. The relevant demographics, clinical, pathological and radiological features were documented.

Results: 30 patients with a mean age of 9.3 yrs and M:F ratio of 13:17 were identified. Pre-operative imaging, including a variable combination of USS, CT and MRI, was available in 26 patients. Lesion size ranged from 7 to 205 mm; mean 82 mm. The tumour was multifocal in 9 and a solitary nodule in 17. In 19 children, arterialisation was a dominant feature, venous or caval thrombosis recognised in 11 and calcification in 8. Lymphadenopathy and distant metastases were a feature in 9 and 6 cases, respectively. CT was the imaging modality most reliably associated with correct diagnosis and pathological sub-type of HCC. Full analysis of results will be presented.

Conclusion: Our experience represents the largest series of paediatric HCC in recent times. This presentation illustrates the radiological characterisation of this rare but important tumour.

Diagnostic / Liver / Transplantation

P-204

Early postoperative bleeding following living donor liver transplantation: clinical impacts and CT findings compared with angiography

S.S. Hong, A.Y. Kim; Seoul/KR

Learning objectives: To illustrate various CT findings of the early postoperative bleeding following LDLT confirmed by angiography. To discuss the clinical impacts of these early postoperative bleedings following LDLT and CT findings or CT angiographic findings compared with angiography according to the various bleeding causes. To evaluate the possible bleeding arteries according to the location of hematoma and contrast leakage on CT scan.

Background: Delayed detection of postoperative arterial bleeding following living donor liver transplantation (LDLT) can be fatal because of most of arterial bleeding becomes suddenly descent in hematocrit and hypotensive. As a result, in most of the cases open surgical revision or interventional embolization is needed.

Imaging findings OR Procedure details: The early postoperative bleeding following LDLT can be caused by problems with vascular anastomosis, rupture of a hepatic artery pseudoaneurysm, inferior phrenic artery bleeding, right renal capsular artery bleeding, intercostals artery bleeding after chest tube insertion site, pancreatoduodenal arcades and jejunal branch bleeding, right adrenal hemorrhage, and abdominal wall hemorrhage. In this exhibit, we will discuss the clinical impacts of these early postoperative bleedings following LDLT and CT findings or CT angiographic findings compared with angiography according to the various bleeding causes. Emphasis is laid on evaluation of the possible bleeding arteries according to location of hematoma and contrast leakage on CT scan.

Conclusion: On serial follow-up CT images, if there are active bleeding findings including increased in size of loculated hematoma, dilated vascular structure, or the extravasation of contrast media, it should be managed surgically or by transcatheter embolization without delay.

P-205

Splenic artery aneurysm in liver transplant patients in Hungary

A. Németh, E. Hartmann, L. Kóbori, Z. Gerlei, V. Weszelits, A. Doros; Budapest/HU

Purpose: The splenic artery aneurysm (SAA) incidence is higher in patients with portal hypertension and cirrhosis than in the average population. The aim of this study is to analyze the results of the clinical and radiological follow up of our liver transplant patients with preoperatively diagnosed SAA.

Material and methods: From 1995 to 2008, a total of 352 orthotopic liver transplantations were performed in 335 patients at our institute. Pre- and 1-year postoperative CT-angiograms of 306 liver transplant patients, age 12.7–63.1 y (mean: 46.1), female-male ratio 16/9 were reviewed for number, size, location and morphology of SAAs. Underlying liver diseases: postviral cirrhosis (17), primary biliary cirrhosis (3), autoimmune (2) ALD, and congenital fibrosis and

Wilson disease 1 case each.

Results: Twenty-five patients had 66 saccular aneurysms (size range: 3–35 mm), in 13 patients multiple. Overall incidence was 8.2%. Sixty aneurysms (91%) located in the distal, 6 in the middle third of the splenic artery. The number of large SAA (>2 cm) was 4. One concomitant renal artery aneurysm was found. Radiological or surgical action for rupture prevention happened in 5 patients. With surgical and radiological intervention of SAA we had no rupture. The control angiographies showed no changes in size and number of the untreated aneurysms.

Conclusion: Large SAA requires surgical or interventional treatment, although, untreated aneurysms showed no progression, and the patients remained free of symptoms.

Diagnostic / Liver / Ultrasound Contrast Agents

P-206

Sequential use of contrast enhanced US and FDG-PET in the assessment of hepatic metastasis resectability in patients with treated colorectal carcinoma

L. Guzmán-Álvarez, D. Cabello-García, M. Culiáñez-Casas, C. Sánchez Toro, A. Medina-Benítez, A. Rodríguez-Fernández, E. González-Flores, D. Garrote Lara, M. Gómez-Río, J.M. Llamas Elvira; Granada/ES

Purpose: Contrast enhanced ultrasonography (CEUS) and FDG-PET have been proposed as diagnostic procedures in order to establish metastatic hepatic disease in patients with treated colorectal carcinoma. The purpose of this study project is to evaluate the use of both procedures in the management of these patients referred to diagnostic accuracy.

Material and methods: Thirty-two patients (mean age: 62 y; 21 male) under follow-up for colorectal carcinoma with suspicion of metastatic hepatic disease have been sequentially explored in blinded conditions using CEUS and FDG-PET (mean interval: 17.2 d). Standard reference used was: lesion pathology (19/32); intraoperative US (5/25); follow up (8/25).

Results: Five patients were free of tumour activity >22 months since initial treatment (true negatives). In three patients, FDG-PET showed systemic dissemination and contraindicated surgery for lesions. In twenty-four patients, CEUS and FDG-PET showed lesions as potentially resectable. Referred to individual lesions (n=68), no tests showed false positives; diagnostic accuracy for lesions was: CEUS: 58 true positive, 10 false negatives (sensitivity: 85%); FDG-PET: 37 true positives, 31 false negatives (sensitivity: 54%), mainly due to the high number of lesions smaller than 10 mm (n=17).

Conclusion: Although both methods are quite useful in determining the treatment decision based on a per patient analysis, the preliminary results in this short cohort shows that CEUS helps the surgeons in their surgical attitude, obtaining much more better results than FDG-PET in order to establish the number, size and localization of liver metastasis in patients with treated colorectal carcinoma, which is determinant in surgical assessment.

P-207

Pattern of enhancement of hepatic metastases on contrast enhanced US: is the classification in hypovascular and hypervascular still valid?

P. Cabassa, E. Gatti, E. Brunelli, E. Orlando, R. Monesi, R. Maroldi; Brescia/IT

Purpose: To describe enhancement and vascularity characteristics of liver metastases on contrast-enhanced ultrasonography (CEUS).

Material and methods: In a three year period from the database of focal liver lesions studied with SonoVue, 71 metastases were identified (gastrointestinal [n=31], lung [n=10], breast [n=7], pancreas [n=10], and other [n=13]). Inclusion criteria were: histologic (biopsy or surgery) proof of malignancy; no previous treatments with thermal ablation or chemoembolization. When more than one lesion was present, a target lesion was chosen for evaluation. CEUS was performed during continuous real time scanning with second generation contrast media (SonoVue) at the standard dose of 2.4 ml with specific contrast settings at low mechanical index (0.1–0.2). Data were recorded prospectively and analyzed retrospectively. Patterns of enhancement were assessed lesion by lesion during

arterial, portal and late phases.

Results: 57/71 (80.3%) lesions showed enhancement during arterial phase. In 42/57 nodules, the enhancement was homogeneous and in 15/57 inhomogeneous. In 41/55 lesions, the enhancement was particularly strong in the early arterial phase (within 20 sec) compared to the late arterial phase. Arterial phase enhancement was present also in well known hypovascular metastasis (i.e. colorectal). All lesions had wash-out during portal and late phases becoming hypoechoic to the surrounding liver.

Conclusion: Most of metastases showed arterial enhancement. Contrary to MDCT and MR, the classification in hypovascular and hypervascular on CEUS is therefore debatable.

P-208

Characterization of focal liver lesions: contrast-enhanced US versus MDCT and MR

T.V. Bartolotta, A. Taibbi, M. Galia, G. Malizia, G. Runza, M. Midiri, R. Lagalla; Palermo/IT

Purpose: To evaluate the diagnostic performance of contrast-enhanced US (CEUS) in comparison with multidetector computed tomography (MDCT) and magnetic resonance (MR) in the characterization of focal hepatic lesions (FHLs).

Material and methods: 139 patients (mean age: 57.6 years) with 163 FHLs (mean size: 3.2 cm), 88 benign (35 hemangiomas, 29 focal nodular hyperplasia, 2 hepatocellular adenomas, 11 focal fatty sparing, 5 regenerating nodules, 3 focal fatty areas, 1 hydatid cyst and 1 hemangiopericytoma) and 75 malignant (46 metastases, 26 hepatocellular carcinoma and four more rare lesions), underwent CEUS after SonoVue® administration. 110/163 FHLs were evaluated with MDCT, 36/163 with MR and the remaining 17/163 with both techniques. Two blinded readers reviewed CEUS images and were asked: 1) to classify each lesion as malignant or benign on a five-point scale; 2) to characterize, if possible, each lesion on the basis of established criteria and 3) if further imaging work-up was needed. Sensitivity, specificity, and diagnostic accuracy were calculated.

Results: CEUS correctly characterized 147/163 (90.2%) lesions, showing high values of sensibility, specificity and diagnostic accuracy either for benign, (86.5, 100 and 92.7%, respectively) and malignant lesions (94.7, 97.8 and 97.5%, respectively) making necessary further imaging work-up in 52/163 (31.9%) cases.

Conclusion: CEUS improves the diagnostic capability of radiologists in the characterization of FHLs with accuracy comparable to that of MDCT and MR, reducing the need for further imaging investigations.

P-209

Multiparametric evaluation of contrast-enhanced behaviour at very low mechanical index contrast-enhanced US of a large series of hepatic adenoma

V. Cantisani¹, P. Ricci¹, M. D'Onofrio², F. Calliada³, D. Sahani⁴, U. D'Ambrosio¹, V. Lombardi¹, R. Passariello¹; ¹Rome/IT, ²Verona/IT, ³Pavia/IT, ⁴Boston, MA/US

Learning objectives: CEUS is an effective technique in identifying micro and macrovascular characteristics of hepatic adenoma. Typically, hepatic adenoma shows early (10–19 seconds), homogeneous enhancement during arterial phase and absence of portal venous phase enhancement.

Background: To describe contrast-enhanced behaviour of histological proven hepatic adenomas studied with low mechanical index (MI) contrast-enhanced US (CEUS).

Imaging findings OR Procedure details: From 2003 and 2006, the databases of four academic hospitals (Università degli studi di Verona, Mass General, Boston, Policlinico Umberto I, University La Sapienza, Rome, and Policlinico San Matteo, Pavia) were reviewed to evaluate the imaging findings of patients with histological proven hepatic adenoma studied with CEUS at low-MI (0.06–0.2). CEUS multiparametric behaviour was analyzed.

Conclusion: 24/25 (96%; 95% CI=80.5–99.3%) showed high intensity of enhancement as scored as 3, while only one (4%; 95% CI=0.7–19.5%) was classified as score 2. The time of contrast arrival ranged between 10 and 19 sec (average 13). All but one of the 25 lesions (96%; 95% CI=80.5–99.3%) showed early homogeneous enhancement during hepatic arterial phase. Nor portal venous phase enhancement was observed in any lesions as all showed rapid washout (100%; 95% CI=86.7–100%). Twenty lesions (80%; 95% CI=60.9–91.1%) were found to be iso to slightly hypoechogenic in the portal phase and 19 were (76%; 95% CI=56.6–88.5%) iso to mildly hypoechogenic whereas 6 lesions (24%; 95% CI=11.5–43.4%) were hypoechogenic during the later phases.

P-210**Hepatocellular cancer response to radiofrequency tumor ablation: contrast-enhanced US**

T.V. Bartolotta, A. Taibbi, M. Galia, G. Malizia, G. Lo Re, M. Midiri, R. Lagalla; Palermo/IT

Learning objectives: To illustrate the spectrum of CEUS findings in the assessment of RFA therapeutic response of HCC.

Background: Radiofrequency ablation (RFA) is increasingly being used as percutaneous treatment of choice for patients with early-stage hepatocellular carcinoma (HCC). An accurate assessment RFA therapeutic response is fundamental, since a complete tumor ablation significantly increases patient survival, whereas residual unablated tumor needs an additional treatment. Recently, contrast enhanced ultrasound (CEUS) has become available for RFA assessment. Advantages and limitations of CEUS are described on the basis of a series of 337 RFA treated HCC.

Imaging findings OR Procedure details: At CEUS, a complete response is the absence of enhancing portion within or at the margin of the ablation zone during the hepatic arterial phase (HAP). Residual unablated tumor is the persistence of an irregular hypervascular area within the treated HCC in the HAP, either located within the edge (ingrowth) or around a treated nodule, and in continuity with its border (outgrowth). A uniform and thin peripheral rim of contrast enhancement surrounding the ablated zone in a rindlike fashion should be regarded as benign reactive hyperaemia, whereas a transient hyperechoic area in the HAP may be an arteriovenous shunting.

Conclusion: Awareness of CEUS findings make the radiologist to confidently detect residual disease after RFA of HCC, thus allowing retreatment even in the same RFA session and resulting in a better patient management.

P-211

Withdrawn by authors

P-212

Withdrawn by authors

Diagnostic / Other / Acute and Post-Traumatic Abdomen**P-213****Plain abdominal radiograph: still useful in the era of MDCT**

E. Kelliher, G. Albuquerque, A. Alzahrani, H. Khosa, P. Mc Carthy; Galway/IE

Learning objectives: To provide a pictorial review of GI and abdominal conditions that may be diagnosed from the PFA (plain abdominal radiograph). To describe and explain the relevant radiological signs. To highlight the value of continuing to perform this simple quick non-invasive non-contrast inexpensive low dose examination, which may, in some cases, render CT unnecessary.

Background: Because of the superior diagnostic sensitivity and specificity of MDCT and its increasing accessibility, patients presenting with an acute abdomen often proceed directly to CT without first having a plain abdominal radiograph (PFA). It is worth remembering that CT has disadvantages, specifically: radiation dose, contrast and cost. Many causes of acute abdominal pain can be ascertained by examining the PFA.

Imaging findings OR Procedure details: Pictorial review of PFAs with CT correlation demonstrating causes of abdominal pain suggested/diagnosed from a PFA through analysis of bowel gas pattern (small/large bowel obstruction, gallstone ileus, gastric/caecal/sigmoid volvulus, congenital malrotation, hernias, intussusception, Hirschsprungs), abnormal gas shadows (aerobilia/portal venous air/intramural air), abnormally located soft tissue (masses/abscesses), abnormal bowel wall (inflammatory bowel disease, ischaemic/pseudomembranous colitis), abnormal calcific densities (appendicolith, biliary calculi, pancreatic calcification, hepatic hydatid disease) and foreign bodies.

Conclusion: Radiologists should promote awareness among clinicians of the continued value of requesting and examining the PFA and radiologists themselves should do so when accepting requests for other modalities as the diagnosis may be apparent from the PFA.

P-214**The imaging approach to right sided abdominal pain**

A. Tokala, D. Kasir, S. Sukumar, V. Rudralingam; Manchester/UK

Learning objectives: 1. To discuss the value of cross sectional imaging in the work up of RSAP. 2. To demonstrate the imaging features of common and unusual alternative diagnosis encountered. 3. To describe the potential imaging pitfalls seen on US and CT.

Background: The management of patients with right sided abdominal pain (RSAP) is increasingly dependant on the imaging findings. The inappropriate choice of imaging modality can lead to misinterpretation. US is the established first line imaging modality in suspected cases of acute cholecystitis and appendicitis. In the appropriate clinical setting, further cross sectional imaging with CT should be performed.

Imaging findings OR Procedure details: 1. The spectrum of imaging findings and pitfalls in common causes of RSAP such as acute appendicitis and acute cholecystitis will be presented. 2. An emphasis will also be placed on the unusual causes of RSAP, for example, acute right sided adrenal hemorrhage, omental infarction, acute appendicitis and right sided diverticulitis.

Conclusion: The appropriate use of US and CT ensure the clinical triage of patients into the correct treatment pathway. This enables the accurate differentiation between surgical and non surgical candidates.

P-215**Torsion of spleen: a CT diagnosis**

A. Ben Ely, S. Strauss, G. Gayer; Zerifin/IL

Purpose: The purpose of this presentation is to report the CT features of splenic torsion, a rare condition which presents as an acute abdomen.

Material and methods: The US and CT studies of five patients with surgically proven torsion of the spleen were reviewed. All patients presented with severe abdominal pain. US was the initial study performed in all patients, followed by CT within the next 24 hours.

Results: US showed a mildly enlarged spleen in three patients. Diminished blood flow on Doppler examination was noted in one case. The spleen was thought to be in its usual location and the diagnosis of torsion of the spleen was not suggested. On CT, a more caudal location of the spleen in the left midabdomen was detected in four patients. Postcontrast CT showed complete lack of enhancement of the splenic parenchyma in three patients, patchy enhancement in one, and very poor, but homogeneous, enhancement in one, indicating partial or complete infarction. A "whirl" appearance representing the twisted splenic pedicle was seen in four patients. Emergency surgery in the five patients confirmed the diagnosis of splenic infarction caused by torsion. Four patients underwent splenectomy and the one of them underwent detorsion with splenopexy.

Conclusion: Imaging plays an essential role in the diagnosis of torsion of the spleen and prompt diagnosis is crucial in order to preserve the spleen.

P-216**Acute abdomen in non-traumatic patients: spectrum of MDCT findings and clinical correlation according to the causes of inflammation and neoplasm and localization of solid and hollow viscera**

K.N. Jee, K.H. Lee, Y. Kim; Cheonan/KR

Learning objectives: To understand the characteristic CT findings and pitfalls of AA in non-traumatic patients according to the inflammatory, neoplastic, vascular causes and localization of solid and hollow viscera 2. To evaluate the correlation of CT findings and clinical severities or medical and surgical conditions in non-traumatic AA.

Background: Acute abdomen (AA) is needed to recognize and understand characteristic CT findings and pitfalls of AA in non-traumatic patients according to the various causes and localization of solid and hollow viscera and to evaluate the correlation of MDCT findings and clinical severities or medical and surgical conditions in non-traumatic AA.

Imaging findings OR Procedure details: 1. Cause and localization; acute (infectious/vascular) inflammation, calculous/tumorous/mechanical obstruction, exacerbation or relapse of chronic inflammation and vascular accidents due to underlying conditions in solid organs of liver, pancreatobiliary and genitourinary systems, hollow viscera and mesentery, etc. 2. Correlation of imaging and clinical severity; medical condition of acute inflammation, emergent interventional

conditions of obstruction of viscus with vascular accident, etc.

Conclusion: MDCT is very helpful to localize and differentiate causes such as calculous/tumorous/mechanical obstruction, exacerbation or relapse of chronic inflammation and vascular accidents due to underlying conditions in solid organs of liver, pancreatobiliary and genitourinary systems, hollow viscera and mesentery, etc. CT findings should be considered combined with clinical findings when we decide the treatment option because clinical and radiological severities are relatively well correlated.

P-217

Air in strange places on the plain abdominal radiograph

E. Kelliher, H. Khosa, T. Ramadan, M. Browne, P. Mc Carthy; Galway/IE

Learning objectives: To highlight the importance of identifying abnormal gas shadows on the PFA. To outline the features of such abnormal gas shadows to facilitate recognition and accurate reporting. To demonstrate the variety of pathology that can cause such appearances.

Background: Prompt recognition of abnormal gas patterns on the plain abdominal radiograph (PFA) is vital to minimise morbidity/mortality. Serious abdominal pathology such as intestinal perforation may be silent when the patient is elderly, on steroids, or unconscious/critically ill/post trauma and so the appreciation of abnormal gas patterns becomes even more important.

Imaging findings OR Procedure details: Air on the PFA is normally confined to the lumen of the GI tract. In a variety of serious pathological conditions, air may occur within solid viscera or within the walls of a viscus (eg. emphysematous cholecystitis or pyelonephritis, abscesses, necrotizing enterocolitis), it may escape into the peritoneal cavity (pneumoperitoneum), or it may occur within the biliary system (aerobilia), portal venous system, abdominal wall (abscesses, hernias) or retroperitoneum. We provide a pictorial review and discussion of possible appearances of pathological gas shadows on the PFA with reference to anatomical structures.

Conclusion: Important pathology may be diagnosed from this simple, quick, inexpensive non-contrast examination through recognition and correct interpretation of abnormal gas shadows. Correct interpretation of the PFA can facilitate further investigations/management and lead to speedier patient diagnosis and treatment.

P-218

Imaging of the acute abdomen in haematology patients

H.G. Delaney, S.A. O'Keefe, M.T. Keogan; Dublin/IE

Purpose: To review the radiological findings in patients with haematological disorders presenting with acute abdominal pain and to determine which particular pathologies and imaging features are more common or unique to this cohort of patients.

Material and methods: A retrospective review of all haematology patients (39) presenting with acute abdominal pain over a nine month period who underwent cross-sectional imaging with CT was performed. The clinical details, radiological findings and final diagnoses were correlated and the imaging features were reviewed.

Results: There were a wide variety of presentations and causes for acute abdominal pain. Some were related to tumour burden including painful organomegaly, bowel obstruction and acute urinary obstruction (11). Others were related to treatment or complications of treatment including graft versus host disease of bowel and neutropenic colitis (12). Two patients developed splenic infarction, while three patients had spontaneous retroperitoneal bleeds. Pathology unrelated to the haematological diagnosis or its treatment was demonstrated in three patients.

Conclusion: Cross-sectional imaging of the acute abdomen is being performed more commonly in patients with haematological disorders. There are a wide variety of causes of abdominal pain including those directly related to disease bulk and complications of treatment. A number of pathologies are unique to, or more common, in these patients and consideration of this with knowledge of the relevant radiological findings is essential in reaching the correct diagnosis.

P-219

Abdominal complications of major gynaecologic surgery: CT examination technique and imaging finding

E. Cucci, M. Ciuffreda, M. Missere, L. Aquilani, M. Barrassi, G. Sallustio; Campobasso/IT

Learning objectives: To describe acquisition technique and imaging findings of CT in abdominal complications of major gynaecologic oncologic surgery.

Background: The initial goal in treatment of patients with gynaecologic malignancies, particularly ovarian cancer, is optimal cytoreduction surgery including total abdominal hysterectomy with bilateral salpingo-oophorectomy, appendectomy, total infragastric omentectomy, peritonectomy limited to the pelvis, the paracolic gutters, and infiltrated diaphragmatic areas, bowel resection limited to the rectosigmoid, if necessary, and removal of bulky lymph nodes to the infrarenal para-aortic level. Morbidity and several complications are possible in the acute phase post surgery.

Imaging findings OR Procedure details: CT imaging is accurate for evaluating the complications in acute phase post major gynaecologic surgery as fistulas (genito-urinary, uro-enteric, entero-cutaneous); vascular complications (retroperitoneal hematoma, hemoperitoneum, renal infarction); dehiscence (anastomotic, cutaneous); and gastro-enteric complications (gastroparesis, intestinal infarction, perforation, occlusion).

Conclusion: Major gynaecological surgery (MGS) is nowadays more commonly performed, especially in oncologic disease, as far as surgical and chemioradiation treatments are improving the patients' survival. Abdominal complications after MGS are not uncommon and may be more severe if not promptly diagnosed. CT, if correctly performed, may be useful for diagnosis, grading and follow-up of such complications. Knowledge of the CT appearance of these complications strongly helps in a timely and correct diagnosis.

P-220

Comparison of observer performance in a non-traumatic acute abdomen CT setting: a prospective study

N.H. Stauffer, P.R. Rau, A. Tempia, C. Picht, D. Guntern, E. Melloul, N. Kotzampassakis, T. Prot, C. Vallet, S. Schmidt, A. Denys; Lausanne/CH

Purpose: Emergency room reading performances have been a point of interest in recent studies comparing radiologists to other physician groups. Our objective was to evaluate the reading performances of radiologists and surgeons in an emergency room setting of non-traumatic abdominal CTs.

Material and methods: Ten readers representing four groups participated in this study: three senior radiologists and visceral surgeons, and two junior radiologists and surgeons. Each observer blindly evaluated 150 multi-slice acute abdominal CTs. The chosen cases represented established proportions of acute abdominal pathologies in a Level-I trauma center. For statistics, each answer was then transformed into a score ranging from 0=all false to 3=all correct. The gold standard was the intraoperative result or the clinical follow-up for non-operated patients.

Results: Senior radiologists had a mean score of 2.38 ± 1.14 , junior radiologists a score of 2.34 ± 1.14 , whereas senior surgeons scored 2.07 ± 1.30 and junior surgeons 1.62 ± 1.42 . No significant difference was found between the two radiologist groups, but results were significantly better for senior surgeons as compared to junior surgeons and for the two radiologist groups as compared to each of the surgeon groups.

Conclusion: Abdominal CT reading in an acute abdomen setting should continue to rely on an evaluation by a radiologist, whether senior or junior. Satisfying reading results can be achieved by senior visceral surgeons, but junior surgeons need more experience for a good reading performance.

P-221

MDCT in evaluation of splanchnic vascular emergencies: spectrum of imaging findings and criteria for diagnosis

S. Romano, G. Tortora, C. Stavolo, N. Gagliardi, L. Romano; Naples/IT

Learning objectives: To illustrate the imaging procedures protocols. To describe the imaging findings of common and unusual acute vascular disease. To discuss the results, limitations and potentiality of the imaging technique, based on the large patients series of our institution.

Background: Conventional angiography has been traditionally considered as

the main imaging and diagnostic procedure for evaluation of patients with acute vascular splanchnic disease. However, in the last years the advanced technology of the CT showed to have a great potentiality in preoperative and pre-interventional evaluation of this kind of patients in Emergency.

Imaging findings OR Procedure details: MDCT examinations considered were performed in emergency in our institution. All patients underwent multi-phase CT scan of the abdomen and pelvis, using a thin collimation and slice thickness. Intravenous contrast administration was performed in all cases. Post processing imaging reconstruction and evaluation were made at a dedicated workstation. Vessel lumen opacification and features, viscera enhancement and appearance as well as the comparison with additional diagnostic, interventional and surgical procedures have been considered.

Conclusion: MDCT could be considered a valuable diagnostic tool in evaluation of patients with suspected splanchnic acute vascular disease.

P-222

From disaster to diagnosis: pitfalls in imaging the acute abdomen

P. Williams, E.M. Armstrong, J. Shirley, B. Fox, S. Jackson; Plymouth/UK

Learning objectives: To improve awareness of the potential pitfalls in imaging patients with an acute abdomen. To provide learning points for both trainees and consultants based upon clinical examples illustrating the varied pitfalls.

Background: Patients with acute abdominal pain can present a diagnostic challenge to the clinical team. Accurate clinical diagnosis is difficult and often unreliable. Imaging, which is routinely requested, has been shown to minimise delay in surgery, reduce unnecessary admissions, and lower patient mortality. Radiologists must therefore understand the various imaging algorithms including when and how each modality is best utilised, as well as interpret the imaging correctly. This educational poster discusses relevant potential pitfalls – including choosing the incorrect investigation, technical errors resulting from contrast administration, phase and timing of imaging, and varied interpretation pitfalls such as missing subtle pathology and misinterpretation of normal findings and abnormalities.

Imaging findings OR Procedure details: We illustrate the potential pitfalls in imaging the acute abdomen with specific examples and provide learning points for both trainees and consultants, including self assessment cases.

Conclusion: Radiologists make a series of complex diagnostic decisions during the patient pathway from initial referral through to image interpretation. An awareness of how to avoid pitfalls at each stage reduces possible life threatening errors.

P-223

MDCT and US in the evaluation of abdominal trauma

C. Urigo, G.D. Pietricola, V. Cossu, A. Canu, M. Coniglio, S. Frau, R. Favero; Latina/IT

Learning objectives: Illustrate the main findings to detect in course of abdominal trauma through US and MDCT providing the imaging/surgical correlation. Discuss when is appropriate to perform MDCT and when US may replace it in post-traumatic abdomen evaluation.

Background: To assess, describe and illustrate US and MDCT findings in the course of abdominal trauma studied in the Emergency Radiology Department, indicating the fundamental role of both imaging modalities and giving the radiologic/surgical correlation of each finding.

Imaging findings OR Procedure details: MDCT represents the gold standard diagnostic method in the course of abdominal trauma. The fundamental findings illustrated are represented by free fluid in the abdomen, liver, splenic or other parenchymal partial or complete lesions, vascular damages, bone fractures and GI involvement. For each we present the correlation with the surgical detection. We furtherly discuss whether US has to be performed preliminarily and if contrast enhanced US may, in some cases, replace MDCT examination.

Conclusion: During the course of abdominal trauma, patients may require an emergency surgery depending on findings that can be provided by different imaging modalities. US is extremely accurate in revealing free fluid into the abdominal cavity but is less accurate than MDCT in detecting parenchymal lesions. MDCT represents a complete and fast imaging modality in the detection of findings fundamental for the patient clinical course. US may, in some cases such as minor traumas, replace MDCT in the evaluation of abdominal injuries.

P-224

Blunt abdominal trauma: CT findings in patients with solid organ, bowel, mesenteric and diaphragmatic injury

B. Graça, F. Cavalheiro, M.F.S. Seco, L. Curvo-Semedo, L. Teixeira, F. Caseiro-Alves; Coimbra/PT

Learning objectives: To recognize the CT signs of solid organ, bowel, mesenteric and diaphragmatic injuries from blunt trauma. To differentiate CT findings indicative of significant injury from those indicative of nonsignificant injury.

Background: Blunt abdominal trauma (BAT) is a common cause of morbidity and mortality among patients admitted to trauma centers after sustaining multiple traumatic injuries. Although abdominal injuries are often suspected in this setting, clinical diagnosis can be challenging due to the lack of specific physical findings in many patients. CT has been shown to be accurate for the diagnosis of solid organ, bowel, mesenteric and diaphragmatic injuries and is the diagnostic test of choice in the evaluation of patients with BAT.

Imaging findings OR Procedure details: In this exhibit we describe and illustrate: 1. The diagnostic evaluation of the patient with BAT. 2. The CT protocols used to perform optimal examinations. 3. The CT findings in: 3.1 Liver trauma; 3.2 Splenic trauma; 3.3 Pancreaticobiliary Trauma; 3.4 Genitourinary Trauma; 3.5 Bowel injury; 3.6 Mesenteric injury; and 3.7 Diaphragmatic injury.

Conclusion: Solid organ, bowel, mesenteric and diaphragmatic injuries from BAT may be significant and require immediate surgery or may be nonsignificant and permit nonsurgical treatment. CT is the diagnostic test of choice in the evaluation of these patients and is instrumental to guide treatment planning.

P-225

Value of the MDCT in blunt abdominal trauma

M.T. Mallebrera, A. Franco, J. Contreras, O. Benitez, B. Gutierrez; Madrid/ES

Learning objectives: To review the radiological aspects of blunt abdominal trauma with particular emphasis on MDCT. This review will provide answers to three basic questions: 1. When to perform a MDCT on a patient who has suffered a blunt abdominal trauma? 2. How to plan and carry out the MDCT? 3. What radiologic findings do we need to be familiar with to provide an accurate radiologic report?

Background: The actual trend in diagnostic imaging with respect to blunt abdominal trauma is to achieve a fast and accurate diagnosis of the traumatic lesions. To this end, a thorough knowledge of the indications, technical aspects and imaging findings of each modality is essential.

Imaging findings OR Procedure details: We divide blunt abdominal trauma patients into three categories: A. Hemodynamically unstable patients. B. Hemodynamically stable patients. C. Hemodynamically stable patients with hematuria. To provide an adequate scanning protocol MDCT to evaluate abdominal damage in as little as 2 minutes, providing data about vascular and visceral lesions. To describe and to illustrate the most important radiologic findings (haemoperitoneum, active haemorrhage and major visceral damage) with examples from our own practice.

Conclusion: Blunt abdominal trauma is a medical emergency. An extensive knowledge of patient classification, the indications of the imaging modalities and technical protocols, together with a familiarity with the imaging findings can greatly improve the quality and response time of the radiological diagnosis.

P-226

Left lower quadrant pain: step-wise approach to evaluate it

J. Arora, G.S. Karnati; Bristol/UK

Learning objectives: To understand the common and uncommon causes of left lower quadrant abdominal pain. To illustrate the imaging findings (plain X-ray, US, and CT) of the various diseases causing left lower quadrant abdominal pain. To understand the appropriate use and role of different imaging modalities.

Background: The left lower quadrant (LLQ) abdominal pain can be a real challenge to the radiologists as unlike right lower quadrant pain its causes are not well understood. The differential diagnosis of left lower quadrant abdominal pain are: sigmoid diverticulitis; leaking abdominal aortic aneurysm; renal colic; epididymitis; incarcerated hernia; bowel obstruction; regional enteritis; pancreatitis; psoas abscess; and in rare instances, situs inversus with acute appendicitis.

Imaging findings OR Procedure details: In this exhibit, we demonstrate imaging findings and tailored approach for rapid and reasonable evaluation of

the diverse diseases causing LLQ abdominal pain. Imaging methods help to establish a correct diagnosis and to differentiate between benign self-limited disorders and those which require immediate intervention. CT and US are the modalities of choice. Apart from the common renal and gynaecologic diseases, diverse bowel and omental lesions are also included in this exhibit.

Conclusion: Understanding of the imaging findings of these various diseases causing LLQ abdominal pain will prove instrumental in early diagnosis and thus proper management. This exhibit provides a practical easy-to-follow algorithm for radiologists that simplifies the imaging recommendations for left lower quadrant pain.

P-227

Plain radiographs of emergency surgical admissions: Who is responsible for these?

A. Kirwadi, V.B. Pakala, S. Evans; Swansea/UK

Purpose: The present workload, working pattern and shortage of out-of-hours staffing does not allow radiologists to report all the plain radiographs immediately. The main objective of the study was to evaluate how many radiographs have been reviewed by the referring clinical team, by a radiologist and note any serious discrepancies between those reports.

Material and methods: 100 consecutively admitted acute surgical patients requiring a plain radiograph were included in our study. Case notes were reviewed to see if the radiographs were reviewed by the clinician and their findings noted. This was compared with the radiologist report for any significant discrepancies.

Results: 60% of the films were reviewed by the referring clinicians while the radiologist reported on 73%. 14% of films were neither reported by the clinician nor the radiologist. Only 2 minor discrepancies were noted.

Conclusion: The IRMER 2000 guidelines state that clinical evaluation of each medical exposure must be made and recorded by both 'the referrer' and 'the practitioner'. We hope that better documentation by clinicians and implementation of PACS will help in reaching this target. Few similar studies have shown that the discrepancy rate between the clinician's and the radiologist's report is very small. Should we restrict the reviewing of films only to those where a clinician is not confident? Developing guidelines with regards to this would help in utilising the available resources for maximum benefit.

P-228

CT findings of bowel and mesentery and solid organ injury following abdominal and pelvic trauma

S.Y. Park¹, S.S. Hwang¹, Y. Ku², Y.J. Lee³, J.Y. Byun³;

¹Suwon/KR, ²Uijeongbu/KR, ³Seoul/KR

Learning objectives: 1. To understanding of image findings of abdominal and pelvic trauma for the purpose of correctly diagnosing and suggesting a guideline for treatment. 2. To demonstrate image findings of various abdominal and pelvic trauma on CT. 3. To discuss the clinical impact according to variable image findings.

Background: CT plays an important role not only for the detection of abdominal and pelvic injuries but also for their appropriate management. In order to make the best use of CT, the radiologist should be aware of the appearance of various types of abdominal and pelvic injuries and the findings that indicate surgery or that may warrant repeat CT studies for monitoring of expectant management.

Imaging findings OR Procedure details: Bowel and mesenteric traumatic lesions include contusion, hematoma, partial or full laceration of the bowel circumference, and bowel transection. Injuries of the mesentery may affect the vascular structures and thus lead to either bleeding or vascular occlusion with subsequent necrosis and eventual perforation of the corresponding bowel structure. Traumatic lesions of solid organ include spleen, liver adrenal gland, kidney pancreas, and urinary bladder.

Conclusion: CT of the trauma patient has become an important diagnostic tool that allows for appropriate triage of these patients. Knowledge of the various appearances of the posttraumatic abdomen and pelvis on CT scans is essential so that the patient can be afforded prompt and effective treatment.

P-229

Contrast induced nephropathy following I/V contrast: absence of evidence is not evidence of absence

S. Krishan, J.A. Guthrie; Leeds/UK

Purpose: The use of contrast media (CM) is common in abdominal CT. Whilst there are data on the incidence of contrast-induced nephropathy (CIN) following cardiac angiography, the incidence of CIN after intravenous CM administration is less well established. The purpose of this retrospective study was to assess the incidence of CIN in an inpatient population.

Material and methods: Consecutive inpatients undergoing intravenous CM enhanced CT from 1st July 2006 to 31st December 2006 were investigated. Serum electrolytes and creatinine before and up to 7 days after intravenous CM were assessed. CIN was defined as an increase of the serum creatinine-level of >0.5 mg/dl or >25% above baseline within 48 hours after contrast agent administration.

Results: 2876 patients were investigated. 85% CT studies were of the abdomen and pelvis. Manifest CIN was seen in 26 patients (0.9%). In those patients who had pre CT creatinine > 250 mmol/L, the incidence increased to 4.6%. A transient rise in serum creatinine (less than 25% above pre-CT value returning to the pre CT levels within a week) occurred in 78 patients (2.7%).

Conclusion: The study population is uncontrolled but unwell enough to occupy a hospital bed and therefore the results are likely to overestimate the incidence of CIN. CIN is an uncommon complication. Intravenous CM seems to be safe and should not be withheld if diagnostically indicated.

P-230

Richter's hernia after laparoscopy

C. Lam, R. Santos, J.M.G. Lourenço, P. Gil, I. Oliveira, Z. Seabra; Lisbon/PT

Learning objectives: We report a case of Richter's hernia after laparoscopy, showing the relevance of CT in the diagnosis, along with a brief literature review.

Background: Richter's hernia is a rare entity and is the protrusion and/or strangulation of only part of the circumference of the intestine's antimesenteric border through a rigid small defect of the abdominal wall. There are only a few references about Richter's hernia after laparoscopy since the first description in 1977. These hernias may rapidly pass into gangrene, yet signs of intestinal obstruction are often absent. Richter's hernia could be life-threatening if the correct diagnosis and early surgery are not performed. CT is the method of choice in the diagnosis.

Imaging findings OR Procedure details: A 52-year-old woman with a history of gastro-esophageal reflux surgery by laparoscopic three weeks earlier presented to the emergency department with an acute onset of abdominal pain, anorexia and nausea. A palpable mass was found in the lower right abdomen. Abdominal CT demonstrated a Richter's hernia of part of the ascending colon through a trocar site. Surgery confirmed the diagnosis and the patient recovered well.

Conclusion: Although Richter's hernia is still associated with a relatively high mortality rate, CT plays an important role in the correct and early diagnosis, allowing prompt treatment.

P-231

Ischemic hepatitis: an unusual presentation of celiac artery compression syndrome

B. Yagci, N. Karabulut, S. Akalin, G. Onem, Y. Kiroglu; Denizli/TR

Purpose: To present imaging findings of a unique case of celiac artery compression syndrome (CACS) in whom massively increased serum transaminase levels (STL) normalized rapidly after surgical division of median arcuate ligament (MAL) fibers.

Material and methods: A 26-year-old male patient with known chronic hepatitis-B presented with abdominal pain, weight loss, and elevated STL. Contrast-enhanced abdominal multislice-CT performed during inspiration showed normal findings. However, the symptoms including "food fear" continued to worsen over the following days. STL increased 10-times during this period.

Results: Doppler US revealed increased velocities at the celiac artery, particularly during expiration. Angiography showed significant expiratory narrowing of the celiac artery origin and widely patent mesenteric arteries. Expiratory abdominal CT clearly demonstrated severe compression of the celiac artery by MAL. After

surgical division of MAL, STL normalized rapidly and the patient experienced dramatic relief of all symptoms.

Conclusion: Hypoxic (ischemic) hepatitis is defined as a massive but rapidly reversible increase in STL due to an imbalance between hepatic oxygen supply and demand. The postoperative decrease in STL suggested ischemic hepatitis due to the CACS. To our knowledge, this association in non-transplant patients has not been reported before. CACS may induce an ischemic hepatitis-like picture, particularly in cases with chronic liver disease. Because the diagnosis of CACS can be overlooked at the routine inspiratory CT, particular attention should be paid to tailor the imaging protocols to include expiratory scan sets.

P-232

MDCT findings of retroperitoneal space: anatomy and pathology

Y. Ku¹, S.L. Lee², S.S. Hwang³; ¹UiJeongbu/KR, ²Seoul/KR, ³Suwon/KR

Learning objectives: Describe the embryogenesis, anatomy of retroperitoneal space and review the concept of the interfascial decompression planes. Identify the MDCT features of related various pathologic features.

Background: Traditional compartmental anatomy does not completely explain the spread of fluid collections in the retroperitoneum. More recent works including embryologic, clinical considerations and anatomic dissections have modified the classic tri-compartmental model and introduce the concept of the interfascial plane. In this exhibit, we will describe the concept of expandable plane (interfascial plane) in which rapidly growing fluid collections may accumulate through the review of embryology and imaging findings.

Imaging findings OR Procedure details: CT observations demonstrated that the rapidly accumulating fluid collections or hematoma tend to escape the retroperitoneal site of origin into laminar variably fused and potentially expandable interfascial planes. Between these planes, potential communicating spaces exist. These are represented by retromesenteric plane (anterior fusion space), retrorenal plane (posterior fusion space) and lateral conal plane. Interfascial fluid collection can spread from the abdominal retroperitoneum into the pelvis along retromesenteric plane and retrorenal plane that form the combined fascial plane at the level of the iliac fossa.

Conclusion: The knowledge of embryology and anatomy of interfascial plane and their interconnection is helpful for the radiologist to determine the extent and spread pathways of the retroperitoneal diseases.

P-233

Evaluation of acute abdominal conditions by CT

L. Curvo-Semedo, J.F. Costa, J. Brito, A. Canelas, B.J.A.M. Gonçalves, M.F.S. Seco, B. Graça, A. Costa, F. Caseiro-Alves; Coimbra/PT

Learning objectives: To address the advantages and drawbacks of CT in the study of acute abdominal conditions. To illustrate various diagnoses readily apparent on CT and to show common mimickers.

Background: The term "acute abdomen" corresponds to a clinical syndrome characterized by sudden onset of abdominal pain requiring emergency treatment, being nowadays one of the commonest conditions in patients admitted to emergency departments. Prompt diagnosis is essential for minimizing morbidity and mortality, but it can be challenging since clinical-laboratory findings are often non-specific, creating the need for efficient imaging techniques. As a result, CT is being increasingly performed in this setting.

Imaging findings OR Procedure details: Acute conditions will be shown according to a topographic classification of pain (one of four abdominal quadrants, epigastric, generalized or flank pain). For each location, examples of the most common conditions will be illustrated, such as acute cholecystitis (RUQ), pancreatitis (LUQ, epigastrium), diverticulitis (LLQ), appendicitis (RLQ), bowel obstruction, GI perforation and mesenteric ischemia (generalized) or urinary colic (flank), as well as other conditions that need to be taken into account in the differential diagnosis.

Conclusion: CT is increasingly being seen as the first-line examination in patients with acute abdomen, lacking the disadvantages of plain films and US and replacing them in a wide spectrum of situations. It has gained the status of "gold-standard" over the last years, particularly after the developments in MDCT.

P-234

Rectus sheath hematoma: CT findings

B. Acu, B. Sarikaya, U. Bekar, Y. Akturk; Tokat/TR

Purpose: Rectus sheath hematoma (RSH) is an uncommon cause of acute abdominal pain. It is an accumulation of blood in the sheath of the rectus abdominis secondary to rupture of an epigastric vessel or muscle tear. We present clinical, laboratory and imaging findings accompanying with literature knowledge.

Material and methods: Between January and July 2007, at ages between 47 and 76, two males and three females of a total five patients with acute abdominal pain and palpable abdominal mass were examined with CT.

Results: At CT examination, two patients in right rectus muscle, two patients in left rectus muscle and one patient in both rectus muscles were seen compatible with hematoma. All of the patients had abdominal mass and have undergone anticoagulant therapy. All of the patients had anemia and leukocytosis. Four patients were treated conservatively and one was showing clinical recovery after a surgery.

Conclusion: RSH is observed frequently by an acute abdominal pain and a palpable mass and mimicking an acute intraabdominal pathology. The most common presenting feature is a painful lower abdominal mass that never crossing the midline. Most important predisposing factor is anticoagulant therapy. At the diagnosis of RSH, CT examination is gold standard. RSH is generally treated conservatively. In conclusion, in old patients with acute abdominal pain, infraumbilical mass, anemia and using anticoagulant therapy, rectus sheath hematoma should be kept in mind. A careful evaluation of the medical history and clinical suspicion will help to make an accurate diagnosis and avoid an unnecessary laparotomy.

P-235

Acute abdomen of vascular origin: a pictorial review with MDCT angiography

I. Vivas, A. Alonso-Burgos, L. Diaz, D. Cano, J. Broncano, J. Arias, J.I. Bilbao; Pamplona/ES

Learning objectives: 1. To show the broad spectrum of causes of abdominal pain of vascular origin. 2. To propose a classification for vascular causes of acute abdominal pain based on "vascular rupture", "vascular occlusion", "diminished flow" and "solid organ ischemia". 3. To present selected cases that illustrate the relevance of image in the clinical management of patients.

Background: MDCT angiography is the preferred method for imaging in emergent abdominal vascular conditions. It enables the acquisition of high-spatial-resolution volumetric data, including small distal visceral branches, as well the aorta and iliac arteries during a single breath hold. Familiarity with the techniques of image acquisition, contrast dynamics, volumetric data post-processing and interpretation is as important as exact knowledge of the physiology of the lesions.

Imaging findings OR Procedure details: We present images following this classification proposal: (1) Vascular rupture - (a) Abdominal aortic aneurysm, (b) Splachnic aneurysm, (c) Intestinal haemorrhage; (2) Vascular occlusion - (a) Intraluminal: thrombosis and embolism, (b) Parietal: Vascular wall pathology, (c) Extraluminal: Infiltrative and mechanic; (3) Diminished vascular flow; (4) Solid organ ischemia.

Conclusion: 1. MDCT and 3D reformation techniques should be considered as the first line imaging tool for the diagnosis of acute abdominal pain of vascular origin. Familiarity with image findings is fundamental to avoid potential diagnostic pitfalls and eventual complications during therapeutic procedures. 2. The information obtained from MDCT is of great usefulness since it allows quick therapeutic decisions.

P-236

Retroperitoneum: pathways in the spread of disease

C. Leal, J. Raposo, A. Vasconcelos, P. Alves, N. Costa, R.M. Marques; Lisbon/PT

Learning objectives: To illustrate the main pathological conditions that involve the retroperitoneum, understanding their spread patterns through the retroperitoneal spaces and interfascial planes, along with an anatomic and embryologic review.

Background: Anatomic and functional knowledge of communications between the retroperitoneal spaces and existence of easily dissectable interfascial planes

(potential spaces) is essential for accurate evaluation of retroperitoneal disease extension, such as inflammatory or infectious conditions, tumors and traumatic lesions.

Imaging findings OR Procedure details: Abdominal CT is the major imaging modality to approach retroperitoneal pathological processes. Pancreatitis, perirenal hematomas, duodenal perforation with pneumoretroperitoneum, colonic diseases (such as retrocecal appendicitis, infiltrating neoplasms and ischemic colitis), abdominal aortic aneurysm rupture and metastatic tumoral spread are some of the nosologic entities revisited.

Conclusion: Embryologic, anatomic, clinical and imaging evidences exist that retroperitoneal fluid collections and infiltrating diseases may rapidly extend to a contiguous space or interfascial plane or even to the pelvis and mediastinum. A review of these data allows a better spread pattern understanding.

P-237

Radiation dose during follow up of acute pancreatitis

S. Stojanovic, V. Njagulj, S. Senicar, D. Hadnadjev;
Novi Sad/RS

Purpose: In Serbia, there is no regulation or survey control about the amount of radiation received by a patient in any period of time. The aim of the study is to analyse retrospectively the mean dose, length of scanning and DLP during the period of one year in patients with diagnosis of acute pancreatitis (AP).

Material and methods: 154 patients (104 male), mean age 54.4±14.7, were examined on 64 MDCT scanner. The entire abdomen is examined, performing all unenhanced and enhanced scans in parenchymal phase. Data is shown in the form of volumetric "CT dose index (CTDI)", "ScanLength (SL)" and "DLP (dose-length product)".

Results: The patient with AP undergoes CT examination usually more than once (1.8). Per phase, average CTDI, in total was 18.9±10.7 mGy, ScanTime 10.8±6.0 sec, and DLP 263.6±323.6 mGycm. No significance is noted regarding the age group. Average values per phase, during one examination, were CTDI 10.63±4.204mGy, ScanTime 6.31±1.5 sek, DLP 68.58±34.48 mGycm. Female patients had significantly longer scanning time, and male patients had significantly higher CTDI value. DLP did not differ between sexes. Low dose protocols were not used.

Conclusion: The national survey program has to be established in order to follow the effective doses from CT examination in different hospitals and to correct and unify the examination protocols with lowest average radiation dose.

P-238

The clinical diagnosis of acute cholecystitis is unreliable

W. Laméris, A. van Randen, P.M.M. Bossuyt, M.A. Boormeester, J. Stoker; Amsterdam/NL

Purpose: The accuracy of the clinical diagnosis and the added value of US and CT in patients with suspected acute cholecystitis (AC) were investigated.

Material and methods: Sensitivity, specificity and post-test probability of the clinical diagnosis AC were calculated in consecutive emergency department patients with acute non-traumatic abdominal pain. The accuracy of the clinical triad (direct tenderness RUQ, fever and leucocytosis) was also assessed. Post-test probabilities after US and CT in suspected patients were calculated to investigate the added value on top of clinical assessment.

Results: Prevalence of AC was 5% (52/1021). AC was the clinical diagnosis in 62 patients and was present in 29, yielding a sensitivity of 56% (95% CI: 42–69%). The clinical triad was 100% sensitive and specific, but present in only 8% of AC. Post-test probability for AC after clinical assessment was 46%, which increased to 88% after a positive US or CT in suspected patients. A negative test result decreased the post-test probability to 16% for US and to 19% for CT. US and CT reduced the 33 false-positive clinical diagnoses to 3 false-positives.

Conclusion: AC was clinically diagnosed in approximately half of cases. The clinical triad was perfectly diagnostic, but only present in 8%. US and CT reduced the false-positive clinical diagnoses equally and had important added value in patients with suspected AC.

P-239

No added value of plain chest and abdominal radiographs in patients with acute abdominal pain at the emergency department

A. van Randen¹, W. Laméris¹, M.P. Gorzeman², J.S.K. Luitse¹, E.J. Hesselink³, D.E.J.G.J. Dolmans⁴, J. Peringa¹, A.A.W. Geloven⁵, P.M.M. Bossuyt¹, M.A. Boormeester¹, J. Stoker¹;
¹Amsterdam/NL, ²Nieuwegein/NL, ³Apeldoorn/NL, ⁴Utrecht/NL, ⁵Hilversum/NL

Purpose: At the emergency department (ED) plain radiographs are often used as initial imaging modality in patients with acute abdominal pain (AAP). We evaluated the added value of plain radiographs on top of clinical assessment.

Material and methods: Patients presenting to the ED with abdominal pain prospectively underwent both supine abdominal and upright chest plain radiographs. The treating physician recorded per patient the most likely diagnoses after clinical assessment and after radiographs. Reference standard was final diagnosis after 6 months follow-up. Sensitivity, specificity and change in primary diagnosis were calculated for diagnoses to be made at radiography as bowel-obstruction, perforated viscus, and urinary tract stones.

Results: 1021 consecutive patients, 566 female, mean age 47, were included. Sensitivity of bowel-obstruction was significant higher after radiographs 74% (95% CI: 0.63–0.84) than after clinical assessment 57% (95% CI: 0.46–0.69) (p<0.01). Primary diagnosis changed in 11 patients from another diagnosis into bowel-obstruction, albeit not significant (p=0.06). Sensitivity of urinary tract stones was higher after radiographs, although not significant, 48% (95% CI: 0.28–0.68) versus 68% (95% CI 0.41–0.79) (p=0.375). Sensitivity of perforated viscus did not change after radiographs 15% (95% CI 0.04–0.40 versus 95% CI: 0.04–0.42) (p=1.00). For urinary tract stones and perforated viscus, primary diagnosis did not change significantly between clinical assessment and radiographs (p=0.375 and p=0.45, respectively).

Conclusion: There is no added value of plain radiographs after clinical evaluation of non-selected patients with AAP at the ED, even for bowel-obstruction.

P-240

Withdrawn by authors

P-241

The value of CT in female patients with suspected appendicitis and an ultrasonography negative for appendicitis

W. Laméris¹, A. van Randen¹, E.M. van Keulen², M.J. Wierzer³, M.P. Simons¹, O.R.C. Busch¹, T.M. van Gulik¹, P.M.M. Bossuyt¹, M.A. Boormeester¹, J. Stoker¹;
¹Amsterdam/NL, ²Hilversum/NL, ³Nieuwegein/NL

Purpose: To study the effect of secondary CT usage in females with suspected appendicitis and negative US.

Material and methods: Consecutive emergency department patients with non-traumatic acute abdominal pain were included. Patients were given a most likely diagnosis based on clinical assessment and underwent abdominal US and CT. The percentage of missed appendicitis and the negative appendectomy rate (false positives (FP)/all positives) were calculated for US usage only and subsequently for US combined with CT in females with an inconclusive or negative US or females with only an inconclusive US.

Results: We included 1021 patients, (55% female; mean age 47 year (19–94)). Acute appendicitis was clinically suspected in 226 females and was present in 104 (pre-test probability: 46%). CT usage in females with an inconclusive US (85/226=38%) would reduce the percentage of missed appendicitis from 24 (25/104) to 8.7% (9/104) as compared to US only, but increase the negative appendectomy rate from 15.9 (15/94) to 20.8% (25/120). CT in all female patients with a negative US (including inconclusives; 132/226=58%) would further reduce the missed appendicitis percentage to 4.8% (5/104), but increase the negative appendectomy rate to 21.4%.

Conclusion: Secondary CT in female patients with suspected appendicitis and a negative or inconclusive US would substantially reduce the percentage of missed appendicitis but would increase the negative appendectomy rate.

Diagnostic / Other / Radiologic-Pathologic Correlation

P-242

CT pulmonary angiogram: a novel approach to GI imaging?

S. Chawla, D.P. Mullan, A. Camenzuli; Liverpool/UK

Learning objectives: To familiarize the radiologist with subtle review areas and pathologies within the GI system as imaged on CTPA examinations. To argue the case for reduced reliance on protocol based investigations and to suggest the need for thorough clinical evaluation prior to imaging.

Background: Computed Tomography Pulmonary Angiograms (CTPAs) have become the main stay of investigation of suspected pulmonary thromboembolism. The classical symptoms of pleuritic chest pain and shortness of breath are notoriously non-specific in clinical practice. Radiologists are aware of the low positive predictive value of the D-dimer assay. Historically, it is well recognized that GI disease can mimic pulmonary pathology both symptomatically and biochemically. The increasing availability of imaging and D-dimers has arguably led to reduced reliance on clinical examination. This has lowered the threshold for performing CTPAs with positive findings often only identified in the GI system.

Imaging findings OR Procedure details: We present in pictorial fashion, a selection of CTPA studies in which the cause of the symptoms and biochemical abnormalities are shown to be due to GI pathologies. We provide selected images of infective, inflammatory and neoplastic processes with reference to salient clinical and anatomical considerations.

Conclusion: CTPAs are frequently carried out for GI pathologies. This in retrospect could have been suspected clinically, thus negating the need for an imaging modality involving significant ionizing radiation to the chest.

P-243

Staging of rectal cancer: how accurate is MRI?

M.G. Mulla, R. Deb, R. Singh; Derby/UK

Purpose: Rectal cancer ranks as the third commonest tumour of the GI tract. With high recurrence rates (30%), accurate staging of these tumours is essential to prevent recurrences. MRI scan is proven to be effective; however, it is important to understand its limitations.

Material and methods: 40 consecutive patients with rectal cancer were included in this retrospective study. All images were reported by two radiologists imaging and all specimens were reported by two histopathologists. MRI staging done preoperatively was compared to post surgery histology staging.

Results: There were 25 males and 15 females with a median age of 70.5 years. Overall agreement in staging (TNM) between the two was 30% (n=12). T stage agreement was assessed by Kappa coefficient (k=0.4583). Sensitivity and specificity for T staging was 0.89 (0.74, 0.96) and 0.67 (13, 0.98), respectively. PPV and NPV for T staging was 0.85 (0.69, 0.94) and 0.15 (0.06, 0.30), respectively. CRM status was accurately staged, except in one patient (94.1%). Accuracy for lymph node staging was 47.5%.

Conclusion: MRI proved very sensitive in identifying the CRM which remains the main factor affecting the outcome of surgery. Differentiating T2 from early T3 still remains a problem as is with T1 and T2 tumours. Identification of involved nodes is also difficult unless they show similar signal characteristics as the tumour. The use of 'paramagnetic iron oxide' MR may be helpful in future.

P-244

Sickle cell disease: spectrum of MRI appearances of the spleen and relevance to clinical management

S. Sawhney, R. Jain, S. Al-Kindi; Muscat/OM

Learning objectives: The spectrum of MRI morphology of the spleen in Sickle cell disease (SCD) reflecting the pathophysiology of splenic sequestration, infarction and 'autosplenectomy'.

Background: Contrary to popular belief, the spleen in SCD does not just 'disappear' (or autosplenectomise). It has varied appearances which may be mistaken for serious pathology and result in unnecessary surgery or splenectomy.

Imaging findings OR Procedure details: Retrospective analysis of MRI of the abdomen performed in 69 patients of SCD referred for evaluation of bone pains

as part of an ongoing project to study the temporal progression of changes in spleens of patients of SCD. Six of these patients had had prior splenectomy. In the remaining 63 patients (age mean±SD 23.3±7.7), a splenic volume of eight to 1546 ml (mean±SD 341.1±291.5) was recorded. The spectrum of splenic morphological appearances ranged from (in increasing order of severity of involvement): a) simple splenomegaly; b) splenomegaly with peripheral nodular or triangular areas of sequestration/infarction leading to small contracted ferrocalcific spleens; c) enlarged hypointense spleens secondary to transfusional iron overload without/with focal nodular areas of (regenerative) functional splenic parenchyma; d) normal sized markedly hypointense spleens reflecting large volume sequestration; and e) small ferrocalcific spleens.

Conclusion: Splenic morphology in SCD is varied and reflects the pathophysiology of SCD. Awareness of the patterns seen and correct interpretation of morphology can help in preventing unnecessary splenectomy.

P-245

Unusual abdominal and pelvic localizations of non-Hodgkin's lymphoma: CT and MRI examination technique and imaging findings

M. Missere, G. Restaino, E. Cucci, A. Piero, M. Barrassi, G. Giordano, S. Storti, G. Sallustio; Campobasso/IT

Learning objectives: The major teaching points of this exhibit are: Apart from typical appearance, NHL may be found in unusual localizations. Both CT and MRI provide useful information for diagnosis and staging of abdominal and pelvic unusual localizations of NHL. Knowledge of the CT and MRI appearance of unusual localizations of NHL strongly helps a timely and correct diagnosis.

Background: Non-Hodgkin lymphomas (NHLs) are frequent tumors. However, extraglandular forms are very unusual, and the location in some organs is extraordinary. In this exhibit, we will describe the epidemiology, classification, pathophysiology and clinic features of NHL. We will also describe CT and MRI technique and imaging findings in unusual abdominal and pelvic localizations of NHL.

Imaging findings OR Procedure details: Epidemiology, classification, pathophysiology and clinical features of NHL. CT and MRI technique for evaluation of abdominal and pelvic NHL. Review of CT and MRI findings in unusual abdominal and pelvic localizations of NHL: liver; biliary tree; gallbladder; spleen; kidney; pancreas; stomach and bowel; ovary and female urethra.

Conclusion: NHL may present in unusual abdominal and pelvic localizations. Radiologists must be aware of these unusual localizations and their CT and MRI appearance in order not to miss crucial diagnostic findings and not to misinterpret the imaging examination results.

P-246

CT and MRI spectrum of presacral lesions

Z. Jiang, W. Peng; Shanghai/CN

Learning objectives: To present the spectrum of CT and MRI findings of presacral lesions. To help develop an imaging algorithm in making a specific diagnosis with clinical and pathologic correlation.

Background: Primary presacral masses may arise from rectum, ovaries, pelvic soft-tissues, or retroperitoneum, and patients with pelvic carcinoma can develop presacral metastasis or recurrence. The differential diagnosis for presacral masses is extensive. The diagnosis can be suggested depending on lesion features and relationship with adjacent organs. We reviewed CT and MRI findings of presacral masses in patients examined at our institution from January 2003 to November 2007 with correlation of symptoms and pathology.

Imaging findings OR Procedure details: Clues of differential diagnosis include special components (fat, calcification, mucus, hemorrhage, necrosis, etc.), contour, pattern of enhancement, and relationship with rectum or sacrum. We present and discuss the imaging features of various presacral masses, which originate from rectum (stromal tumor, adenocarcinoma), ovaries (teratoma, cystadenoma), pelvic primary masses (neural tumor, liposarcoma, leiomyosarcoma, lymphoma, perivascular epithelioid cell neoplasm), metastatic or recurrent tumours, and non-neoplastic lesions such as endometrial cyst and abscess.

Conclusion: A wide variety of lesions occur in the presacral space. The knowledge of imaging characteristics and clinicopathologic behavior of these lesions allows the diagnosis and may suggest an adequate treatment.

P-247**Evaluation of abdominal lesions with diffusion weighted imaging**

T. Gerukis, A. Petridis, K. Anastasiadou, M. Pilavaki, A. Pantazopoulou, C. Karatziou, V. Kalpakidis, P. Palladas; Thessaloniki/GR

Purpose: To exhibit the implementation of diffusion-weighted imaging (DWI) with the use of apparent diffusion coefficient (ADC) measurements in the study of variable (histologically proven) abdominal lesions.

Material and methods: Single-shot echo-planar DWI was added to the routine abdomen MR examination in 61 patients with abdominal lesions. Quantitative analysis of ADC was made by region of interest measurements in normal and pathologic tissue of different abdominal organs (liver 24, pancreas 2, kidney 4, adrenal 7, bowel 8, ovaries 3, bladder 1, peritoneum 3 patients).

Results: The mean ADC of malignant lesions was in all occasions lower than that of benign lesions. The mean ADC value of liver was 1.31 (x 10⁻³ mm² sec⁻¹), of the spleen 1.23, of the kidneys 2.25, of the adrenals 1.85 and of the pancreas 1.71. Liver ADCs showed no significant difference from 6 hepatocellular carcinomas or 11 metastatic lesions (1.64). ADC in 6 patients with colon tumor recurrences 1.13, one pancreatic cancer 1.45, one adrenal metastasis 1.32 (no significant difference from 5 adenomas – 1.31).

Conclusion: ADC calculation of abdominal organs and lesions can give further information and may be used as a tool (in conjunction to the other available sequences and techniques) in successful characterization of malignant lesions. Further accumulative experience is needed to define the ranges of pathologic in each occasion.

P-248**Abdominal wall: a pictorial review of the normal anatomy and pathology**

J.C. Quintero, D. Hernández, I. Urra, L. Castro, I. Guasch, C. Pozuelo; Badalona/ES

Learning objectives: The aim of this exhibit is to review normal anatomy of the abdominal wall by CT and to present the more usual pathologies of the abdominal wall diagnosed in our institution.

Background: We revised all of the reports of five years old of abdominal CT made in our institution. 9525 reports of abdominal CT were performed in the last four years at our institution. We encountered 302 cases (3.17%) of pathology of the abdominal wall and retrospectively reviewed two senior experienced radiologists who were unaware of CT findings from the other. Usually the studies consist: oral contrast, 5 mm collimation, pitch: 1.5, 100 ml of contrast medium, rate: 2.5 ml/sec, delay: 70 sec. We illustrate the most representative images that show the abdominal wall and its components: muscles, fascias layers, aponeurosis, ligaments, skeletal, vessels and nerves.

Imaging findings OR Procedure details: Herniary pathology (194): Spigelian, inguinal, incisional, lumbar, etc. Not herniary pathology (108): congenital lesions (urachal abnormalities and omphalomesenteric duct abnormalities), fluid collections (haematoma, abscess and cellulites and urinoma), neoplasm (primary malignancies, metastatic disease and benign lesions) and miscellaneous (vascular lesions, vascular grafts, calcifications and subcutaneous gas).

Conclusion: Cross-sectional imaging provides an excellent, non-invasive means of evaluating these processes. Specific observations on the nature, location, extent, and underlying causes can be made, therapy planned and instituted, and follow-up accomplished.

P-249**That the radiologist should know about the spleen?**

J.C. Quintero, C. Roqué, D. Hernández, A. Olazábal, I. Guasch; Badalona/ES

Learning objectives: 1) To illustrate the spectrum of congenital and acquired abnormalities spleen. 2) To determine the current role of US, CT and MRI in the detection and characterization of focal spleen lesions.

Background: The spleen has the same relationship to the circulatory system that the lymph nodes have to the lymphatic system. A wide range of splenic variations and abnormalities can affect the spleen and may be detected on abdominal imaging while one simultaneously evaluates the remaining intraabdominal structures.

Imaging findings OR Procedure details: We reviewed retrospectively 51

patients with normal, splenic variations and abnormalities spleen diagnosed in our institution. We present a comprehensive algorithmic approach to diagnose various abnormalities of the spleen: 1) Normal anatomy and congenital variations (11); 2) Traumatic conditions (9); 3) Vascular affections (5); 4) Infections (4); 5) Cysts (5); 6) Benign neoplasms: hemangioma (3), hamartomas (1), lymphangiomas, and inflammatory pseudotumor (1); 7) Malignant neoplasms: primary, lymphoma (5), and metastasis (4); and 8) Miscellaneous conditions: sarcoidosis (1), amyloidosis (1), throrotrastosis, and extramedullary hematopoiesis (1).

Conclusion: In discussing the normal anatomy, congenital variations, and acquired abnormalities such as those resulting from trauma, infection, infarction, cysts, and neoplasm. US, CT and MRI all play an important role in the detection and characterization of focal splenic lesions, and with sufficient clinical information they enable the differential diagnosis of these lesions.

P-250**Mesenteric tumors: CT findings of primary and secondary tumors and differential diagnosis**

A. Lourbakou, A. Anagnostara, S. Mylona, S. Ntai, A. Katsarou, N. Batakis; Athens/GR

Purpose: CT is the main method in establishing the diagnosis of mesenteric tumors. Though the primary mesenteric tumors are rare, mesentery is commonly affected by metastatic or inflammatory lesions of the peritoneal cavity. The purpose of this study is to present the imaging findings of these entities.

Material and methods: In a 12-month period, 23 patients with CT findings of mesenteric tumors were studied in our department. **Results:** Three of them were diagnosed with primary tumors (lipoma, desmoid tumor and sarcoma). The diagnosis was confirmed by CT guided biopsy. Seven of them had typical imaging findings of mesenteric lipodystrophy. There was no need for histological confirmation. One patient was diagnosed with carcinoid tumor, one with GIST, four presented with peritoneal spread from ovarian and GI tumors, two suffered from lymphoma, one from amyloidosis with mesenteric infiltration, one from tuberculosis, and one from mesenteric metastasis of melanoma. In one out of 23 patients, mesenteric multiple abscesses were observed and one patient presented with echinococcus cyst with mesenteric spread. CT revealed the mesenteric pathology in all cases. The imaging findings of the above mentioned entities in correlation with the rest of the clinical findings had led in certain cases to the differential diagnosis.

Conclusion: CT imaging with or without CT-guided biopsy is efficient in establishing the diagnosis in mesenteric disease.

P-251**Normal anatomic relationship of peritoneal reflections and diseases of peritoneum using multiplanar images**

Y. Kim¹, S.Y. Song², O.K. Cho², B.H. Koh²; ¹Kuri/KR, ²Seoul/KR

Learning objectives: To display normal peritoneal reflections using multiplanar images. To illustrate usual and unusual peritoneal diseases. To find the imaging characteristics of individual disease.

Background: Omentum, mesentery, ligaments and peritoneum are anatomically complicated areas to fully assess CT images. Peritoneum can be affected by various diseases, and several different forms are manifested.

Imaging findings OR Procedure details: We reviewed normal peritoneal reflection, ligament, mesentery and omentum using multiplanar CT images. We classified MDCT findings of peritoneal disease as follows: disseminated, nodular, cystic forms. Selected cases are presented and the imaging characteristics are discussed. Peritoneal diseases include inflammatory diseases (tuberculous peritonitis, bacterial peritonitis, and actinomycosis) and peritoneal carcinomatosis (disseminated, nodular and cystic type).

Conclusion: A review of the normal peritoneal anatomy, the pathology and imaging characteristics of disseminated peritoneal disease is presented. Although these CT appearances overlap, classifying them by pattern is helpful in narrowing the range of the differential diagnosis.

P-252**CT-imaging of splenic lesions**

S. Ntai, S. Mylona, G. Karapostolakis, A. Anagnostara, A. Katsarou, N. Batakis; Athens/GR

Learning objectives: Computed Tomography (CT) is an excellent imaging modality for demonstrating the size, shape and position of the spleen as well as for depicting intrasplenic pathologic features. The purpose of this study is to discuss the congenital and acquired abnormalities of the spleen and present their CT appearance. The examination technique and contrast protocol are also part of this presentation.

Background: The medical records of 91 patients (55 men, 36 women, age range 18–76, mean age 56.4 years) with intrasplenic lesions were retrospectively reviewed. Location, enhancement patterns, presence of calcifications or cystic components was in all cases evaluated.

Imaging findings OR Procedure details: The clinical history of the patients must always be taken into consideration since the imaging findings of different entities may be overlapping. The abnormalities encountered and described in this study include congenital variations, traumatic and infectious lesions, vascular abnormalities, benign and malignant neoplasms, whereas the cases presented demonstrate both the value and the limitations of the method.

Conclusion: A wide variety of splenic variations and abnormalities may be detected on abdominal CT scans while one simultaneously evaluates the remaining intraabdominal structures.

P-253**Spectrum of radiologic findings of abdominal solitary fibrous tumor**

H.J. Kim, S.S. Lee, S.H. Park, K.W. Kim, H.J. Won, A.Y. Kim, P.N. Kim, M. Lee, H.K. Ha; Seoul/KR

Learning objectives: To describe the spectrum of abdominal manifestations of solitary fibrous tumor.

Background: Solitary fibrous tumors are spindle-cell neoplasms that most commonly arise in the pleura. However, they also been reported at extrapleural locations. Solitary fibrous tumor (SFT) rarely arises in the abdomen. To our knowledge, there are only case reports of abdominal solitary fibrous tumor in the English literature. Therefore, we will describe the abdominal manifestations of solitary fibrous tumor.

Imaging findings OR Procedure details: This educational exhibit demonstrates the various spectrums of radiologic findings of abdominal solitary fibrous tumor proven by the surgery. Eight patients with abdominal solitary fibrous tumor and abdominal CT scans or pelvic MRI were included in this study. Involved abdominal organs included the retroperitoneum, pancreas, kidney, and perivesical space.

Conclusion: Although abdominal solitary fibrous tumor rarely occur, it should be included in the differential diagnosis if the well-defined hypervascular mass is noted in the retroperitoneum on CT or MRI.

P-254**A pilot study assessing the feasibility of adrenal gland volume measurement by MRI**

L. Grant, A. Napolitano, S. Miller, K. Stephens, S. Mc Hugh, A.K. Dixon; Cambridge/UK

Purpose: To determine whether MRI can measure adrenal gland volume (AGV) in normal human volunteers and to determine the intra and inter-observer variations and repeatability.

Material and methods: This was a simple single cohort, sequential design, 2 part study involving 4 MRI examinations per subject. Part 1: subjects underwent a single MRI examination to determine feasibility for the technique. Part 2: the volunteers were examined twice in one day (1 hour apart) and again one week later. Information was collected on four healthy subjects (three male and one female). Two different investigators estimated the area of the adrenal gland for each of the 3 mm contiguous slices on two separate occasions. The volume of the adrenal gland (in cm³) was calculated. To estimate inter and intra reader variability, a repeated-measures mixed model was fitted with adrenal volume as the dependent variable. In order to estimate any bias between readers, Bland-Altman methodology was applied.

Results: Total volume variation from all sources is approximately 14% of a 3 cm³ adrenal gland. Variation over time is small (5% of a 3 cm³ adrenal gland). Variation due to within and between investigator is larger (9% of a 3 cm³ adrenal gland). Image reading by a second investigator could reduce variability.

Conclusion: MR analysis of AGV is suitable for detecting incremental changes within the range seen in adrenal gland disease.

P-255**CT imaging of hernias in the inguinal region**

S.A. Joffe¹, V. Hatzoglou², S. Okon², M. Horowitz², Z. Patel²; ¹Beth Shemesh/IL, ²New York, NY/US

Learning objectives: 1) To review the anatomy of the inguinal region. 2) To demonstrate the CT anatomy and CT imaging features of hernias in the inguinal region. 3) To demonstrate CT imaging features of complications of these hernias.

Background: Evaluation of hernias in the inguinal region is a common indication for CT imaging of the abdomen and pelvis. In addition, CT frequently detects these hernias incidentally.

Imaging findings OR Procedure details: Knowledge of the anatomy of the inguinal region including normal CT anatomy is essential for differentiating the different types of hernias. CT imaging techniques for evaluating inguinal hernias include the valsalva maneuver. CT can differentiate among indirect inguinal hernias, direct inguinal hernias, and femoral hernias. CT helps demonstrate the contents of these hernias, including fat, fluid, bowel, bladder, and ovary. In addition, CT can identify complications of inguinal hernias, including incarceration, strangulation, and bowel obstruction.

Conclusion: This exhibit will explain how to differentiate indirect and direct inguinal hernias and femoral hernias on CT, how to identify structures within these hernias, and how to recognize complications of these hernias.

P-256**Imaging diagnosis of sclerosing peritonitis and its complications**

D. Emlik, M. Yeksan, I. Guney, O. Koc, S. Gumus, K. Odev; Konya/TR

Purpose: Sclerosing peritonitis (SP) is a rare but serious complication of chronic ambulatory peritoneal dialysis that occurs with an incidence of between 0.06 and 7.3%. The purpose of this study was to discuss serious complications such as small bowel, large bowel obstruction, necrosis and peritoneal thickening.

Material and methods: A 33 years-old woman with chronic renal failure involvement having CAPD for ten years was presented. Plain films of abdomen, ultrasonography and abdomen CT were performed.

Results: Enhanced abdominal CT showed dilatation of small and large bowels. Enhanced abdomen CT also revealed enhancement of the peritoneal membranes, peritoneal thickening and presence of intraperitoneal fluid collection. Moreover, there were peritoneal and vascular calcifications in association with liver and splenic capsule calcifications. Such radiological changes in this patient on peritoneal dialysis were consistent with a diagnosis of SP. The patient's condition deteriorated during the peritoneal dialysis and died due to infection. The SP diagnosis was suggested by imaging findings and confirmed by peritoneal biopsy.

Conclusion: Although a rare complication, small and large bowel obstruction due to SP should be considered in any patient on prolonged ambulatory peritoneal dialysis. CT is an accurate method for early diagnosis and follow-up of SP.

P-257**The various manifestations of extra-nodal lymphoma in the abdomen and pelvis: a pictorial review**

A. Rajesh, R. Kirke, R. Verma; Leicester/UK

Learning objectives: To illustrate and discuss the different manifestations of extra-nodal lymphomatous involvement in the abdomen and pelvis.

Background: Malignant lymphomas are differentiated into Hodgkin's and non-Hodgkin's-lymphoma (NHL). Lymphoma can affect nearly all tissues and involve extra-nodal locations. This review describes the typical and rarer atypical manifestations of abdominal lymphoma involving the solid abdominal viscera and bowel.

Imaging findings OR Procedure details: Extra-nodal involvement from lymphoma can affect any organ and can present as isolated organ involvement or as a part of multi-organ involvement. The use of MDCT is increasing in the evaluation of the abdomen and a variety of lymphoproliferative pathology is being detected either as an incidental finding in an acute abdomen or a part of a diagnostic work up. Imaging also aids in the staging of the disease and in detection of related complications. We discuss and review the radiologic appearances of histopathologically proven cases of extra-nodal lymphoma in the abdominal viscera, gastrointestinal tract and in rarer locations such as the

testes.

Conclusion: An understanding of the spectrum of organ involvement in lymphoproliferative disease is necessary for aiding diagnosis and appropriate patient management.

P-258

The radiological diagnosis of adenomyomatosis of the gallbladder

H. Stunell, C.F. Murphy, E. Ward, J.M. O'Brien, T. Geoghegan, W. Torreggiani; Dublin/IE

Learning objectives: We describe the diagnosis of gallbladder adenomyomatosis on US, CT and MRI, and correlate the characteristic pathological findings with those first described on cholecystography.

Background: Adenomyomatosis is a relatively common abnormality of the gallbladder with a reported incidence of 2.8–5%. It is characterized pathologically by excessive proliferation of the surface epithelium and hypertrophy of the muscularis propria, with invagination of the mucosa into the thickened muscularis, forming characteristic Rokitansky-Aschoff sinuses. Occasionally, focal adenomyomatosis may mimic gallbladder carcinoma, making accurate diagnosis of this as a distinct pathological entity essential.

Imaging findings OR Procedure details: Visualization of the characteristic Rokitansky-Aschoff sinuses on US may be difficult due to factors such as obesity, gallbladder calculi and interruption of the beam by bowel gas and the diagnosis is now made more commonly on cross-sectional imaging. Contrast-enhanced CT in the arterial phase best shows enhancement of the mucosal layer of the gallbladder and therefore, the mucosal outpouching into the thickened muscularis. However, we have found MRI using a heavily T2-weighted HASTE sequence to most accurately depict the characteristic features of adenomyomatosis of the gallbladder and associated biliary tract disease.

Conclusion: While CT has been shown to be superior to US and cholecystography, MRI using T2-weighted images has been shown to be the most accurate modality for diagnosing gallbladder adenomyomatosis, with a reported accuracy of over 90%.

P-259

Patterns of lymphadenopathy in GI malignancies

M. Duarte, R. Santos, M. Bispo, J. Alpendre, A. Marques, J. Castaño, Z. Seabra; Lisbon/PT

Learning objectives: To illustrate patterns of lymphatic spread from different primary GI malignancies.

Background: Different primary malignancies have different lymphatic drainage pathways. Proper assessment of lymphatic spread requires careful evaluation of specific pathways. CT plays a central role in diagnosing, staging, management and follow-up of GI malignancies. It is a non-invasive, available diagnostic tool which also allows determination of the most appropriate approach for nodal sampling and helps in the detection of recurrent disease.

Imaging findings OR Procedure details: The authors make a comprehensive review on pathways for lymphatic spread in GI malignancies including oesophagus, stomach, liver, pancreas, biliary system, small bowel and colon. Schematic representations and CT images illustrate these pathways. TDM criteria for pathologic lymph nodes including location, number, location-related size, morphology, density and patterns of contrast uptake are reviewed.

Conclusion: Awareness of preferential pathways of lymphatic drainage from different primary GI malignancies allows better assessment of lymphatic nodes involvement and is a precious aid for accurate staging of malignancies.

P-260

Pelvic retroperitoneal cystic masses: CT and pathologic findings

D.M. Yang, H.C. Kim; Seoul/KR

Learning objectives: 1. To demonstrate the anatomy of pelvic retroperitoneum. 2. To illustrate the CT imaging findings of various types of pelvic retroperitoneal cysts. 3. To evaluate the distinguishing points between many types of retroperitoneal cysts.

Background: Pelvic retroperitoneal cystic masses (PRCM), which arise within the retroperitoneal space but outside the major organs of that compartment, are uncommon. However, the widespread use of computed tomography (CT) for evaluating abdominal and retroperitoneal diseases has increased the detection

rate of retroperitoneal cystic lesions. CT is an ideal tool for assessment of retroperitoneal disease because it provides discrete sectional images of the organs and retroperitoneal compartments. Differential diagnosis of retroperitoneal cystic masses includes cystic teratoma, epidermoid cyst, tailgut cyst, cystic change of neurilemmoma and extraskeletal Ewing's sarcoma, perianal mucinous carcinoma, lymphocele, urinoma, and hematoma.

Imaging findings OR Procedure details: 1. Anatomy of pelvic retroperitoneum 2. Various types of PRCM including cystic teratoma, epidermoid cyst, tailgut cyst, cystic change of neurilemmoma and extraskeletal Ewing's sarcoma, perianal mucinous carcinoma, lymphocele, urinoma, and hematoma 3. Distinguishing points between many types of retroperitoneal cysts.

Conclusion: 1. There is a substantial overlap of CT findings in various pelvic retroperitoneal cysts. 2. Clinical history and certain details seen at CT assist in making correct diagnosis. 3. Familiarity with the CT features of various PRCM facilitates accurate diagnosis.

P-261

Heterogenous fat distribution in adrenal nodules: a voxel by voxel analysis of CT attenuation using chemical shift MRI

L. Lanka, K.S. Jhaveri, M.A. Haider; Toronto, ON/CA

Purpose: Heterogeneity can be seen in adrenal adenomas on CT. Mean attenuation does not account for heterogeneity and histograms can be affected by noise. The purpose of this study was to determine the range of attenuation that can be seen in fat rich versus fat poor adenoma regions using voxel by voxel comparative chemical shift MRI (CSMRI) analysis.

Material and methods: A single unenhanced CT and CSMRI slice could be co-registered for 23/36 adenomas using ImageJ software allowing for voxel by voxel comparison. Lipid rich voxels were defined as having >25% drop in signal intensity on CSMRI. Five of 23 (22%) adenomas were heterogenous (HetAd) having at least 2% and no more than 98% lipid poor voxels.

Results: The mean attenuation of HetAd was 12 HU (8–23 HU). The mean attenuation was >10 HU in all lipid poor regions. On a voxel by voxel basis, 15% (520/3548) of voxels were lipid poor. There was a significant correlation between signal drop on CSMRI and CT attenuation ($r=-0.632$, $p<0.001$). Mean CT attenuation was significantly higher in lipid poor voxels (27.7 HU vs 10.8 HU, $p<0.0001$). On an adenoma by adenoma basis, 4 (36/957) to 42% (289/677) of the voxels in each adenoma were lipid poor.

Conclusion: True lipid poor regions can occupy sizeable subregions of HetAd. The location of measurement within a nodule could affect the diagnosis of benignity.

P-262

Abdominal hydatid disease: a pictorial review of unusual findings and pathologic features

D. Emlik, D. Kiresi, C. Kadiyoran, S. Gumus, K. Odev; Konya/TR

Purpose: The aim of this study is to illustrate examples of the diagnostic imaging modalities. We also discuss the main differential diagnosis.

Material and methods: We illustrate a variety of radiological findings on US, CT and MRI in cases seen in our institution. Typical findings, unusual locations (pancreas, kidney, diaphragm, peritoneum, adnexial and perivesical) and complicated cases (peritoneal seeding, biliary communications) are described. Secondary involvement due to peritoneal seeding may be seen in almost any anatomic location and may cause important problems in the differential diagnosis.

Results: Hydatid disease was correctly diagnosed by the combination of clinical history, imaging findings and serologic test results.

Conclusion: Hydatid disease should be considered in the differential diagnosis in all patients presenting cystic lesions of the abdomen in areas where the disease is endemic.

P-263

Abdominopelvic actinomycosis: CT and MRI findings

H.J. Kim¹, S. Yoon², K.A. Kim¹; ¹Sungnam-si, Kyonggi-do/KR, ²Seoul/KR

Learning objectives: To review the imaging features of abdominopelvic actinomycosis in CT and MRI.

Background: Actinomycosis is an uncommon disease in the abdomen and pelvis. It is a chronic suppurative infection caused by actinomyces israelii. It is characterized

by multiple abscesses, draining sinuses, and abundant granulation tissue. It shows infiltrative nature and easily invades normal anatomic barrier, cross fascial planes, and invades multiple compartments. Its imaging findings overlap with neoplastic and inflammatory conditions.

Imaging findings OR Procedure details: We reviewed the CT and MRI of 15 patients with abdominopelvic actinomycosis. The involving sites were appendix (1), appendix and cecum (1), omentum (1), urachal remnant (2), and ovary (10). Appendiceal actinomycosis shows thickening of appendix. Actinomycosis of appendix and cecum shows bulbous thickening of appendix with contiguous cecal thickening. Actinomycosis of omentum shows bulky infiltrative solid mass with dense enhancement and multiple small abscess cavities, contiguous with the transverse and ascending colon. Actinomycosis of urachal remnant shows infiltrative densely enhancing mass with infiltrative border with multiple small abscess cavities along urachal course. Ovarian actinomycosis reveals unilateral or bilateral adnexal mass with pure cystic or solid and cystic mass with infiltrative border.

Conclusion: Abdominopelvic actinomycosis involves many organs. Awareness of its characteristic imaging findings can help in the differential diagnosis of abdominal and pelvic mass.

P-264

Withdrawn by authors

P-265

Normal anatomy and various abnormalities of the splanchnic arteries: MDCT angiography and 3D imaging

H.Y. Han, S.J. Park, H.S. Choe; Daejeon/KR

Learning objectives: To review the MDCT angiographic and 3D images of the normal anatomy, anatomical variant, and various abnormalities involving splanchnic arteries.

Background: To review imaging findings of the normal anatomy, anatomical variant, and pathologic processes involving celiac trunk and mesenteric arteries.

Imaging findings OR Procedure details: Review of MDCT imaging findings of the various abnormalities involving celiac trunk and mesenteric arteries. 1. Normal anatomy and anatomical variant - celiomesenteric trunk with/without aneurysm, superior mesenteric artery (SMA) syndrome, intestinal malrotation. 2. Acute arterial impairment - Celiac trunk dissection, isolated SMA dissection, thromboembolism, traumatic vascular injury. 3. Chronic arterial insufficiency. 4. Inflammatory or tumorous conditions affecting celiomesenteric arteries.

Conclusion: MDCT angiography and 3D images allow for optimal depiction of the anatomy and its anatomical variant of the celiac trunk and mesenteric arteries and show various causes of the vascular impairment.

P-266

Imaging spectrum of the extraabdominal mass lesions at the pelvic component of the conventional abdomino-pelvic cross-sectional examinations

D. Yildirim¹, H.T. Sanal², M. Tasar², M. Kocaoglu², B. Tiryaki¹; ¹Istanbul/TR, ²Ankara/TR

Learning objectives: In the pelvic region, with abdominopelvic CT imaging other than gastrointestinal, urinary and genital systems, a diversity of lesions can be seen.

Background: In abdominopelvic cross sectional imaging, a spectrum of pathologies other than gastrointestinal and urogenital systems can be seen in pelvic region. We aim to classify pelvic mass lesions which do not correspond with their prediagnoses.

Imaging findings OR Procedure details: 290 cases which have been reported as having pelvic masses on CT between May 2005 and June 2007 were reviewed respectively. With the pathology reports of 23 cases and 2 years follow up results of the rest, the imaging protocols, prediagnoses, and the images were re-reviewed.

Conclusion: Neoplastic mass lesion (n=71) (32 benign, 24 primary malignancy of the bone and soft tissues around the pelvic rim, 15 metastatic lesion), infectious-inflammatory mass (n=54), postoperative-posttraumatic changes (n=68), Paget disease (n=1), fibrous dysplasia (n=1), pelvic lipomatosis (n=1), bone island (n=29), Klipel-Trenaunay Syndrome (n=1), bone variation (n=59), and pelvic kidney (n=5) were found. Extraintestinal, extraurinary and extragenital masses comprised 4.2% of the 6900 cases.

P-267

Bilateral extraadrenal perirenal myelolipomas: CT features

O. Temizoz, H. Genchellac, M.K. Demir, E. Unlu, H. Ozdemir; Edirne/TR

Purpose: The purpose of this report is the demonstration of CT findings in this disease.

Material and methods: Abdominal computed tomography (CT).

Results: Myelolipomas are rare, benign tumors composed in varying proportions of adipose tissue and hematopoietic cells. These lesions are typically found in adrenal glands. However, they are rare in extra-adrenal sites and are difficult to diagnose with imaging studies. The unusual location of these tumors present an imaging studies challenge. Distinguishing these lesions from other tumors including adipose tissue and hemopoietic cells may also be difficult even at pathologic examinations. The distinction between extra-adrenal myelolipomas and malignant tumors such as liposarcomas is crucial to avoid an invasive procedure. Although sporadic case reports involving perirenal sites of myelolipomas have surfaced in the literature, only a case of bilateral extraadrenal perirenal myelolipomas with imaging findings have been reported to date.

Conclusion: We herein present a comprehensive report of the CT imaging characteristics of a pathologically proven case of bilateral extraadrenal perirenal myelolipomas.

P-268

Withdrawn by authors

P-269

Optimization of scanning parameters of 64MDCT of abdomen and pelvis

P. Paolantonio¹, R. Ferrari², P. Lucchesi², F. Vecchietti², M. Maceroni², A. Laghi²; ¹Rome/IT, ²Latina/IT

Purpose: We propose a scanning protocol optimized for abdomen and pelvis evaluation using a 64MDCT scanner.

Material and methods: On a 64MDCT scanner, we optimized the following protocol for abdomen and pelvis evaluation: detector configuration: 64 x 0.625; 120 kv; for tube current setting a smart-mA system were used (range 100–800 mA); noise index 28; pitch 1.3. This scanning protocol was acquired before and during i.v. administration of iodinate contrast medium. Hepatic arterial phase, portal venous phase and equilibrium phase were acquired using a bouls-tracking system for hepatic arterial phase acquisition with 15 sec. of delay between aortic threshold of 100 HU. We used this scanning protocol in 150 patients referring for abdomen and pelvis CT scan. Data sets were transferred on a off-line workstation with MPR and VR capabilities. Image analysis was performed increasing the slice thickness from the native 0.4 mm up to 2.5 mm. Image analysis was performed from two radiologist in consensus and was focused to a quantitative assessment of image quality of both axial images and MPR reconstructions.

Results: Image quality referring to image noise of both axial and MPR reconstructions was judged optimal in all cases. The isotropic voxel properties lead to an optimal quality of the MPR reconstruction.

Conclusion: The scanning protocol proposed for 64MDCT scanner in the evaluation of abdomen and pelvis enables optimal image quality and excellent spatial resolution on z-axis.

Diagnostic / Other / Ultrasound

P-270

Chronic hepatic venous outflow obstruction: US in the diagnosis and rationalizing approach towards management

R. Jain¹, S. Sawhney¹, S.K. Acharya²; ¹Muscat/OM, ²New Delhi/IN

Purpose: To identify the spectrum of Ultrasonographic findings in chronic hepatic venous outflow obstruction (HVOO).

Material and methods: A prospective study on 100 consecutive patients aged 3 to 69 years (mean±SD 27.1±11) with histologically proven HVOO. US was performed in all patients. Inferior-venacava (IVC) angiograms were performed in

40 patients for correlation with US, including 26 endovascular interventional procedures.

Results: With IVC angiograms as gold standard, US was 100% sensitive for diagnosis of HVOO; and site, type and severity of IVC abnormality. US provided additional information about liver parenchyma, hepatic-veins (HV) and intrahepatic collaterals. Three distinctive types of IVC/HV disease were identified: Type I–22/100 patients–Membranous occlusion of the IVC at cavo-atrial junction by 2.1±.08 mm thin membrane; Type II–72/100 patients–Steno-occlusive narrowing - 41±25 mm long-of intrahepatic IVC 1 cm below cavo-atrial junction; Type III–6/100 patients - IVC was normal. All types were associated with hepatic vein abnormalities of varying severity. Types I and II showed significant differences in age at presentation 35.23±8.66 v/s 25.13±10.83 years ($p<0.001$), HV abnormalities–HV score 4.18 v/s 6.43 ($p<0.001$), and response to endovascular therapy, respectively.

Conclusion: US is adequate for diagnosis and classification of HVOO into: Type I – Membranous, and Type II – Steno-occlusive IVC abnormalities. Percutaneous interventional procedures are most effective for Type I disease, and less so for Type II. US is helpful in the diagnosis of HVOO and rationalising patient management.

P-271

Causes and patterns of abdominal lymphadenopathy in pediatric patients

M.G. Papadaki Athens/GR

Learning objectives: To present the different causes of AL in children. To highlight the specific characteristics of the lymph nodes. To emphasise the importance of additional findings that may assist in the correct diagnosis.

Background: Abdominal lymphadenopathy (AL) is a very common finding during abdominal ultrasonography in pediatric patients. A clinical context explaining the cause is often difficult to define, while location, characteristics and additional findings may help to narrow the differential diagnosis.

Imaging findings OR Procedure details: Several pathologic conditions cause AL, the most common being viral mesenteric adenitis. Of inflammatory nature are also lymph nodes accompanying appendicitis and Crohn's disease. Non-Hodgkin lymphomas of the bowel are the most common malignancy manifesting with AL while other malignancies may also spread through abdominal lymph nodes. When studying enlarged lymph nodes, it is mandatory to define their location, either intra- or retroperitoneal. Specific characteristics should be examined: their size and shape, the presence or absence and the thickness of the nodal hilum, the structural pattern of the cortex and the blood flow patterns. Ultrasonographic evaluation should include all abdominal solid organs, components of the peritoneal cavity, the retroperitoneum and the bowel wall looking for evidence that may contribute to the diagnosis.

Conclusion: Knowledge of differential diagnosis in pediatric patients with AL, specific characteristics of the lymph nodes and additional findings may contribute significantly to the correct diagnosis.

P-272

Role of endoanal US in the management of women with clinical diagnosis of 3rd/4th degree obstetric-related perineal tears

K. Thiruppathy, R. Cohen, A. Emmanuel, S. Halligan, S.A. Taylor; London/UK

Purpose: To correlate endoanal USS findings with symptoms and anal manometry in women with clinical diagnosis of 3rd/4th degree obstetric-related perineal tears.

Material and methods: 101 consecutive women with clinically diagnosed 3rd/4th degree obstetric tears (and undergoing primary repair) underwent endoanal US, anorectal physiology (resting and squeeze pressures) and completed bowel function scores (Wexner incontinence scores). Comparison was made between women with radiologically confirmed 3rd/4th tears with ultrasonically intact sphincters (1st/2nd degree tear) using chi square testing and unpaired t testing as appropriate on statistical advice.

Results: US revealed that 32/101(32%) had no evidence of sphincter injury (i.e. 1st/2nd degree tear). Significantly, more women reported faecal incontinence (FI) in the group with actual sphincter injury (61 vs 34%, $p=0.01$). 14% (10/69) of those with ultrasonically confirmed tears had persisting sphincter defects despite primary repair. Anal resting pressure was not significantly different both between the 3rd/4th and 1st/2nd degree tear groups (59 vs 65 mmHg, $p=0.13$), but

squeeze pressure was lower in those with confirmed 3rd/4th tears (57 vs 73 mmHg, $p=0.003$).

Conclusion: One-third of patients clinically diagnosed with 3rd/4th degree tears in fact have intact sphincters on US. This group report less FI and retain a stronger anal squeeze pressure than those with ultrasonically confirmed sphincter disruption. Endoanal US has an important role in the correct management of patients even with clinically diagnosed sphincter disruption.

Diagnostic / Pancreas

P-273

Relapse of autoimmune pancreatitis

N. Takahashi, S.T. Chari, A. Sugumar, J.G. Fletcher, A. Kawashima; Rochester, NY/US

Purpose: To evaluate the patterns of relapse in patients with autoimmune pancreatitis (AIP) and to identify findings at presentation that may predict the relapse.

Material and methods: 70 patients with AIP who had follow-up imaging study were included. Imaging studies at presentation were evaluated for pattern of pancreatic involvement and presence of extrapancreatic involvement. Serum IgG4 levels and mode of treatment were recorded. Follow-up imaging studies were evaluated for presence of relapse or progression of AIP. Findings at presentation were compared between patients with and without relapse.

Results: Median follow-up duration was 13 months (1–146 months). 26 (37%) of 70 patients had relapse or progression of AIP. 12 patients had relapse in biliary tree, 11 in pancreas, 8 in kidney, and 4 in other organs (2 in lung, 2 in liver, 1 in pleura, 1 in retroperitoneum). Relapse in organs that were uninvolved at presentation was uncommon. Relapse occurred between 6–60 months (median 19 months). When compared between patients with and without relapse, mean age (60 vs. 59 y-o), mean serum IgG4 levels (446 vs. 453 mg/dL), pattern of pancreatic enlargement (diffuse/focal/normal-atrophy: 48/22/30% vs. 36/28/15%), or presence of extrapancreatic involvement (biliary/kidney/retroperitoneum: 71/33/17% vs. 56/34/13%) at presentation and mode of treatment (steroid/surgery/none: 58/27/15% vs. 64/25/11%) were not significantly different.

Conclusion: Relapse of AIP is relatively common. It is difficult to predict the relapse of AIP from the findings at presentation.

P-274

Evaluation of age-related changes of pancreatic tissue on diffusion weighted MRI

S. Bayramoglu, O. Kilickesmez, N. Guner, T. Cimilli, G. Yirik, S. Aksoy, E. Hocaoglu; Istanbul/TR

Purpose: Pancreas demonstrates significant morphological changes during the life. The dimensions and weight of pancreas begin to increase in newborn till adulthood and it gradually decreases after the fourth decade. The morphological changes were reported on US and CT imaging while the cytologic changes were declared only in autopsy series. The purpose of our study was investigate the reflection of these changes on diffusion weighted MRI (DWI-MRI).

Material and methods: One hundred and forty patients aged between 1 and 87 were studied in a consecutive series. Patients with major abdominal, major-minor hepatopancreaticobiliary pathologies and history of diabetes, pancreatitis and alcohol abuse were excluded. ADC measurements of pancreatic head, corpus and tail were recorded. The mean ADC value was calculated for each patient. The statistical differences of ADC values and sex differences were investigated in each decade. Each decade was compared using Oneway Anova and Post Hoc Tukey HSD tests. The correlation between age and pancreatic ADC values was evaluated with Pearson correlation analysis.

Results: Mean ADC values of pancreas showed a linear negative correlation after third decade ($r:-0.842$; $p:0.001$; $p<0.01$). ADC values of each decade were different and the differences were more significant in doubling decades ($p<0.01$). There was no significant difference between males and females.

Conclusion: DWI reflects the morphological and cytological changes of pancreatic tissue.

P-275**What is the role of diffusion-weighted MRI in the evaluation of pancreatic carcinoma?**

T. Cimilli, N. Guner, S. Bayramoglu, E. Öztürk, A. Kayhan, O. Kilickesmez, A. Karahasanoglu; Istanbul/TR

Purpose: The aim of this study was to demonstrate the feasibility of body diffusion-weighted (DW) MRI in the evaluation of presence and extent of pancreatic carcinoma (PC).

Material and methods: DW images were obtained on axial plane scanning with a single-shot echo planar spin-echo sequence with a body coil in fifteen patients with PC and in fifteen normal volunteers aged same as those of patient group. We measured the apparent diffusion coefficient (ADC) value in a circular region of interest (ROI) within the normal pancreas in control group and within the PC and also the surrounding tissue in patient group.

Results: On diffusion-weighted images, fourteen of fifteen carcinomas showed high signal intensity relative to the surrounding tissue. The ADC values in the carcinoma were significantly lower compared to that of surrounding tissue and normal pancreas in fourteen patients ($p < 0.01$). In one patient with a diagnosis of mucin-producing tumour, ADC value was significantly higher than normal pancreas.

Conclusion: DW images can be helpful in detecting the presence and the extent of PC.

P-276**Diffusion-weighted MRI of pancreatic tumors**

F. Kotake¹, R. Iwashiro², M. Yoshimura², K. Saito², M. Matsushita¹, Y. Takahashi¹, T. Ozuki¹; ¹Ibaraki/JP, ²Tokyo/JP

Purpose: To evaluate the diagnostic contribution of diffusion-weighted imaging using apparent diffusion coefficient (ADC) values to the characterization of pancreatic tumors and differentiation of benign and malignant lesions.

Material and methods: The study included 27 patients with pancreatic tumors who underwent upper abdominal MRI examinations. Chemical shift selective-diffusion-weighted images were performed with the following parameters: 2600/76/6 (TR/TE/excitations); echo train length 51; slice thickness/gap 5.0 mm/1.0 mm and b-values were set at 0 and 1000 sec/mm². We set the region of interest in the center of the pancreatic tumors, except for cystic lesions and necrosis, and then measured the ADC value.

Results: The mean ADC values ($\times 10^{-3} \text{mm}^2/\text{sec}$) were 1.01 ± 0.09 for carcinomas ($n=16$), 0.58 ± 0.02 for malignant lymphomas ($n=2$), 0.78 for mucinous cystadenocarcinoma ($n=1$), 0.95 ± 0.05 for metastatic tumors ($n=2$), 1.32 for insulinoma ($n=1$), 1.46 for solid-pseudopapillary tumor ($n=1$), 1.22 ± 0.11 for autoimmune pancreatitis ($n=3$), and 1.65 for tumor-forming pancreatitis ($n=1$). The ADC values in the malignant lymphoma were significantly lower compared to that of the other pancreatic tumors ($p=0.0017$). The mean ADC value of benign lesions (1.35 ± 0.19) was significantly higher than that of malignant lesions (0.95 ± 0.16) ($p < 0.0001$). When an ADC value smaller than 1.05 was used for predicting malignancy, the diagnostic sensitivity, specificity and accuracy were 86, 100 and 89%, respectively.

Conclusion: Diffusion-weighted imaging with quantitative ADC measurements can be useful in the differential diagnosis of pancreatic tumors.

P-277**Pancreatic adenocarcinoma: state of the art imaging using MDCT and MRI**

M. Zins¹, I. Boulay-Coletta¹, L. Huwart², E. Petit¹; ¹Paris/FR, ²Le Kremlin-Bicêtre/FR

Learning objectives: To detail state-of-the-art MDCT and MRI protocols in imaging the pancreas for suspicion of tumor. To discuss respective advantages of MDCT and MRI using state-of-the-art 2D and 3D techniques in the assessment of pancreatic adenocarcinoma. To illustrate 64 MDCT and high resolution 3D MRI results in the diagnosis and staging of pancreatic adenocarcinoma.

Background: The assessment of pancreatic adenocarcinoma is a difficult challenge for the radiologist and needs state-of-the-art imaging techniques for precise evaluation and adapted therapeutic approach.

Imaging findings OR Procedure details: 1. 64 row MDCT protocol for diagnosis and staging pancreatic adenocarcinoma. 2. MRI protocol for pancreatic imaging with emphasis on new 3D sequences. 3. Case studies of pancreatic cancer with comparison of both modalities. 4. Pitfalls and limitations of CT. 5. Pitfalls and

limitations of MRI. 6. Conclusion with diagnostic algorithm.

Conclusion: MDCT using 3D multiplanar reconstructions remains the imaging modality of reference in the diagnosis and staging of pancreatic adenocarcinoma. MDCT has the potential to improve the accuracy of pancreatic cancer staging for surgical resectability. However, some limitations and pitfalls still remain and high resolution MRI using new 3D sequences is now a strong competitor for CT.

P-278

Withdrawn by authors

P-279**Prognostic significance of the volume of the primary tumor and metastasis imaging characteristics with survival and PTEN gene expression in patients with inoperable or metastatic pancreatic cancer treated with gemcitabine combined with gefitinib in a phase II trial**

A. Kalogera-Fountzila, X. Mavropoulou, E. Psoma, M. Potsi, V. Karadimou, B. Demirler-Simsir, A.S. Dimitriadis; Thessaloniki/GR

Purpose: To evaluate the response to treatment of inoperable/metastatic pancreatic cancer and correlate the imaging findings with survival and gene profile.

Material and methods: 54 patients were registered in a phase II study of the Hellenic Cooperative Oncology Group (HeCOG), Athens, GREECE. Gemcitabine (G) (1000 mg/m²) was administered weekly for 7 cycles. Gefitinib (250 mg) was given orally. RESIST criteria were used to evaluate the response to treatment. In 43 patients, the volume of the primary tumor was calculated using Volumio software.

Results: Ten patients (19%) completed treatment while 36 (67%) progressed before the completion of the treatment. Three patients (6%) had partial response and 11 (20%) had stable disease. After a median follow-up of 9 months, median survival time was 7.4 months, while median time to disease progression (TTP) was 3.9 months. The one-year survival rate was 23%. Neither the volume nor any other imaging characteristic was significant to survival and PTEN expression. We noticed that target and non-target lesions in baseline images had a complete response to therapy, with appearance of new lesions, a fact significantly associated with increased survival ($p=0.022$). PTEN expression was noticed in 7/30 patients and was the only marker significantly associated with disappearance of old lesions and appearance of new ($p=0.003$).

Conclusion: There are limitations of our study due to the small number of patients. Larger numbers are needed to confirm that gene profile correlates with response to treatment pattern.

P-280**Imaging of pancreatoduodenal groove**

B. Viamonte, L.I. Melão, A. Almeida, M. Castro, N. Silva, R.G. Cunha; Porto/PT

Learning objectives: 1. Review the normal anatomy of the PDG. 2. Present imaging features and key diagnostic findings of the diseases involving the PDG.

Background: The pancreatoduodenal groove (PDG) is a potential space bordered by the head of the pancreas, duodenum, and common bile duct. Diseases arising from or involving the PDG can be categorized into four types: diseases associated with the pancreas, duodenum, lymph nodes, and distal common bile duct.

Imaging findings OR Procedure details: A didactic format will be utilized and organized based on imaging findings and clinical features. Differential diagnosis with a discussion of specific entities will follow. All patients underwent an MRI examination on a 1.5/3 T system and a CT investigation in a 64 slice scanner.

Conclusion: Knowledge of the features of each disease may allow one to make a specific diagnosis, which assists in clinical management and helps to prevent unnecessary surgical intervention.

P-281**Accessory pancreatic duct and minor duodenal papilla: visibility, examination technique and imaging findings at secretin-enhanced MRCP**

G. Restaino, M.V. Occhionero, M. Missere, M. Ciuffreda, E. Cucci, G. Mannetta, G. Sallustio; Campobasso/IT

Learning objectives: Many variants of APD and MIP exist. Proper S-MRCP examination provides good conspicuity of these structures. Morphological and functional evaluations of APD and MIP add important information in patients evaluated with S-MRCP for pancreatic disease.

Background: Accessory pancreatic duct (APD), due to hard visibility and presumed lower clinical significance than main pancreatic duct, is usually disregarded by radiologists reporting MRCP. Nevertheless, beside its role in pancreas divisum (PD), its patency lowers the risk of developing acute pancreatitis either spontaneous and after ERCP. Minor duodenal papilla (MIP) is difficult to locate radiologically, but may host diseases, like several types of endocrine tumors, and its function is crucial in PD.

Imaging findings OR Procedure details: We reviewed 200 S-MRCP performed at our Institution from 2004 to 2007 and focused on APD with regard to: visibility, type (long, intermediate, short, ansa), morphology of distal end (stick, branch, saccular, spindle, cudgel), caliber and patency; on MIP with regard to visibility, location, size and morphology. We also assessed the APD and MIP conspicuity in various S-MRCP sequences: T2w-SSFSE, b-SSFP, 2D-MRCP w/o secretin, 3D-MRCP (with MIP, MPR), 3D-LAVA (with minIP, MPR).

Conclusion: Morphological and functional evaluation of APD and MIP adds important information to those provided by S-MRCP. Newer MR sequences allow good conspicuity of these structures. Knowledge of normal and variant morphology of APD and MIP is crucial to correct image interpretation.

P-282*Withdrawn by authors***P-283****Imaging findings of groove pancreatitis**

V. Tang, K. Uzoka; Manchester/UK

Learning objectives: Describe groove pancreatitis and its appearance on various imaging modalities.

Background: Groove pancreatitis is an uncommon form of chronic focal pancreatitis that affects the pancreatoduodenal groove between the pancreatic head, duodenum and common bile duct. It causes fibrous scarring of the duodenal wall, smooth stricture of the common bile duct and rarely stricture of the pancreatic duct. Its importance lies in the similarity of imaging appearances to carcinoma of the pancreatic head affecting the pancreatoduodenal groove.

Imaging findings OR Procedure details: We describe our imaging experience of groove pancreatitis in our hepatobiliary unit. We illustrate the varied appearances of groove pancreatitis on CT, MRI and ERCP. A characteristic sheet of mass is noted in the pancreatoduodenal groove which is hypodense on CT, hypointense on T1 and iso to marginally hyperintense to the normal pancreatic parenchyma on T2 weighted images. Cystic changes within and thickening of the duodenal wall are noted. A smooth stricture of the common bile duct is present on MRCP and ERCP.

Conclusion: Although certain imaging features can distinguish groove pancreatitis from pancreatic carcinoma, it remains difficult to differentiate the two conditions and histology is often required for correct diagnosis. A mass in the pancreatoduodenal groove in a patient with abdominal pain and vomiting should prompt the radiologist to consider groove pancreatitis as a differential diagnosis in order to avoid unnecessary surgical intervention.

P-284**Peripancreatic lymphatic invasion of the pancreatic carcinoma: imaging demonstration with multi-detector row CT**M. Sai¹, H. Mori², K. Kosen¹, M. Kiyonaga², Y. Yamada², S. Matsumoto²; ¹Yufu-shi/JP, ²Oita/JP

Learning objectives: 1. To understand the normal CT anatomy of PLN. 2. To demonstrate the multi-detector row CT (MDCT) imaging of PLN invaded by the pancreatic carcinoma. **Background** The peripancreatic lymphatic networks (PLN)

are frequently involved with pancreatobiliary carcinoma, affecting the prognosis. However, little attention has been paid to the CT imaging of normal and pathological conditions of PLN.

Imaging findings OR Procedure details: In this education exhibit, we will demonstrate the normal PLN obtained by imaging reconstruction every 1 mm with multiplanar reformation using MDCT. Furthermore, we will review the CT images of PLN invaded by the pancreatic carcinoma. The normal peripancreatic lymphatics were usually detected as "linear structures" on MDCT. On the other hand, the peripancreatic lymphatic invasion of pancreatic carcinoma was frequently identified as "reticular", "tubular" or "soft tissue mass" appearances in the peripancreatic fat tissues on MDCT. The peripancreatic lymphatic invasion of pancreatic carcinoma on MDCT was more frequently detected around the common hepatic artery, celiac artery, and superior mesenteric artery.

Conclusion: Knowledge of the CT imaging of normal and abnormal PLN is essential for determining the accurate staging of pancreatic carcinoma.

P-285**Imaging acute pancreatitis**

B. Koo, S. Freeman, A. Shaw; Cambridge/UK

Learning objectives: To review the role of the radiologist in the management of patients with AP. This ranges from establishing the diagnosis and aetiology, the merits of using imaging-based severity scores for prognosis, recognition of complications and, finally, when and how interventional procedures should be performed. **Background** Acute pancreatitis (AP) is an increasingly common clinical problem which is associated with a significant morbidity and mortality. The radiologist may encounter patients for a number of reasons, from diagnosis to therapy. It is vital that the radiologist and clinician understand when, why and how to image patients optimally, together with the indications and techniques of therapeutic procedures.

Imaging findings OR Procedure details: CT is the mainstay of imaging patients with pancreatitis, with US and MRI reserved for specific indications. This review will demonstrate the findings of AP, the value of imaging-based severity scores, the complications arising and how some of these may be managed by radiological means. We also explore the roles of US, CT and MRI in establishing the underlying aetiology of the disease.

Conclusion: The radiologist may play a key role in the management of patients with AP, but in order to fulfil this, one needs to be aware not only of the imaging techniques and findings, but when to initiate intervention.

P-286**Morphological and functional characterization of mucinous lesions of pancreas: a comparative study of MDCT, PET and fused PET-CT**

D. Sahani, N. Sainani, S. Fritz, M. Blake, V. Deshpande, C. Fernandes-del Castillo, A. Fischman; Boston, MA/US

Purpose: Characterize mucinous pancreatic lesions on MDCT and establish features predicting malignancy. Distinguish malignant lesions, based on increased FDG uptake. Correlate areas of increased FDG activity with morphologic features on MDCT. Compare performance of MDCT, PET and PET-CT.

Material and methods: 28 suspected mucinous lesions in 20 patients (M:F 9:11, Age 33-84 yrs), evaluated with dual phase pancreatic 16-MDCT with abdomen FDG-PET and surgery, were included in this prospective study. One reader evaluated MDCT features and lesions were categorized into benign/malignant. Another reader analyzed FDG-PET; areas of highest FDG uptake were quantified with standard uptake value (SUV). Areas of increased uptake on PET were correlated with morphological features on MDCT on fused PET-CT images. Pathology served as gold standard.

Results: Pathologically, 12 lesions were main-duct IPMNs, 12 side-branch IPMNs, 1 MCN, 1 SPPN and 2 unclassified cysts. 21/28 lesions were benign and 7/28 malignant. MDCT accurately characterized lesions in 75%. MDCT features favoring malignancy were gross PD dilatation, thick wall/septae and mural nodule. Areas of increased FDG uptake correlated with thick wall/septae and mural nodule on MDCT. Sensitivity and specificity of MDCT, PET and PET-CT for malignancy were 86 and 91%, 43 and 95% and 86 and 86%, respectively.

Conclusion: Dual-phase 16-MDCT reliably characterizes mucinous lesions and prediction of malignancy. Increased FDG uptake is highly specific for malignancy and can complement MDCT to increase confidence of malignancy.

P-287*Withdrawn by authors***P-288****Visual assessment of high-b value diffusion-weighted MRI in the differential diagnosis of pancreatic lesions: preliminary results**

F. Donati, P. Boraschi, R. Gigoni, C. Bertucci, S. Salemi, M.C. Cossu, F. Falaschi, C. Bartolozzi; Pisa/IT

Purpose: To determine the usefulness of visual assessment of high-b value diffusion-weighted MRI (DW-MRI) in the differential diagnosis of pancreatic lesions.**Material and methods:** Ten patients with malignant pancreatic lesion confirmed at surgery (ductal adenocarcinoma, n=8; metastasis, n=1, papillary mucinous carcinoma, n=1) and 15 patients who were being followed-up at our institution because of pancreatic disease other than malignancy (focal chronic pancreatitis, n=2; autoimmune pancreatitis, n=1; IPMT, n=5; serous cystadenoma, n=5; pseudocyst, n=2) were included in our study group. All patients underwent MRI at 1.5 T device (Signa EXCITE; GE Healthcare). DW-MRI was performed using a breath-hold single-shot echo-planar sequence with b gradient factor values of 300, 500, 700 and 1000 sec/mm² in three orthogonal directions. All DW images were blindly interpreted by two reviewers in conference that graded the presence of lesions on a three-point scale on the basis of their signal intensity on high-b value, as follows: 0, absent (no signal); 1, undetermined (mild to moderate signal); 2, present (strong signal).**Results:** The reviewers graded as "2" all adenocarcinomas, pancreatic metastasis and autoimmune pancreatitis (false positive), whereas papillary mucinous carcinoma was defined as undetermined (false negative). All the other pancreatic lesions show "no signal" on high-b value DWI. The sensitivity and specificity of high-b value DW-MRI for the detection of pancreatic malignancy were 90 and 93%, respectively.**Conclusion:** Visual assessment of high-b value DW-MRI might be helpful in the differential diagnosis of pancreatic lesions.**INTERVENTIONAL****Interventional / GI Tract****P-289****Placement of 85 fiducials in 23 patients under CT guidance for cyberknife stereotactic radiosurgery of abdomen malignant lesions: an initial experience**

E. Sotiropoulou, A. Bouga, F. Laspas, N. Salvaras, V. Kosmas, L. Thanos; Athens/GR

Purpose: The aim of this study is to present our initial experience in positioning gold fiducials as tumor landmarks under CT guidance to facilitate treatment with Cyberknife system of abdomen malignant lesions.**Material and methods:** During the last 8 months, we positioned in our department a total of 85 fiducials in 23 patients. Eight patients had liver metastatic lesions from NSCLC or colon cancer (number of fiducials placed per case: 4, 3, 4, 3, 4, 4, 4, 3), 5 patients had nodes metastases from ovary cancer (number of fiducials placed per case: 2, 3, 3, 3, 4), 3 patients had adrenals metastases from lung cancer (number of fiducials placed per case: 4, 5, 3), 5 patients had pancreatic malignant lesions (number of fiducials placed per case: 3, 4, 4, 4, 4), one patient had retroperitoneal leiomyosarcoma (5 fiducial placed) and one patient had peritoneal sarcoma (5 fiducial placed). Fiducial positioning under CT guidance followed the same procedure as CT guided biopsy. Once the tip was seen at a correct position on CT images, fiducials were advanced through the 18 G Chiba needle. The tip of the needle was readjusted in order to put the fiducials in different sites within the lesion.**Results:** 84/85 fiducials were implanted successfully (98.8%); there was migration of 1 fiducial. Major complications did not occur.**Conclusion:** Fiducial placement under CT guidance seems to be a safe and efficient procedure.**P-290****The appearance and management of colorectal stent complications**

K. Mason, E.M. Armstrong, J. Shirley, S. Jackson, B. Fox; Plymouth/UK

Learning objectives: To illustrate the radiological appearance of the complications associated with colorectal stent placement and demonstrate how the varying complications can be managed.**Background** In patients presenting with large bowel obstruction, the morbidity and mortality of emergency surgery remains high and self-expanding metal stent insertion is commonly used as an alternative. Stenting can be performed using fluoroscopic or endoscopic guidance or a combination of both. The local complications associated with colorectal stents include rectal bleeding, perforation, stent migration, stent fracture and stent blockage due to tumour in growth. Perforation can be caused by the initial stent insertion, stricture dilatation or due to stent erosion through the colonic wall. It is important that these complications are both detected early and effectively managed in order to optimise a patient's treatment or palliation.**Imaging findings OR Procedure details:** We provide a radiological review of the complications associated with colorectal stents and outline the management options available for treating them using video demonstration of the techniques used in our department.**Conclusion:** It is important that radiologists are able to recognise the complications associated with colorectal stent insertion and appreciate the management options available. This will allow prompt patient treatment and avoid unnecessary delays.**P-291****CT enterographic findings of most common small bowel disorders**

G. Caruso, G. Salvaggio, S. Pardo, A. Campisi, F. Sorrentino, R. Lagalla; Palermo/IT

Learning objectives: CT enterographic findings of most common SBD.**Background** Increased spatial and temporal resolutions of multi-detector row computed tomography (CT) have made CT a first-line modality for the examination of small bowel disorders (SBD). With large volumes of ingested neutral enteric contrast material, it permits better display of the small bowel lumen and wall.**Imaging findings OR Procedure details:** We report CT enterographic findings in the most common diseases encountered in our series, including neoplastic lesions (lymphoma, GI stromal tumor, carcinoid tumor and adenocarcinoma) and non-neoplastic lesions. Non-neoplastic lesions include inflammatory diseases (Crohn's disease, diverticulitis and epiploic appendagites) and non-inflammatory diseases (intussusception, volvulus and ischemia).**Conclusion:** Knowledge of typical imaging features of most common SBD can simplify the diagnosis and be of value in management.**P-292****Setting up a laparoscopic gastric banding service: implications for the radiology department**

A.J. Sambrook, A. Thrower, A. Lowe, C. Kay, J. May; Bradford/UK

Purpose: Laparoscopic insertion of gastric bands is one of several surgical techniques used to treat obesity. Following insertion of a band, radiological inflation/deflation is necessary in order to ensure optimal function. The purpose of this study is to review our local experience of the implications for the radiology department when setting up a laparoscopic banding service.**Material and methods:** A retrospective audit of gastric bands placed in our institution (April 2005–September 2007) was performed. 19 cases were reviewed. Costs were derived using the business case figures for our institution.**Results:** Mean weight loss was 21.4 kg (range 2–50 kg). The average number of band adjustments was 4 (range 2–9) with a time interval between adjustments of 2–3 months. In 4 cases, urgent band volume reduction was necessary due to complete dysphagia approximately 2 days after the previous adjustment. A single patient needed emergency admission to remove the band due to position slip. The cost per adjustment was €07 with a mean total cost per patient of €228 (€14–2763).**Conclusion:** Participation in a gastric banding service requires on average 4 adjustments per case at a cost of €228 per patient. The requirement for band readjustment and emergency admissions must be factored in when setting up a laparoscopic gastric banding service.

P-293**Early experience with long dwelling ascitic drainage system**

V. Arora, A. Razack, G. Alluvada; Hull/UK

Learning objectives: Pleurx drain should be considered for palliation of recurrent malignant ascites in terminally ill patients. **Background** Malignant ascites is a common distressing symptom in cancer patients requiring repeated drainages particularly in later stages due to rapid re-accumulation. Pleurx catheters which are long term indwelling catheters have been used in malignant recurrent pleural effusions. We have used these catheters for relief from malignant ascites.

Imaging findings OR Procedure details: Pleurx drain (Denver biomedical) is a long fenestrated silicon catheter with silicon valve mechanism and a polyester cuff. The two way valve can only open with a specific matched drainage vacuum bottle. We inserted this catheter in ten patients suffering from advanced malignancies for long term ascitic drainage, with US guidance under local anesthesia. Technical success was 100% with no immediate complication. The catheter was tunnelled under the skin and the tube taped to the abdominal wall. As ascites re-accumulates, a vacuum bottle is attached to the tube and further drainage undertaken by the patient, carer or community nurse at home. Follow up showed preference by patients, avoiding repeated interventions and hospital admissions. The catheter has good life span with low complication rate.

Conclusion: Pleurx drain can be used for long term palliation of recurrent malignant ascites. It is safe with low complication rate, high technical success rate, avoids repeated hospital admissions and improves quality of life.

P-294**Esophageal mucocele causing angina symptoms treated with percutaneous drainage**

K. Güven, E. Terzibasoglu, A. Ucar, B. Bakir; Istanbul/TR

Purpose: To stress on the effectiveness of percutaneous drainage of a symptomatic esophageal mucocele.

Material and methods: A 52-year-old man suffered from chest pain and discomfort after the esophageal resection and colonic interposition operation due to esophageal carcinoma. Electrocardiogram (ECG) revealed ST segment depression suggestive of coronary hypoperfusion. CT examination revealed 58x46 mm well-defined fluid collection at the posterior of the base of the heart next to the thoracic descending aorta. At CT guidance via the intercostal approach, the cavity was punctured and a 6 french locked pig-tail catheter was introduced to the cavity. After the drainage, symptoms disappeared and ECG was returned to normal.

Results: Esophageal by-pass surgery is performed for benign esophageal strictures, perforations and ruptures, congenital tracheal and esophageal fistulas, esophageal and gastric neoplasms. Blind loop esophageal segments which are ligated proximally and distally contain squamous and glandular epithelium causing secretion collections. They are generally asymptomatic in adults but there are some complications such as infection, ulceration, compression of nearby organs and malign transformation. In our case, the symptomatic esophageal mucocele was treated with percutaneous drainage successfully and did not occur in 6 months follow-up.

Conclusion: Percutaneous drainage of esophageal mucoceles after surgery is an alternative treatment to surgery and can be easily performed under CT guidance.

Interventional / Liver / Other**P-295****Our experience of percutaneous treatment of liver hydatid cysts: 15 years results**

D. Emlik, D. Kiresi, S. Gumus, K. Odev; Konya/TR

Purpose: To evaluate the long-term effectiveness of percutaneous treatment of liver hydatid cysts (LHC).

Material and methods: Sixty one patients with 84 LHC affected by liver echinococcosis were treated using puncture, aspiration injection and reaspiration (PAIR) technique under sonographic guidance. Patients with cysts larger than 6 cm in diameter underwent PAIR followed by percutaneous drainage (PAIR-PD).

The cysts were treated with 20% hypertonic saline solution or 0.5% silver nitrate. All patients went follow-up examinations for 1 month to 6 years after aspiration. Clinical and radiologic examinations and laboratory analysis were performed every month for the first 6 months and then at 3 months intervals.

Results: A progressive disease in diameter in seventy six cysts (90%); calcification of the cyst wall, cystic or both in five cysts (6%) and complete disappearance of three cysts (4%) in three patients who had been monitored for over 15 years. Five patients developed urticaria, 6 developed fever. One patient developed a biliary fistula after the first aspiration attempt. Two patients developed infection of the cyst cavity after PAIR-PD. Anaphylactic reaction developed in 2 patients and successfully treated with antiallergic medication. Abdominal dissemination was not encountered in any patient over the follow up period of 15 years.

Conclusion: Percutaneous treatment of LHC has fewer complications and is much less costly than surgical treatment. This procedure is an effective and reliable treatment in selective cases.

P-296**Percutaneous treatment of simple liver cysts with alcohol sclerotherapy**

F. Islim, O. Temizoz, D. Akinci, M.N. Ozmen, O. Akhan; Ankara/TR

Purpose: To evaluate the therapeutic efficacy of percutaneous treatment of simple liver cysts (SLC) with alcohol sclerotherapy.

Material and methods: During the period 1993–2007, 31 SLC in twenty six patients (sixteen women, ten men; age range 9–79 years, mean age of 51.2±17.1) were treated by alcohol sclerotherapy. The cyst volumes were 10–1550 mL (mean 188.8 mL). Patients were followed up 1–168 months (mean 46.9 months). 24 of them were treated with single session alcohol sclerotherapy by 19 G needle. Single session catheter drainage and sclerotherapy was performed in 5 cysts. Prolonged catheter drainage and multiple sclerotherapy were applied to two cysts whose volumes were greater than 500 ml. Differences in cystic volumes before and after therapy were examined using the Wilcoxon signed-rank test.

Results: Technical success was achieved in all patients (100%). The average volume reduction was 93.9% (range 50–100%; p<0.001) in all patients. The mean volume reduction rate was 97% in 25 cysts which were followed for at least 1 year. The remaining 6 cysts with less than 1 year follow up had an 81% mean volume reduction rate. An abscess as a major complication was developed in only one patient who was treated percutaneous drainage and antibiotherapy later.

Conclusion: Percutaneous alcohol sclerotherapy is a safe and effective treatment for the management of SLC.

P-297**Liver cell transplantation: state of the art**

J. Tisnado, T. Murphy, U.R. Prasad, R. Fisher, M.K. Sydnor, D. Komorowski, D. Leung; Richmond, VA/US

Purpose: Orthotopic liver transplantation (OLT) is the definitive method to manage patients with fulminant, acute and chronic liver failure. Unfortunately, organ availability is limited in USA. A "bridge" is needed to keep patients alive until a cadaver or a living donor is found. About 10,000 patients are waiting for a liver. Many will die waiting. Recently, right lobe living donor transplantation (RLLDT) has become accepted and organ pool increased 10-fold. One method to keep patients with fulminant failure alive is liver cell transplantation (LCT), i.e., the hepatocytes infusion from donor livers into the recipient's liver or spleen.

Material and methods: LCT provides function until a liver is available, or improves function in patients too sick for OLT or RLLDT, in patients with expected 100% mortality in 24 hours. Hepatocytes (200–1000 million) are harvested, cultured, frozen and stored. When needed, cells are thawed and infused in the spleen via splenic artery, or in the liver via the portal vein. Thereafter, hepatocytes colonize in the splenic pulp or hepatic parenchyma and provide hepatic function.

Results: We performed LCT in >20 patients. We present our encouraging experience. This new method is a "bridge" until OLT and/or RLLDT can be performed.

Conclusion: IR must be ready to catheterize the splenic artery or portal vein procedures required on short notice during 24/7. The future of LCT is exciting; therefore, this review.

Interventional / Liver / Tumour ablation / Follow-up imaging and outcome

P-298

Pilot study of transarterial chemoembolization with pirarubicin and amiodarone for unresectable HCC

B. Guiu, R. Loffroy, S. Guiu, J.P. Cercueil, C. Colin, F. Bonnetain, M. Boulin, F. Ghiringhelli, P. Hillon, L. Bedenne, D. Krausé, B. Chauffert; Dijon/FR

Purpose: As we previously reported that an in vitro emulsion of pirarubicin, amiodarone and lipiodol was more stable and cytotoxic than a classical doxorubicin-lipiodol mixture, we designed a pilot study to evaluate efficacy and toxicity of a transarterial chemoembolization (TACE) procedure using this combination.

Material and methods: Forty-three patients were included and underwent TACE for unresectable HCC. CT scans were performed to assess tumor response (RECIST) and lipiodol uptake after the first session. Median follow-up lasted 30 months. Endpoints were overall and progression-free survival. Univariate and multivariate Cox analyses were performed.

Results: Mean tumor size was 9.5 cm (1–20 cm) and 30/43 were multifocal or diffuse. CLIP-score was 0 in 7/40, and 1 in 16/40. Mean number of TACE sessions was 3.5 (1–11). There were 3 treatment-related deaths. Twelve (28%) partial responses and 29 (67%) stable diseases were observed. Median overall and progression-free survivals were 29 months (95% CI 13.8–45) and 15 months (95% CI 11.5–20.8), respectively. CLIP-score ≤ 1 ($p=0.042$) and lipiodol uptake $>25\%$ ($p=0.003$) were independent prognostic factors for better overall survival.

Conclusion: This new TACE procedure is safe, gives high overall survival and merits phase III investigation for comparison with classical treatment such as doxorubicin-lipiodol TACE.

P-299

The role of percutaneous CT guided radiofrequency ablation in intrahepatic recurrence of HCC in patients initially treated with hepatectomy

E. Sotiropoulou, P. Filippousis, M. Seferos, P. Tsgouli, A. Bouga, L. Thanos; Athens/GR

Purpose: To evaluate the efficacy of radiofrequency ablation (RFA) in patients with intrahepatic recurrence of HCC.

Material and methods: From December 2003 until December 2007, 41 patients with 56 recurrences of HCC, who were initially treated with partial hepatectomy underwent a total of 75 RFA sessions. The number of lesions ranged between 1 and 3 with a mean size of 2.95 cm. 45 minutes before RFA, 3 mg bromazepam per os and 0.05 gr pethidine hydrochlorique intramuscularly were administered. RFA was performed using expandable electrodes. A pulsed RF energy was applied for 12 to 15 min. A dual-phase dynamic contrast enhanced CT was performed after the electrode removal to evaluate the immediate lesion's response to the ablation. Follow up was performed at 1, 3, and 6 months post-RFA and every 6 months afterwards.

Results: Complete response was seen in 48/56 lesions (85.7%), whereas the rest 8/56 showed partial necrosis and underwent a second RFA. Six patients (14.6%) who presented new lesions within a year, and 5 patients (12.2%) who presented with local tumor progression at the ablated site 6–12 months after the first RFA session, underwent a second RFA as well. Overall survival was 29.61 \pm 12.6 months. 1-, 2-, 3- and 4- year survival rate was: 95.12, 73.2, 41.5 and 10%, respectively. Major complications did not occur.

Conclusion: RFA of intrahepatic recurrence of HCC post hepatectomy seems to be an efficient treatment modality.

Interventional / Liver / Tumour ablation / Technical aspects

P-300

Percutaneous radiofrequency ablation of HCC in patients with ascites: can this method be equally efficient?

A. Lourbakou, S. Mylona, S. Ntai, E. Daskalaki, G. Karapostolakis, N. Batakis; Athens/GR

Purpose: To evaluate the contribution of percutaneous radiofrequency ablation (RFA) as treatment of HCC in cirrhotic patients with ascites.

Material and methods: In a period of seven years, 198 cirrhotic patients (153 men, 35 women, and average age 62.5 y) with HCC (2.4–4.8 cm) proceeded for RFA under CT-guidance. 32/198 had ascites. The re-evaluation after RFA was performed with dual phase CT after I.V. contrast enhancement. Regions with lack of enhancement were characterised as necrotic, and regions with maximum enhancement were estimated as residual disease. In these cases a second RFA session was performed.

Results: A total necrosis was found in 87.5% of patients with ascites and in 88.6% of patients without ascites (no statistically important difference, $p=1.00$). In patients with residual disease a second RFA session was performed. No major complications were observed. Patients with ascites had no peritoneal spread in the puncture channel or elsewhere in the abdomen.

Conclusion: Percutaneous RFA for treatment of HCC patients with ascites seems to be as safe and efficient as in patients without a ascites.

Interventional / Other / Abdominal vascular

P-301

Chronic Hepatic Venous Outflow Obstruction: Transluminal membranotomy with balloon dilatation.

R. Jain¹, S. Sawhney¹, S.K. Acharya², P. Sahni²; ¹Muscat/OM, ²New Delhi/IN

Purpose: To evaluate effectiveness of percutaneous inferior vena cava (IVC) balloon dilatation and stenting in chronic hepatic venous outflow obstruction (HVVO).

Material and methods: Percutaneous transfemoral endoluminal membranotomy, balloon dilatation, and placement of self-expanding metallic stents in the intrahepatic vena cava were performed in 26 patients with chronic HVVO.

Results: Two distinct responses were identified depending on type of IVC abnormality: Type I – 14 patients - Membranous occlusion of the IVC at the cavo-atrial junction by 2.1 \pm 0.8 mm membrane; one-time puncture and balloon dilatation was curative for all 14 patients - follow-up US up to 2 years demonstrated IVC patency (RRR=1, ARR=1, NNT=1). Type II – 12 patients - Steno-occlusive narrowing - 41 \pm 25 mm long of intrahepatic IVC - balloon dilatation (12/12), metallic stents (8/12) - mean diameter of IVC increased from 2 to 9 mm; cavo-atrial pressure gradient dropped from a mean of 16 to 3 mmHg. Of eight patients who had stent placements, seven maintained IVC patency, one died of hepatic venous thrombosis; four patients who did not have stent placement showed recurrent stenosis - repeated balloon dilatations required (average 2.2 per year) to maintain IVC patency (RRR=0.875 (95% CI- 0.22, 0.98), ARR=0.875 (95% CI- 0.65, 1.1), NNT=1.143 (95% CI- 0.9, 1.55)).

Conclusion: Type I – Membranous IVC occlusion – membranotomy and balloon dilatation were curative. Type II – Steno-occlusive – did not respond effectively without stent placement; repeated balloon dilatations and/or metallic stents required for maintaining patency.

P-302

Retrospective study of proximal versus distal main splenic artery embolization

P.R. Rau, N.H. Stauffer, A. Denys; Lausanne/CH

Purpose: Proximal splenic artery embolization (SAE) is supposed to be better tolerated as compared to standard distal or segmental embolization, nevertheless, fulfilling the same treatment objectives. A smaller post-interventional complication rate in terms of infarction and infection is advocated. The objective was to test this hypothesis in our study.

Material and methods: 73 consecutive patients undergoing proximal vs. distal or segmental SAE over a time period of 5 years were included in this study. Age, sex, and clinical history leading to SAE were noted. Pre-interventional imaging was reviewed for each patient, and grade of splenic injury and degree of hemoperitoneum were noted. Finally, we checked all digitally available patient records for clinical and radiological follow-up in order to assess post-interventional complications. These were examined on a four point scale, from 0=none, to 3=important complications.

Results: Complications following proximal SAE (N=11, median=1.0, range=0–2, mean=0.64) did not differ significantly from distal SAE (N=62, median=1.0, range=0–3, mean=0.87), U=303.0, Z=-0.63, p=0.30, r=-0.07.

Conclusion: Proximal SAE is a safe and efficacious intervention as compared to distal and segmental SAE. Concerning possible post-interventional complications, there is a slight but non-significant tendency in favour of proximal SAE. There is no elevation of the secondary splenectomy rate in the proximal SAE-group. These results allow us to pursue a prospective study which might reveal a significant advantage in favour of proximal SAE.

P-303

Percutaneous treatment of two hydatid cysts in the adrenal gland

O. Akhan, D. Kaya, B. Ustunsoz, D. Akinci; Ankara/TR

Purpose: To demonstrate radiological features and evaluate the results of the percutaneous treatment of the hydatid cyst (HC) of the adrenal gland for the first time in the literature.

Material and methods: Two patients with two HCs of the adrenal gland underwent percutaneous treatment. The first patient was a 72-year old man in which radiological studies disclosed an 8x11x13 cm cystic mass with structures resembling germinative membrane in the left suprarenal region. The second patient was 43-year old female with a 4.5x3.5x3.0 cm cystic mass. The CE 3A HC was considered in the first patient and CE 2 in the second patient according to WHO classification. The interventions were performed under sonographic and fluoroscopic guidance. Among the percutaneous techniques, "catheterization technique with hypertonic saline and alcohol" were chosen for the management.

Results: No procedure related complications were encountered in the patients. Hospital stay was one day for each patient. A substantial decrease (more than 90%) in the size of the cysts was observed in both patients. No sign of viability was observed during the 45 months for the first and 26 months for the second patient.

Conclusion: Percutaneous treatment of adrenal HC is a safe and effective procedure and should be considered as a serious alternative to surgery.

P-304

Partial splenic embolotherapy

S. Karakose, A. Karabacakoglu, S. Yol, E. Ertekin; Konya/TR

Purpose: The purpose of this study was to evaluate the effectiveness of partial splenic arter embolization in patients with splenomegaly and with or without hypersplenism.

Material and methods: Thirty-four patients (18 men, 14 women, mean age 48, range 34–80) with splenomegaly and thrombocytopenia underwent selective transcatheter splenic arter branches embolization with PVA, microspheres, gelfoam particles and mechanical fibrinated coils. They were not suitable for the surgical splenectomy. Eight of them were refused surgery and for the remaining 24 patients the surgeons had suggested radiological interventional procedures. Transcatheter embolization was applied to the main and distal branches of the splenic artery. In every case, 1 or 2 main branches of the splenic artery were not embolized, since we believe that non-infracted spleen segments may continue to provide immunologic functions. During embolization, super selective catheterization was supplied by micro catheters for the protection of the non-splenic vascular beds.

Results: After splenic embolization, platelet counts had increased in all patients. Fifty-nine days after embolization, the portion of infarcted spleen tissue was calculated between 40–65% according to CT images. 1 week, 3 months, and 6 months after the procedure, CT and US examinations were performed. There was a significant decrease in the dimensions of the spleens. Our patients required post-procedural analgesics for an average of 2–11 days. No major complication was seen.

Conclusion: Selective and partial embolization of splenic arterial branches will provide easy, safe and rapid splenic vascular occlusion as an effective alternative therapy to surgical splenectomy.

Interventional / Pancreas

P-305

Standardization of MDCT criteria of patients qualifying for endoscopic treatment of organized pancreatic necrosis and assessment of therapeutic effect

J.M. Pienkowska, E. Szurowska, J. Wierzbowski, M. Studniarek; Gdansk/PL

Purpose: The therapeutic success of endoscopic treatment of organized pancreatic necrosis depends on the appropriate selection of patients. The aims of this study were the analysis of the MDCT criteria of patients qualifying for endoscopic drainage of pancreatic fluid collection (PFC) and the evaluation of the therapeutic effect.

Material and methods: 40 patients in the period from 6–8 weeks after acute phase of pancreatitis with PFC underwent MDCT. The indications for sterile pancreatic necrosis drainage were: a difficult to relieve abdominal pain, symptoms of delayed stomach emptying, anorexia and body weight loss. Transmural, less frequently percutaneous with simultaneous transpapillary aggressive drainage was applied in all patients. In 35 of patients, multiple drainages (2–5) were positioned and left in place for a period for 7–90 days. MDCT was performed in all patients before and after endoscopic drainage. Topography of PFC, size, number and location of the collections were analyzed.

Results: The size of detected PFC was 45–115 mm (mean 65 mm), the number was 1–3 (mean 1.8). The best position of the drainages location was determined on the strength of the MDCT. The appropriate criteria of evaluation affected that resolution of fluid collections was achieved in all selected lesions. Recurrence occurred in 6 patients, and four of them underwent repetition of the procedure.

Conclusion: MDCT is a useful method for patient selected, therapy planning and monitoring drainage of organized pancreatic necrosis resulted in good therapeutic outcomes.





A

Abdel Aziz A.: SS 9.10
 Acar M.: P-150
 Acharya S.: P-270, P-301
 Acu B.: P-234
 Adamonis W.: P-143, P-172
 Aduna M.: P-053
 Agrawal S.: P-134
 Aguirre I.: P-053
 Ahmad R.: SS 1.02, SS 6.07, SS 13.09
 Aisen A.: SS 2.06, SS 4.10, SS 9.03
 Akalin S.: P-231
 Akata D.: P-098, P-149, P-158
 Akay H.: P-032
 Akhan O.: P-098, P-149, P-158, P-296,
 P-303, SS 14.10, SS 15.10
 Akinci D.: P-296, P-303, SS 14.10,
 SS 15.10
 Akisik F.: SS 2.06, SS 4.10, SS 9.03
 Aksoy S.: P-181, P-274
 Akturk Y.: P-234
 Akyildiz H.: SS 5.10
 Al-Ansari N.: SS 13.07
 Al-Kindi S.: P-244
 Alaimo V.: SS 7.02
 Albuquerque G.: P-213
 Alexander G.: P-171
 Alkadhhi H.: PG 1.03
 Allison M.: P-171
 Allum W.: SS 3.01
 Alluvada G.: P-085, P-293
 Almac Z.: P-109
 Almeida A.: P-280
 Alonso-Burgos A.: P-235
 Alpendre J.: P-259
 Alt C.: SS 4.05
 Alves E.: P-114
 Alves P.: P-137, P-236
 Alzahrani A.: P-213
 Amitai M.: SS 11.10
 Amonkar S.: P-183
 Anagnostara A.: P-250, P-252
 Anastasiadou K.: P-247
 Anderson H.: P-095
 Ansari H.: P-004
 Anselmino M.: P-136
 Antonelli L.: SS 9.07
 Apter S.: SS 11.10
 Aquilani L.: P-219
 Arevalo J.: P-053
 Arias J.: P-235
 Armitage S.: SS 5.09
 Armstrong E.: P-142, P-222, P-290
 Arora J.: P-226
 Arora V.: P-293
 Arraiza M.: P-038
 Arslan D.: P-056
 Arthurs O.: P-076
 Asakura K.: P-018
 Aschoff A.: PG 4.02, SS 8.04
 Ashikaga R.: P-029
 Atchley J.: SS 1.04

Atkin W.: SS 1.09
 Attia H.: SS 9.10
 Aufort S.: SS 9.05
 Avidan B.: SS 11.10
 Avventurieri G.: SS 5.05
 Awad D.: P-019, P-084
 Aydin S.: P-181
 Aydogdu Kiresi D.: P-141
 Ayuso C.: P-116
 Ayuso Colella C.: P-047
 Ayuso J.: P-116

B

Ba-Ssalamah A.: PG 3.01, SS 4.04
 Bacigalupo L.: P-039, P-126
 Baek S.: P-128
 Bagni B.: SS 8.07
 Bainbridge A.: SS 11.05, SS 11.06
 Bakir B.: P-294
 Balaguer F.: P-116
 Baldwin R.: SS 6.07
 Balik E.: P-109
 Ballesta M.: P-016
 Bangash T.: SS 2.07
 Baratella E.: SS 7.02
 Barbachano Y.: SS 3.01
 Bardine A.: P-136
 Barentsz J.: P-035
 Bargellini I.: SS 10.06, SS 10.08
 Barluenga E.: P-196
 Barrassi M.: P-219, P-245
 Barratt D.: SS 8.01
 Bartolotta T.: P-156, P-160, P-208, P-210,
 SS 5.08
 Bartolozzi C.: P-055, P-064, P-106,
 P-107, P-108, P-136, P-288, PG 2.02,
 SS 3.06, SS 4.09, SS 6.04, SS 10.06,
 SS 10.08, SS 12.10, SS 14.06
 Bartone G.: P-082
 Bartumeus P.: P-180
 Baruah R.: P-123
 Barxias M.: P-024
 Başaran C.: P-006
 Bashir O.: P-062
 Baski M.: SS 7.06
 Batakis N.: P-250, P-252, P-300
 Battaglia V.: P-055, SS 3.06, SS 4.09
 Baudin G.: SS 15.02
 Bayrak A.: P-032
 Bayramoglu S.: P-147, P-181, P-274,
 P-275
 Baysal B.: P-138
 Baysal H.: P-138
 Bazzocchi A.: SS 10.07
 Bazzocchi M.: P-009, SS 9.04
 Becker C.: PG 4.04, SS 15.01
 Bedenne L.: P-298
 Beets-Tan R.: P-105, P-112, P-117,
 SS 8.08, SS 8.10, SS 13.06
 Beets G.: P-105, P-112, P-117, SS 8.08,
 SS 8.10, SS 13.06
 Bekar U.: P-234

Belcari A.: SS 3.06
 Bell J.: P-193, SS 13.03
 Bella G.: SS 13.07
 Bellomi M.: SS 7.04
 Belo-Soares P.: P-078
 Ben Ely A.: P-215
 Benitez O.: P-225
 Beomonte Zobel B.: P-057, P-058,
 SS 9.07, SS 11.01, SS 13.01
 Bérczi V.: P-061, P-119, P-127
 Berggruen S.: P-165, SS 2.05
 Bergin D.: SS 1.03
 Berman P.: SS 15.08
 Bernardin G.: SS 15.02
 Berthier F.: SS 15.02
 Bertini L.: P-059, SS 11.03
 Bertucci C.: P-288
 Besa Correa C.: P-001
 Bethke A.: SS 14.01
 Bhayana D.: SS 2.01
 Bilbao J.: P-235
 Bilici A.: P-198
 Bipat S.: SS 1.10
 Birchall J.: P-092
 Biscaldi E.: P-126, SS 13.02
 Bispo M.: P-259
 Bisschops R.: P-192
 Biyani D.: SS 13.03
 Blackshaw W.: P-019
 Blake M.: P-286
 Blanc P.: SS 9.05
 Blomqvist L.: P-033
 Boermester M.: P-238, P-239, P-240,
 P-241, SS 5.02, SS 5.04, SS 5.06
 Boggi U.: SS 4.09
 Bomanji J.: P-046, SS 6.09
 Bonnetain F.: P-298
 Bonomo L.: P-121, P-129, SS 12.03
 Bonvin F.: SS 10.06
 Boon K.: SS 6.10
 Boraschi P.: P-055, P-288, SS 14.06,
 SY 5.03
 Borhani A.: P-007
 Borrego P.: P-024
 Borrelli O.: SS 11.07
 Bossuyt P.: P-238, P-239, P-240, P-241,
 SS 5.02, SS 5.04, SS 5.06
 Bouchot O.: SS 15.06
 Bouga A.: P-289, P-299
 Boulay-Coletta I.: P-027, P-277
 Boulin M.: P-298
 Bouma W.: P-240, SS 5.06
 Bourreille A.: P-130
 Bova V.: P-160
 Boyes S.: SS 12.06
 Bozzi E.: SS 10.08, SS 12.10
 Bracken J.: P-045
 Brambs H.: SS 8.04
 Brancatelli G.: P-146, SS 5.08, SS 12.08
 Braude P.: SS 6.05
 Breitenstein S.: P-167, SS 14.05
 Brenot R.: SS 15.06
 Breuer J.: SS 12.05

Brito J.: P-118, P-148, P-233
 Broncano J.: P-235
 Brown C.: P-051
 Brown G.: SS 3.01
 Browne M.: P-217
 Bruegel M.: SS 2.10
 Bruel J.: SS 9.05
 Brunelli E.: P-207
 Bruno O.: P-146, SS 12.08
 Buccianti P.: P-108
 Buckley D.: P-122, P-135
 Buecker A.: SS 12.07
 Bulakbasi N.: P-182
 Buls N.: SS 10.02
 Bulut E.: SS 14.10
 Burling D.: SS 1.02, SS 6.03, SS 6.07,
 SS 11.02, SS 13.09, SY 7.01
 Burns P.: SS 2.01
 Busch O.: P-241
 Bydder M.: SS 9.01
 Byun J.: P-096, P-228

C

Cabassa P.: P-188, P-207, SS 2.02,
 SS 7.01, SS 9.09
 Cabello-García D.: P-206
 Caddeo G.: P-162
 Calliada F.: P-209
 Camenzuli A.: P-242
 Campani D.: SS 4.09, SS 10.06
 Campbell S.: P-104
 Campisi A.: P-291
 Campos C.: P-115
 Canelas A.: P-078, P-233, P-264
 Cannizzaro F.: P-160
 Cano D.: P-038, P-235
 Cantisani V.: P-209, P-212
 Canu A.: P-223
 Cappelli A.: SS 10.07
 Cappelli C.: SS 3.06, SS 4.09
 Caprasecca S.: SS 3.09
 Caproni G.: SS 4.09
 Caramella D.: SS 4.09
 Carizzoni S.: SS 7.01
 Carmignani G.: SS 6.04
 Carneiro A.: P-163
 Carnicer J.: P-191
 Carroll N.: P-011
 Carrozzo F.: SS 3.03, SS 8.03
 Caruso G.: P-291
 Carvalho V.: P-118
 Casciani E.: P-059, SS 3.09, SS 5.05,
 SS 11.03
 Caseiro-Alves F.: P-078, P-118, P-148,
 P-153, P-224, P-233, P-264
 Caserta N.: P-023, P-069
 Castagna M.: P-108
 Castaño J.: P-259
 Castorino A.: SS 11.08
 Castro L.: P-248
 Castro M.: P-280

Catalano C.: P-212, SS 7.06, SS 7.08,
 SS 12.03
 Cattani G.: P-046, SS 6.09
 Cavalheiro F.: P-153, P-224
 Cercueil J.: P-169, P-298, SS 15.06
 Cereser L.: P-009, SS 9.04
 Cerri F.: P-106, P-107, SS 6.04
 Chan V.: SS 2.07
 Chandarana H.: P-072
 Chari S.: P-273
 Chatoor D.: P-067
 Chatzimichail K.: SS 2.03
 Chauffert B.: P-298
 Chawla S.: P-242
 Chayvialle J.: P-159
 Chen K.: SS 12.03
 Chenevert T.: SS 14.04
 Cheng D.: P-068
 Chetri K.: P-123
 Chevallier P.: SS 15.02
 Chiorean M.: P-131
 Cho H.: P-075
 Cho J.: P-025, P-073, P-113, P-179
 Cho K.: SS 14.09
 Cho O.: P-251
 Choe H.: P-265
 Choi D.: P-111
 Choi H.: P-025
 Choi J.: P-093, P-094, P-144, P-168,
 SS 2.08, SS 7.10, SS 14.07
 Chun H.: P-111, SS 8.09
 Chung J.: P-087, SS 2.08
 Chung K.: P-103
 Chung S.: P-187
 Cianci R.: P-101
 Cianni R.: SS 10.09
 Ciccantelli B.: SS 3.03
 Ciccio C.: SS 13.05
 Ciftci T.: SS 14.10, SS 15.10
 Cigdem K.: P-032
 Cimilli T.: P-147, P-181, P-274, P-275
 Cimsit C.: P-138
 Cinque T.: P-082
 Cioffi U.: P-097
 Cioni R.: SS 10.06
 Citone M.: SS 15.07
 Ciuffreda M.: P-021, P-219, P-281
 Clavien P.: SS 14.05
 Cohen R.: P-272
 Colin C.: P-298
 Collins C.: SS 2.07
 Comai A.: P-089
 Combescure C.: SS 9.05
 Como G.: P-009
 Condat B.: SS 12.08
 Coniglio M.: P-223
 Contreras J.: P-225
 Cortesi E.: P-212
 Coskun M.: P-006
 Coskun T.: SS 12.04
 Cossu M.: P-288
 Cossu V.: P-223
 Costa A.: P-013, P-055, P-233

Costa J.: P-148, P-233
 Costa N.: P-137, P-236
 Cousens C.: P-142
 Cova M.: SS 7.02
 Crespo I.: P-038
 Crippa S.: SS 4.07
 Crocetti L.: SS 10.08, SS 12.10
 Cucchiara S.: SS 11.07
 Cucci E.: P-021, P-219, P-245, P-281
 Culiáñez-Casas M.: P-206
 Cunha M.: P-023, P-069
 Cunha R.: P-280
 Curran C.: SS 3.08
 Curvo-Semedo L.: P-148, P-153, P-224,
 P-233
 Cusati B.: P-010, P-012
 Cybulska A.: P-090

D

D'Ambrosio U.: P-209, P-212
 D'Amico D.: SS 3.09, SS 11.03
 D'Andrea G.: SS 7.04
 D'Assignies G.: SS 7.03
 D'Onofrio M.: P-209, P-089, SS 4.01,
 SY 2.03
 Damilakis J.: PG 1.02
 Danieli R.: SS 13.05
 Danse E.: SS 15.09
 Das J.: SS 2.07
 Das P.: SS 1.02
 Daskalaki E.: P-300
 David M.: SS 15.06
 David V.: SS 15.07
 Davies S.: P-171
 De A.: P-104
 De Bruine A.: P-105, P-112, P-117,
 SS 8.08, SS 8.10
 De Cecco C.: P-042, P-152, SS 12.02,
 SS 15.07
 De Cicco M.: SS 5.05
 De Filippis G.: SS 7.08
 De Juan C.: P-116
 De Maria M.: P-160, SS 12.08
 De Mey J.: SS 10.02
 De Oliveira M.: SS 14.05
 De Simone M.: P-097
 De Simone P.: SS 10.06
 De Vargas Macchiucca M.: SS 5.05,
 SS 13.07
 De Vita E.: SS 11.05, SS 11.06
 De Vries A.: SS 1.05, SS 1.10
 De la Espriella T.: P-003
 Deb R.: P-243
 Del Val Montañana A.: P-180
 Del Vescovo R.: P-057, P-058, SS 9.07,
 SS 11.01, SS 13.01
 Debets J.: SS 8.10
 Dekker E.: SS 1.05, SS 1.10
 Dekker H.: P-035, SS 1.05, SS 1.10
 Delaney H.: P-218
 Delgado S.: P-116

Della Longa G.: P-057, P-058, SS 9.07, SS 11.01, SS 13.01
 Della Monica P.: SS 1.06
 Della Pina M.: SS 10.08, SS 12.10
 Demir M.: P-267
 Demirler Simsir B.: P-077, P-279
 Denys A.: P-220, P-302
 Deshpande A.: P-104
 Deshpande V.: P-286, SS 4.07
 Desmond A.: SS 3.08
 Di Costanzo G.: P-010, P-012
 Di Martino M.: SS 7.06, SS 7.08
 Dias S.: P-013, P-079
 Diaz L.: P-235
 Dickson J.: P-046, SS 6.09
 Dicle O.: P-014, P-125
 Dieguez Costa E.: P-024
 Dimitriadis A.: P-077, P-279
 Dixon A.: P-254
 Dobrowolska-Zachwieja A.: P-050, P-054
 Dogan S.: P-181
 Dohmen J.: SS 8.08, SS 13.06
 Dolmans D.: P-239
 Dominguez-Oronoz R.: P-003, P-005
 Donati F.: P-055, P-288, SS 14.06
 Donkervoort S.: P-240
 Doros A.: P-205
 Dragosavac S.: P-023, P-069
 Drews M.: P-050, P-054
 Duarte M.: P-259
 Düşünceli E.: P-200
 Dunjic Kratovac M.: SS 2.09
 Dupas B.: P-130
 Dvoyris M.: P-132

E

Economou G.: SS 2.03
 Eiber M.: SS 2.10
 El Gabaly H.: SS 9.10
 Ell P.: P-046, SS 6.09
 Elmas N.: PG 4.01
 Emlik D.: P-141, P-256, P-262, P-295
 Emmanuel A.: P-067, P-272
 Engelen S.: P-105, P-112, P-117, SS 8.08, SS 8.10, SS 13.06
 Engelken F.: P-100, SS 4.03
 Engellandt K.: SS 14.01
 Engin G.: P-109
 Erden A.: P-161, P-200
 Erden I.: P-161
 Erdur B.: SS 5.03
 Ergun O.: SS 15.10
 Erley C.: P-202
 Ernst A.: SS 8.04
 Erol B.: P-158
 Ertekin E.: P-304
 Erturk S.: SS 11.04
 Esposito G.: SS 9.04
 Essmat G.: SS 9.10
 Etkind S.: SS 5.09
 Evans S.: P-227

F

Faccioli N.: P-089, SS 4.01
 Faggioni L.: SS 14.06
 Faivre S.: SS 7.03
 Falaschi F.: P-055, P-288, SS 14.06
 Fanelli F.: SS 14.08
 Farquhar S.: SS 1.04
 Fasciani A.: SS 13.02
 Fasih N.: P-080, P-184
 Favero R.: P-223
 Fazio N.: SS 7.04
 Febrer Febrer M.: P-074
 Fedeli G.: P-121
 Fernandes-del Castillo C.: P-286, SS 4.07
 Ferrari R.: P-036, P-042, P-043, P-049, P-152, P-190, P-269, SS 1.08, SS 6.08, SS 12.02, SS 13.04
 Ferrero S.: SS 13.02
 Ferris J.: P-007
 Filippone A.: P-101
 Filippini F.: SS 10.06
 Filippousis P.: P-299
 Fina P.: SS 15.07
 Fiocchi F.: SS 8.07
 Fischman A.: P-286
 Fisher R.: P-297
 Fitzgerald E.: P-081
 Fletcher J.: P-273
 Fockens P.: SS 1.05, SS 1.10
 Fogari E.: P-188, SS 2.02
 Forasassi F.: SS 3.06
 Foufa K.: P-176
 Fox B.: P-142, P-222, P-290
 Frampas E.: P-130
 Francica G.: SS 12.09
 Franco A.: P-225
 Frangos A.: SS 1.03
 Fraser-Hill M.: P-080
 Fraser C.: SS 11.02
 Frau S.: P-223
 Frauenfelder T.: P-166, P-167, SS 12.01, SY 5.02
 Freeman A.: P-076
 Freeman S.: P-285
 Freire P.: P-118
 Fries P.: SS 12.07
 Fritz S.: P-286, SS 4.07
 Froehlich J.: SS 11.04
 Frota Barroso D.: P-180
 Fruzzetti E.: P-108
 Furlan A.: P-007, P-009, SS 9.04
 Furukawa H.: P-018

G

Gaa J.: SS 2.10
 Gabata T.: P-185
 Gaffke G.: SS 14.01
 Gagliardi N.: P-221, SS 5.07
 Galati F.: SS 7.06, SS 7.08
 Galia M.: P-156, P-208, P-210, SS 5.08
 Galloway S.: P-066

Gallix B.: SS 9.05
 Galluzzo A.: P-146, SS 12.08
 Gamblin T.: P-007
 Gan S.: P-134, SS 14.03
 Ganter C.: SS 2.10
 Garbarino V.: SS 3.03, SS 8.03, SS 11.07
 Garcia Bosch O.: P-047
 Garlaschi A.: P-126
 Garrote Lara D.: P-206
 Gatti E.: P-188, P-207, SS 7.01, SS 9.09
 Gavalakis N.: P-176
 Gavazzi E.: SS 2.02
 Gaya A.: SS 2.04
 Gayer G.: P-215
 Geiger D.: SS 7.06, SS 7.08
 Geisthoff U.: SS 12.07
 Geller D.: P-007
 Geloven A.: P-239
 Gelsi E.: SS 15.02
 Genchellac H.: P-267
 Geoghegan J.: SS 2.07
 Geoghegan T.: P-258
 Gerlei Z.: P-205
 Gerukis T.: P-247
 Ghiringhelli F.: P-298
 Gholamrezanezhad A.: SS 15.04
 Ghosh S.: P-017, SS 13.09
 Giampalma E.: SS 10.07
 Gibbons N.: SS 1.04
 Gigoni R.: P-055, P-288, SS 14.06
 Gil P.: P-114, P-230
 Gillams A.: SS 10.04, SS 10.10
 Gillen C.: SS 6.07
 Gimson A.: P-171
 Giordano G.: P-039, P-245
 Giraud M.: P-146
 Girometti R.: P-009, SS 9.04
 Gironès Vilà J.: P-074
 Gispert-Herrero S.: P-003, P-005
 Giusti P.: P-064, P-106, P-107, P-108, P-136
 Giusti S.: P-064, P-106, P-107, P-108, P-136
 Glynne-Jones R.: SS 13.08
 Go P.: P-240
 Godfrey E.: P-011, P-171, SS 5.09
 Goehde S.: P-056
 Goetzinger P.: SS 4.04
 Göke B.: SS 11.09
 Goffette P.: SS 15.09
 Goh V.: PG 1.04, SS 2.04, SS 3.07, SS 13.08
 Gokan T.: P-154
 Gokharman D.: P-030
 Golfieri R.: SS 10.07
 Golubovic M.: P-099
 Gomes M.: P-199
 Gomez A.: P-076
 Gómez-Río M.: P-206
 Gómez F.: P-016
 Gonçalves B.: P-148, P-153, P-233
 Goncalves L.: P-013, P-079
 González-Flores E.: P-206

Gonzalez-Junyent C.: P-191
 Gonzalez B.: P-024
 Gooszen H.: SS 5.04
 Gorzeman M.: P-239
 Goswami H.: P-123
 Gottlieb P.: P-132
 Gourtsoyianni S.: SS 5.01, SS 8.05, SS 9.02
 Gourtsoyiannis N.: SS 8.05, SS 9.02, SS 14.08
 Graça B.: P-078, P-118, P-153, P-224, P-233, P-264
 Grant L.: P-254
 Graser A.: P-072
 Grassi R.: SS 8.02
 Grasso R.: SS 11.01
 Grazioli L.: SS 12.03, SY 8.02
 Greco L.: SS 15.07
 Greenhalgh R.: P-046, SS 6.09, SS 8.01, SS 11.05, SS 11.06
 Grenacher L.: SS 4.02, SS 4.05
 Grieve F.: P-004, P-193
 Griffin N.: P-171
 Groves A.: P-046, SS 6.09
 Grunshaw N.: SS 14.02
 Gualdi G.: P-059, SS 3.09, SS 5.05, SS 11.03
 Guasch I.: P-248, P-249
 Guerrisi A.: P-212, SS 7.06, SS 7.08
 Guibal A.: P-159
 Guidi L.: P-121
 Guindi M.: SS 7.05, SS 7.07, SS 7.09
 Guiu B.: P-169, P-298, SS 15.06
 Guiu S.: P-169, P-298
 Gumus S.: P-141, P-256, P-262, P-295
 Guner N.: P-274, P-275
 Guney I.: P-256
 Guntern D.: P-220
 Gupta A.: SS 6.03, SS 6.07, SS 11.02
 Guthrie J.: P-229, SS 12.06
 Gutierrez B.: P-225
 Güven K.: P-294
 Guvenc I.: P-182
 Guyennon A.: P-159
 Guzmán-Álvarez L.: P-206

H

Ha H.: P-044, P-253
 Habib F.: SS 8.03
 Hadnadjev D.: P-237
 Haider M.: P-051, P-261, SS 7.05, SS 7.07, SS 7.09
 Haji A.: P-028
 Halligan S.: P-046, P-067, P-272, PG 3.04, SS 1.07, SS 1.09, SS 3.07, SS 6.01, SS 6.06, SS 6.09, SS 8.01, SS 11.05, SS 11.06, SY 3.01
 Hamilton G.: SS 9.01
 Hamilton P.: P-068
 Hammerstingl R.: SY 4.02
 Hampson F.: P-076
 Han H.: P-113, P-265

Hanaoka N.: P-023, P-069
 Haritanti A.: P-077
 Harji D.: SS 14.03
 Haroon A.: P-086
 Harsoula A.: P-077
 Hartmann E.: P-205
 Hashimoto M.: P-155
 Hassan C.: SS 1.08
 Hassib A.: SS 9.10
 Hattori Y.: P-282
 Hatzidakis A.: SS 14.08
 Hatzoglou V.: P-255
 Hawkes D.: SS 6.01, SS 8.01
 Hayashi T.: P-154
 Haycock A.: SS 6.03
 Hayirlioglu A.: P-138
 Hazarika S.: P-123
 Heaton N.: P-203
 Hébuterne X.: SS 15.02
 Heesewijk J.: SS 5.06
 Heianna J.: P-155
 Heiken J.: PG 2.04
 Henneman O.: SS 5.02
 Hermans J.: SS 15.03
 Hernández D.: P-191, P-248, P-249
 Hesselink E.: P-239, SS 5.04
 Heye T.: SS 3.04, SS 4.06
 Higginson A.: SS 1.04
 Hillon P.: P-169, P-298
 Hocaoglu E.: P-181, P-274
 Hodnett P.: P-048, P-081
 Holm T.: P-033
 Holzapfel K.: SS 2.10
 Honeyfield L.: SS 6.07
 Hong H.: SS 2.08
 Hong S.: P-140, P-204
 Hoogduin J.: P-174
 Hoogeveen Y.: P-035
 Horowitz M.: P-255
 Hosch W.: SS 3.04, SS 4.06
 Hosseinzadeh K.: P-007
 Howard W.: P-095
 Hu Y.: SS 8.01
 Huang D.: P-170
 Huete Garin A.: P-001
 Humphries D.: P-011
 Huppert P.: SS 10.01
 Hussain H.: SS 14.04
 Huwart L.: P-277
 Hwang S.: P-228, P-232

I

lafrate F.: P-036, P-043, SS 1.08, SS 6.08
 Ichikawa T.: P-031
 Idilman R.: P-161
 Igci E.: P-014, P-125
 Inuma G.: SS 6.06
 Ilharco J.: P-118
 Ilica A.: P-198
 Illangovan R.: SS 11.02
 Ilsen B.: SS 10.02
 Imai Y.: P-031

Imaoka I.: P-029
 Inci E.: P-181
 Indinnimeo M.: SS 8.03
 Iotti V.: SS 8.07
 Iozzino M.: SS 10.09
 Islim F.: P-296, SS 14.10
 Iwashiro R.: P-276
 Iwata Y.: P-031
 Izycka-Świeszewska E.: P-143, P-172

J

Jackson S.: P-222, P-290
 Jagirdar N.: P-086
 Jain R.: P-178, P-244, P-270, P-301
 Jain S.: P-095
 Jaju D.: P-178
 Jakubowski W.: P-090
 James A.: P-063
 Jang H.: SS 2.01, SS 7.05, SS 7.07, SS 7.09
 Jauch K.: SS 3.10, SS 8.06
 Jedrzejczyk M.: P-090
 Jee K.: P-216, SS 3.02
 Jeong H.: P-113
 Jeong I.: SS 3.02
 Jhaveri K.: P-261
 Jiang Z.: P-246
 Jiménez J.: P-196
 Jimenez-Juan L.: P-068, P-268
 Jobling J.: SS 15.05
 Joerg D.: P-056
 Joffe S.: P-255
 Johnson R.: P-022
 Johnson T.: P-072, SS 14.04
 Jonas E.: SY 6.01
 Jones R.: P-086
 Joubert I.: P-171
 Jouve J.: P-169
 Jullès M.: P-027
 Juttmann J.: SS 5.04

K

Kacar M.: P-030
 Kadiyoran C.: P-262
 Kakde D.: SS 3.05
 Kalogera-Fountzila A.: P-279
 Kalpakidis V.: P-247
 Kamel R.: SS 9.10
 Kampanarou S.: SS 2.03
 Kandel S.: P-100, SS 4.03
 Kane P.: P-028, P-170, P-194, P-203
 Kappers D.: P-174
 Kara E.: SS 12.04
 Karabacakoglu A.: P-304
 Karabulut N.: P-231, SS 5.03
 Karademir I.: P-182
 Karadimou V.: P-279
 Karahan O.: SS 5.10
 Karahasanoglu A.: P-275
 Karakose S.: P-304

- Karaman H.: SS 15.08
 Karani J.: P-028, P-170, P-194, P-203
 Karanikas C.: SS 2.03
 Karaosmanoglu D.: P-098, P-149, P-158
 Karapostolakis G.: P-252, P-300
 Karatzou C.: P-247
 Karcaaltincaba M.: P-098, P-149, P-158
 Karlo C.: P-167, SS 12.01
 Karnati G.: P-226
 Karolemeas K.: SS 9.02
 Kasir D.: P-019, P-022, P-066, P-071, P-214
 Katsarou A.: P-250, P-252
 Katulska K.: P-050, P-054
 Kauczor H.: SS 3.04, SS 4.02, SS 4.05, SS 4.06
 Kauffmann G.: SS 3.04, SS 4.02, SS 4.05, SS 4.06
 Kawada S.: P-031
 Kawashima A.: P-273
 Kay C.: P-052, P-292
 Kaya D.: P-303
 Kaya Y.: SS 12.04
 Kayahan Ulu E.: P-006
 Kayhan A.: P-147, P-275
 Kaytan Saglam E.: P-109
 Kelekis D.: SS 2.03
 Kelliher E.: P-213, P-217
 Kelly D.: SS 1.01
 Keogan M.: P-218
 Kessels A.: P-105
 Khalili K.: SS 7.05, SS 7.07, SS 7.09
 Khan A.: SS 14.04
 Khan L.: SS 7.09
 Khosa H.: P-213, P-217
 Kilickesmez O.: P-147, P-181, P-274, P-275
 Kilicoglu G.: P-056, P-175
 Kilinc I.: P-032
 Kim A.: P-044, P-204, P-253
 Kim B.: SS 7.10, SS 8.09
 Kim H.: P-008, P-070, P-139, P-253, P-260, P-263, SS 4.08, SS 7.10, SS 14.07
 Kim J.: P-044, P-087, P-113, P-133, P-140, P-144, P-278, P-278, SS 2.08, SS 4.08, SS 4.08, SS 14.07
 Kim K.: P-093, P-094, P-144, P-168, P-253, P-263, P-278, SS 2.08, SS 4.08, SS 14.07
 Kim M.: P-111, PG 2.03, SS 2.08, SS 8.09, SS 14.07
 Kim P.: P-253
 Kim S.: P-094, P-168, SS 8.09, SS 8.09
 Kim T.: P-133, P-144, P-278, SS 2.01, SS 4.08, SS 7.05, SS 7.07, SS 7.09
 Kim Y.: P-103, P-216, P-251, P-278, SS 3.02, SS 4.08
 Kinebuchi Y.: P-154
 Kirby J.: SS 14.09
 Kirchhoff C.: SS 3.10, SS 8.06, SS 11.09
 Kirchhoff S.: SS 3.10, SS 8.06, SS 11.09
 Kiresi D.: P-262, P-295
 Kirke R.: P-257
 Kiroglu Y.: P-231, SS 5.03
 Kirwadi A.: P-227
 Kitahara T.: P-154
 Kiyonaga M.: P-088, P-284
 Klauss M.: SS 4.02, SS 4.05
 Kloeters C.: P-100, SS 4.03
 Ko Y.: P-008, P-070, P-139
 Kobashi Y.: P-020
 Kobayashi S.: P-185, P-186
 Kóbori L.: P-205
 Koc O.: P-256
 Koc Z.: P-195, P-197, P-201
 Koçak B.: SS 5.03
 Kocaoglu M.: P-182, P-266
 Koda W.: P-185
 Kodama R.: P-020
 Koelblinger C.: SS 4.04
 Koh B.: P-251
 Kohl C.: SS 9.01
 Koizumi J.: P-031
 Koloszar J.: SS 6.02
 Komorowski D.: P-297
 Konsten J.: SS 8.10
 Koo B.: P-285
 Kornmann M.: SS 8.04
 Korutz A.: P-165, SS 2.05
 Kosar P.: P-030
 Kosar U.: P-030
 Kosen K.: P-088, P-284
 Kosmas V.: P-289
 Kotake F.: P-276
 Kotterer O.: SS 10.01
 Kotzampassakis N.: P-220
 Kozaka K.: P-186
 Krak N.: SS 15.03
 Krausé D.: P-169, P-298, SS 15.06
 Kreis M.: SS 3.10, SS 8.06
 Kretz B.: SS 15.06
 Krishan S.: P-229
 Krokidis M.: SS 14.08
 Krug L.: SS 4.03
 Krysztopik R.: P-065
 Ku Y.: P-096, P-228, P-232
 Kulinna-Cosentini C.: SS 4.04
 Kumano S.: P-029
 Kumar H.: SS 14.03
 Kurochka S.: P-013, P-079
 Kuru I.: P-138
 Kuwabara M.: P-029
 Kwon H.: P-073
-
- L**
-
- La Grutta L.: SS 5.08
 Labib S.: SS 9.10
 Lad S.: P-051
 Lagalla R.: P-156, P-208, P-210, P-291, SS 5.08
 Laghi A.: P-036, P-042, P-043, P-049, P-152, P-190, P-269, PG 3.03, SS 1.08, SS 6.08, SS 12.02, SS 13.04
 Lahaye M.: P-105, P-112, P-117, SS 8.08, SS 8.10, SS 13.06
 Lam C.: P-002, P-230
 Lambert A.: P-169
 Lambregts D.: P-117
 Laméris W.: P-238, P-239, P-240, P-241, SS 5.02, SS 5.04, SS 5.06
 Lanciotti S.: SS 5.05
 Lang R.: SS 8.06
 Laniado M.: SS 14.01
 Lanka L.: P-261
 Larena J.: P-053
 Laspas F.: P-289
 Latham T.: P-095
 Latief K.: P-062
 Latif A.: SS 2.07
 Lauenstein T.: P-056
 Laurent V.: SY 2.02
 Lazaro S.: P-053
 Lazic L.: SS 2.09
 Leal C.: P-137, P-236
 Leaute F.: P-130
 Lee C.: P-093, P-094, P-168
 Lee D.: P-008, P-070, P-139
 Lee H.: P-145
 Lee J.: P-093, P-094, P-128, P-133, P-144, P-168, P-278, SS 4.08, SS 7.10
 Lee K.: P-216
 Lee M.: P-253
 Lee S.: P-044, P-096, P-103, P-111, P-232, P-253, SS 8.09, SS 13.03
 Lee W.: SS 7.10
 Lee Y.: P-075, P-124, P-228, SS 3.02
 Lees W.: SS 10.04, SS 10.10
 Lefere P.: SY 3.03
 Lefkopoulos A.: P-077
 Leiner T.: P-117
 Leite C.: P-079
 Lembcke A.: SS 4.03
 Lemos A.: P-097
 Lencioni R.: SS 10.08, SS 12.10
 Lerut J.: SS 15.09
 Leung D.: P-297
 Lev-Toaff A.: SS 1.03
 Lewis D.: P-170, P-194, P-203
 Liaw J.: SS 3.07, SS 13.08
 Liedenbaum M.: SS 1.05, SS 1.10, SS 6.10
 Lienemann A.: SS 3.10, SS 8.06, SS 11.09
 Liew C.: P-004, P-177, P-183, P-193
 Ligabue G.: SS 8.07
 Lilic G.: SS 2.09
 Lim H.: P-111, P-145
 Lim J.: P-008, P-070, P-139, SS 2.08, SS 14.07
 Lim K.: SS 14.02
 Lin C.: SS 2.06, SS 4.10, SS 9.03
 Lindholm J.: P-033
 Linke K.: P-050, P-054
 Liong S.: P-019, P-022, P-071, P-084
 Llamas Elvira J.: P-206
 Lloret M.: P-016

Lo Re G.: P-210, SS 5.08
 Loffroy R.: P-169, P-298, SS 15.06
 Lomas D.: P-171
 Lombard-Boahs C.: P-159
 Lombardi V.: P-209
 Lombardo P.: P-082, SS 5.07
 Loubakou A.: P-250, P-300
 Lourenço J.: P-002, P-114, P-230
 Love M.: P-060
 Lowe A.: P-052, P-292
 Lucchesi P.: P-042, P-049, P-190, P-269,
 SS 13.04
 Luitse J.: P-239
 Lukács L.: SS 6.02
 Luppi G.: SS 8.07

M

Macari M.: P-072
 Macchiarella V.: P-160
 Maccioni F.: SS 3.03, SS 8.03, SS 11.07,
 SS 11.08, SS 13.07, SY 4.01
 Maceroni M.: P-049, P-269
 Madroñal N.: P-016
 Maglente D.: P-131, PG 3.02
 Maher M.: P-015, P-048, P-081, SS 1.01,
 SS 3.08
 Maia R.: P-199
 Mainardi P.: P-089
 Mainta E.: SS 2.03
 Maisto F.: SS 8.02
 Maksimovic R.: SS 2.09
 Malago R.: SS 4.01
 Malizia G.: P-208, P-210
 Mallarini G.: P-083, P-091, P-151, P-157,
 P-162
 Mallebrera M.: P-225
 Malone D.: SS 2.07
 Mancino S.: SS 13.05
 Mancuso P.: SS 7.04
 Manfredi R.: SY 5.01
 Maniaci M.: P-156
 Maniatis V.: P-176
 Manika C.: P-077
 Mańkowska-Wierzbicka D.: P-050, P-054
 Mannetta G.: P-281
 Marcelli G.: SS 5.05
 Marigliano C.: P-212
 Marin D.: SS 7.06, SS 7.08
 Marincek B.: P-167, SS 12.01, SS 13.10,
 SS 14.05, SY 5.02
 Marini M.: P-036, SS 3.03, SS 8.03,
 SS 11.07, SS 11.08, SS 13.07
 Maris T.: SS 9.02
 Maroldi R.: P-188, P-207, SS 2.02,
 SS 7.01, SS 9.09
 Maroto Genover A.: P-074
 Marques A.: P-002, P-259
 Marques C.: P-148, P-153
 Marques R.: P-137, P-236
 Marshall M.: SS 1.02, SS 6.03, SS 6.07,
 SS 11.02, SS 13.09
 Marsman H.: P-173, SS 9.08

Marti-Bonmati L.: P-180
 Martin D.: SY 7.03
 Martinelli M.: SS 3.03, SS 11.08, SS 13.07
 Martinez-Alvarez Y.: P-003
 Mason K.: P-290
 Masselli G.: SS 3.09, SS 11.03
 Massmann A.: SS 12.07
 Masulovic D.: SS 2.09
 Matsui O.: P-186, P-282, PG 4.03
 Matsumoto S.: P-088, P-284
 Matsushita M.: P-276
 Mauro E.: SS 12.10
 Mavropoulou X.: P-279
 May J.: P-292
 Mayol J.: P-016
 Mazzeo S.: SS 3.06, SS 4.09
 Mc Carthy P.: P-213, P-217
 Mc Dermott S.: SS 2.07
 Mc Gregor C.: P-068
 Mc Hugh S.: P-254
 Mc Laughlin P.: SS 1.01
 Mc Leod R.: P-051
 Mc Sweeney S.: P-015, P-048, P-081,
 SS 1.01, SS 3.08
 Mc Williams S.: SS 1.01, SS 3.08
 Medina-Benítez A.: P-206
 Melão L.: P-280
 Melani E.: P-039
 Melloul E.: P-220
 Mendes V.: P-013, P-079
 Mennesson N.: P-159
 Merino-Casabiel X.: P-003, P-005
 Mészáros N.: SS 6.02
 Meurette G.: P-130
 Meyer H.: P-100, SS 4.03
 Mezzetta L.: P-169
 Midia M.: SS 14.09
 Midiri M.: P-156, P-160, P-208, P-210,
 SS 5.08
 Milenkovic R.: SS 2.09
 Miller B.: SS 14.03
 Miller S.: P-254
 Minami T.: P-185
 Minordi L.: P-121, P-129
 Miranda I.: P-005
 Mirk P.: P-129
 Mirpour S.: SS 15.04
 Missere M.: P-021, P-219, P-245, P-281
 Molin V.: SS 15.06
 Mombelloni S.: SS 7.01, SS 9.09
 Monesi R.: P-207, SS 2.02
 Montanaro F.: P-026
 Montisci R.: P-151
 Montserrat E.: P-191
 Moore A.: SS 6.07
 Morak M.: SS 15.03
 Morcos S.: P-202
 Mori H.: P-088, P-284
 Morigoni V.: P-064, P-106, P-107, P-136
 Moriguchi M.: P-018
 Morita D.: P-023, P-069
 Morone M.: SS 9.09
 Morrin M.: P-041, P-045, SY 1.04

Morrison P.: SS 10.03
 Mourad M.: SS 15.09
 Mourelo S.: P-196
 Muckian J.: SS 6.03, SS 6.07
 Mulla M.: P-092, P-189, P-243
 Mullan D.: P-242
 Mulrennan S.: P-084
 Murakami T.: P-029
 Murphy C.: P-258
 Murphy T.: P-297
 Mylona S.: P-250, P-252, P-300

N

Nair J.: SS 3.05
 Nakajima Y.: P-020
 Nakanuma Y.: P-186
 Naldini G.: P-106, P-107
 Nam K.: P-025, P-073, P-179
 Nandalur K.: SS 14.04
 Napolitano A.: P-254
 Narayanaswamy S.: P-122
 Narbone P.: P-188, SS 7.01
 Narin Anil B.: P-056, P-175
 Nazaroglu H.: P-032
 Nederveen A.: P-173, P-174, SS 9.08
 Németh A.: P-205
 Neri E.: SS 6.04, SY 7.02
 Nese N.: SS 12.04
 Ngatchu T.: SS 14.03
 Nicolaus M.: SS 11.09
 Nikapota A.: SS 13.08
 Nilsson S.: P-099
 Njagulj V.: P-237
 Nocera V.: P-026, SS 9.06, SS 10.05,
 SS 12.09
 Notarianni E.: SS 10.09
 Novaria L.: SS 3.06
 Novellas S.: SS 15.02
 Novo S.: P-024
 Ntai S.: P-250, P-252, P-300

O

O'Brien J.: P-258
 O'Keefe S.: P-218
 O'Regan K.: P-015, P-048, SS 3.08
 Obuz F.: P-014, P-125
 Occhicone F.: P-058, SS 13.01
 Occhionero M.: P-021, P-281
 Odev K.: P-141, P-256, P-262, P-295
 Oh J.: P-025, P-073, P-179
 Oh S.: P-096
 Oh T.: P-177, P-193
 Ohgiya Y.: P-154
 Okada M.: P-029
 Okamoto H.: P-020
 Okon S.: P-255
 Olazábal A.: P-249
 Oliveira I.: P-002, P-230
 Onem G.: P-231
 Onur E.: P-125
 Op De Beeck B.: SS 10.02

Opdenakker L.: SS 8.08, SS 13.06
 Oppezzi M.: P-126
 Orabona P.: P-026
 Orgera G.: SS 14.08
 Orlando E.: P-207, SS 2.02
 Osorio Fernández M.: P-074
 Ozbalci E.: P-147
 Özden A.: P-161
 Ozdemir H.: P-267
 Ozkan F.: SS 14.10
 Ozmen C.: P-032
 Ozmen M.: P-098, P-149, P-158, P-296,
 SS 14.10, SS 15.10
 Ozturk A.: P-006
 Öztürk E.: P-275
 Ozuki T.: P-276

P

Padhani A.: SS 2.04
 Pagés Llinás M.: P-116
 Pakala V.: P-227
 Palabiyik F.: P-147
 Palladas P.: P-247
 Pallan A.: P-134, SS 14.03
 Palmieri F.: P-010, P-012
 Palmieri S.: SS 9.09
 Palumbo P.: SS 3.09
 Pamies J.: P-016
 Panes J.: P-047
 Pantazopoulou A.: P-247
 Paolantonio P.: P-042, P-043, P-049,
 P-152, P-190, P-269, SS 6.08,
 SS 12.02, SS 13.04
 Papadaki M.: P-271
 Papadopoulos A.: P-176
 Papagrigoriadis S.: P-028
 Papanikolaou N.: SS 8.05, SS 9.02
 Paprzycki W.: P-050, P-054
 Pardo S.: P-291
 Park B.: P-103
 Park C.: P-093, P-094, P-168
 Park J.: P-145
 Park M.: P-144, P-278, SS 2.08, SS 4.08,
 SS 14.07
 Park S.: P-044, P-145, P-228, P-253,
 P-265
 Park Y.: SS 7.10
 Parmeggiani D.: SS 10.05
 Passariello R.: P-209, P-212, SS 7.06,
 SS 7.08, SS 14.08
 Patak M.: SS 11.04
 Patel Z.: P-255
 Peddu P.: P-170, P-194
 Pekindil G.: SS 12.04
 Peng W.: P-246
 Peringa J.: P-239
 Pernas J.: P-191
 Perrone A.: P-036
 Petit E.: P-277
 Petralia G.: SS 7.04
 Petridis A.: P-247
 Petrowsky H.: SS 12.01

Petruzzi P.: SS 10.06, SS 10.08
 Phillips A.: P-065, P-120
 Picarelli A.: P-059, SS 3.09
 Piccione E.: P-057, P-058, SS 9.07,
 SS 13.01
 Pichi A.: SS 1.08
 Picht C.: P-220
 Pickhardt P.: SS 1.08, SY 3.02
 Pięnkowska J.: P-037, P-143, P-172,
 P-305
 Piermattei A.: SS 3.09
 Pierro A.: P-021, P-245
 Pietricola G.: P-223
 Pilavaki M.: P-247
 Pilleul F.: P-159
 Pimenta M.: P-163
 Pina Vaz C.: P-013, P-079
 Pineda-Sanchez V.: P-003, P-005
 Pino A.: SS 11.08
 Pires J.: P-199
 Piscopo A.: SS 10.05
 Pittalis A.: SS 3.09
 Pittiani F.: P-188
 Pizzolato R.: SS 7.02
 Plessier A.: SS 12.08
 Poletti E.: P-059, SS 3.09, SS 11.03
 Poloni G.: P-121, P-129
 Pomoni A.: SS 2.03
 Pontillo Contillo B.: SS 4.09
 Portmann B.: P-203
 Post P.: SS 8.08, SS 13.06
 Postgate A.: SS 11.02
 Potsi M.: P-077, P-279
 Power N.: P-017
 Pozuelo C.: P-248
 Pozzi Mucelli R.: P-089, SS 4.01
 Prasad U.: P-297
 Preto A.: P-163
 Priest A.: P-171
 Principe F.: SS 4.01
 Prot T.: P-220
 Psoma E.: P-279
 Ptohis N.: SS 2.03
 Puckett M.: P-122, P-135
 Punwani S.: SS 6.01, SS 11.05, SS 11.06
 Puri S.: P-092
 Putignano L.: P-156

Q

Quaglia A.: P-194
 Quaiá E.: SS 7.02
 Quattrocchi C.: SS 11.01
 Quigley E.: P-015
 Quintero J.: P-196, P-248, P-249

R

Radecka E.: P-099
 Radeff B.: SS 3.04, SS 4.06
 Radice D.: SS 7.04
 Ragozzino A.: P-010, P-012

Rajashanker B.: P-004, P-177, P-193
 Rajesh A.: P-104, P-257
 Ramírez Fuentes C.: P-180
 Ramírez O.: P-016
 Ramadan T.: P-217
 Rambla J.: P-016
 Ramos I.: P-163
 Raposo J.: P-137, P-236
 Raptopoulos V.: SS 5.01
 Rathi V.: SS 3.05
 Rau P.: P-220, P-302
 Raviv-Zilka L.: SS 11.10
 Rawlinson J.: SS 14.09
 Raymond E.: SS 7.03
 Razack A.: P-085, P-293
 Rebonato A.: SS 15.07
 Regge D.: SS 6.04, SY 1.01, SY 1.02,
 SY 1.05
 Reginelli A.: SS 8.02
 Reiner C.: P-167, SS 12.01, SS 13.10,
 SS 14.05
 Reis F.: P-199
 Reiser M.: SS 3.10, SS 8.06, SS 11.09,
 SS 12.05
 Remorgida V.: SS 13.02
 Rengo M.: P-043, P-152, P-190, SS 6.08,
 SS 12.02, SS 13.04
 Resmini E.: P-039
 Restaino G.: P-021, P-245, P-281
 Ribeiro M.: P-199
 Ricart E.: P-047
 Ricci P.: P-209, P-212
 Rice P.: P-060
 Richardson C.: SS 3.01
 Richardson M.: SS 14.03
 Richter G.: SS 4.02, SS 4.05, SS 4.06
 Riddell A.: SS 3.01
 Rimola J.: P-047
 Ripa C.: P-026, SS 9.06, SS 10.05
 Robinson C.: SS 1.09, SS 6.01
 Robinson P.: SS 12.06
 Rocha D.: P-163
 Rock B.: P-135
 Rodgers P.: P-104
 Rodríguez-Fernández A.: P-206
 Rodríguez S.: P-116
 Rodríguez-Justo M.: SS 11.05, SS 11.06
 Rodríguez Gomez S.: P-047
 Rogalla P.: P-100, PG 1.01, SS 4.03
 Rollandi G.: P-039, P-126, SS 13.02
 Rollvén E.: P-033
 Romano L.: P-082, P-202, P-221,
 SS 5.07, SS 12.03
 Romano S.: P-082, P-221, SS 5.07
 Romano V.: P-100
 Romero J.: SS 5.01
 Roqué C.: P-196, P-249
 Ros P.: P-191, PG 1.05, SY 1.03
 Roseman A.: P-011
 Rossi M.: SS 15.07
 Rotondo A.: SS 8.02
 Roussakis A.: P-176
 Roy-Choudhury S.: P-134, SS 14.03

Rubbia-Brandt L.: SS 15.01
 Rudralingam V.: P-022, P-066, P-071,
 P-214
 Ruers T.: P-035
 Rummeny E.: SS 2.10
 Runza G.: P-208
 Russo A.: SS 8.02
 Rustin G.: SS 2.04
 Ryan M.: P-015, P-048, P-081, SS 1.01
 Ryan S.: P-028, P-170
 Ryu Y.: P-185
 Rzepko R.: P-172

S

Saba L.: P-083, P-091, P-151, P-157,
 P-162
 Sahani D.: P-202, P-209, P-286, SS 4.07
 Sahni P.: P-301
 Sai M.: P-088, P-284
 Sainani N.: P-286, SS 4.07
 Saito K.: P-276
 Salem R.: P-165, SS 2.05
 Salemi S.: P-055, P-288, SS 14.06
 Sallustio G.: P-021, P-219, P-245, P-281
 Saltarelli A.: SS 10.09
 Salvaggio G.: P-291
 Salvaras N.: P-289
 Salvatori R.: SS 10.09
 Sambrook A.: P-052, P-292
 Sampere J.: P-196
 Samyn M.: P-203
 Sanada J.: P-185
 Sanal H.: P-266
 Sánchez Toro C.: P-206
 Sandrasegaran K.: P-131, SS 2.06,
 SS 4.10, SS 9.03
 Sanfilippo R.: P-151
 Sansoni I.: P-057, P-058, SS 9.07,
 SS 11.01, SS 13.01
 Santos P.: P-199
 Santos R.: P-002, P-114, P-230, P-259
 Sarikaya B.: P-234
 Sarrazin J.: P-068
 Sawada A.: P-018
 Sawhney S.: P-178, P-244, P-270, P-301
 Sayedee K.: SS 6.07
 Schettini D.: P-126
 Schiano A.: SS 9.06
 Schillaci O.: SS 13.05
 Schima W.: SS 4.04, SY 4.03
 Schirra J.: SS 11.09
 Schmidt S.: P-220
 Schmitz B.: SS 8.04
 Schneider G.: SS 12.07, SY 8.03
 Schueller G.: SS 4.04
 Seabra Z.: P-002, P-230, P-259
 Secil M.: P-014, P-125
 Seco M.: P-078, P-153, P-224, P-233
 Seferos M.: P-299
 Sellars M.: P-203
 Semedo L.: P-264
 Senicar S.: P-237

Senol S.: SS 5.10
 Senturk S.: P-032, P-198
 Seppala R.: P-080
 Serter S.: SS 12.04
 Set P.: P-076
 Shanahan F.: SS 3.08
 Sharifov R.: P-109
 Shaw A.: P-171, P-285, SS 5.09
 Sheikh Y.: P-081
 Sheridan M.: SS 12.06
 Sherman M.: SS 7.05, SS 7.07, SS 7.09
 Sherman S.: SS 4.10
 Shiehorteza M.: SS 9.01
 Shimono T.: P-029
 Shimoyama K.: P-020
 Shin K.: P-113
 Shinjo H.: P-154
 Shirley J.: P-222, P-290
 Shon Y.: P-124
 Sidhu P.: SY 8.01
 Silva M.: P-002
 Silva N.: P-280
 Silverman S.: P-150, SS 10.03
 Simonetti G.: SS 13.05
 Simons M.: P-241
 Simsek M.: P-056, P-175
 Singh R.: P-092, P-189, P-243
 Sirlin C.: SS 9.01
 Skehan S.: SS 2.07
 Slapa R.: P-090
 Slattery M.: P-041, P-045
 Smith J.: SS 12.06
 Solopova A.: SS 13.10
 Sommavilla C.: SS 12.07
 Song K.: P-113
 Song M.: P-103
 Song S.: P-111, P-251
 Sordelli I.: P-026, SS 9.06,
 SS 10.05, SS 12.09
 Soriano Viladomiu J.: P-074
 Sorrentino F.: P-291
 Sosna J.: SS 15.08
 Sotiropoulou E.: P-289, P-299
 Spahr L.: SS 15.01
 Sperlongano P.: SS 10.05
 Squifflet J.: SS 15.09
 Squillaci E.: SS 13.05
 Stagnitti A.: P-036, SS 1.08
 Stajgis M.: P-050, P-054
 Staltari I.: SS 11.08
 Stamoulis E.: P-176
 Stauffer N.: P-220, P-302
 Stavolo C.: P-221, SS 5.07
 Steinberg E.: SS 15.06
 Stephens K.: P-254
 Sternberg J.: P-097
 Stirling J.: SS 2.04
 Stojanovic S.: P-237
 Stoker J.: P-173, P-174, P-238, P-239,
 P-240, P-241, SS 1.05, SS 1.10,
 SS 5.02, SS 5.04, SS 5.06, SS 6.10,
 SS 9.08
 Storti S.: P-245

Storto M.: P-101
 Stoupis C.: SS 11.04
 Strasser S.: SS 15.01
 Strauss S.: P-215
 Stroszczyński C.: SS 14.01
 Studniarek M.: P-037, P-143, P-172,
 P-305
 Stunell H.: P-258
 Subramanian K.: P-063
 Sugumar A.: P-273
 Sukumar S.: P-019, P-022, P-066, P-071,
 P-084, P-183, P-214
 Sung D.: P-103
 Sung J.: P-113
 Sydnor M.: P-297
 Szopinski K.: P-090
 Surowska E.: P-037, P-143, P-172,
 P-305

T

Tagliafico A.: P-039
 Taibbi A.: P-156, P-160, P-208, P-210
 Takahashi N.: P-273
 Takahashi Y.: P-276
 Takeyama N.: P-154
 Tam M.: P-095
 Tanaka K.: SS 9.10
 Tandon L.: P-183
 Tang V.: P-283
 Tanteles S.: SS 2.03
 Tarantino L.: P-026, SS 9.06,
 SS 10.05, SS 12.09
 Tarján Z.: SS 6.02
 Tasar M.: P-266
 Tatti S.: P-150, SS 10.03
 Tayfun C.: P-182
 Taylor J.: SS 10.04
 Taylor N.: SS 2.04
 Taylor S.: P-046, P-067, P-272, SS 6.01,
 SS 6.06, SS 6.07, SS 6.09, SS 8.01,
 SS 11.05, SS 11.06
 Teixeira L.: P-078, P-224
 Temizoz O.: P-267, P-296, SS 15.10
 Tempia A.: P-220
 Ten Hove W.: SS 5.02, SS 5.06
 Ten Kate F.: P-173, SS 9.08
 Tengg-Koblik H.: SS 4.02
 Terraz S.: SS 15.01
 Terzibasoglu E.: P-294
 Thanos L.: P-289, P-299
 Thayur N.: P-065
 Thipphavong S.: P-080, P-184
 Thiruppathy K.: P-067, P-272
 Thomas B.: P-063
 Thomsen H.: P-202
 Thornton E.: P-041, P-045
 Thoufeeq M.: P-086
 Thrower A.: P-052, P-292
 Thurley P.: SS 15.05
 Tiryaki B.: P-266
 Tisnado J.: P-297
 Tokala A.: P-214

AUTHORS' INDEX

Tokmak N.: P-197
 Tolan D.: SS 8.01
 Torrão H.: P-013, P-079
 Torreggiani W.: P-258
 Torricelli P.: SS 8.07
 Tortora G.: P-221
 Tóth G.: P-061, P-110, P-119, P-127
 Tóth L.: P-061, P-110, P-119, P-127
 Treanor D.: SS 12.06
 Tsagouli P.: P-299
 Tsiftsis D.: SS 8.05
 Tuncali K.: P-150, SS 10.03
 Tuncbilek I.: P-030
 Turini F.: SS 6.04
 Türkçüer I.: SS 5.03
 Turupoli E.: P-061, P-110, P-119, P-127
 Tutcu S.: SS 12.04
 Tutuian R.: SS 13.10
 Tzovara J.: P-176

U

Ucar A.: P-014, P-294
 Ulusan S.: P-195, P-197, P-201
 Unlu E.: P-267
 Urich M.: SS 12.05
 Urigo C.: P-223, SS 10.09
 Urria I.: P-248
 Ustunsoz B.: P-303
 Üstüner E.: P-200
 Uysal F.: P-014
 Uysal Ramadan S.: P-030
 Uzoka K.: P-283

V

Valeriano S.: P-101
 Vallet C.: P-220
 Valls Masot L.: P-074
 Van de Velde C.: P-112, P-117, SS 8.08, SS 8.10, SS 13.06
 Van Eijck C.: SS 15.03
 Van Engelshoven J.: P-105, P-112, SS 8.08, SS 13.06
 Van Es W.: SS 5.02, SS 5.06
 Van Gulik T.: P-173, P-241, SS 9.08
 Van Keulen E.: P-241, SS 5.02, SS 5.06
 Van Leeuwen M.: P-192, SS 5.02, SS 5.06
 Van Meyenfeldt M.: P-112, SS 8.08, SS 8.10
 Van Ramshorst B.: SS 5.04, SS 5.06
 Van Randen A.: P-238, P-239, P-240, P-241, SS 5.02, SS 5.04, SS 5.06
 Van Rijn A.: SS 1.05, SS 1.10
 Van Vliet A.: P-174
 Van Werven J.: P-173, P-174, SS 9.08
 Vandenberk P.: P-174
 Vandenbroucke F.: SS 10.02
 Vandendries C.: P-027
 Vardaki H.: P-176
 Vasconcelos A.: P-137, P-236
 Vasserman M.: P-132

Vecchietti F.: P-042, P-043, P-049, P-152, P-190, P-269, SS 6.08, SS 12.02, SS 13.04
 Vecchioli A.: P-121, P-129
 Venâncio J.: P-115
 Venema H.: SS 6.10
 Verkooyen H.: SS 8.10
 Verma R.: P-104, P-257
 Viamonte B.: P-280
 Vígváry Z.: P-110
 Vignali C.: SS 10.06, SS 10.08
 Vilgrain V.: P-146, PG 2.01, SS 7.03, SS 12.08, SY 2.01, SY 2.04
 Viola F.: SS 11.07
 Virmani S.: SS 6.05
 Vivas I.: P-038, P-235
 Von Wagner C.: SS 1.09
 Vora P.: SS 14.09
 Vos B.: SS 12.05
 Voth M.: P-117
 Vuillierme M.: P-146

W

Wajs E.: P-174
 Waldherr C.: SS 11.04
 Wamsteker E.: SS 14.04
 Ward E.: P-258
 Ward J.: SS 12.06
 Wardle J.: SS 1.09
 Watarai J.: P-155
 Watson A.: SS 13.03
 Weadock W.: SS 14.04
 Weinmann H.: SS 12.05
 Weishaupt D.: P-167, SS 12.01, SS 13.10, SS 14.05
 Weldon J.: SS 6.07
 Wellsted D.: SS 3.07
 Welzel T.: SS 4.05
 Weszelits V.: P-205
 Whitley S.: P-068
 Whitmarsh G.: P-120
 Wierzbowski J.: P-037, P-305
 Wietholtz H.: SS 10.01
 Wiezer M.: P-241
 Williams L.: P-022, P-066, P-071
 Williams P.: P-222
 Willig A.: P-105
 Wilson D.: SS 12.06
 Wilson N.: SS 5.09
 Wilson S.: SS 2.01
 Won H.: P-253
 Woo J.: P-187
 Wotherspoon A.: SS 3.01
 Wray A.: P-060
 Wyatt J.: SS 12.06
 Wylie P.: SS 1.02, SS 6.03, SS 6.07, SS 13.09

X

Xu J.: SS 12.03

Y

Yagci B.: P-231
 Yaghmai V.: P-165, SS 2.05
 Yagyu Y.: P-029
 Yakar T.: P-195, P-201
 Yamada Y.: P-088, P-284
 Yamaner S.: P-109
 Yang D.: P-260
 Yang I.: P-187
 Yarmenitis S.: SS 8.05, SS 9.02
 Yasuda K.: P-155
 Yeksan M.: P-256
 Yi B.: P-145
 Yigitbasi R.: P-138
 Yikilmaz A.: SS 5.10
 Yildirim Donmez F.: P-006
 Yildirim D.: P-266
 Yirik G.: P-181, P-274
 Yol S.: P-304
 Yoo H.: SS 2.08, SS 14.07
 Yoon K.: P-124
 Yoon S.: P-075, P-124, P-263
 Yoshimura M.: P-276
 Yu J.: P-087, SS 4.08
 Yutaka S.: SS 6.06

Z

Zadrozny D.: P-143, P-172
 Zalcman M.: SS 6.05
 Zamboni G.: SS 4.01, SS 5.01
 Zappa M.: SS 7.03
 Zausig N.: SS 4.06
 Zech C.: SS 12.05, SY 6.02
 Zen Y.: P-185, P-186
 Zhang J.: SS 6.06
 Zins M.: P-027, P-277
 Zuiani C.: P-009, SS 9.04

NOTES

See you at
ESGAR '09



VALENCIA / ES

EUROPEAN SOCIETY OF GASTROINTESTINAL AND ABDOMINAL RADIOLOGY

ESGAR 2009



JUNE 23 – 26

20TH ANNUAL MEETING AND POSTGRADUATE COURSE

MEETING PRESIDENT

Dr. Luis Martí-Bonmatí
Dr Peset University Hospital
Resonancia Magnética. Servicio de Radiología
Gaspar Aguilar, 90
ES – 46017 Valencia, Spain

CENTRAL ESGAR OFFICE

Neutorgasse 9/2a
AT – 1010 Vienna, Austria
Phone: +43 1 535 89 27
Fax: +43 1 535 70 37
E-Mail: office@esgar.org
www.esgar.org

GE Healthcare

Now the CT you trust protects patients with less dose.

The new LightSpeed® VCT XT reduces cardiac CTA dose by up to 70% with uncompromised image quality. It captures the right images at exactly the right moments, reducing your patient's exposure. With only the best images to read and reconstruct, you can reach a diagnosis quickly and confidently. Less dose. Better patient care. That's **CT Re-imagined.**

Get the whole story on low dose and see remarkable images at www.gehealthcare.com/LowDoseCT



GE imagination at work